

**NEUROPROTECTIVE EFFECTS OF ROOIBOS AGAINST H₂O₂-INDUCED
CYTOTOXICITY IN HUMAN NEUROBLASTOMA SH-SY5Y CELLS**

BY

ELIAS CHIPOFYA

**Thesis submitted in fulfilment of the requirements for the degree
Master of Science: Biomedical Technology
in the Faculty of Health and Wellness Sciences
at the Cape Peninsula University of Technology, Bellville**

Supervisor: Prof Jeanine L Marnewick

Co-supervisor: Dr Taskeen F Docrat

February 2024

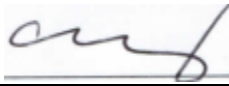
CPUT copyright information

The dissertation/thesis may not be published either in part (in scholarly, scientific, or technical journals) or as a monograph unless permission has been obtained from the University.

DECLARATION

I, Elias Chipofya, declare that the contents of this dissertation/thesis represent my own unaided work, and that the dissertation/thesis has not previously been submitted for academic examination towards any qualification. Furthermore, it represents my own opinions and not necessarily those of the Cape Peninsula University of Technology.

Elias Chipofya,



Signed

13th March 2024

Date

ABSTRACT

Oxidative stress, a key player in neurodegenerative disorders such as Alzheimer's and Parkinson's disease, is a critical target for therapeutic interventions. Plant polyphenols demonstrate substantial neuroprotective effects in numerous neurodegenerative disorders, underpinning future preclinical and clinical studies. South African Rooibos (*Aspalathus linearis*) herbal tea, which is widely consumed for its health benefits and caffeine-free nature, has been shown to positively affect various processes observed in the pathogenesis of neurodegenerative disorders. In this study, we investigate the neuroprotective potential of fermented and unfermented aqueous and ethanolic Rooibos extracts on neuroblastoma cells, addressing a critical gap in current research. Aqueous and ethanolic extracts [15-500 µg/mL] were evaluated in an SH-SY5Y cellular model subjected to oxidative stress induced by hydrogen peroxide (H₂O₂). The antioxidant properties of the extracts were measured using cell-free systems. The total antioxidant content and capacity of the Rooibos extracts were determined by measuring using total polyphenol content (TPC), trolox equivalent antioxidant capacity (TEAC) and ferric ion reducing antioxidant power (FRAP). HPLC was employed to quantify major phenolic compounds, revealing aspalathin as the predominant polyphenol. The 3-(4,5-dimethylthiazol-2-yl)-2,5-diphenyltetrazolium bromide (MTT) assay was used to assess the maximum non-toxic dosage (MNTD) of Rooibos extracts against SH-SY5Y cells. Subsequently, the cells were pretreated with the MNTDs of Rooibos extracts, and thereafter exposed for 3 hours to 150 µM H₂O₂. The effect of Rooibos extracts on cell viability and metabolic activity was determined using MTT and intracellular adenosine triphosphate (ATP) assays; oxidative status was assessed using thiobarbituric acid reactive substance (TBARS), conjugated diene (CDs), protein carboxylation, and reduced glutathione (GSH) assays; and endogenous antioxidant enzyme activity in SH-SY5Y cells was assessed using superoxide dismutase (SOD) and catalase (CAT) colorimetric assays. In addition, the activities of lactate dehydrogenase (LDH) and caspase -3/7, -8, and -9 were used to measure cellular death. Rooibos extracts exhibited a dose-dependent increase in antioxidant capacity in cell-free systems. The results showed that treatment with Rooibos extracts did not reduce cell viability of SH-SY5Y cells. Furthermore, when SH-SY5Y cells were exposed to H₂O₂, Rooibos extracts exhibited dose-dependent cytoprotective effects. Rooibos fermented aqueous extract at 60 µg/mL increased ($P \leq 0.05$) intracellular ATP levels, while the fermented ethanolic extract at 125 and 250 µg/mL increased ($P \leq 0.001$) intracellular ATP levels and ($P \leq 0.001$), respectively. Both unfermented and fermented aqueous and ethanolic extracts reduced CDs, an early marker of lipid peroxidation ($P \leq 0.01$, and $P \leq 0.001$, when compared to cells treated only with H₂O₂), except for fermented aqueous extract at 60 µg/mL, where CDS formation was comparable

to cells treated only with H₂O₂. Furthermore, a significant decrease in protein carbonyls was observed in cells pre-treated with 250 µg/mL of unfermented aqueous Rooibos extract (P≤0.01), 125 and 250 µg/mL of unfermented ethanolic Rooibos extract (P≤0.001) and (P≤0.05), respectively and 250 µg/mL of fermented ethanolic Rooibos extract (P≤0.001) compared to cells treated only with H₂O₂. Pre-treatment with 60 µg/mL of unfermented ethanolic Rooibos extract prevented H₂O₂ depletion of reduced GSH (P<0.05). Both Rooibos extracts significantly (P≤0.01, P≤0.001) restored endogenous antioxidant enzyme, CAT activity, with varying effects on SOD enzyme activity in the cells. The current study demonstrates that Rooibos, a renowned South African herbal tea at certain concentrations, may enhance the endogenous antioxidant defence system in oxidatively challenged H₂O₂ human neuroblastoma SH-SY5Y cells. However, this was not the case for all concentrations tested in this model, implying that Rooibos may possess pro-oxidant properties at certain concentrations. The interactions between Rooibos and H₂O₂ must be further elucidated. Nevertheless, these findings suggest a compelling avenue for the use of Rooibos in preventative strategies against neurodegenerative disorders, including Alzheimer's disease and Parkinson's disease.

Keywords: Neurodegenerative disorders; oxidative stress; antioxidant activity; Rooibos; neuroprotection.

ACKNOWLEDGMENTS

I wish to thank:

- The Lord Almighty for His enabling grace and mercy in my life. Every day, I see His love in my life, and I shall be eternally grateful.
- Professor J.L. Marnewick, my supervisor, for your motherly support and kindness. Thank you for giving me everything I requested for as soon as I asked. I am appreciative of the attentive guidance, encouragement, and unending support I received during my studies.
- Dr. T.F Docrat, my co-supervisor, for her contributions to this work. Throughout my studies, she has provided me with exceptional guidance, many appropriate suggestions, valuable advice, insightful discussion, and support.
- Mr. F Rautenbach from the Oxidative Stress Research Laboratory at the Applied Microbial and Health Biotechnology Institute (AMHBI), Cape Peninsula University of Technology (CPUT) for his technical assistance, encouragement, and recommendations throughout the entire study.
- Dr. Graham Beastall and Dr. Mike Hallworth, my International Federation of Clinical Chemistry and Laboratory Medicine (IFCC) mentors, thank you for your continuous support and advice in shaping my professional career.
- Colleagues and colleagues who provided invaluable support and assistance throughout this program.
- Staff and colleagues at the Oxidative Stress Research Laboratory at the Applied Microbial and Health Biotechnology Institute (AMHBI) who have contributed to my success.
- The financial assistance of the South African Rooibos Council (SARC) and CPUT towards this research is acknowledged. Opinions expressed in this thesis and the conclusions arrived at, are those of the author, and are not necessarily to be attributed to the SARC and CPUT.

DEDICATION

I dedicate this thesis to the glory of God Almighty, the one who created plants for mankind's use and commanded man to use these herbs and trees for food and medicine, as recorded in the Holy Bible's books of Genesis and Revelation.

To the glory of God, I also dedicate this dissertation to my wife, Madalitso, who has been a continuous source of support and encouragement throughout the challenges of academia and life. I am very grateful to have you in my life.

This work is also dedicated to my parents, Mr, and Mrs Chipofya, who have always loved me unconditionally and have never stopped praying for my protection and salvation, and whose good examples have inspired me to strive hard for the things I seek in life.

OUTPUTS

- **Elias Chipofya**, Taskeen F Docrat, Jeanine L Marnewick. The neuroprotective effects of Rooibos extracts against H₂O₂-induced oxidative stress in human neuroblastoma SH-SY5Y cells. The 25th WORDLAB-EUROMEDLAB ROMA 2023, Rome, 21-25 May 2023, Italy (Presenting author for poster presentation).
- **Elias Chipofya**, Taskeen F Docrat and Jeanine L Marnewick. The neuroprotective effect of Rooibos herbal tea against Alzheimer's disease: A Review. Submitted to Nutritional Neuroscience, 13 February 2023. (1st author of manuscript).
- **Elias Chipofya**, Taskeen F Docrat, Jeanine L Marnewick. The neuroprotective effects of Rooibos extracts against H₂O₂-induced oxidative stress in human neuroblastoma SH-SY5Y cells. CPUT postgraduate conference 2023. SARETEC Auditorium in Bellville. 1 March 2023. (Presenting author for oral presentation).
- **Elias Chipofya**, Taskeen F Docrat, Jeanine L Marnewick. protective effects of Rooibos extracts against H₂O₂-induced neurotoxicity in human neuroblastoma SHSY5Y cells: a proposal CPUT postgraduate conference 2021. Online. 30 November 2021. (Presenting author for poster presentation).

TABLE OF CONTENTS

DECLARATION	ii
ABSTRACT	iii
ACKNOWLEDGMENTS.....	v
DEDICATION.....	vi
OUTPUTS.....	vii
TABLE OF CONTENTS	viii
LIST OF TABLES.....	xii
LIST OF FIGURES	xiii
ABBREVIATION	xv
GLOSSARY	xix
APPENDICES.....	xx
1. CHAPTER ONE: INTRODUCTION.....	1
1.1. Background.....	1
1.2. Study rationale.....	4
1.3. Research aims and objectives.	6
1.3.1. Aim of the study.....	6
1.3.2. Objectives.....	6
2. CHAPTER TWO: LITERATURE REVIEW.....	7
2.1. Rooibos herbal tea.....	7
2.2. Antioxidant defence systems of the body.....	10
2.2.1. Glutathione	12
2.2.2. Superoxide dismutases.....	14
2.2.3. Catalase	16
2.3. Reactive oxygen species	16
2.4. Hydrogen peroxide.....	19
2.5. Neurodegeneration	20

2.6.	Oxidative stress	22
2.6.1.	Oxidative stress and the pathogenesis of Alzheimer’s disease	22
2.6.2.	Oxidative stress and cellular pathologies in Parkinson’s disease	23
2.7.	Protein damage	24
2.8.	Lipid damage	25
2.9.	Cell death	27
2.9.1.	Apoptosis.....	27
2.9.2.	Necrosis.....	30
2.10.	Human neuroblastoma SH-SY5Y cell line.....	32
3.	CHAPTER THREE: METHODOLOGY	34
3.1.	Materials.....	34
3.2.	Preparation of the Rooibos extracts	35
3.3.	Extracts screening	36
3.4.	Total Polyphenol determination of Rooibos extracts.....	36
3.5.	Ferric ion reducing antioxidant power (FRAP) Assay	37
3.6.	Trolox Equivalent Antioxidant Capacity (TEAC) Assay.....	39
3.7.	High-performance liquid chromatography analysis of Rooibos extracts.....	41
3.8.	Cell culture and maintenance.....	41
3.8.1.	Trypan blue dye exclusion assay	42
3.8.2.	Hydrogen peroxide preparation.....	43
3.8.3.	Determination of optimal concentrations of H ₂ O ₂ using Methylthiazol tetrazolium dye reduction (MTT) cell viability assay	43
3.8.4.	Rooibos concentration screening.....	45
3.8.5.	The ATP quantification assay	45
3.8.6.	Oxidative stress biomarkers.....	47
3.8.6.1.	Conjugated dienes.....	47
3.8.6.2.	The thiobarbituric acid reactive substance assay	48
3.8.7.	Protein extraction, quantification, and standardization	49

3.8.7.1.	Protein Extraction	49
3.8.7.2.	Protein Quantification.....	50
3.8.8.	Quantification of protein carbonylation	50
3.9.	Redox status.....	51
3.9.1.	Reduced glutathione assay.....	51
3.10.	Antioxidant enzyme activity.....	53
3.10.1.	Superoxide dismutase activity.....	53
3.10.2.	Catalase activity.....	54
3.11.	Cellular Death.....	55
3.11.1.	Analysis of caspase activity	55
3.11.2.	The lactate dehydrogenase assay	57
3.12.	Statistical Methods.....	58
4.	CHAPTER FOUR: RESULTS	59
4.1.	Determination of total phenolic content of Rooibos extracts	59
4.2.	Determination of ferric reducing antioxidant power of Rooibos extracts	60
4.3.	Determination of Trolox Equivalent Antioxidant Capacity of Rooibos extracts	61
4.4.	High-performance liquid chromatography analysis of unfermented and fermented Rooibos extracts.....	62
4.5.	H ₂ O ₂ cytotoxicity on the metabolic activity of SH-SY5Y cells.....	66
4.6.	The effect of Rooibos extracts on cell viability in SH-SY5Y cells	66
4.7.	The effect of Rooibos extracts on SH-SY5Y cell metabolic activity under induced H ₂ O ₂ cytotoxic conditions.	67
4.8.	The effect of Rooibos extracts on intracellular ATP	69
4.9.	The effect of Rooibos extracts on oxidative damage biomarkers in SH-SY5Y cells.....	71
4.9.1.	The effect of the Rooibos extracts on lipid peroxidation in H ₂ O ₂ -challenged cultured SH-SY5Y cells.	72
4.9.1.1.	The effects of the Rooibos extracts on conjugated Dienes.....	72
4.9.1.2.	The effect of Rooibos extracts on thiobarbituric acid reactive substances (TBARS) 73	

4.9.2. The effects of Rooibos Extracts on Protein Carbonylation in H ₂ O ₂ -challenged cultured SH-SY5Y cells.....	75
4.10. The effects of Rooibos extracts on reduced glutathione (GSH) in H ₂ O ₂ -challenged cultured SH-SY5Y cells.	77
4.11. The effect of Rooibos extracts pre-treatment on SOD activity in SH-SY5Y cells exposed to 150 µM H ₂ O ₂ for 3 hours.....	78
4.12. The effects of Rooibos extracts pre-treatment on CAT activity in SH-SY5Y cells exposed to 150 µM H ₂ O ₂ for 3 hours.....	80
4.13. Cellular Death.....	81
4.13.1. Effects of Rooibos extract pre-treatment on H ₂ O ₂ -induced caspase-8, -9, and -3/7 activation in SH-SY5Y cells exposed to 150 µM H ₂ O ₂ for 3 hours.	81
4.13.2. Effects of Rooibos extract pre-treatment on H ₂ O ₂ -induced LDH activation in SH-SY5Y cells exposed to 150 µM H ₂ O ₂ for 3 hours.....	84
5. CHAPTER FIVE: DISCUSSION.....	86
5.1. Conclusion.....	99
5.2. Study limitations and future recommendations.....	99
6. REFERENCES	100
7. APPENDIX.....	129

LIST OF TABLES

Table 2.1: Classification of the common phenolic composition of Rooibos (<i>Aspalathus linearis</i>).9	
Table 3.1: Treatment groups used in the investigation of neuroprotective effects of Rooibos extracts on H ₂ O ₂ -induced cytotoxicity in SH-SY5Y cells.45	45
Table 4.1: The total phenolic content of ethanolic, and aqueous extractions compared according to the type of Rooibos.60	60
Table 4.2: Ferric reducing antioxidant power of ethanolic, and aqueous extractions compared according to the type of Rooibos.61	61
Table 4.3: Trolox equivalent antioxidant capacity of ethanolic, and aqueous extractions compared according to the type of Rooibos.62	62
Table 4.4: Quantitative data of flavonoids detected in ethanolic, and aqueous extracts compared according to the type of Rooibos.63	63

LIST OF FIGURES

Figure 2.1: Glutathione formation and recycling.	14
Figure 2.2: The mechanism of lipid peroxidation	26
Figure 3.1: The two forms of processed Rooibos plant materials (fermented and unfermented Rooibos) used in this study.	35
Figure 3.2: The 96-well microplate used in the total polyphenol content determination.	37
Figure 3.3: Plate layout for the total polyphenol content assay.....	37
Figure 3.4: The 96-well microplate used in the ferric reducing antioxidant potential assay	38
Figure 3.5: Plate layout for the ferric reducing antioxidant potential assay	38
Figure 3.6: The 96-well microplate used in the trolox equivalent antioxidant capacity assay	40
Figure 3.7: Plate layout for the trolox equivalent antioxidant capacity assay.	40
Figure 3.8: Schematic representation of dead cells stained with trypan blue.....	42
Figure 3.9: 3-(4,5-Dimethylthiazol-2-yl)-2,5-diphenyl-2H-tetrazolium bromide (MTT) assay principle.	44
Figure 3.10: The bioluminescence-based adenosine triphosphate quantification assay principle.	46
Figure 3.11: A schematic and simplified representation for determining conjugated dienes.	47
Figure 3.12: The principle of the thiobarbituric acid reactive substance assay.	49
Figure 3.13: The reaction of the protein carbonyl group with 2,4-dinitrophenylhydrazine (DNPH).	50
Figure 3.14: Principle of the GSH-Glo™ Glutathione Assay.	52
Figure 3.15: Schematic of the superoxide dismutase (SOD) activity assay principle.	53
Figure 3.16: Schematic of the catalase colorimetric activity assay principle.	54
Figure 3.17: Schematic representation of the Caspase-Glo® assay principle.	56
Figure 3.18: The schematic representation of the lactate dehydrogenase (LDH) release assay principle.	57
Figure 4.1: High-performance liquid chromatography (HPLC) chromatogram of unfermented Rooibos extracts used in the study.....	64
Figure 4.2: High-performance liquid chromatography (HPLC) chromatogram of fermented Rooibos extracts	65
Figure 4.3: Cytotoxicity profile of H ₂ O ₂ (3 hours) in the 3-(4,5-dimethylthiazol-2-yl)-2,5-diphenyl-2H-tetrazolium bromide (MTT) assay expressed as % cell viability.	66
Figure 4.4: The effects of a 24-hour Rooibos treatment.	67

Figure 4.5: Effect of Rooibos extracts on the metabolic output of SH-SY5Y cells challenged with 150 μM H_2O_2 using the 3-(4,5-dimethylthiazol-2-yl)-2,5-diphenyl-2H-tetrazolium bromide (MTT) assay.69

Figure 4.6: Analysis of the effect of 24- Rooibos extracts pretreatment followed by 3-hour H_2O_2 treatment on intracellular adenosine triphosphate (ATP) levels in SH-SY5Y cells.71

Figure 4.7: Conjugated diene levels in SH-SY5Y cells pre-treated with different concentrations of Rooibos extracts for 24 hours, followed by 150 μM H_2O_2 treatment for 3 hours.....73

Figure 4.8: Malondialdehyde (MDA) levels in SH-SY5Y cells treated for 24 hours with different concentrations of Rooibos extracts, followed by 3 hours with 150 μM H_2O_274

Figure 4.9: The effects of 24-hour treatment of Rooibos extracts, followed by on protein damage in 150 μM H_2O_2 (3 hours) - challenged cultured SH-SY5Y cells.76

Figure 4.10: Effects of Rooibos extracts on reduced glutathione (GSH) levels in SH-SY5Y cells treated for 24 hours with different concentrations of Rooibos extracts, followed by 3 hours with 150 μM H_2O_278

Figure 4.11: The superoxide dismutase (SOD) activity in SH-SY5Y cells pre-treated with different concentrations of Rooibos extracts for 24 hours, followed by 150 μM H_2O_2 treatment for 3 hours.79

Figure 4.12: Catalase (CAT) activity in SH-SY5Y cells pre-treated with different concentrations of Rooibos extracts for 24 hours, followed by 150 μM H_2O_2 treatment for 3 hours.....81

Figure 4.13: Caspase 8 activity in SH-SY5Y cells pre-treated with different concentrations of Rooibos extracts for 24 hours, followed by 150 μM H_2O_2 treatment for 3 hours.....82

Figure 4.14: Caspase 9 activity in SH-SY5Y cells pre-treated with different concentrations of Rooibos extracts for 24 hours, followed by 150 μM H_2O_2 treatment for 3 hours.....83

Figure 4.15: Caspase 3/7 activity in SH-SY5Y cells pre-treated with different concentrations of Rooibos extracts for 24 hours, followed by 150 μM H_2O_2 treatment for 3 hours.....84

Figure 4.16: The lactate dehydrogenase (LDH) activity in SH-SY5Y cells pre-treated with different concentrations of Rooibos extracts for 24 hours, followed by 150 μM H_2O_2 treatment for 3 hours.85

ABBREVIATION

Acronyms/Abbreviations	Definition/Explanation
°C	Degree Celsius
µg/mL	Micrograms per millilitre
µL	Microliter
³ O ₂	Triplet ground state of oxygen
4HNE	4-hydroxynonenal
AAE	Ascorbic acid equivalent
ABTS ^{•+}	2,3'-Azinobis (3-ethylbenzothiazoline-6-sulfonic acid) radical cation
AD	Alzheimer's disease
ANOVA	Analysis of variance
AOC	Antioxidant capacity
AP-1	Activator protein 1
Apaf-1	Multimeric apoptotic protease activating factor 1
ASC	Neutral amino acid transport system
ATCC	American Type Culture Collection
ATP	Adenosine triphosphate
Aβ	Amyloid beta peptide
BAK	Bcl-2 homologous antagonist
BAX	Bcl-2-like protein 4
BBB	Blood-brain barrier
Bcl-2	B-cell lymphoma
BHT	Butylated hydroxytoluene
BSA	Bovine serum albumin
Ca ²⁺	Calcium ion
CARD	Caspase recruitment domain
CAT	Catalase
CDs	Conjugated dienes
CNS	Central nervous system
COX	Cyclooxygenase
CSF	Cerebrospinal fluid
Cu	Copper
CV	Coefficients of variation
CYP450	Cytochrome p450

Cyt c	Cytochrome c
DAAO	D-amino acid oxidase
dATP	Deoxyadenosine triphosphate
DED	Death effector domain
DEP	Diesel exhaust particle
dH ₂ O	Distilled water
DHCs	Dihydrochalcones
DISC	Death-inducing signalling complex
DMEM	Dulbecco's Modified Eagle Medium
DMSO	Dimethylsulfoxide
DNA	Deoxyribonucleic acid
DNPH	2,4-Dinitrophenylhydrazine
ER	Endoplasmic reticulum
ETC	Electron transport chain
ETPT	Electron transfer-proton transfer
FADD	Fas-associated protein with death domain,
Fas	First apoptosis signal
Fe	Iron
FeCl ₃ ·6H ₂ O	Iron chloride hexahydrate solution
FRAP	Ferric reducing antioxidant power
GAE	Gallic acid equivalent
Gox	Glucose oxidase
GPx	Glutathione peroxidase
GR	Glutathione reductase
GS	Glutathione synthetase
GSH	Superoxide dismutase
GSSG	Glutathione disulfide
GST	Glutathione S-transferase
H ⁺	Hydrogen ions
H ₂ O	Water
H ₂ O ₂	Hydrogen peroxide
H ₃ PO ₄	Phosphoric acid
hAPP	Human amyloid precursor protein
HCl	Hydrochloric acid

HPLC	High performance liquid chromatography
HRP	Horseradish peroxidase
HUVECs	Human umbilical vein endothelial cells
IL-1 β	Interleukin 1 beta
IL-6	Interleukin 6
K ₂ S ₂ O ₈	Potassium persulfate
LDH	Lactate dehydrogenase
LOX	Lipoxygenase
LPO	Lipid peroxidation
MAO	Monoamine oxidase
MAPT	Microtubule-associated protein tau
MDA	Malondialdehyde
Mg ²⁺	Magnesium ions
mM	Millimolar
MNTD	Maximum non-toxic dosage
MPP ⁺	1-Methyl-4-phenylpyridinium
mRNA	Messenger ribonucleic acid
mTorr	Millitorr
MTT	3-(4,5-Dimethylthiazol-2-yl)-2,5-diphenyl-2H-tetrazolium bromide
Na ₂ CO ₃	Sodium carbonate
NAD ⁺	Nicotinamide adenine dinucleotide
NADPH	Reduced nicotinamide adenine dinucleotide phosphate
NaOH	Sodium hydroxide
NDDs	Neurodegenerative disorders
NF- κ B	Nuclear factor kappa light chain enhancer of activated B cells
NGF	Nerve growth factor
NKA	Sodium-potassium ATPase pump
NOXs	Nicotinamide adenine dinucleotide phosphate oxidases
O ₂	Molecular oxygen
O ₂ ^{•-}	Superoxide anion radicals
OD	Optical density
OS	Oxidative stress
PARP1	Poly (ADPribose) polymerase 1
PARylation	Poly (ADPribosyl)ation

PBS	Phosphate-buffered saline
PCs	Protein carbonyls
PD	Parkinson's disease
pH	Potential of hydrogen or Power of hydrogen
Prx	Peroxiredoxin
PUFAs	Polyunsaturated fatty acids
RNS	Reactive nitrogen species
ROS	Reactive oxygen species
RPM	Revolutions per minute
SD	Standard deviation
SETPT	Single-electron transfer-proton transfer
-SO ₂ H	Sulfinic acid
-SO ₃ H	Sulphonic acid
SOD	Superoxide dismutase
-SOH	Sulfenic acid
SPLET	Sequential proton loss electron transfer
TAC	Total antioxidant capacity
TBA	2-Thiobarbituric acid
TBARS	Thiobarbituric acid reactive substance
<i>t</i> -BHP	<i>tert</i> -Butyl-hydroperoxide
TCA	Trichloroacetic acid
TE	Trolox equivalents
TEAC	Trolox equivalent antioxidant capacity
TNF	Tumour necrosis factor
TNF α	Tumour necrosis factor alpha
TPC	Total polyphenolic content
TPTZ	2,4,6-Tri[2-pyridyl]-s-triazine
TRADD	TNF receptor associated death domain
Trx	Thioredoxin
Uox	Urate oxidase
WHO	World Health Organization
XOD	Xanthine oxidase
γ -GCS	γ -Glutamylcysteine synthetase

GLOSSARY

Terms	Definition/Explanation
Alzheimer's disease	An age-related disease characterised by the development of amyloid plaques and neurofibrillary tangles in the brain parenchyma.
Antioxidant	Any substance that, when present in low concentrations relative to the oxidisable substrate, significantly delays or inhibits oxidation of that substrate.
Free radical	Any species that contains one or more unpaired electrons.
Limit of detection	The lowest concentration of an analyte in a sample that can be consistently detected with a certain probability (usually at 95% confidence).
Lipid peroxidation	A complex process involving the interaction of oxygen-derived free radicals with polyunsaturated fatty acids, resulting in a variety of highly reactive electrophilic aldehydes.
Neurodegeneration	A complex multifactorial central nervous system disorder characterised by chronic progressive loss of the structure and function of neuronal cells, as well as possible neuronal death, resulting in behavioural and mental impairment
Parkinson's disease	A progressive neurodegenerative disorder characterized pathologically by dopaminergic neuron loss in the substantia nigra, and the presence of protein inclusions known as Lewy bodies.
Protein carbonylation	The process by which reactive carbonyl moieties such as aldehyde, ketone, and lactam are introduced into proteins.
Reactive oxygen species	A collective term for oxygen-derived small and highly reactive molecules.

APPENDICIES

Appendix 1: Recipe for preparation of TPC reagents	129
Appendix 2: Recipe for preparation of FRAP reagents	130
Appendix 3: Recipe for preparation of TEAC reagents	132
Appendix 4: Recipe for preparation of TBARS reagents.....	133
Appendix 5: Recipe for preparation of protein carbonyl reagents	134
Appendix 6: Optimal H ₂ O ₂ concentrations	134
Appendix 7: The effect of 2-hour Rooibos extracts pretreatment followed by 3-hour H ₂ O ₂ treatment on SH-SY5Y cell metabolic activity	135
Appendix 8: Intracellular ATP levels after SH-SY5Y cells pretreated with Rooibos extracts for 2 hours followed by 3-hour treatment with H ₂ O ₂	135
Appendix 9: Protein quantitation and standardisation after SH-SY5Y cells pretreated with Rooibos extracts from 24 hours followed by H ₂ O ₂ treatment for 3 hours	136
Appendix 10: Estimate the quantity of flavonoids identified in unfermented ethanolic and aqueous Rooibos extracts.	136
Appendix 11: Estimate the quantity of flavonoids identified in fermented ethanolic and aqueous Rooibos extracts.	137
Appendix 12: The effects of a 24-hour unfermented aqueous Rooibos extract treatment.....	137
Appendix 13: Effect of unfermented aqueous Rooibos extracts on the metabolic output of SH-SY5Y cells challenged with 150 µM H ₂ O ₂ using the 3-(4,5-dimethylthiazol-2-yl)-2,5-diphenyl-2H-tetrazolium bromide (MTT) assay	138
Appendix 14: The total phenolic content of unfermented, and fermented Rooibos compared according to the extraction methods.....	138
Appendix 15: Ferric reducing antioxidant power of unfermented, and fermented Rooibos compared according to the extraction methods.	139
Appendix 16: Trolox equivalent antioxidant capacity of unfermented, and fermented Rooibos compared according to the extraction methods.	139
Appendix 17: Ethics certificate	140

1. CHAPTER ONE: INTRODUCTION

1.1. Background

The global impact of neurodegenerative disorders (NDDs) like Alzheimer's disease (AD) and Parkinson's disease (PD) has grown drastically in recent years, especially in countries with an ageing population. This trend is predicted to persist and eventually reach pandemic proportions (Dekker et al., 2020; Holbrook et al., 2021). Alzheimer's disease is the most common and progressive age-related NDD that causes cognitive, functional, and behavioural impairments (Holbrook et al., 2021; Chen, 2022). It affects between 23 and 35 million people worldwide (Chen, 2022). Parkinson's disease, which affects around 6 million people worldwide, is the world's second most common NDD after AD (Holbrook et al., 2021). Improved healthcare systems correlate with increasing average life expectancy and lower mortality for communicable diseases on the African continent, and NDDs are becoming a major public health challenge (Dekker et al., 2020; Nelson et al., 2020; Quarshie et al., 2021). The World Health Organization (WHO) estimates that Africa's average life expectancy is currently 61.2 years and is expected to increase further (Dekker et al., 2020). It is estimated that by 2050, ~139 million individuals in developing nations, including Africa, will outlive the average life expectancy in developed nations (Blanckenberg et al., 2013). This will significantly impact the socioeconomic burden of global healthcare. Neurodegenerative disorder complications significantly impact healthcare delivery, associated economic costs, and patient quality of life. Furthermore, indirect costs (income loss) are related to the patient's inability to work and reduced family income (Cilia et al., 2011; Erukainure et al., 2020a). Suffering psychological distress and shouldering burdens while caring for an individual with NDD relative affects not only the caregiver's quality of life and health, but also their productivity as an individual and their ability to provide quality care for the ill relative, thus worsening the ill relative's health and decreasing the likelihood of recovery or health improvements. Survival after being diagnosed with a NDD ranges between 3 and 10 years, with an average survival of less than five years. Biological sex, poor mental health, and disease severity have all been linked to increased mortality (Lwi et al., 2017).

Neurodegenerative disorders are incurable and debilitating conditions that cause a loss of nervous system function due to neuronal death (Maciotta et al., 2013; Gudoityte et al., 2021; Kulkarni, 2021). Those who suffer from this condition struggle with movement (ataxia), speech, breathing, and general mental function (dementias) because neurons find it difficult to regenerate (Kulkarni, 2021).

Numerous studies have shown that oxidative stress (OS), transition metal dysmetabolism, inflammation, microbiota, environmental pollution, and diet all play a role in NDDs (Grochowska et al., 2019; Agapouda et al., 2020; Erukainure et al., 2020a; Toledo et al., 2022). Various potential targets for neuroprotective agents are still being investigated to mitigate these factors, particularly OS (Erukainure et al., 2020a), which is recognised as an essential factor in neurodegeneration (Gudoityte et al., 2021). Oxidative stress arises when the production of reactive oxygen species (ROS) surpasses the intracellular antioxidant capacity (AOC) (Huang et al., 2014; Jin & Wang, 2019; Huang et al., 2020). When ROS, including hydrogen peroxide (H₂O₂), are produced in excess, they stimulate free radical reactions, resulting in protein and lipid damage (Jin & Wang, 2019). Oxidative stress causes neuronal death, which is a critical factor in developing NDDs (Huang et al., 2014; Huang et al., 2020). The brain is extremely sensitive to OS due to its high oxygen (O₂) consumption and metabolic rate, high content of polyunsaturated fatty acids (PUFAs), impaired ability to repair following injury, and low levels of antioxidant enzymes in comparison to other organs (Huang et al., 2014; Ataie et al., 2016; Huang et al., 2020).

Furthermore, OS has been linked to a disruption in brain glucose uptake, which leads to neuronal dysfunction (Erukainure et al., 2020b). Additionally, high levels of ROS and reactive nitrogen species (RNS) have been linked to neuroinflammation (Gudoityte et al., 2021). Furthermore, when antioxidant defences are compromised, the subsequent OS can cause mitochondrial damage, culminating in cellular malfunction, senescence, and cell death (Agapouda et al., 2020).

Neurodegenerative disorders are typically detected later in life when affected individuals exhibit symptoms, thus prevention is critical to reducing the disease burden (Agapouda et al., 2020; Xie et al., 2022). There is a growing demand for practical solutions to prevent the adverse effects that age-related conditions and NDDs have on healthcare systems (Huang et al., 2014; Ataie et al., 2016; Jin & Wang, 2019). Current NDD treatments are intended to alleviate symptoms but have little effect on preventing disease progression. Furthermore, they are frequently associated with negative side effects which include dizziness, hormonal imbalance, and in serious cases, it may result in cancer (Gülcan & Orhan, 2020; Mathur et al., 2023; Ul Islam et al., 2020). These interventions cannot prevent neurodegeneration, and there is no known cure to date (Gülcan & Orhan, 2020).

Natural substances may promise to prevent or treat NDDs (Rahman, 2020). Furthermore, the reported effects of bioactive polyphenols are linked to their ability to prevent or improve the symptoms of age-related diseases (Erukainure et al., 2020a; Abdul & Marnewick, 2021), including NDDs (Erukainure et al., 2020b). Plants have yielded a variety of active compounds, including anticholinesterases (physostigmine and neostigmine), opioid alkaloids, and galantamine, which have demonstrated a remarkable multipotent ability to provide relief from symptoms. Furthermore, seven of the 26 natural drugs approved in the last ten years were for treating NDDs, including three for PD. This highlights the significance of such products in drug discovery (Rahman, 2020).

In Africa, particularly in southern Africa, the use of phytomedicines is widely accepted as part of ethnopharmacology (also known as herbal medicine or phytotherapy) and continues to be the first point of contact for a significant proportion of the population (approximately 70%-95%) seeking primary healthcare needs (Rahman, 2020; Abdul & Marnewick, 2021). The WHO recognises the importance of ethnopharmacology, particularly in Africa, which has a long history of phytomedicine use and knowledgeable indigenous practitioners. Furthermore, the WHO encourages African member nations to promote and incorporate ethnopharmacology into their healthcare systems because it is regarded as an economically viable strategy (Abdul & Marnewick, 2021).

Several preclinical studies have revealed that natural beverages, notably herbal teas, have been demonstrated to prevent oxidative damage and thereby slow the progression of NDDs (Hong et al., 2014). Rooibos herbal tea is a good source of dietary antioxidants because of its special blend of bioactive phytochemicals, which include aspalathin, luteolin, quercetin, vitexin, and many more (Marnewick et al., 2000; Hong et al., 2014; Abdul & Marnewick, 2021). It has been reported that luteolin, quercetin, and vitexin may have neuroprotective properties (Swaminathan et al., 2019; Babaei et al., 2020; Maccioni et al., 2022).

Rooibos, or *Aspalathus linearis* (Burm. F.) R. Dahlgren (Fabaceae), is a strictly endemic plant found only in parts of the broader Cape Floristic Region of South Africa (Erlwanger & Ibrahim,

2017). The flat acuminate leaves and stems of the plant are used to prepare Rooibos, a popular herbal tea that has been used for its medicinal benefits in South Africa since the 1700s and contains only minimal quantities of tannins and no caffeine (Marnewick et al., 2000; Hong et al., 2014; Marnewick et al., 2011; Erlwanger & Ibrahim, 2017; Abdul & Marnewick, 2021).

Rooibos is commercially processed to produce either unfermented (green) or fermented/traditional Rooibos (Orlando et al., 2019). The primary flavonoid in unfermented Rooibos, aspalathin, is present in 7 % of fermented Rooibos herbal teas. The fermentation of aspalathin results in the production of flavanones and unknown polymeric compounds. However, it has been demonstrated that fermented Rooibos has additional active components, specifically aspalathin oxidation products, which enhance its potent antioxidant effect (Von Gadow et al., 1997).

It has been reported that dietary antioxidants may have adverse side effects if they are not appropriately administered or combined with other medications. In contrast to their supposed ability to prevent disease, excessive antioxidant consumption has also actually been linked to the pathophysiology and aetiology of diseases (Swaminathan et al., 2019). Complex polyphenols, such as tannins, can bind to iron in the intestine and prevent absorption, resulting in anaemia. They can also influence the regulation of iron homeostasis. Furthermore, the negative impact of these constituents on digestive system functioning may be due not just to enzyme inhibition, but also to their influence on the intestinal microbiota. Polyphenols can modify the microbiota profile by promoting some species and suppressing others, resulting in a change in the ratio of important bacterial groups. In addition, dysbiosis causes inflammation and immunological dysregulation, and it is linked to a variety of diseases, including irritable bowel syndrome, functional dyspepsia, metabolic disorders (diabetes, obesity, and non-alcoholic fatty liver disease), colon cancer, inflammatory bowel diseases (Crohn's disease and ulcerative colitis), cardiovascular disease, and small intestinal bacterial overgrowth (Duda-Chodak & Tarko, 2023). Therefore, the advantages of Rooibos herbal tea and its optimal dosage require further study. Additionally, *in vitro* concentrations should be calculated using anecdotal dosages to extrapolate *in vitro* data for *in vivo* use (Hoosen, 2019).

1.2. Study rationale

Human commercial cell lines are mostly immortalized cell lines derived from tumorigenic cells, which have the advantage of allowing unlimited and relatively easy culture, less subject to the ethical concerns of human primary cell cultures (Lopez et al., 2022). Cancer-derived cell lines are undifferentiated and usually very proliferative by nature (Mongelli et al., 2020). Probably the most used human cell line in neural cell biology research is the SH-SY5Y cell line from the American Type Culture Collection (ATCC® CRL-2266™). This neuroblastic cell line is a triple-cloned subline of the SK-N-SH cell line (ATCC® HTB-11™), which was established in the 1970s using cultures from a bone marrow biopsy that showed metastatic neuroblastoma, a tumour arising from the neural crest, in a 4-year-old child (Mongelli et al., 2020; Lopez et al., 2022). Undifferentiated SH-SY5Y cells are useful for studying how neurotoxicants impact the immature nervous system that could shed light on the causes of neurodegeneration in targeted studies or by large-scale techniques (Lopez et al., 2022), because they proliferate rapidly and are easy to handle (Shipley et al., 2016; Strother et al., 2021). Several studies have demonstrated that the undifferentiated SH-SY5Y cell line is an appropriate model to measure general endpoints of neurotoxicity such as cell viability, mitochondrial function, and OS (Lopez et al., 2022).

Dietary antioxidants, such as Rooibos, are gaining scholarly attention since they are less expensive and have very few side effects when compared to drugs and synthetic chemicals (Kee et al., 2013; Hong et al., 2014). However, more quality investigations and innovations are undoubtedly needed to back up these conclusions. It is also worth noting that dietary antioxidants have been described as an alternative for enhancing cellular capacity to endure apoptotic triggers (Feng & Wang, 2012; Fujita et al., 2012). Furthermore, compounds that suppress apoptosis have been proposed as a possible treatment or prevention for neurodegeneration (Carrasco et al., 2003). Additionally, cytotoxicity assays can be used to ascertain a compound's neuroprotective properties in SH-SY5Y cells in high-throughput testing (Cetin et al., 2022).

Since the neuroprotective properties of Rooibos herbal tea have not been extensively studied, more investigation is required to completely comprehend its health-promoting properties. Previous research has shown that fermented Rooibos only has neuroprotective activity and no anxiogenic impact, thus, a more thorough profile of both fermented and unfermented Rooibos is required (Hong et al., 2014; Akinrinmade et al., 2017; Pyrzanowska et al., 2019). Furthermore, the pharmacologically active constituents of Rooibos can affect a variety of processes, potentially modulating the risk of neurodegeneration. However, we still have gaps in understanding the mechanisms involved (Akinrinmade et al., 2017; López et al., 2022; Pyrzanowska, 2022).

An increase in OS is implicated in mechanisms that lead to complex multifactorial disorders known as neurodegeneration in the central nervous system (Ataie et al., 2016). It is worth noting that neuronal cell death has been identified as a hallmark feature of neurodegeneration. However, it is unclear whether neuronal cell death occurs because of apoptosis or necrosis in diseased states (Albarracin et al., 2012). Understanding the mechanisms involved in peroxide detoxification and toxicity in SH-SY5Y cells, and their interactions in antioxidative defence will help our understanding of physiological peroxide metabolism in the brain. Furthermore, such knowledge will help elucidate pathophysiological changes in NDDs including AD and PD and develop new therapeutic options to prevent peroxide-mediated OS in the brain (Dringen et al., 2005).

1.3. Research aims and objectives.

1.3.1. Aim of the study

To investigate the neuroprotective activity of fermented and unfermented Rooibos extracts in H₂O₂-challenged neuroblastoma SH-SY5Y cells. We additionally aim to determine the oxidative biomarker profile and the mechanisms involved in related cell death pathways.

1.3.2. Objectives

- i. To investigate the antioxidant profile of aqueous and ethanolic Rooibos extracts utilising two antioxidant assays (Ferric reducing antioxidant power [FRAP] and Trolox Equivalent Antioxidant Capacity [TEAC]).
- ii. To determine the total polyphenolic content (TPC) and High-performance liquid chromatography (HPLC) of Rooibos extracts.
- iii. To determine the safe and non-toxic doses of fermented and unfermented Rooibos extracts that maintain the viability of SH-SY5Y cells using the 3-(4,5-dimethylthiazol-2-yl)-2,5-diphenyl-2H-tetrazolium bromide (MTT) assay
- iv. To determine the various concentrations of H₂O₂ that can induce the death of at least 50% of the SH-SY5Y cells for different time intervals.
- v. To determine cell viability following pretreatment with Rooibos extracts before exposure to H₂O₂ using the MTT assay
- vi. To determine the metabolic effects of Rooibos pretreatment using the intracellular adenosine triphosphate (ATP) assay
- vii. To determine the levels of malondialdehyde (MDA) and conjugated dienes (CDs) formed by lipid peroxidising systems as oxidative stress indicators, as well as the extent of protein carbonylation.

- viii. To determine the effects of pre-treatment with selected concentrations of Rooibos extracts on antioxidant status of SH-SY5Y cells after H₂O₂ toxicity
- ix. To evaluate caspase 3/7, -8 and 9 activities in SH-SY5Y cells following pre-treatment with selected concentration of Rooibos extracts and exposure to H₂O₂
- x. To determine the level of lactate dehydrogenase (LDH) activity in SH-SY5Y cells after pre-treatment with selected concentrations of Rooibos extracts and H₂O₂ toxicity

2. CHAPTER TWO: LITERATURE REVIEW

2.1. Rooibos herbal tea

The use of medicinal plants such as Rooibos as practically viable commercial intervention strategies is gaining traction globally, particularly in developing countries (Ajuwon et al., 2013; Abdul & Marnewick, 2021). It is interesting to note that with rapid demographic and nutritional

transitions, NDDs will become a serious public health burden in developing countries (Alvi et al., 2021; López et al., 2021).

South Africa traditionally uses Rooibos herbal tea (brewed using *Aspalathus linearis* stems and leaves), also known as tisane, as an indigenous herbal health beverage (Marnewick, 2009; Abdul & Marnewick, 2021). Indeed, indigenous people in the Western Cape province of South Africa's Cederberg region have been processing the plant's stems and leaves to make herbal infusions since the late 1700s (Marnewick, 2009). Traditionally, it was sipped hot and strong with milk or sugar. Nowadays, the hot brew Rooibos is usually made with one tea bag (~2.4 g) and freshly boiled water, with an infusion time of 2 to 5 minutes to release colour and flavour (Joubert et al., 2008; Marnewick, 2010).

The consumption of Rooibos has increased because of its naturally sweet taste, low cost, and good safety record. Most importantly, due to its high antioxidant activity and distinct phenolic components, which are directly linked to its health-promoting properties (Carrier et al., 2021; Takalani et al., 2022). In comparison to other herbal teas like honeybush (*Cyclopia intermedia*) and black tea (*Camellia sinensis*), Rooibos is also devoid of caffeine and has a lower tannin level (about 3% in the leaves). Thus, it has been proposed to be beneficial for individuals who are nervous, and sensitive to caffeine, infants, and expecting mothers (Joubert et al., 2008; Marnewick, 2010; Takalani et al., 2022). It is believed that the unique polyphenolic compounds found in Rooibos contribute to its phytopharmaceutical effect. These compounds can influence many processes, potentially reducing the risk of dementia (Pyrzanowska, 2022; Takalani et al., 2022), with anecdotal evidence linking Rooibos consumption to 1) lipid peroxidation (LPO) inhibition and augmentation of GSH as main regulator of cellular redox status in rats exposed to chronic immobilisation (Hong et al., 2014), and 2) reduced brain oedema and neuronal apoptosis in adult male Wistar rats (Akinrinmade et al., 2017). Additionally, it has been demonstrated that Rooibos protects the liver through an antioxidative mechanism (Millar et al., 2020).

Given the importance of Rooibos herbal tea's phenolic composition in determining product properties, selecting *Aspalathus linearis* plant material, combined with an up-scalable isolation procedure, is of particular interest to obtain enough pure compounds that can then be used for structure determination and biological activity (Beelders et al., 2012; de Beer et al., 2015).

The isolation and structure determination of compounds from *Aspalathus linearis* revealed a variety of polyphenolic compounds, including phenolic acids (e.g., caffeic), the phenolic precursor phenylpyruvic acid-2-O- β -glucoside, and flavonoids. Rooibos flavonoids that have been identified and quantified include dihydrochalcone (DHCs) (e.g., aspalathin), flavonols (e.g., quercetin), flavones (e.g., vitexin), and flavanones (e.g., naringenin) (Table 2.1) (Pyrzanowska, 2022). The monomeric flavonoids aspalathin and nothofagin as well as linearthin are three rare and unique polyphenols of particular interest (de Beer et al., 2015; Mgwatyu et al., 2020).

Table 2.1: Classification of the common phenolic composition of Rooibos (*Aspalathus linearis*).

Rooibos (<i>Aspalathus linearis</i>) polyphenols	Phenolic acid	Caffeic, Ferrulic, Protocatechuic acid		
	Flavonoid precursors	Phenylpyruvic acid-2-O- β -glucoside		
	Flavonoids	Flavones	Apigenin, Luteolin, Orientin, Osoorientin, Vitexin, Isovitexin, Chrysoeriol	
		Flavonols	Hyperoside, Quercetin, Rutin, Quercitrin	
		Flavanones	Hesperidin, Eriodictyol, Naringenin	
Dihydrochalcones		Aspalathin, Nothofagin		

Significant, unwanted variation in Rooibos polyphenolic constituents may occur because of the plant material's origin (i.e., geographical location and harvest season), plant material components (i.e., leaves and stems), manufacturing conditions and time, and brewing algorithm. However, the commercially available simultaneous HPLC quantification method of these bioactive compounds allows for variation monitoring and ensures the quality of Rooibos products (Beelders et al., 2012; Pyrzanowska, 2022).

On the market, Rooibos comes in two forms: unfermented/green and fermented/traditional (Orlando et al., 2019; Pyrzanowska, 2022). Clinical evidence shows that consuming six cups of Rooibos herbal tea daily has a beneficial role in the context of cardiovascular disease and OS modulation Marnewick et al., (2011), and six cups of Rooibos herbal tea is recommended as a minimum daily consumption to have a beneficial health effect. Joubert & de Beer, (2012). Other studies (including *in vitro* and experimental animal studies) have shown substantial evidence for its neuroprotective effects (Hong et al., 2014; Akinrinmade et al., 2017; Pyrzanowska et al., 2019; Pyrzanowska et al., 2021; López et al., 2022; Omoruyi et al., 2023).

Significant quantitative differences have reportedly been observed in the phenolic composition of fermented and unfermented Rooibos (Pyrzanowska, 2022), with the former containing higher levels of aspalathin and nothofagin and exhibiting higher antioxidant activity (López et al., 2022; Mulaudzi et al., 2022; Vhangani et al., 2022). Rooibos fermentation involves cutting, bruising, wetting, and oxidizing the needle-shaped plant leaves in the open air to develop the distinctive reddish-brown colour, whereas unfermented rooibos retains its green colour (Sirotkin, 2021; López et al., 2022). Polyphenol oxidising enzymes catalyse the oxidation of phenolic compounds into highly reactive o-quinones at the start of the fermentation process. When Rooibos plant material is bruised and hydrated during processing, optimal reaction conditions for the polyphenol oxidising enzymes are created. Furthermore, water not only acts as a reaction medium but also aids in the transport of substrates and reactions during the enzymatic reaction (Tobin, 2018). The DHC aspalathin is oxidised to isoorientin and orientin during the second (non-enzymatic) processing step in the fermentation of Rooibos (Tobin, 2018; López et al., 2022).

2.2. Antioxidant defence systems of the body

The highly developed antioxidant defence system in humans works in concert to eliminate excess ROS while maintaining their beneficial effects (Demirci-Çekiç et al., 2022). When present at concentrations lower than the oxidising substrate in the cell, an antioxidant substance is responsible for regulating redox balance/homeostasis by restraining and retarding the oxidation of oxidisable substrates (Kurutas, 2016; Zhang et al., 2020; Demirci-Çekiç et al., 2022).

The components of the antioxidant defence system include both enzymatic and non-enzymatic species; the most notable examples of these are glutathione peroxidase (GPx), CAT, and SOD (Gonzalez-Pinto et al., 2012; Kurutas, 2016; Demirci-Çekiç et al., 2022). Non-enzymatic antioxidants include melatonin, vitamins E and C, carotenoids, thiol antioxidants (lipoic acid, glutathione, and thioredoxin), and flavonoids (Kurutas, 2016), and their defence mechanism is mostly reliant on GSH, an important water-soluble antioxidant (Gonzalez-Pinto et al., 2012; Demirci-Çekiç et al., 2022).

Antioxidants can be endogenous (produced by metabolism) or exogenous (from the diet) (Kurutas, 2016; Yanowsky-Escatell et al., 2020). Plants that include vitamins A, C, and E, as well as β -carotene, polyphenols, and flavonoids, are a good source of exogenous antioxidants (Widhiantara et al., 2021). The extracellular and intracellular fluid of the organism, as well as the cell membrane, may contain these antioxidants. A distinct antioxidant spectrum is required because lipid-soluble antioxidants, such as vitamin E, and carotenoids, are present in the hydrophobic lipid core of the membranes. Lipid-soluble antioxidants are essential for preventing peroxidation of PUFAs in biological membranes. However, during the hydrophilic phase, water-soluble antioxidants such as GSH, polyphenols, and vitamin C are essential for scavenging ROS (Munteanu & Apetrei, 2021).

The non-enzymatic antioxidant capacity is a biomarker for the body's antioxidant network (Kurutas, 2016). Non-enzymatic antioxidant capacity considers all exogenous antioxidants and their synergistic effects; therefore, endogenous antioxidants can be bolstered with exogenous antioxidants (Kurutas, 2016; Akinrinmade et al., 2017).

Enzymatic antioxidants are often called preventive antioxidants because they are the first line of cellular defence (Gonzalez-Pinto et al., 2012; Costa, Losada-Barreiro, et al., 2021). The cellular generation of reactive species or free radicals is inhibited or halted by their high catalytic properties. Furthermore, enzymatic antioxidants rapidly neutralize any molecule that possesses the potential to become a free radical or any free radical that could encourage the production of additional radicals. Most importantly, metal ion binding proteins (e.g., transferrin and ceruloplasmin) with high iron and copper affinities, prevent iron and copper from becoming free

radicals or deactivating radicals before they reach the stage of radical propagation by chelating or sequestering iron and copper (Costa, Losada, et al., 2021).

Non-enzymatic antioxidants, also known as chain-breaking antioxidants, are the second line of cellular defence (Gonzalez-Pinto et al., 2012; Costa, Losada, et al., 2021). Once the peroxidation chain commences, these compounds neutralize a limited number of free radicals that impede, postpone, or terminate the propagation stage by trapping lipid radicals. It is worth noting that excessive or diminished second-line antioxidant stores may result in uncontrollably high levels of oxidative stress. Furthermore, non-enzymatic antioxidants neutralize free radicals in four main ways: electron transfer-proton transfer (ETPT), sequential proton loss electron transfer (SPLET), single-electron transfer-proton transfer (SETPT), and transfer of hydrogen atoms to peroxy radicals (Costa, Losada, et al., 2021). Since some preventative and chain-breaking antioxidants can replenish chain-breaking antioxidants used up during the inhibitory reaction, they work in synergy. Citric acid, lecithin, ascorbic acid, and ascorbyl palmitate are a few examples (Costa, Losada, et al., 2021).

Consuming natural antioxidants or antioxidant-fortified foods can protect the brain from oxidative damage (Huang et al., 2014; Ataie et al., 2016). With the exacerbated oxidative insults and weakened antioxidant defence systems present in the brains of NDD patients, preventing OS and maintaining intracellular redox balance may be an effective way to slow the progression of age-related neurodegeneration (Huang et al., 2014). Furthermore, a variety of dietary antioxidants demonstrate neuroprotective properties in both *in vitro* and *in vivo* models of neuronal death (Ataie et al., 2016).

2.2.1. Glutathione

The reduced form of glutathione, or GSH; L-glutamyl-L-cysteinyl-glycine, is an indispensable component of the antioxidant system in the brain (Chen et al., 2022; Kinoshita et al., 2022). Glutathione is a powerful water-soluble antioxidant that plays a key role in preventing OS (Ho et al., 2022). Glutathione's strong negative redox potential combined with higher intracellular concentrations (up to 15 mM) results in a high reducing power (Chavan et al., 2005; Mancilla et al., 2015). This characteristic supports its strong antioxidant activity, its role as an enzyme

cofactor, and its intricate thiol exchange system, which hierarchically controls cell function (Chavan et al., 2005; Ho et al., 2022). Glutathione appears to be depleted throughout the body with each year, particularly in older people (Ho et al., 2022). Studies conducted on animals and *in vitro* have demonstrated that GSH depletion is a crucial factor in OS-induced neuronal death and is linked to neuronal loss in several NDDs, such as AD and PD. Therefore, glutathione depletion may be a viable therapeutic target for halting or reducing neurodegeneration (Singh et al., 2019; Chen, 2022).

Intracellular GSH levels are maintained via *de novo* and salvage synthesis pathways (Iskusnykh et al., 2022). The production of glutathione from its constituent amino acids occurs in two steps. γ -glutamylcysteine synthetase (γ -GCS) catalyses the first step, which amalgamates cysteine and glutamic acid, while GSH synthetase (GS) catalyses the next step, which involves the addition of glycine. γ -glutamylcysteine is the catalyser for the rate-limiting step in the *de novo* synthesis of GSH. Moreover, the synthesis process may be impacted by the availability of L-cysteine through the neutral amino acid transport system ASC, the reduction of cystine received through the cystine/glutamate exchanger, also referred to as system X_c⁻ (Han et al., 1997; Lv et al., 2019; Cheng et al., 2021), and glutathione's feedback competitive inhibition (Cheng et al., 2021). Interestingly, extracellular oxidation of cysteine to cystine reduces the availability of L-cysteine in OS (Han et al., 1997). During the detoxification of H₂O₂ or other organic hydroperoxides, the enzyme glutathione peroxidase (GPx) oxidises GSH to glutathione disulfide (GSSG). Glutathione reductase (GR) can convert the oxidised form, GSSG, back to GSH. The GST (glutathione S-transferase) converts GSH to nontoxic products, resulting in xenobiotic compound detoxification (Figure 2.1) (Iskusnykh et al., 2022).

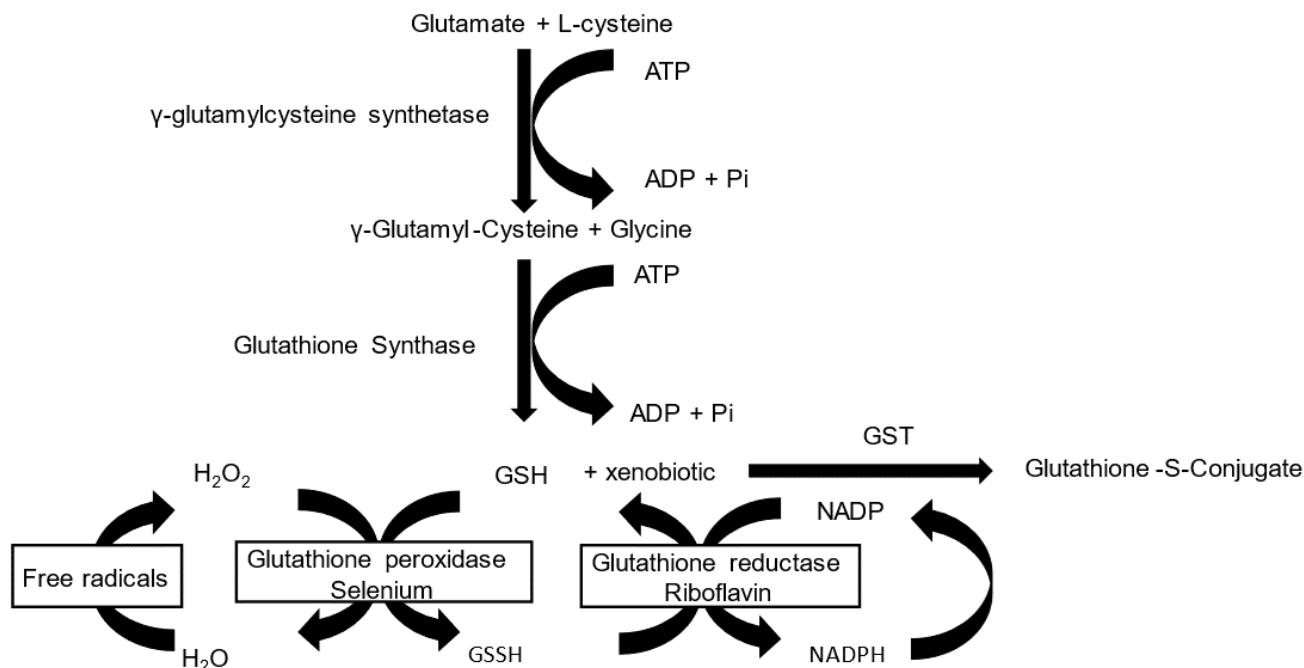


Figure 2.1: Glutathione formation and recycling.

Reduced glutathione (GSH) is produced by two mechanisms: de novo synthesis and GSSG recycling. De novo synthesis is a two-step reaction catalysed by glutamine-cysteine ligase and glutathione synthase. Glutathione reductase is an enzyme that catalyses the conversion of GSSG to GSH. The enzyme glutathione peroxidase converts H_2O_2 to water H_2O . Abbreviations: ATP = adenosine triphosphate, ADP = adenosine diphosphate, Pi = inorganic phosphate, H_2O = water, H_2O_2 = Hydrogen peroxide, NADP: nicotinamide adenine dinucleotide phosphate, NADPH = Reduced nicotinamide adenine dinucleotide phosphate, GST = glutathione S-transferase, GSSG = glutathione disulfide

2.2.2. Superoxide dismutases

Superoxide dismutases (SODs), which are members of the oxidoreductase family, are redox-active metalloenzymes that require O_2 to survive (Saxena et al., 2022). Superoxide dismutases, which are found in a variety of intracellular compartments as well as the extracellular space, are the first line of defence against illness or injury caused by ROS (Mohideen et al., 2022). Superoxide dismutases are enzymes that facilitate the conversion of superoxide anion ($O_2^{\cdot-}$) to H_2O_2 and O_2 . This reaction occurs primarily at the site of $O_2^{\cdot-}$ generation, a reaction that requires one proton per superoxide reacted but not externally reacted but no external reductant or energy from the cell (Day, 2009; Sheng et al., 2014), and is thus an important component of biological antioxidant defence (Winterbourn, 2020; Tretter et al., 2022).

Superoxide dismutases exist in three isoforms in mammals, depending on the metals in the active site. Two of these are copper/zinc SOD, or SOD1, which is a homodimer of 32 kDa found in the cytoplasm, and SOD3, a tetrameric glycoprotein of 135 kDa located in the outer mitochondrial space (Winterbourn, 2020; Rosa et al., 2021; Tretter et al., 2022). Copper is involved in catalysis, whereas zinc is involved in structure (Winterbourn, 2020). The third is an 88 kDa homotetramer of manganese superoxide dismutase (Mn-SOD), also referred to as SOD2, which is restricted to the inner mitochondrial space (Winterbourn, 2020; Rosa et al., 2021; Tretter et al., 2022). Superoxide dismutases all function in the same way. It is worth noting that SODs are highly enzymatic selective, however, Cu/Zn-SOD has peroxidase activity and reacts with H_2O_2 (Winterbourn, 2020).

When considering the endogenous antioxidant system involved in H_2O_2 production and removal, all the enzymes involved can be recognized as having a dual role that runs parallel, both physiological and pathological (Rosa et al., 2021). Superoxide dismutase activity may thus have a positive and negative effect (Winterbourn, 2020; Rosa et al., 2021). It can function as an antioxidant enzyme when its activity is synchronized with the thioredoxin (Trx)-dependent peroxiredoxin (Prx) enzymes, CAT, GPx, and/or both, which neutralize H_2O_2 accumulation by converting it to H_2O (Rosa et al., 2021). In this way, SODs reduce the harmful effects of superoxide and other free radicals that result from secondary reactions. It is also worth noting that SODs play an important role in preventing peroxynitrite formation and mitochondrial dysfunction by inhibiting the oxidative modification of nitric oxide (Mohideen et al., 2022). Secondly, SODs may function as a pro-oxidant due to the accumulation of H_2O_2 , which can result in an excess of ROS and cell toxicity (Winterbourn, 2020; Rosa et al., 2021). By preventing superoxide from acting as a reductant and being transformed into O_2 (as in the reduction of cytochrome c) or from generating an addition product (e.g., peroxynitrite), SODs increase the amount of H_2O_2 . If it prevents superoxide from acting as an oxidant, as iron-sulfur proteins do, the amount of H_2O_2 produced is reduced in half. How SODs interact with these activities might affect the amount and subsequent effects of H_2O_2 generated. If eliminating superoxide shifts an otherwise unfavourable balance, SODs can also increase the amount of H_2O_2 generated (Winterbourn, 2020). Superoxide dismutase is therefore important in the development of different medicinal formulations that are intended to treat a range of devastating disorders, including AD (Saxena et al., 2022). Research has demonstrated that overexpression of SOD-2 protects cognitive impairment in an AD animal model by reducing hippocampal superoxide (Massaad et al., 2009). Similarly, administering SOD mimics to aged mice for 6 months alleviated age-related decline in performance during fear

conditioning tasks and decreased LPO, deoxyribonucleic acid (DNA) oxidation, and ROS levels (Clausen et al., 2010). Another study has shown that supplementing with SOD-1 and adenosylmethionine synergistically reduced the worsening of AD-like symptoms induced by a B vitamin deficit in mice (Cavallaro et al., 2017). Antioxidant treatment, especially EUK-207, a SOD mimic, inhibited the progression of tau phosphorylation and, as a result, improved clinical symptoms in 3X-Tg-AD, an aggressive mouse model of AD (Clausen et al., 2012).

2.2.3. Catalase

Catalase (CAT), a haem-containing oxidoreductase enzyme, is a central antioxidant enzyme that, along with SODs and GPxs, serves as the primary defence against OS (Christiansen et al., 2004; Ali et al., 2022; Oboh et al., 2023). Under cellular conditions, CAT reduces the toxic effects of H₂O₂ by catalysing its decomposition into H₂O and O₂ (Christiansen et al., 2004; Ali et al., 2022). Catalase efficiently decomposes H₂O₂ without requiring any additional reducing equivalents, thus no energy from the cell is needed (Day, 2009). Catalases' haem groups are shielded by being buried in a non-polar pocket with narrow hydrophobic channels that help with H₂O₂ selectivity (Day, 2009; Nandi et al., 2019). It is noteworthy that CAT can oxidise short-chain alcohols to their corresponding aldehydes. Thus, it also possesses peroxidase activity (Oshino et al., 1973). Depletion of CAT leads to an increase in the level of H₂O₂ in cells, which causes extensive cell injury (Singh & Singh, 2019) and has been strongly associated with the pathophysiology of NDDs such as AD (Ali et al., 2022). However, overexpression of CAT in neural cells has been shown to protect against H₂O₂-induced toxicity (Mann et al., 1997). Therefore, the therapeutic principle of preventing free radical injury by CAT is emerging as a promising enzyme in the biotechnology and pharmaceutical industries (Ali et al., 2022).

2.3. Reactive oxygen species

Reactive oxygen species (ROS) are reactive molecules formed because of the incomplete oxidation of O₂ to produce H₂O (Galaup et al., 2022; Kumari et al., 2022). Most biomolecules tend to react thermodynamically with it, hence, O₂ itself may be considered a reactive species. Nevertheless, they are kinetically prevented by the oxygen triplet ground state (³O₂). This is not the case for singlet oxygen, a member of the family of ROS (Juan et al., 2021; Galaup et al., 2022). Two unpaired electrons in distinct molecular orbitals with parallel spins make up molecular oxygen (Juan et al., 2021). There are two types of ROS molecules: free radicals and non-radicals (Kumari et al., 2022; Yu et al., 2022). The term "free radical" (O₂^{·-} and hydroxyl radical [[·]OH]) refers to an atom, molecule, or ion that has an unpaired valence electron in its outer orbital, while

non-radical species like singlet oxygen and H_2O_2 are oxidative agents that can also turn into radicals (Kumari et al., 2022; Mongirdienė et al., 2022; Yun et al., 2022). ROS, especially H_2O_2 , $\cdot OH$, and $O_2^{\cdot -}$, appear to be the most toxic factor in the biological system when they are produced in excess and exhibit higher pathogenically responses (Waki et al., 2012; Agapouda et al., 2020; Kumari et al., 2022).

The most important characteristics of ROS are their short life span and extreme reactivity (Juan et al., 2021; Yun et al., 2022); however, their chemical reactivity varies and is dependent on their specific targets (Sies, 2020; Yun et al., 2022). Reactive oxygen species are produced endogenously and exogenously, indicating that they are influenced by internal and external sources (Park et al., 2015; Kumari et al., 2022). Radiation or drug exposure can result in exogenous ROS (Park et al., 2015). Endogenous ROS are formed as a result of reduction-oxidation (redox) reactions that occur naturally in the cell (Sies & Jones, 2020). Typical cell metabolic activities include enzymatic production by peroxidases, nicotinamide adenine dinucleotide phosphate oxidases (NOXs) (which catalyse the process known as a respiratory burst), cyclooxygenases, transition metal-mediated pathways (the Fenton reaction), and so on (Bartosz, 2003; Villalpando-Rodriguez & Gibson, 2021). But the majority of endogenous cellular ROS are produced by mitochondria as byproducts of oxidative phosphorylation that takes place in the electron transport chain (ETC), which accounts for 1 % to 3 % of total electron generation and where 85 % of O_2 is metabolised (Agapouda et al., 2020; Galaup et al., 2022). Two high-production sites in the ETC, complex I and III, are responsible for directly releasing ROS into the intermembranous space and the cristae lumen (Agapouda et al., 2020; Sies & Jones, 2020). Mitochondrial proteins' cysteine residues oxidise because the mitochondrial ETC generates ROS, altering the function of the proteins (Villalpando-Rodriguez & Gibson, 2021). It is worth noting that thiol-based protein modification is the primary mechanism by which ROS mediate their biological effects (Sies & Jones, 2020).

One interesting approach to understanding the aetiology of NDDs is to track the formation of ROS (Galaup et al., 2022). However, because of their short half-life, determining the level of free radicals *in vivo* is difficult (Gonzalez-Pinto et al., 2012), hence OS can be investigated indirectly by measuring antioxidant defence systems (Gonzalez-Pinto et al., 2012; Khovarnagh & Seyedalipour, 2021).

Reactive oxygen species participate in many physiological processes, including the regulation of intracellular transcription factor activation (cytokines, insulin, growth factors, activator protein 1 [AP-1], nuclear factor kappa light chain enhancer of activated B cells [NF- κ B], and many more), despite their toxic effects at high concentrations. This makes ROS important in human physiology (Zhang et al., 2022; Liu et al., 2022). Furthermore, by controlling the release of apoptotic components like cytochrome c, ROS may induce apoptosis (Park et al., 2015; Lampinen et al., 2022; Zhang et al., 2022).

Biological antioxidants and endogenous antioxidant enzymes like GPx tightly regulate ROS generation under physiological conditions to maintain the balance between ROS production and their elimination (Huang et al., 2014; Agapouda et al., 2020; Sies & Jones, 2020; Zhang et al., 2022). If the organism's strong antioxidant system fails to suppress ROS production, it can lead to problems. This is because a high concentration of ROS has the potential to initiate a chain reaction involving free radicals, which can damage macromolecules (e.g., lipids and proteins) (Jin & Wang, 2019; Huang et al., 2020).

Reactive oxygen species can impair mitochondrial efficiency and interfere with the flow of hydrogen (H^+) ions, which generates the mitochondrial membrane potential in exchange for the ATP molecule when their levels increase beyond a certain threshold. Thus, ROS can interfere with the ETC, resulting in an imbalance in energy homeostasis and cell death (Liu et al., 2022). Therefore, in a normal physiological state, the cell maintains a controlled level of ROS to maintain homeostasis (Zhang et al., 2022). In some cases, such as the prevention or treatment of NDDs, it is necessary to change one's lifestyle by supplementing with exogenous antioxidants that either limit the formation of ROS or break the chain of free radical reactions (Jin & Wang, 2019).

Most treatments have tried antioxidants, which includes using coenzyme Q, vitamins C and E, N-acetylcysteine, and compounds derived from CAT, to address ROS. Apart from adopting healthy lifestyle habits like exercise and diet, the antioxidant treatment additionally incorporates plant polyphenolic compounds like resveratrol, curcumin, and quercetin to improve brain function (Kalani et al., 2023). Rooibos herbal tea and its pharmacologically active constituents have the potential to positively modulate many processes observed in the pathogenesis of NDDs, as are other polyphenol-rich dietary products. However, there is a dearth of research on nervous system cells directly and in pre-clinical *in vivo* models of neurodegeneration, highlighting the need for more investigation (Pyrzanowska, 2022).

2.4. Hydrogen peroxide

One of the most studied ROS is H_2O_2 , which is also one of the most important ROS in cell metabolism (Agapouda et al., 2020; Kumari et al., 2022; Rosini & Pollegioni, 2022). Hydrogen peroxide, a strong oxidant can be generated either indirectly through superoxide dismutation or directly through O_2 two-electron reduction via an oxidation-reduction reaction (Kumari et al., 2022; Martemucci et al., 2022). Most important is that enzyme reactions produce the majority of H_2O_2 (Martemucci et al., 2022).

In microsomes, peroxisomes, and mitochondria, the presence of oxidases (flavin-containing enzymes) such as uricase or urate oxidase (Uox), glucose oxidase (Gox), and D-amino acid oxidase (DAAO) may result in the direct synthesis of H_2O_2 via the transfer of two electrons to O_2 (Martemucci et al., 2022; Rosini & Pollegioni, 2022). In the brain, the most common sources of H_2O_2 are spontaneous superoxide dismutations catalysed by the enzyme SOD and monoamine oxidase (MAO) activity (Liu et al., 2022).

Hydrogen peroxide is liposoluble and can therefore easily cross membranes and react with other species (Fragoso-Morales et al., 2021; Martemucci et al., 2022; Rosini & Pollegioni, 2022). In addition, H_2O_2 can directly react with cellular macromolecules, resulting in protein and lipid damage as well as cell death (Jin & Wang, 2019; Huang et al., 2014; Park et al., 2015; Rosini & Pollegioni, 2022). Most importantly, H_2O_2 can indirectly mediate oxidative damage after non-enzymatic reactions such as the Haber-Weiss and Fenton reactions. The Fenton reaction can be triggered by metal ions, which catalyse the conversion of H_2O_2 to a highly reactive $\cdot OH$ (Rosini & Pollegioni, 2022).

In the iron-dependent Fenton reaction, the highly reactive $\cdot OH$ of amyloid beta peptide ($A\beta$) during the growth and enlargement of $A\beta$ plaques in AD brains can promote H_2O_2 production (Yang et al., 2016; Martemucci et al., 2022). The excessive accumulation of inflammatory cytokines, (including tumour necrosis factor-alpha [$TNF\alpha$], interleukin 1 beta [$IL-1\beta$], and $IL-6$), can be induced by the produced $\cdot OH$. This, in turn, can attract microglia to encircle the active plaques (Yang et al., 2016; Richard & Mousa, 2022). Furthermore, the microglia in the surrounding area produce more H_2O_2 , which contributes to neuronal death (Yang et al., 2016). Furthermore, it should be noted that ROS and H_2O_2 can both independently trigger inflammatory pathways, which

can lead to neuronal dysfunction (Kalani et al., 2023). Consequently, maintaining the intracellular H_2O_2 equilibrium and eliminating $A\beta$ s are linked to AD treatment (Yang et al., 2016).

Hydrogen peroxide is well known to function as a secondary messenger and to cause cysteine-centred oxidative post-translational modifications (oxPTMs), which impact cellular processes and trigger downstream signaling cascades (Jin & Wang, 2019; Lee et al., 2021), therefore, antioxidants tightly regulate the intracellular concentration of H_2O_2 in peripheral tissue targets in the low nanomolar range (approximately 1-100 nM) (Sies & Jones, 2020). Hydrogen peroxide is essential for many normal and aberrant neural cell functions, but its concentration in the brains of living things including people and mice is rarely reported, and it is not known how the concentration of H_2O_2 changes in diseases like AD (Yang et al., 2016).

Cellular H_2O_2 modifies thiol groups in cysteine residues in the central nervous system (CNS) into various sulfated acid groups such as sulfenic acid (-SOH), sulfinic acid (-SO₂H), and sulphonic acid (-SO₃H), with increasing oxidation as H_2O_2 exposure increases (Lee et al., 2021). Several studies have shown that H_2O_2 exposure can activate caspases, a unique family of cysteine proteases: particularly caspase-3 (Park et al., 2015; Jin & Wang, 2019), a key component of executing programmed cell death (apoptosis) (Jin & Wang, 2019; Huang et al., 2020). It is also worth noting that H_2O_2 is commonly used *in vitro* to induce OS (Park et al., 2015; Huang et al., 2020) and inhibits cell growth in a variety of cell lines, including SH-SY5Y cells (Park et al., 2015).

2.5. Neurodegeneration

Neurodegeneration is a complicated multifactorial CNS condition characterised by the gradual loss of neuronal cell structure and function, as well as possible neuronal death, resulting in behavioural and mental impairment (Angelova et al., 2021; Crispi & Filosa, 2021; Icer et al., 2021; Dong & Yong, 2022; Pyrzanowska, 2022). Diseases with neurodegeneration as a distinguishing feature are collectively referred to as NDDs, which include AD and PD (Lamprey et al., 2022). Because neurodegeneration and disease progression are largely incurable, it underscores the enormous challenges in biology and medicine in identifying the underlying molecular signaling pathways that drive neuronal cell death and developing effective therapeutics for NDDs (Moreno-García et al., 2021; Dong & Yong, 2022). Several factors, including OS, excitotoxicity, protein aggregation, vascular dysfunction, and neuroinflammation, are known to contribute to neurodegeneration, and these processes culminate in the death of certain neuronal populations, resulting in cognitive and/or motor impairments (Kwakowsky et al., 2023). However, OS acts as

a bridge between current academic hypotheses (excitotoxicity hypothesis, protein aggregation hypothesis, inflammation hypothesis, metal ions hypothesis, and OS hypothesis) and neurodegeneration mechanisms associated with NDDs such as AD (Bai, Guo, Ye, et al., 2022). Thus, increased OS associated with brain aging has been identified as a hallmark of neurodegeneration (Moreno-García et al., 2021).

Synapse malfunction, neural network dysfunction, and the accumulation of physiochemically modified synaptic protein variations in the brain have all been linked to neurodegeneration (Lamprey et al., 2022). Many NDDs begin as asymptomatic accumulations of certain proteins in different brain regions, which subsequently spread to other brain regions (Davis et al., 2018). Several proteins have been linked to NDDs; however, there are currently no effective treatments to mitigate the negative impact these proteins play in the aetiology and development of NDDs (Cetin et al., 2022).

The word "synaptopathy," which is gaining popularity, describes early pathophysiological events that precede neuronal death and degeneration as well as abnormalities in synaptic structure and function that are a major predictor of NDDs (Imbriani et al., 2022). In AD patients, there may also be a direct causal relationship between OS and synaptic dysfunction, which contributes to early disease mechanisms before any symptoms of A β or Tau pathology (Tönnies & Trushina, 2017). Furthermore, several studies have shown that OS causes phosphorylation of tau protein in neuronal cells *in vitro* (Zhu et al., 2005; Su et al., 2010; Naini & Yanicostas, 2015). Beside the accumulation of phosphorylated tau protein within neurons, another prominent feature of AD pathogenesis is the A β toxicity. It is also interesting to note that there are numerous indications that when A β is introduced as an oligomer into lipid bilayer, induces OS (Butterfield et al., 2013). The discovery of biomarkers or therapeutic targets for NDDs provides valuable insight into neurodegenerative pathophysiology (Behl et al., 2021). Furthermore, several oxidative markers (including LPO and protein oxidation) are elevated in brain regions of patients with neurodegeneration (Moreno-García et al., 2021). This highlights the importance of understanding the primary role of OS in neurodegeneration pathophysiology (Behl et al., 2021).

To assure future treatment success, the focus has recently switched toward treatments that target multiple aspects of neurodegeneration, and the targeting of individual neural networks offers numerous potential therapeutic targets. Furthermore, instead of treating NDDs as the disease progresses, pharmaceutical designs increasingly prioritize prevention strategies before the onset

of the symptoms. By considering the dysfunction of brain networks in NDDs, the aetiology of these incurable conditions might be better understood. This will provide a new understanding of the basic processes underlying brain circuit remodelling and function. Targeting neuronal dysfunction early in these diseases may also present novel and enhanced therapeutic and modulatory options (Kwakowsky et al., 2023).

2.6. Oxidative stress

The overproduction of ROS, particularly $O_2^{\cdot-}$, and H_2O_2 , causes OS, as does the overburdening of intracellular antioxidants (Huang et al., 2014; Jin & Wang, 2019; Agapouda et al., 2020; Huang et al., 2020; Bai, Guo, Ye, et al., 2022). Through aging, OS has been identified as a cause of many diseases, including NDDs such as AD and PD (Lee et al., 2021; Taurone et al., 2022). Antioxidants are essential in cellular defence against OS and are effective in disease prevention, treatment, and management of these devastating age-related conditions (Erukainure, Matsabisa, et al., 2020).

Aging is associated with a decrease in antioxidant defences and a persistent production of ROS. These factors can cause mitochondrial dysfunction and cell damage, which are involved in the processes of age-related disorders such as NDDs (Agapouda et al., 2020; Zhang et al., 2021; Bai, Guo, Ye, et al., 2022; Chen, 2022). It has been documented that some ETC enzyme loss or failure leads to a decrease in mitochondrial membrane potential and the release of cytochrome c, hence impairing mitochondrial function (Bai, Guo, Ye, et al., 2022; Chen, 2022). The accumulation of misfolded proteins specific to NDDs is amplified by neuronal mitochondrial dysfunction caused by increased ROS production (Zhang et al., 2021). In AD, these include the $A\beta$ peptide and hyperphosphorylated tau protein (Zhang et al., 2021; Chen, 2022), as well as α -synuclein in the pathological progression of PD (Levin et al., 2011; Haque et al., 2022).

2.6.1. Oxidative stress and the pathogenesis of Alzheimer's disease

The brain miscompartmentalization and dyshomeostasis of transition metals, as well as their increased combination with $A\beta$ to form metal- $A\beta$ species like iron (Fe) (II/III) - $A\beta$ and copper (Cu) (I/II)- $A\beta$, are correlated with increased OS in AD patients' brains. More evidence supports the role of OS in the activation and overexpression of related oxidases (reduced nicotinamide adenine dinucleotide phosphate [NADPH] enzymes; MAO-B). This eventually aggravates neuronal cell apoptosis and promotes AD pathogenesis by increasing ROS production and eventually inducing OS and mitochondrial dysfunction. However, these metal ions are required as cofactors for

several catalytic enzymes, including antioxidant enzymes and neurotransmission, which involves the synthesis of neurotransmitters, myelination, and synaptic plasticity (Kim & Lee, 2021; Bai, Guo, Ye, et al., 2022). Consequently, a metal chelation strategy has been suggested as a treatment for AD to reduce the risk of neurodegeneration brought on by these metals. Nevertheless, focusing only on metal ions will not be sufficient to fully cure the condition (Kim & Lee, 2021).

2.6.2. Oxidative stress and cellular pathologies in Parkinson's disease

The most compelling theory contends that neuronal mitochondrial dysfunction causes OS, which can promote α -synuclein toxicity in PD (Levin et al., 2011; Haque et al., 2022; Iranshahy et al., 2022). Small oligomeric α -synuclein aggregates, as opposed to microscopically detectable α -synuclein deposits, are toxic particle species that play an important role in cell death (Levin et al., 2011). Oxidative stress in dopamine neurons can cause LPO of PUFAs, which can result in the formation of nitrotyrosine, 4-hydroxynonenal (4HNE), and acrolein, which can promote the formation of secondary β -sheets and oligomers (Haque et al., 2022; Iranshahy et al., 2022). Metal ions have been shown to induce conformational changes and aggregation of α -synuclein *in vitro* (Uversky et al., 2001). By causing a shift in the ratio of ferrous to ferric iron towards ferric oxidation, OS affects the α -synuclein's ability to aggregate which result into ferroptosis (Levin et al., 2011). It is worth noting that in recent years, the involvement of ferroptosis in PD has become a research hotspot, owing to evidence of aberrant iron deposition and lipid peroxidation damage in PD patients' brains (Lu et al., 2023).

It has been demonstrated that there is a positive correlation between α -synuclein and mitochondrial dysfunction. This is because mitochondrial dysfunction is associated with several defects in the mitochondria, such as fragmentation of the mitochondria, inhibition of complex-I (the first enzyme in the mitochondrial ETC) and mitophagy activity, and disruption of the mitochondrial membrane potential (Haque et al., 2022; Iranshahy et al., 2022). Therefore, the correlation between mitochondrial components and α -synuclein aggregation may be a good target for developing of a novel treatment approach to treat PD (Haque et al., 2022).

Neuronal cells require a constant supply of energy and are thus extremely sensitive to changes in mitochondrial function (Głuchowska et al., 2021; Tefera et al., 2021). Therefore, neurons typically require continuous glucose availability from the blood, as stored energy in the brain is low (Tefera et al., 2021). Several studies have revealed that increased OS correlates with

decreased brain glucose uptake due to downregulation of brain GLUTs (Erukainure et al., 2019; Erukainure, et al., 2020b). It is important to note that glucose is vital in OS defence because it is metabolised via the pentose phosphate pathway to produce NADPH, which is required to keep GSH in its antioxidant-reduced state (Tefera et al., 2021). However, brain glucose hypometabolism is a hallmark feature of AD and PD progression, indicating an insufficient supply of blood-derived glucose to meet energy requirements (Hascup et al., 2022; Olofinisan et al., 2022). Brain glucose hypometabolism is associated with increased ROS generation and, ultimately, OS, contributing to neuronal dysfunction and metabolic imbalance (Olofinisan et al., 2022).

2.7. Protein damage

Carbohydrates, lipids, proteins, and nucleic acids are constantly exposed to oxidants (Kehm et al., 2021). Proteins are a prime target for oxidizing agents because of their high rate of interaction with different oxidants and their abundance in cells, plasma, and tissues (Al Smadi et al., 2021; Demirci-Çekiç et al., 2022). Highly reactive ROS, such as $\cdot\text{OH}$, which is produced by radiolysis of H_2O_2 or by the Fenton reaction (Al Smadi et al., 2021), can modify the amino acid residues of proteins (including lysine, arginine, proline, and threonine) and protein backbones, resulting in the formation of many oxidative products, including protein oxidation adducts (Akagawa, 2021; Al Smadi et al., 2021; Demirci-Çekiç et al., 2022). Reversible changes are inherent in physiological processes and serve as a signalling cascade; yet non-reversible changes may contribute to the causes of age-related diseases (Kehm et al., 2021). Indeed, protein modification and subsequent protein accumulation have been observed in tissue proteins during aging and in the development of various diseases, such as NDDs (Akagawa, 2021; Kehm et al., 2021; Demirci-Çekiç et al., 2022).

There is some evidence that protein modification affects protein stability and activity, as it may enhance proteolysis by inhibiting enzymatic action (Al Smadi et al., 2021; Demirci-Çekiç et al., 2022). However, the severity of such modification is determined by the ratio of altered molecules, the type of oxidant, and the protein structure (Al Smadi et al., 2021). Thiol-based protein modification is the primary mechanism through which ROS exert their biological effects (Sies & Jones, 2020).

Protein carbonylation is the process by which reactive carbonyl moieties (such as aldehyde, ketone, and lactam) are incorporated into proteins, and it is thought to be an important marker of

oxidative protein degradation (Akagawa, 2021). Thus, protein carbonyls are the most widely used biomarkers for measuring oxidative protein damage (Al Smadi et al., 2021; Kehm et al., 2021; Demirci-Çekiç et al., 2022) due to their relatively early formation during OS, higher stability in comparison to other oxidative products, and ease of measurement (Kehm et al., 2021).

2.8. Lipid damage

Lipids play a crucial role in the formation of intracellular membrane-bounded organelles such as the Golgi apparatus, and endoplasmic reticulum (ER) (Demirci-Çekiç et al., 2022; Jain & Zoncu, 2022). Cell membranes comprise a phospholipid bilayer with embedded proteins that protect the cell and function as a barrier to specific molecules (Demirci-Çekiç et al., 2022; Nasri et al., 2022). Membrane fluidity, which is heavily dependent on the dynamics of PUFAs acyl chain with reactive allylic hydrogens from the cellular membrane, can regulate membrane function by influencing integral membrane protein arrangements, membrane permeability, and transmembrane transport activity (Asghari & Aghdam, 2010; Lopes et al., 2021; Demirci-Çekiç et al., 2022). Due to the nature of unsaturated bonds, PUFAs are easily oxidised, resulting in a variety of metabolites as well as ROS (Lopes et al., 2021; Demirci-Çekiç et al., 2022).

Peroxidation is the process by which oxidants such as free radicals attack PUFAs with more than two cis-double bonds and oxidise their esters. It is worth noting that the major PUFAs that are important targets of LPO are linoleic, docosahexaenoic acid, and arachidonic acids (Angelova et al., 2021; Demirci-Çekiç et al., 2022). The brain has the second highest lipid content after adipose tissue, indicating an elevated level of lipid turnover in this organ (Angelova et al., 2021).

The overall process of LPO in biological systems is divided into three stages: initiation, propagation, and termination. The abstraction of allylic hydrogen from PUFA by a free radical initiates LPO, resulting in the formation of the carbon-centred lipid radical (L^{\cdot}) (Jaganjac et al., 2021; Demirci-Çekiç et al., 2022), which eventually transforms into a more stable CD structure (Demirci-Çekiç et al., 2022). During the propagation phase, the CDs react with O_2 to form a highly reactive L^{\cdot} , which abstracts hydrogen from another lipid molecule, resulting in the formation of a new L^{\cdot} (this is referred to as a "chain reaction") and a lipid peroxy radicals (LOO^{\cdot}) (Jaganjac et al., 2021; Demirci-Çekiç et al., 2022). Non-radical compounds such as cytotoxic and genotoxic aldehydes, as well as their lipid hydroperoxide precursors, are generated during the termination stage. The accumulation of these molecules is dangerous because they form a Schiff base with amino groups, inactivate certain enzymes, and interact with the thiol group (Demirci-Çekiç et al.,

2022). Chain-breaking antioxidants, such as polyphenols, can inhibit the free radical chain mechanism of LPO (Jaganjac et al., 2021; Demirci-Çekiç et al., 2022; Farhoosh, 2022). Chain-breaking antioxidants are known to modulate LPO kinetics by reacting with LOO^\bullet and converting them into oxidatively stable products (Figure 2.2) (Demirci-Çekiç et al., 2022; Farhoosh, 2022).

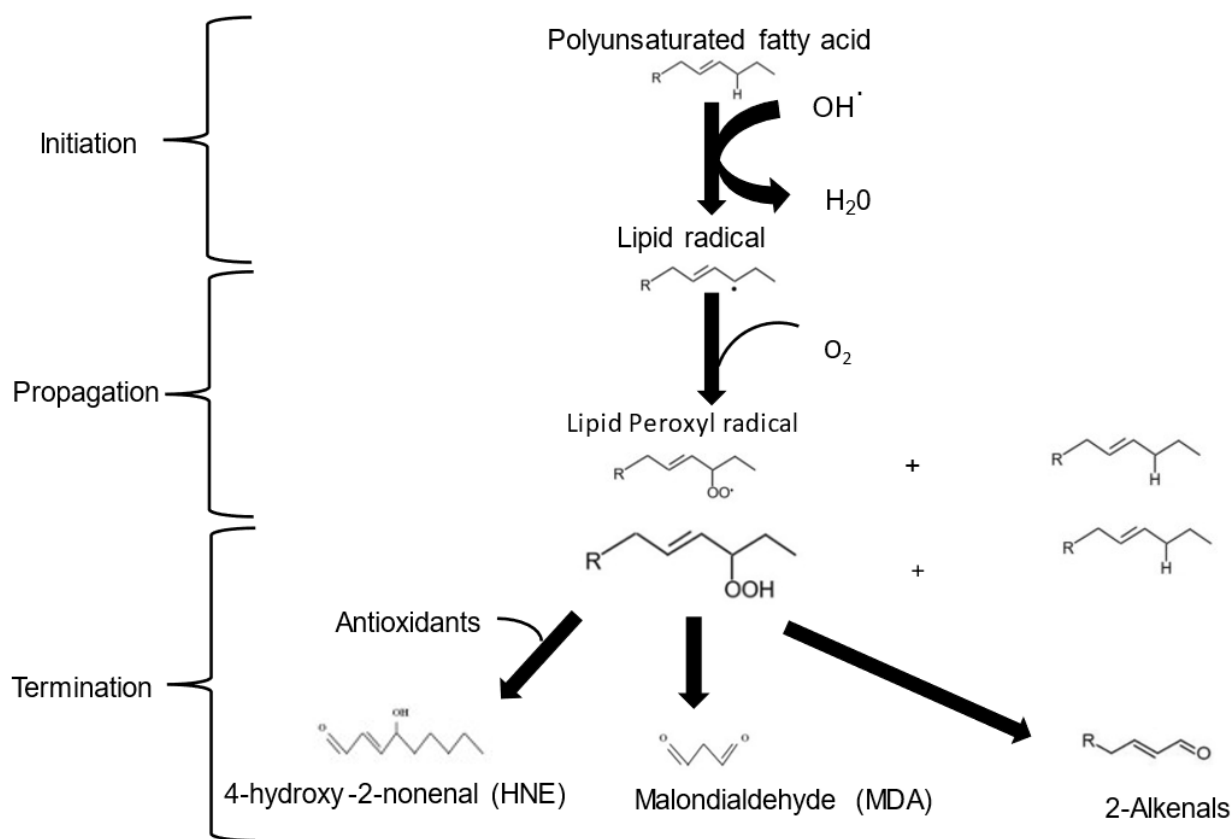


Figure 2.2: The mechanism of lipid peroxidation

Lipid peroxidation occurs via two distinct mechanisms: non-enzymatic and enzymatic (Angelova et al., 2021; Jaganjac et al., 2021; Demirci-Çekiç et al., 2022). Non-enzymatic lipid peroxidation is initiated by the Fenton and Haber-Weiss reaction in the presence of a suitable transition metal or by the above-mentioned random effects of ROS (Demirci-Çekiç et al., 2022). The most important peroxidases are phospholipase A2, cyclooxygenase (COX), lipoxygenase (LOX), and cytochrome p450 (CYP450). Hydrolysis is catalysed by COX, LOX, and CYP450, resulting in lipid endoperoxides, lipid hydroperoxides, and epoxyeicosatrienoic acids, respectively (Angelova et al., 2021; Jaganjac et al., 2021; Demirci-Çekiç et al., 2022).

Lipid peroxidation products are constantly produced. Thus, LPO is a major biomarker for OS (Angelova et al., 2021; Al Smadi et al., 2021; Kehm et al., 2021; Demirci-Çekiç et al., 2022). However, LPO is also important in cell physiology, such as phospholipase activation (lipolytic enzymes that hydrolyse phospholipids such as PUFAs at specific ester bonds yielding free fatty acids and lysophospholipids) (Balboa & Balsinde, 2021). Glutathione peroxidase can halt LPO and reduce peroxides to alcohol using GSH as a substrate (Angelova et al., 2021). More importantly, when the generation of LPO products exceeds the intracellular antioxidant capacity, the LPO products (specifically MDA and 4HNE) can cause damage to proteins and DNA, resulting in necrosis, apoptosis, or ferroptosis (Angelova et al., 2021; Balboa & Balsinde, 2021; Kehm et al., 2021; Demirci-Çekiç et al., 2022). Thus, LPO is a hallmark of most NDDs, including AD and PD (Angelova et al., 2021; Demirci-Çekiç et al., 2022), and is potentially one of the most promising targets for the diagnosis and development of novel therapeutic strategies for these disorders (Angelova et al., 2021; Kehm et al., 2021; Demirci-Çekiç et al., 2022). Several studies have shown that LPO alters membrane permeability, transportation, and fluidity (Oliveira et al., 2021; Demirci-Çekiç et al., 2022), as well as disrupting extracellular ion balance (Demirci-Çekiç et al., 2022). Although studies have been conducted on the relationship between LPO and antioxidant mode of action, more research is needed (Cháfer-Pericás, 2021). Unravelling the cell death and LPO pathways remains a top priority for therapeutic development (Behl et al., 2021).

2.9. Cell death

2.9.1. Apoptosis

Apoptosis, also known as programmed cell death, (Erekat, 2022) is a highly regulated, energy-dependent cellular process that involves the genetically programmed removal of damaged, redundant, or irreparable cells (Erekat, 2017; Fakhri et al., 2022; Erekat, 2022). On the molecular level, apoptotic cell death has been divided into three stages: initiation, execution, and termination (Krueger et al., 2001). It is also worth noting that the primary molecular components of apoptosis in neurons are the same as those in non-neuronal cell types, and apoptosis has been observed in numerous NDDs (Erekat, 2018; Erekat, 2022). Furthermore, several approaches for

recognising apoptotic cells and analysing biochemical, molecular, and morphological alterations that result in cell death have been established (Oancea et al., 2006; Cetin et al., 2022). Cell shrinkage, chromatin condensation (which increases the number of distinct spaces within the nucleus), DNA fragmentation, membrane blebbing, and the formation of apoptotic bodies, which contain fragmented chromatin and organelles and are phagocytosed by surrounding cells without any associated inflammation, are all visible under a microscope (Erekat, 2017; Erekat, 2018; Erekat, 2022). Whereas the most well-known biochemical hallmarks of apoptosis are an array of internucleosomal DNA fragmentation and activated caspases (Oancea et al., 2006; Erekat, 2018; Schmidt et al., 2021). In addition, caspase activation can be examined using a variety of approaches, including colorimetric assays (Carrasco et al., 2003; Oancea et al., 2006). These advanced assays are often employed as validation tests after a more robust method of determining cell death has been performed (Cetin et al., 2022).

Several studies have indicated that apoptosis plays an important role in both healthy and pathological conditions. In physiological conditions, apoptosis maintains homeostasis by eliminating aged cells to conserve cell populations in tissues during development (Erekat, 2022; Fakhri et al., 2022; Heydarnezhad Asl et al., 2022). Furthermore, neuronal death is necessary for the formation of appropriate circuitry during nervous system growth and maturation (Erekat, 2018; Erekat, 2022). Apoptosis, on the other hand, occurs pathologically as a defensive mechanism, such as during an immune response or when cells are damaged by harmful chemicals such as H₂O₂ (Erekat, 2022; Fakhri et al., 2022; Heydarnezhad Asl et al., 2022). It is worth emphasising that excessive apoptosis may be a hallmark of NDDs, which are characterised by the selective loss of vulnerable populations of neurons, resulting in motor symptoms and cognitive impairment (Carrasco et al., 2003; Erekat, 2018; Schmidt et al., 2021; Erekat, 2022; Heydarnezhad Asl et al., 2022). However, the processes that lead to neuronal death, as well as the exact mechanism of neuronal death, remain unknown (Luchi et al., 2021; Moujalled et al., 2021). Therefore, much more research is needed, both fundamental research in neurodegenerative experimental animals and clinical trials, to provide a precise understanding of the role of apoptosis in brain diseases, so that this knowledge can be used to generate truly transformative advances in their treatment (Moujalled et al., 2021).

Caspases, a class of enzymes noted for their cysteine protease activity, cause neuronal death, culminating in the cytomorphological changes associated with programmed cell death, also known as apoptosis (Carrasco et al., 2003; Erekat, 2017; Mahrus et al., 2008; Araya et al., 2021;

Heydarnezhad Asl et al., 2022). In caspase active sites, catalytic cysteine residues cleave substrates on the carboxy side of aspartate residues, resulting in cell dissociation during apoptosis (Carrasco et al., 2003; Araya et al., 2021; Erekat, 2022). The caspase recognition site is determined by three to four amino acids, which is followed by the cleavage site (aspartic acid residue) (Carrasco et al., 2003; Araya et al., 2021). Caspases are constitutively expressed in normal cells as inactive zymogens known as pro-caspases, which have three domains: the N-terminus prodomain, which contains either a caspase recruitment domain (CARD) or a death effector domain (DED) (a cytoplasmic domain containing approximately 80 amino acid subunits (Makoni & Nichols, 2021) Pro-caspases lack protease activity and are triggered by proteolytic cleavage between the p20 and p10 subunits or between the p20 subunit and the prodomain in response to apoptotic stimuli (Carrasco et al., 2003; Oancea et al., 2006; Erekat, 2017; Makoni & Nichols, 2021; Erekat, 2022).

Caspases are classified according to their structure or function. Inflammatory caspases (caspases 1, 4, 5, 11, and 12) have a role in immune responses to microbial infections by mediating the proteolytic activation of inflammatory cytokines. Caspases that are the principal causes of apoptotic cell death are classed as (1) initiator caspases such as caspases 2, 8, 9, and 10 and (2) executioner or effector caspases such as caspases 3, 6, and 7 (Oancea et al., 2006; Erekat, 2017; Erekat, 2018; Makoni & Nichols, 2021; Erekat, 2022; Heydarnezhad Asl et al., 2022). Caspase-6, on the other hand, can function as an executioner caspase as well as an initiator and inflammatory caspase (Makoni & Nichols, 2021). Caspase-3 is the most essential executioner caspase in apoptosis, and it is activated via both intrinsic (caspase 9) and extrinsic (caspase 8) pathways (Carrasco et al., 2003; Erekat, 2017; Erekat, 2022) and thereby coordinates the damage of cellular integrity or structures (Erekat, 2017).

There are two well-described pathways that regulate apoptosis induction: the extrinsic pathway and the intrinsic pathway, and both eventually lead to a single pathway - the execution phase of apoptosis (Chen et al., 2002; Putcha et al., 2002; Erekat, 2022). Cytochrome c (Cyt c) initiates the intrinsic route of apoptosis when apoptotic stimuli induce its release from the mitochondria into the cytoplasm. Thus, mitochondrial integrity and activity are essential for the intrinsic pathway (Kermer et al., 2004; Erekat, 2018; Erekat, 2022). Apoptosis can be induced by intracellular damage, which causes BID, a BH3-only protein, to be cleaved, resulting in the release of Cyt c. Cytochrome c acts as a cofactor in the development of a multimeric apoptotic protease activating factor 1 (Apaf-1)/cyt c complex. In the presence of ATP or deoxyadenosine triphosphate (dATP),

this complex recruit procaspase 9, leading to the development of an apoptosome. Procaspase-9 is activated by proteolysis within the apoptosome. Caspase-9 dissociates from this complex after activation, activating executioner caspases 3, 6, and 7 (Putcha et al., 2002; Erekat, 2018; Araya et al., 2021; Erekat, 2022). This pathway is strictly regulated by a group of B-cell lymphoma (Bcl-2) family proteins with either proapoptotic (e.g., Bcl-2-like protein 4 [BAX]) or antiapoptotic (e.g., Bcl-2-l homologous antagonist [BAK]) characteristics. While Bcl-2 inhibits mitochondrial cytochrome c release, Bax enhances it following activation. Thus, regulated protein-protein interactions activate the intrinsic pathway within the cell (Oancea et al., 2006; Erekat, 2018; Erekat, 2022).

The extrinsic pathway, on the other hand, activates caspases via cell-surface death receptors such as tumour necrosis factor (TNF)/nerve growth factor (NGF), which are regulated by the expression levels of triggering ligands (e.g., FAS ligand). (Kermer et al., 2004; Erekat, 2018; Erekat, 2022). When Fas interacts with its ligand (FasL), a death-inducing signalling complex (DISC) forms, which recruits procaspase-8 (Putcha et al., 2002; Erekat, 2018; Erekat, 2022). When procaspase-8 is autoproteolytically cleaved, it forms active caspase-8 (Putcha et al., 2002), which possesses DED at its N-terminus and can either directly or indirectly induce caspase-3, 6, and 7 activations, which mediate the execution phase of apoptosis. Thus, an upstream caspase usually proteolytically activates the executioner caspases (Putcha et al., 2002; Kermer et al., 2004; Araya et al., 2021; Erekat, 2022; Erekat, 2022). Studies have revealed that caspase-8 is activated in neurons following numerous death stimuli, including OS (Chen et al., 2002; Kermer et al., 2004).

Caspases 3, 6, and 7 can be activated by either the intrinsic or extrinsic pathways, resulting in the cleavage of several proteins that regulate diverse cellular functions during apoptosis. These executioner caspases cleave proteins that can halt cell cycle progression, signal transduction, and inactivating apoptosis protein inhibitors via Bcl-2 family protein cleavage, facilitating nuclear and cytoskeletal disassembly, and recognizing dying cells for phagocytosis and subsequent clearance, all of which contribute to the distinct morphological changes associated with apoptosis (Oancea et al., 2006; Erekat, 2018). Therefore, using antioxidants to inhibit caspase activation in the context of cell death stimuli like OS, may reduce or even halt caspase-dependent cell death.

2.9.2. Necrosis

Necrosis is the most common type of cell death in neurodegeneration (Padanilam, 2003; Saleem, 2021). Necrosis is an unprogrammed cell death process that occurs when cells are subjected to

extreme stress because of a disruption in normal cell function (Artal-Sanz & Tavernarakis, 2005). Necrosis in neurons is triggered by significant ATP depletion (Datta et al., 2020; Saleem, 2021). Early events in necrosis include an increase in intracellular calcium (Ca^{2+}) concentration and the generation of ROS, which culminate in events that cause irreversible cell injury (Moujalled et al., 2021).

Excessive poly (ADP-ribose) polymerase 1 (PARP1) activation toward poly(ADP-ribosylation) (PARylation), which catalyses its formation from donor nicotinamide adenine dinucleotide (NAD^+), is a major cause of necrotic cell death. As a result, excessive activation of PARP-1 depletes the NAD^+ pool, eventually leading to ATP depletion (Li et al., 2021). Most importantly, ATP aids in the preservation of neuronal resting potential via the Na^+/K^+ ATPase (NKA) pump (an active transporter), which promotes the maintenance of an ion gradient across membranes and the uptake and release of neurotransmitters in the cell (Johar et al., 2014; Datta et al., 2020). Thus, this function is critical for both cell death and cell survival (Suhail, 2010).

Failure of NKA activity has been linked to the development of several NDDs including AD and PD (Johar et al., 2014). When NKA activity fails to maintain Na^+ and K^+ gradients between cells' internal and extracellular compartments, Na^+ accumulates within the cell, resulting in cellular oedema. Blebs form within the cell because of the continuous formation of oedema. These blebs fuse, and cellular debris accumulates within the huge, fused blebs. Finally, blebs rupture and their contents are released into the surrounding extracellular space, triggering inflammatory responses (Datta et al., 2020).

In neurons, inappropriate modulation of NKA activity leads to altered neuronal excitability and compromised activity of Na^+ -coupled transporters such as $\text{Na}^+/\text{Ca}^{2+}$ exchangers, leading in inappropriate regulation of the cytosolic free Ca^{2+} concentration (Shrivastava et al., 2020). When Ca^{2+} accumulates in cells, mitochondrial activity diminishes, leading in an increase in ROS and a reduction in ATP levels, resulting in necrotic cell death (Li et al., 2021). The morphology of necrosis is marked by widespread swelling of cell membranes, which is typically accompanied by severe vacuolation of the cytoplasm, mitochondrial swelling, and plasma membrane rupture. Cellular contents are thereby released into the intracellular space, triggering inflammatory responses (Artal-Sanz & Tavernarakis, 2005). The release of LDH is commonly used as a marker for necrotic cell death. When cells are lethally injured, the activity of LDH in the incubation medium can be used to assess loss of membrane integrity (Kendig & Tarloff, 2007).

2.10. Human neuroblastoma SH-SY5Y cell line

The neuroblastoma cell line SH-SY5Y, derived from the SK-N-SH cell subline (established from a bone marrow biopsy of a 4-year-old female child), is the most common immortalized human cell line used to obtain neuronal culture *in vitro*. It is widely used in neurotoxicity studies and *in vitro* models of NDDs, including AD and PD even in the undifferentiated state and these cultures contain both floating and adherent cells (D'Aloia et al., 2024; Hoffmann et al., 2023; Lopez-Suarez et al., 2022; Strother et al., 2021). Adherent cells have two distinct phenotypes: neuroblast-like 'N' cells that express neuron-specific biochemical markers like dopamine- β -hydroxylase and non-neuronal substrate adhesive cells, and epithelial-like 'S' cells that lack neuronal markers (Strother et al., 2021). Undifferentiated SH-SY5Y cells proliferate indefinitely, grow in clusters, and can form clumps of spherical cells on top of one another, non-polarized cell bodies with few, shorter processes, and bigger cell bodies (Loghen et al., 2023; Sahin et al., 2021). To overcome the challenges associated with having a heterogeneous cell population, SH-SY5Y cells can be encouraged to differentiate into neuron-like cells (Lopez-Suarez et al., 2022; Strother et al., 2021). When SH-SY5Y cells are differentiated with differentiation-inducing agents such as retinoic acid, they exit the cell cycle and shift to a morphology like that of primary neurons, with smaller cell bodies, which are frequently polarized, present extended neurites, and excitable membranes with distinct properties (such as potassium conductance) as compared to undifferentiated cells (Lopez-Suarez et al., 2022).

Because SH-SY5Y cells are human-derived, they express various human-specific proteins and protein isoforms that are not naturally seen in primary rodent cell cultures (Hoffmann et al., 2023). The SH-SY5Y cells are simple to handle and culture (Strother et al., 2021; Bell & Zempel, 2022), which is useful for both biochemical manipulation and analysis (Strother et al., 2021). The SH-SY5Y cell line is usually cultured in DMEM or a mixture of DMEM/F12 growth mediums (Loghen et al., 2023). Usually, the medium is supplemented with 10% fetal bovine serum as it encourages cell proliferation and contains of growth factors which support survival and proliferation (Loghen et al., 2023; Strother et al., 2021). To encourage the differentiation of cell lines, serum concentrations are usually reduced to between 1 % and 5 %, inhibiting proliferation and supporting differentiation (Strother et al., 2021).

The undifferentiated SH-SY5Y cell line is a good model for measuring neurotoxicity-related endpoints such as cell viability, mitochondrial function, and OS. Furthermore, neuroblastic cells

provide an excellent model for investigating potential carcinogenicity using endpoints such as cell proliferation and migration. Even if a compound may impact these endpoints in SH-SY5Y cells, this does not prove that it is neurotoxic; rather, it demonstrates that it is cytotoxic in this model (Lopez-Suarez et al., 2022).

3. CHAPTER THREE: METHODOLOGY

In this study, unfermented and fermented Rooibos water and ethanol extracts were investigated for their potential neuroprotective effects on SH-SH5Y cells using an *in vitro* technique. The materials and procedures used are described in detail below.

3.1. Materials

Chemicals: L-ascorbic acid, 2,2-azino-di-3-ethylbenzthiazoline sulfonate (ABTS), Folin Ciocalteu's phenol reagent, gallic acid, trifluoroacetic acid (TCA), Trolox (6-hydroxy-2,5,7,8-tetramethylchroman-2-carboxylic acid), methanol, 2-thiobarbituric acid (TBA), glacial acetic acid, and 2,4,6-tri[2-pyridyl]-s-triazine (TPTZ), sodium carbonate (Na_2CO_3) iron chloride hexahydrate ($\text{FeCl}_3 \cdot 6\text{H}_2\text{O}$), potassium persulfate. Sodium acetate, malondialdehyde (MDA), ethanol, and hydrochloric (HCl), cyclohexane, phosphoric acid (H_3PO_4), butylated hydroxytoluene (BHT), 2,4-dinitrophenylhydrazine (DNPH), sodium hydroxide (NaOH), butanol, ethyl acetate, and guanidine hydrochloride, Dimethyl sulfoxide (DMSO), trypan blue dye, H_2O_2 were purchased from Merck (Johannesburg, South Africa). Chloroform (Kimix Chemical and Lab Supplies, South Africa).

Thermo Fisher (Johannesburg, ZA) provided bovine serum albumin (BSA), fetal bovine serum (FBS), M-PER™ Mammalian protein extraction reagent, Dulbecco's Modified Eagles Medium (DMEM), Halt™ phosphatase, penicillin-streptomycin, Halt™ protease inhibitor, Pierce™ bicinchoninic acid (BCA) Protein Assay kit, CAT colorimetric activity kit, and SOD colorimetric activity kits. Dulbecco's Phosphate-Buffered Saline (PBS) was supplied by WhiteSci (Cape Town, ZA). Trypsin EDTA (Lonza Group Ltd., Verviers, Belgium). The Caspase -8, -9, -3/7 protease activity kits and the GSH-Glo™ Glutathione assay kit were provided by Promega (Madison, USA). The LDH cytotoxicity detection kit was provided by Roche (Germany).

Consumables: Flasks, 23 cm cell scrapers, 96-well plates, 2 mL microcentrifuge tubes, 50 mL conical tubes, and 15 mL centrifuge tubes were all provided by WhiteSci (Cape Town, South Africa). The SH-SY5Y cell lines were obtained from the ATCC (American Type Culture Collection). Lasec (Cape Town, ZA) supplied powder-free nitrile examination gloves and Reagent reservoirs (50 mL).

Plants: Freshly dried and ground unfermented and fermented Rooibos plant materials with the batch numbers: U15/03/JJ and PO6/59/11, respectively were obtained commercially (Rooibos Ltd, Clanwilliam) (Figure 3.1).

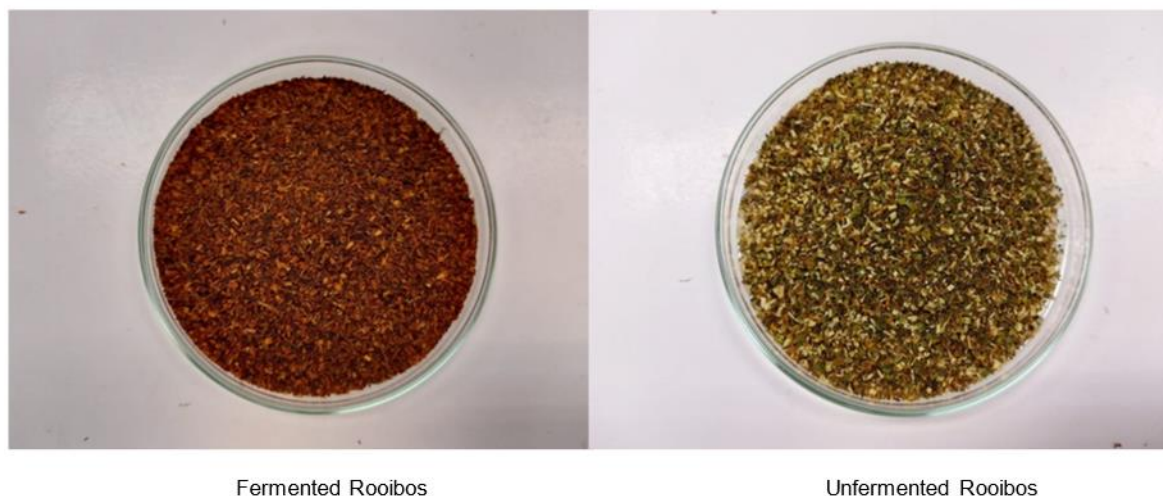


Figure 3.1: The two forms of processed Rooibos plant materials (fermented and unfermented Rooibos) used in this study.

The fermentation/chemical oxidation process results in the distinctive reddish-brown colour of fermented Rooibos, whilst unfermented Rooibos plant material is immediately dried after harvest and thus retains its green colour.

3.2. Preparation of the Rooibos extracts

Commercially available fermented (Batch number: PO6/59/11) and unfermented (Batch number: U15/03/JJ) Rooibos plant material was obtained from Rooibos Ltd (Clanwilliam, South Africa). Aqueous extracts were prepared by adding freshly boiled water (200 mL) to fermented and unfermented Rooibos plant material (2.5 g, the equivalent of a teabag). According to Piek *et al.*, the mixture was stirred and steeped for 10 minutes (Piek *et al.*, 2019). The extracts were filtered through Munktell 3HW 320 mm filter paper and freeze-dried in stainless steel trays with extract solution using a Virtis Genesis 25EL freeze dryer (SP Scientific, Stone Ridge, NY, USA). First, the solutions were frozen for 90 minutes on pre-cooled -45 °C shelves. The shelf temperature was raised to -30 °C at a rate of 1.3 °C/minute for primary drying (below the collapse temperature). During primary drying, the shelf temperature was adjusted to 30 °C for 24 hours, while the chamber pressure was kept at 75 mTorr (for ice sublimation). During primary drying, the average product temperature ranged from -37 to -38 °C. The end of primary drying was signalled by a rise in product temperature above the shelf temperature and a corresponding reduction in dew point to a constant value. Secondary drying (evaporation of water in the amorphous phase) was accomplished by increasing the shelf temperature from 0.1 °C/minute to 0 °C. The temperature was maintained at 0 °C for 30 minutes, followed by another heating phase at 0.1 °C/minute to 10

°C. Temperature and pressure were kept at 10 °C and 75 mTorr for 280 minutes. The powders that resulted were weighed and stored at -80 °C until use.

For the ethanolic extraction, 50 g of the fermented and unfermented Rooibos plant materials were steeped overnight in 80 % ethanol (250 mL). A rotary evaporator (Buch, Postfach, Switzerland) was used to evaporate the ethanol extracts at 40 °C. The resulting residues were freeze-dried as explained above, and the powders were weighed and stored at -80 °C until further use.

3.3. Extracts screening

The stock concentration of unfermented and fermented Rooibos, aqueous, and ethanolic extracts [2 mg/mL] were reconstituted by dissolving 50 mg of freeze-dried samples in 25 mL autoclaved distilled water (dH₂O). From the stock, Rooibos extracts were prepared by dilution with dH₂O in the following concentration range: 15, 30, 60, 125, 250, and 500 µg/mL.

3.4. Total Polyphenol determination of Rooibos extracts

The TPC of different Rooibos extracts was determined by the Folin-Ciocalteu spectrophotometric method (Singleton et al., 1999). The previously modifications described procedure by (Ajuwon et al., 2013) was used, and all experiments were performed in triplicate (Figure 3.2) and (Figure 3.3). In brief, 25 µL of various Rooibos extract concentrations of 15, 30, 60, 125, 250, and 500 µg/mL were transferred into appropriate wells in a 96-well clear plate, followed by 125 µL of 0.2 N Folin-Ciocalteu reagent. The mixtures were mixed with 100 µL of 7.5 % w/v sodium carbonate (Na₂CO₃) solution to create basic conditions (pH 10) for the redox reagent (Folin-Ciocalteu reagent) to reluctantly oxidise the phenolic compounds present in sample matrices. Following a two-hour incubation at room temperature (in a dark environment), absorbance at 765 nm was measured with a multiplate reader (SpectraMax i3X, San Jose, CA, USA). The gallic acid standard curve had six values ranging from 0 to 500 mg/L. The data were represented in gallic acid equivalent (GAE) units per litre (mg/L). Recipes for the buffers in Appendix 1.

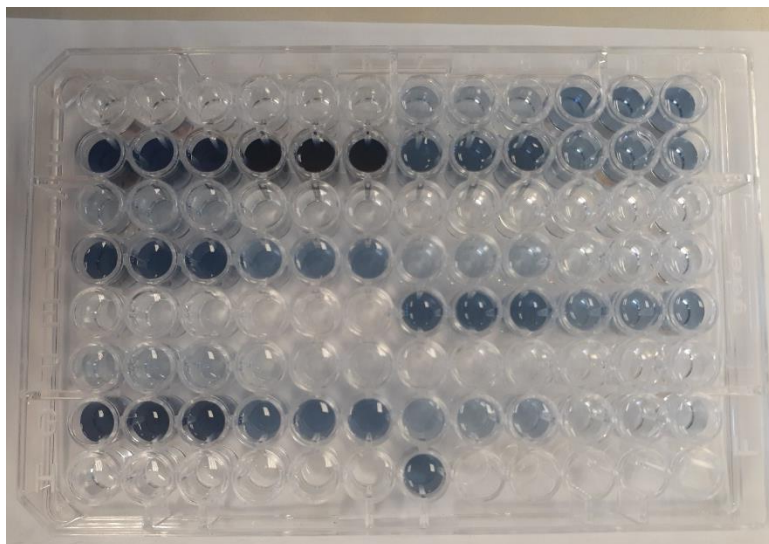


Figure 3.2: The 96-well microplate used in the total polyphenol content determination.

The reaction between the Folin-Ciocalteu reagent and phenolic compounds in each Rooibos extract yields a blue colour complex, and the intensity of the blue colour is proportional to the quantity of polyphenol compounds present.

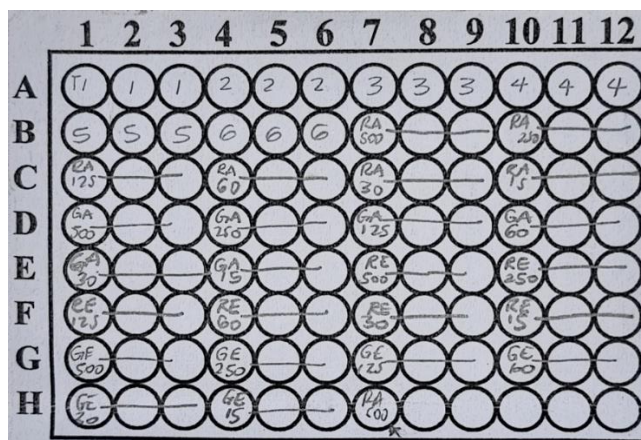


Figure 3.3: Plate layout for the total polyphenol content assay

Numbers 1-6 are standards. Rooibos extracts key: RA = fermented aqueous, GA = unfermented aqueous, RE = fermented ethanol, GE = unfermented ethanol

3.5. Ferric ion reducing antioxidant power (FRAP) Assay

The FRAP assay is based on a sample's antioxidant ability to convert a colourless ferric tripyridyl triazine complex to a blue ferrous complex at low pH, which is measured spectrophotometrically at 593 nm (Figure 3.4) and (Figure 3.5) (Benzie & Strain, 1996). The FRAP experiment was performed with a few modifications as described by Hussein et al. (2022). In brief, 10 µL of

fermented and unfermented Rooibos extracts at concentrations of 15, 30, 60, 125, 250, and 500 $\mu\text{g}/\text{mL}$ or ascorbic acid as standard were mixed with 300 μL of FRAP reagent (10:1:1, v/v/v of acetate buffer at 300 mM, pH 3.6, tripyridyl triazine (TPTZ) at 10 mM in 40 mM HCl, and $\text{FeCl}_3 \cdot 6\text{H}_2\text{O}$ at 20 mM) in a 96-well clear plate and incubated for 30 min at room temperature. After incubation, the plate was read at 593 nm using a multiplate reader (SpectraMax i3X, San Jose, CA, USA). The results were expressed as micromole ascorbic acid equivalent per litre (μmol AAE)/L. Recipes for the buffers in Appendix 2.

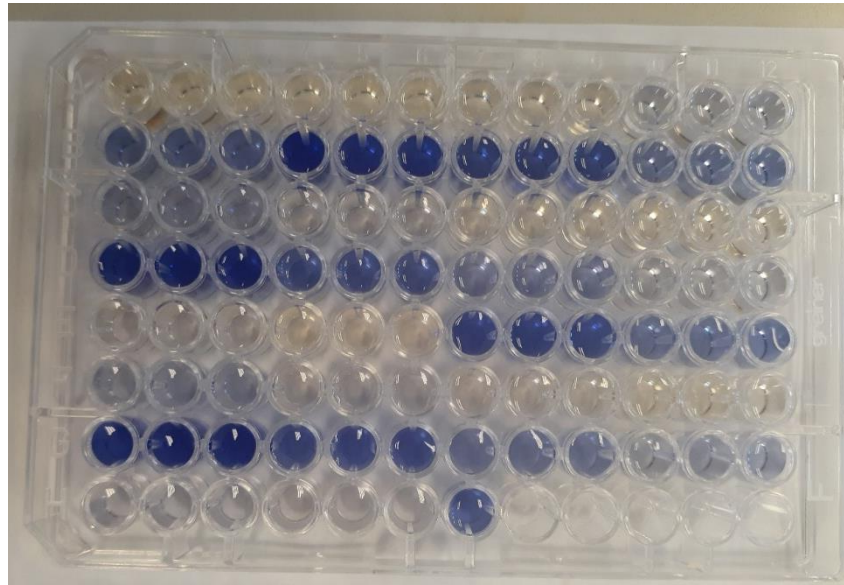


Figure 3.4: The 96-well microplate used in the ferric reducing antioxidant potential assay

The ferric-reducing antioxidant power assay makes use of an electron transfer reaction in which a ferric salt is utilised as an oxidant. In this assay, the yellow colour test solution changes to green and blue depending on the reducing power of Rooibos extracts.

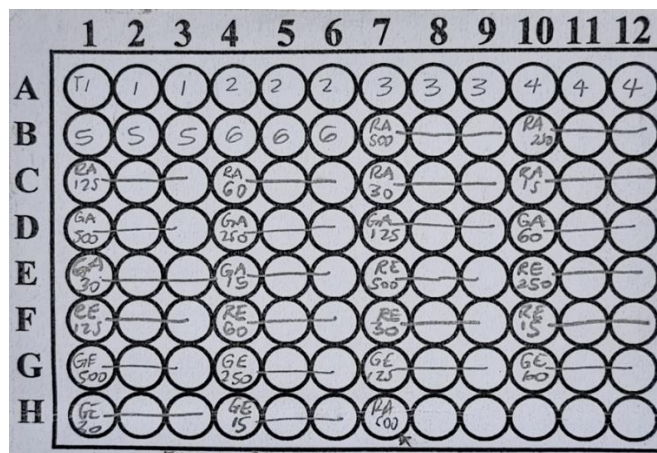


Figure 3.5: Plate layout for the ferric reducing antioxidant potential assay

Numbers 1-6 are standards. Rooibos extracts key: RA = fermented aqueous, GA = unfermented aqueous, RE = fermented ethanol, GE = unfermented ethanol

3.6. Trolox Equivalent Antioxidant Capacity (TEAC) Assay

The Trolox equivalent antioxidant capacity of both Rooibos extracts was measured using the method described by Re et al. (1999). The assay is based on the direct production of the blue/green 2,3'-azinobi (3-ethylbenzothiazoline-6-sulfonic acid) (ABTS^{•+}) radical cation and potassium persulfate. The reaction has a significant absorption band at 734 nm (Figure 3.6) and (Figure 3.7). When the ABTS^{•+} radical, an unstable form that may absorb light at different wavelengths, accept an electron from the antioxidant in the sample, the blue/green chromophore fades to pale blue or colourless, indicating ABTS, stable form regeneration.

In brief, the stock solutions were prepared using the previously described methods (Ajuwon et al., 2013; Hussein et al., 2022) and contained freshly prepared 7 mM ABTS and 140 mM of potassium persulfate (K₂S₂O₈) solution to 5 mL solution to 5mL of ABTS solution. The two solutions were mixed and allowed to react for 24 hours in the dark at room temperature before use. The working solution was diluted 1:20 with dH₂O, obtaining an absorbance of 1.50 at 734 nm. In brief, each sample or standard (25 µL) was mixed in a 96-well clear plate with a 275 µL ABTS^{•+} solution. After 30 minutes of incubation at room temperature, the plate was read at a wavelength of 734 nm in a plate reader (SpectraMax i3X, San Jose, CA, USA). Trolox (6-hydroxy-2,5,7,8-tetramethylchroman-2-carboxylic acid) was used as an antioxidant standard, with concentrations ranging between 0 and 500 µM. The results were expressed in micromole Trolox equivalents per litre (µM TE)/L. Recipes for the buffers in Appendix 3.

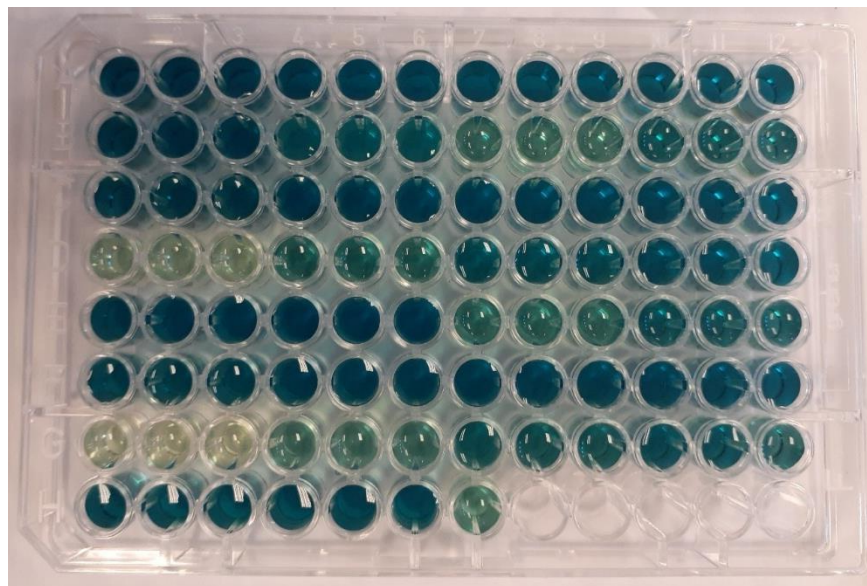


Figure 3.6: The 96-well microplate used in the trolox equivalent antioxidant capacity assay

Although the TEAC assay is usually classified as an electron transfer (ET)-based method, the hydrogen atom transfer (HAT) mechanism also applies. The extent of discoloration of the blue-green colour, measured as a decrease in absorbance, is determined by the duration of the reaction, the inherent antioxidant activity, and the concentration of each Rooibos extract.

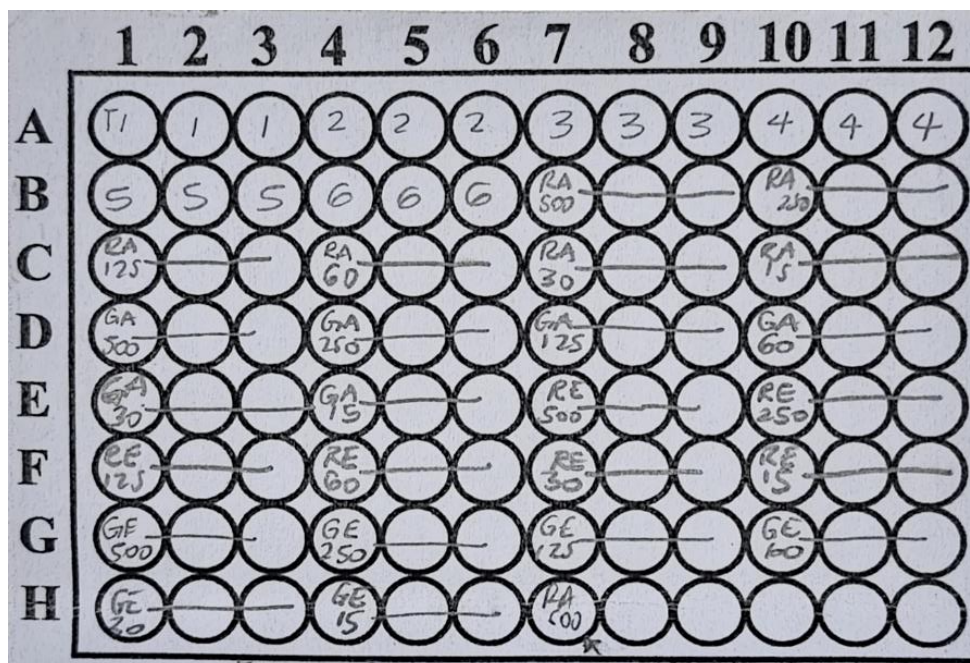


Figure 3.7: Plate layout for the trolox equivalent antioxidant capacity assay.

Numbers 1-6 are standards. Rooibos extracts key: RA = fermented aqueous, GA = unfermented aqueous, RE = fermented ethanol, GE = unfermented ethanol

3.7. High-performance liquid chromatography analysis of Rooibos extracts.

The stock concentration of 2 mg/mL for each extract was centrifuged at 4000 rpm (Eppendorf centrifuge 5810/5810: Rotor diameter: 18 cm) for 5 minutes. Using an adapted method described by Bramati et al. (2002), chromatographic separation was performed on an Agilent Technology 1200 series HPLC system. The HPLC system (which contained a G1315C diode array) was equipped with a multiple wavelength detector (a G1311A quaternary pump, a G1329A autosampler, and a G1322A degasser) with wavelengths set at 287 nm for aspalathin and 360 nm for the other Rooibos components. For separation, a 5 m YMC-Pack Pro C18 (i.d.) column was used. Water (A) with 300 µL/L trifluoroacetic acid and methanol (B) with 300 µL/L trifluoroacetic acid were used as mobile phases. The mobile phases were water (A) with 300 µL/L trifluoroacetic acid and methanol (B) with 300 µL/L trifluoroacetic acid. The gradient elution began at 80 % A and 20 % B, then changed to 20 % A and 80 % B after 5 minutes, and then returned to 80 % A and 20 % B after 25 minutes and back to 80% A after 28 minutes. The column temperature was set to 23°C, the overall run time was 5 minutes, and the flow rate was 1 mL/min. The injection volume was set at 20 µL. The contents of the Rooibos extracts were quantified by comparing the retention time and/or peak area to standards. Due to a lack of HPLC availability, a single run and injection were completed. To ensure analytical consistency and reliability, Rooibos extracts undergo assessment in the laboratory on a regular basis using standardised protocols. This involves utilising sample preparation techniques which promote consistency and minimise variability. As part of our quality control procedures, Periodic assessments on the performance of HPLC equipment and analytical methods are also done. As a result, a single run and injection are deemed sufficient for this study as per laboratory manager recommendation.

3.8. Cell culture and maintenance

The ATCC supplied human neuroblastoma SH-SY5Y cell lines, which were cultured in DMEM supplemented with 10 % FBS and 1 % penicillin-streptomycin. At 37 °C in a humidified 5 % CO₂ atmosphere, the cells were grown in 75 cm³ culture flasks. After 3 to 4 days of incubation, the cells were harvested for subculturing or cryopreserving for long-term storage when they attained a culturing density of 80-100 % confluence. The Faculty of Health and Wellness Sciences Human Research Ethics Committee (CPUT/HWS-REC 2022/H11) has approved the use of these cells for medical and scientific research at Cape Peninsula University of Technology (Appendix 17).

3.8.1. Trypan blue dye exclusion assay

The trypan blue stain assay, which was developed about a century ago, is the most extensively used approach for estimating the number of living cells (Kamiloglu et al., 2020; Nowak et al., 2018; da Cruz et al., 2022). This technique assumes that healthy, living cells have intact cell membranes that resist staining by trypan blue, whereas dead, damaged cells take up the stain (Figure 3.8) (Kamiloglu et al., 2020; da Cruz et al., 2022; Feles et al., 2022). Trypan blue stain can thus be used to assess the integrity of cellular membranes (Nowak et al., 2018; da Cruz et al., 2022).

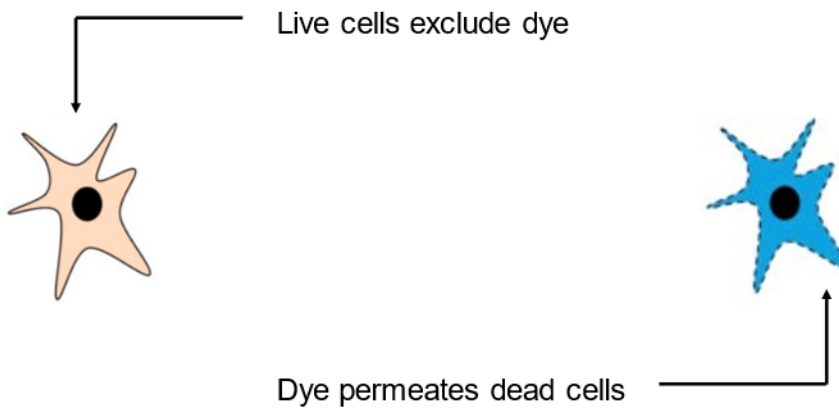


Figure 3.8: Schematic representation of dead cells stained with trypan blue.

In this experiment, 50 μL of well mixed cell suspension was added to an equal volume of 0.3 % trypan blue solution (Sigma Aldrich) in a 2 mL clean Eppendorf tube and the mixture was allowed to stain for 2 min at room temperature in the dark. After staining a clean cover slip was placed on the improved Neubauer haemocytometer, which was then loaded with 10 μL of cell solution and immediately examined at low magnification. In cell counting, only living, unstained cells (with intact membranes) were used. The total number of cells counted per mL was determined using the formula (Equation 1).

$$\text{Total cells/mL} = \frac{(\text{Total cells counted} \times \text{Dilution factor} \times 10,000\text{cells/mL})}{\text{Number of squares counted}}$$

Equation 1: Formula for haemocytometer cell counting.

After counting the cells, they were diluted to a concentration (20,000 cells/well and each well takes 200 μ L of cell suspension) that enabled easy preparation for the subsequent experiments.

3.8.2. Hydrogen peroxide preparation

Hydrogen peroxide (H_2O_2), an azure-blue covalently bonded liquid (Halliwell et al., 2000), is thought to have the most influence on cell fate since it can move rapidly through membranes (Agapouda et al., 2020). It is also worth noting that H_2O_2 is water-miscible (Halliwell et al., 2000). To prepare a 1000 μ M H_2O_2 stock solution, 5 μ L of concentrated H_2O_2 (30 % w/w in H_2O) was diluted with 49.995 mL of dH_2O and stored at 4 $^{\circ}$ C. The H_2O_2 concentrations (50, 100, 150, 200, 400, 600, 800, and 1000 μ M) (prepared by diluting the stock solution with DMEM) were used for optimisation.

3.8.3. Determination of optimal concentrations of H_2O_2 using Methylthiazol tetrazolium dye reduction (MTT) cell viability assay

SH-SY5Y cells treated with different concentrations of H_2O_2 was assessed using the colorimetric [3, (4, 5-dimethylthiazol-2-yl)-2, 5-diphenyl tetrazolium bromide] (MTT) assay. This assay is used to determine cell viability as a measure of mitochondrial activity (Kamiloglu et al., 2020; da Cruz et al., 2022). The principle of the MTT assay is based on the ability of metabolically active/viable cells to convert the yellow water-soluble MTT tetrazolium salt to its purple insoluble formazan product (Figure 3.9). This reaction requires the activity of two mitochondrial enzymes, succinate dehydrogenase and NAD(P)H-dependent cellular oxidoreductase. The needle-like formazan crystal is spectrophotometrically (600 nm) measured after dissolving in DMSO. The intensity of the formazan colour determines the number of metabolically active/viable cells.

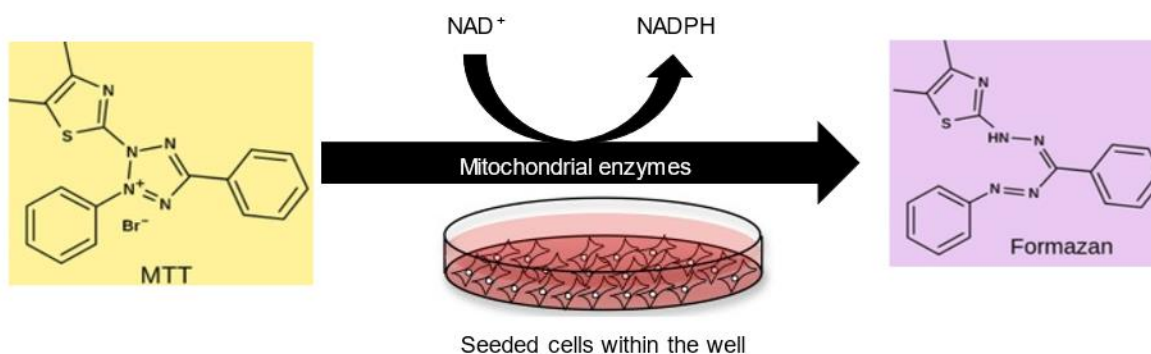


Figure 3.9: 3-(4,5-Dimethylthiazol-2-yl)-2,5-diphenyl-2H-tetrazolium bromide (MTT) assay principle.

The yellow MTT solution was removed, and the formazan solvent dimethyl sulfoxide (DMSO) was added, resulting in a purple colour.

In brief, cells were planted in a 96-well microtiter plate at a density of 2.0×10^4 cells per well and grown for 24 hours to promote attachment. Following cell attachment, cells were treated in triplicate for 1, 2, 3, and 24 hours to a range of H_2O_2 concentrations (50, 100, 150, 400, and 1000 μM) to induce OS. The control cells were incubated in DMEM. With a few adjustments, the approach described by Docrat et al (2018) was used to determine cell viability. 20 μL of the MTT salt solution (5 mg in 1 mL of 0.1 M PBS) was dispensed into the cell wells, followed by 100 μL of DMEM, and the plate was incubated for 3 hours at 37 $^\circ\text{C}$ with 5 % CO_2 . After incubation, the supernatants were aspirated and DMSO (100 μL /well) was added before incubating at 37 $^\circ\text{C}$ with 5 % CO_2 for 30 minutes. A multiplate reader (SpectraMax i3X, San Jose, CA, USA) was used to measure the optical density (OD) at 570 nm and 670 nm as a reference. The data is presented as a percentage of cell viability ($n=3$), and the optimal concentrations for H_2O_2 were calculated using the approximately 50% inhibition concentration and used in all subsequent assays. Using this formula (

Equation 2) cell viability was calculated as a percentage.

$$\% \text{ Cell viability} = (\text{individual OD treated cells} \div \text{average OD control cells}) \times 100$$

Equation 2: Formula for cell viability

3.8.4. Rooibos concentration screening

The MTT assay was used to determine cytotoxicity in SH-SY5Y cells following exposure to Rooibos extracts. Cells were seeded at a density of 2.0×10^4 cells per well in a 96-well microtiter plate and cultured for 24 hours before being treated with Rooibos extracts [0 to 500 $\mu\text{g}/\text{mL}$] for 2 and 24 hours, respectively. The cytoprotective effects and possible mechanism of Rooibos extracts on H_2O_2 -induced cytotoxicity in SH-SY5Y cells were investigated using different Rooibos treatment dosages, as indicated in table 3.1. The extract's final concentrations were prepared by diluting the stock [2mg/mL] with DMEM. Cells were pre-treated with 15, 30, 60, 125, 250, and 500 $\mu\text{g}/\text{mL}$ unfermented Rooibos extracts and fermented Rooibos extracts for 2 hours and 24 hours, respectively, before being exposed to the optimal H_2O_2 concentrations for 3 hours, as established in Section 3.8.3. above. The negative control cells received only DMEM, whereas the positive control cells received H_2O_2 . While 150 μM H_2O_2 for 3 hours was chosen as the optimal dosage, low, medium, and high concentrations of Rooibos extracts were chosen to be 60, 125, and 250 $\mu\text{g}/\text{mL}$, respectively. This model was used for subsequent assays.

Table 3.1: Treatment groups used in the investigation of neuroprotective effects of Rooibos extracts on H_2O_2 -induced cytotoxicity in SH-SY5Y cells.

Group	Unfermented Rooibos		Fermented Rooibos	
	Aqueous	Ethanol	Aqueous	Ethanol
1	Control (untreated cell)	Control (untreated cell)	Control (untreated cell)	Control (untreated cell)
2	H_2O_2 only (150 μM)	H_2O_2 only (150 μM)	H_2O_2 only (150 μM)	H_2O_2 only (150 μM)
3	15 $\mu\text{g}/\text{mL}$ + 150 μM H_2O_2	15 $\mu\text{g}/\text{mL}$ + 150 μM H_2O_2	15 $\mu\text{g}/\text{mL}$ + 150 μM H_2O_2	15 $\mu\text{g}/\text{mL}$ + 150 μM H_2O_2
4	30 $\mu\text{g}/\text{mL}$ + 150 μM H_2O_2	30 $\mu\text{g}/\text{mL}$ + 150 μM H_2O_2	30 $\mu\text{g}/\text{mL}$ + 150 μM H_2O_2	30 $\mu\text{g}/\text{mL}$ + 150 μM H_2O_2
5	60 $\mu\text{g}/\text{mL}$ + 150 μM H_2O_2	60 $\mu\text{g}/\text{mL}$ + 150 μM H_2O_2	60 $\mu\text{g}/\text{mL}$ + 150 μM H_2O_2	60 $\mu\text{g}/\text{mL}$ + 150 μM H_2O_2
6	125 $\mu\text{g}/\text{mL}$ + 150 μM H_2O_2	125 $\mu\text{g}/\text{mL}$ + 150 μM H_2O_2	125 $\mu\text{g}/\text{mL}$ + 150 μM H_2O_2	125 $\mu\text{g}/\text{mL}$ + 150 μM H_2O_2
7	250 $\mu\text{g}/\text{mL}$ + 150 μM H_2O_2	250 $\mu\text{g}/\text{mL}$ + 150 μM H_2O_2	250 $\mu\text{g}/\text{mL}$ + 150 μM H_2O_2	250 $\mu\text{g}/\text{mL}$ + 150 μM H_2O_2
8	500 $\mu\text{g}/\text{mL}$ + 150 μM H_2O_2	500 $\mu\text{g}/\text{mL}$ + 150 μM H_2O_2	500 $\mu\text{g}/\text{mL}$ + 150 μM H_2O_2	500 $\mu\text{g}/\text{mL}$ + 150 μM H_2O_2

Human neuroblastoma SH-SY5Y cells were exposed for 2 and 24 hours to six different Rooibos treatment combinations before being treated for 3 hours with 150 μM hydrogen peroxide (H_2O_2).

3.8.5. The ATP quantification assay

To detect ATP luminescence, the Cell Titer-Glo® kit (Promega, Madison, USA) was used with slight modifications, as previously described by Docrat et al. (2018). The principle of this assay as a measure of cellular metabolic activity and viability is based on the luciferase-catalysed conversion of luciferin to oxyluciferin in the presence of magnesium ions (Mg^{2+}), ATP, and O_2 (Docrat et al., 2018; Nowak et al., 2018). All metabolically active cells contain ATP, which serves as the primary immediate donor of energy in the luciferase reaction (Sánchez et al., 2013). When cells are lysed, the luciferase reaction emits light (luminescence) in proportion to the intracellular ATP concentration (Figure 3.10) (Sánchez et al., 2013; Docrat et al., 2018; Nowak et al., 2018; Agapouda et al., 2020).

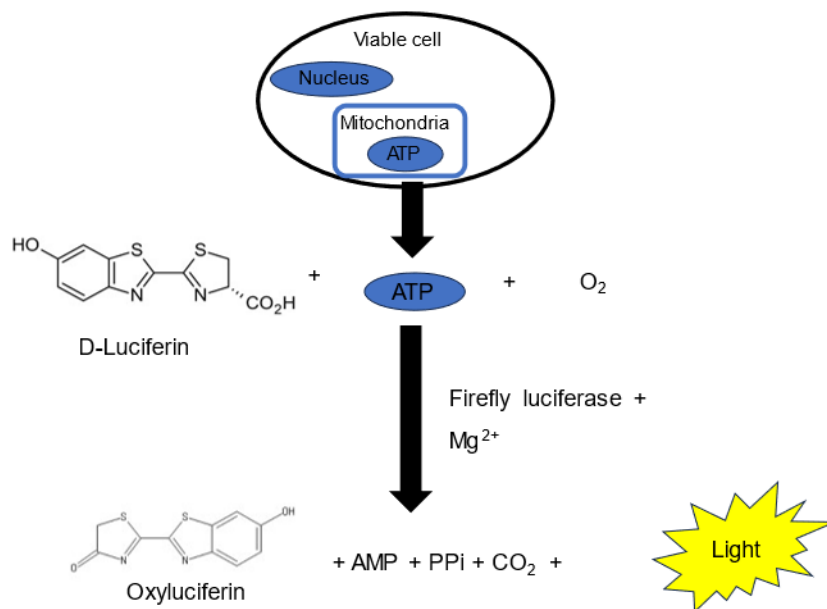


Figure 3.10: The bioluminescence-based adenosine triphosphate quantification assay principle.

The presence of Mg^{2+} and ATP in the luciferase reaction enhances the conversion of luciferin to oxyluciferin. As a result, energy is released in the form of light in proportion to the intracellular ATP concentration. Abbreviations: Mg^{2+} = magnesium, ATP = adenosine triphosphate, AMP = adenosine monophosphate, PPi = inorganic pyrophosphate

In brief, SH-SY5Y cells were seeded (2.0×10^4 cells/well) in a 96-well microtiter luminometer plate and incubated for 24 hours for attachment. Following cell attachment, cells were pre-treated in triplicate for 2 hours and 24 hours with various Rooibos extracts concentrations (15, 30, 60, 125, 250, and 500 $\mu\text{g}/\text{mL}$). Following incubation, the supernatants were aspirated and discarded. Cells were exposed to the optimal H_2O_2 concentrations for 3 hours. Supernatants were aspirated and

discarded after incubation. To remove any residual media, the wells were rinsed with 100 μL PBS (0.1 M). 25 μL of the Cell Titer-Glo® kit assay reagent and 25 μL of 0.1 M PBS were added to each well of the plate. This facilitated cell lysis and the luciferase-based reaction. The plate was then incubated at room temperature for 30 minutes in the dark. Using a multiplate reader (SpectraMax i3X, San Jose, CA, USA), the luminous signal was linearly correlated to ATP concentration. The concentrations of ATP were measured in Relative Light Units (RLU).

3.8.6. Oxidative stress biomarkers

The following assays were conducted using a concentration range for Rooibos extract pre-treatment for 24 hours. This was optimal based on the metabolic assays.

3.8.6.1. Conjugated dienes

Lipid hydroperoxides are PUFAs with CDs that can be detected spectroscopically by measuring the dienes' absorbance at 232-235 nm (Figure 3.11) (Situnayake et al., 1990; Abeyrathne et al., 2021).

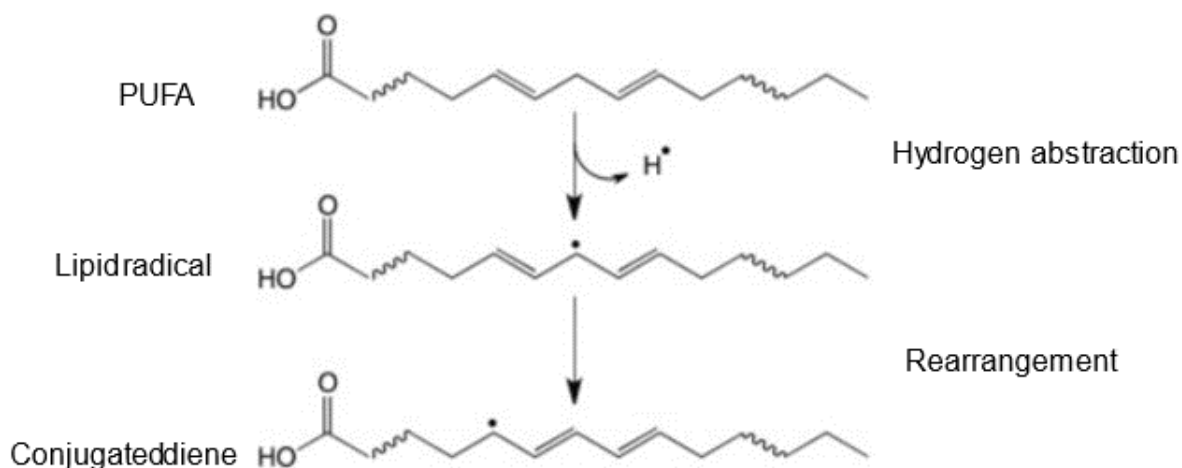


Figure 3.11: A schematic and simplified representation for determining conjugated dienes.

Conjugated dienes are oxidised polyunsaturated fatty acids that result from a molecular rearrangement of carbon-centred radicals, resulting in an increase in UV absorbance at 230-235 nm. Abbreviations: PUFA = polyunsaturated fatty acids, H• = radical

Conjugated dienes were analysed by the method of Recknagel & Glende, (1984), with minor modifications. The method used is simple and determines all conjugated forms of dienes in lipids during the early stages of lipid oxidation. In brief SH-SY5Y cells were seeded in 25 cm³ flasks with a cell density of 3.5×10^4 cells/cm². When the cells reached the culturing density of 80 % confluence (approximately 3.5×10^4 cells/cm²) after 24 hours of incubation, they were pretreated with Rooibos extracts and incubated for another 24 hours. Then the cells were treated with 150 μ M H₂O₂ for 3 hours. To ensure removal of any residual media, the cell sheet was rinsed with 400 μ L of 0.1 M PBS, twice and then a rubber policeman was used to gently dislodge adhered cells. The pellet was then sonicated for 15 minutes in 1 mL of cold diluted CAT assay buffer using a UMC5 sonicator. The mixture was centrifuged at 10,000 x g for 15 minutes at 4°C, the supernatant was collected, and the assay was carried out immediately. Lipids were extracted using the Folch method (Folch et al., 1957), with 100 μ L of sample pipetted into a 2 mL Eppendorf tube and 400 μ L of 2:1 chloroform-methanol (v/v) added, vortex-mixed for 10 seconds, and centrifuged (Eppendorf 5810 R, Germany) at 10000 x g for 10 minutes at room temperature. Following that, 300 μ L of the chloroform phase (bottom layer) was transferred into a clean tube. The sample was then air-dried for 24 hours in a standard laboratory hood with the lid open to allow the chloroform to evaporate. The dried samples were vortex-mixed for 10 seconds in 1000 μ L cyclohexane, which has no UV absorption at 232-234 nm (Kodali et al., 2020). 300 μ L of the sample was transferred into a clear 96-well microplate and measured at 232 nm with a SpectraMax i3X (San Jose, CA, USA) platform plate reader against a cyclohexane blank. Using the molar extinction coefficient 2.95×10^4 M⁻¹cm⁻¹, absorbance units were converted to molar units (Ahotupa, 1996). The results were represented in μ mol/L to provide an estimate of the actual level of CD in the sample.

3.8.6.2. The thiobarbituric acid reactive substance assay

The TBARS assay has been widely used in physiological systems as a generic metric of LPO (Ghani et al., 2017; Tsikas, 2017). This assay measures the levels of MDA formed by lipid peroxidising systems. 2-thiobarbituric acid (TBA) has been widely used as a reagent for the colorimetric measurement of MDA in biological samples as a biomarker for OS because of its stability and the high molar extinction value of the resultant adduct at 532 nm. The procedure involves the condensation between TBA molecules and an MDA molecule (2:1), which yields a red-coloured derivative (Figure 3.12) (Erdelmeier et al., 1998).

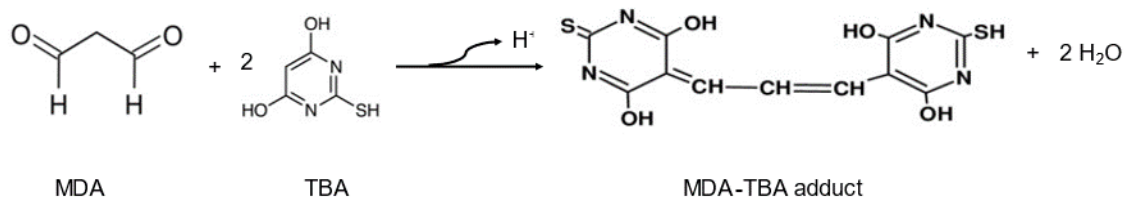


Figure 3.12: The principle of the thiobarbituric acid reactive substance assay.

When heated in an acidic solution, one molecule of malonaldehyde (MDA) interacts with two molecules of thiobarbituric acid (TBA) to generate a unique Schiff base compound with a pink colour that can be quantified using visible (at 532-535 nm) spectrophotometers.

The procedure described by Docrat et al., (2018) was followed. In brief, 200 µL of supernatants were mixed with 200 µL of 2 % phosphoric acid (H₃PO₄) in pre-labelled glass test tubes. Following that, each tube received 400 µL of TBA/Butylated hydroxytoluene (BHT) solution and 200 µL 7% H₃PO₄. To remove background absorbance, 400 µL of 3 mM HCl was added to the blank, which was utilised as a negative control. MDA (1 µL) was added to the positive control test tube. Vortex-mixed samples were incubated at 100 °C for 15 minutes to facilitate MDA adduct hydrolysis before being allowed to cool at room temperature. The assay's sensitivity was enhanced by adding butanol (1500 µL), which precipitates the MDA-TBA adduct after cooling. After vortex-mixed for 30 seconds, the samples were allowed to settle until two different phases were observed. The upper butanol layer (100 µL) was then aliquoted in triplicate into a 96-well microtiter plate and measured at 532 nm using a multiplate reader (SpectraMax i3X, San Jose, CA, USA) with a reference wavelength of 600 nm. The data (n=3) were expressed as MDA concentrations (mM), which were computed using the equation below (*Equation 3*). Recipes for the buffers Appendix 4.

$$MDA \text{ concentration} = [(individual \ OD \ of \ the \ sample - average \ OD \ blank) \div 156] * 1000$$

Equation 3: Calculation to determine MDA concentration (in mM), where 156 is the extinction coefficient of the MDA-TBA adduct (Devasagayam et al., 2003).

3.8.7. Protein extraction, quantification, and standardization

3.8.7.1. Protein Extraction

Human neuroblastoma SH-SY5Y cells were seeded in 25 cm³ flasks with a cell density of 3.5 × 10⁴ cells/cm². When the cells reached the culturing density of 80 % confluence (approximately 3.5 × 10⁴ cells/cm²) after 24 hours of incubation, they were pretreated with Rooibos extracts [60, 125,

and 250 µg/mL] for 24 hours. Following a 1 mL PBS wash, 250 µL of M-PER™ Mammalian protein extraction reagent supplemented with Halt™ phosphatase and Halt™ protease inhibitor cocktails (a final concentration of 1X) was added to the cells and shaken for 30 minutes. Cells were mechanically extracted using a cell scraper and transferred to 1.5 mL microcentrifuge pre-labelled tubes, then stored at -80 °C until use.

3.8.7.2. Protein Quantification

The crude protein extract was quantified using the Pierce™ bicinchoninic acid (BCA) Protein Assay kit according to the manufacturer's instructions. Under alkaline conditions, the BCA relies on the stoichiometric reduction of Cu^{2+} to Cu^+ via peptide bonds in the protein. The Cu^+ chelates two BCA molecules, resulting in a purple complex (BCA- Cu^+ complex) with an absorbance peak at 562 nm. As a result, absorption is correlated with sample protein content, which can then be quantified using a calibration curve (Nilles et al., 2022). In brief, 9 standard solutions of bovine serum albumin (BSA) were prepared by serially diluting the 2000 µg/mL stock solution. In each well of a 96-well plate, 25 µL of BSA standard or sample was added in duplicate. The plate was agitated for 30 seconds before incubating at 37 °C for 30 minutes with 200 µL of the working solution (a 50:1 mixture of reagent A and reagent B from the kit). At 562 nm, absorbance was measured using a multiplate reader (SpectraMax i3X, San Jose, CA, USA). The standard curve protein concentrations have been standardised to 1 mg/mL (Appendix 9).

3.8.8. Quantification of protein carbonylation

The protein carbonyl levels were determined using a procedure described by Docrat et al., (2020), which involved reacting the carbonyl groups with 2,4-dinitrophenylhydrazine (DNPH) to generate 2,4-dinitrophenylhydrazone, which was then spectrophotometrically quantified (Figure 3.13) (Kehm et al., 2021).

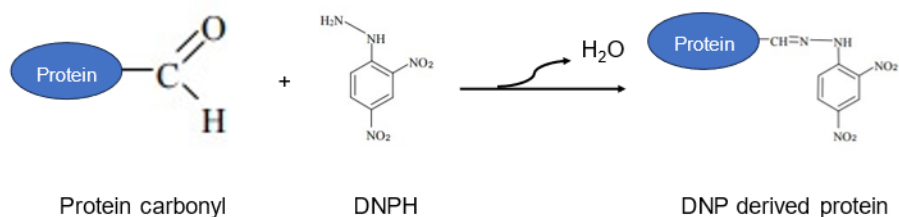


Figure 3.13: The reaction of the protein carbonyl group with 2,4-dinitrophenylhydrazine (DNPH).

The nucleophilic addition, commonly known as the condensation reaction, results in a DNP-derived protein (2,4-dinitrophenyl hydrazone). It is worth noting that the reaction results in the loss of one water molecule.

In brief, the standardised protein (100 µL) and DNPH (400 µL) was mixed with a vortex at room temperature for 1 hour, every 15 minutes to ensure complete carbonyl group derivatisation. 100 µL of control treatment was added to 400 µL of 2.5 M HCl (to serve as a blank). Following incubation, proteins were precipitated with 500 µL of 20 % w/v trichloroacetic acid (TCA) in dH₂O, using a vortex, and centrifuged (2000 × g for 10 min). To prevent the degradation of proteins, the procedure was carried out on ice. Each sample's pellet was washed twice with 500 µL of ethanol-ethyl acetate (1:1 v/v) to remove any unbound DNPH. To neutralize the DNPH-derivatized protein, 250 µL of 6 M guanidine hydrochloride was added. To remove any insoluble material, the samples were centrifuged (2,000 ×g, 10 min, room temperature) and then incubated (37°C, 10 min). The absorbance at 370 nm was measured using a multiplate reader (SpectraMax i3X, San Jose, CA, USA) after the supernatant (100 µL) was transferred in triplicate to a 96-well microtiter plate. The carbonyl concentration was calculated using the equation below (Equation 4), and the results were represented in nanomoles per milligram. Recipes for the buffers in Appendix 5.

$$\text{Carbonyl concentration} = \frac{[(\text{individual absorbance sample} - \text{Average absorbance blank}) \div 22,000] * 106}{1}$$

Equation 4: Equation for calculating protein carbonyl concentration in nmol/mg, where 1cm is the pathlength and the extinction coefficient of the DNP is 22, 000 (Augustyniak et al., 2015).

3.9. Redox status

3.9.1. Reduced glutathione assay

The most important non-enzymatic antioxidant molecule is GSH, a low-molecular-weight thiol present in cells at millimolar quantities (Cazzola et al., 2021). The GSH-Glo™ Glutathione Assay was used to determine for changes in the intracellular level of GSH as an oxidative stress marker.

Using luminescence principles, the GSH-Glo™ test detects low GSH levels in cells. In this experiment, GST catalyses the conversion of a luciferin derivative to luciferin in the presence of GSH. The signal generated is proportional to the amount of GSH in the sample (Figure 3.14).

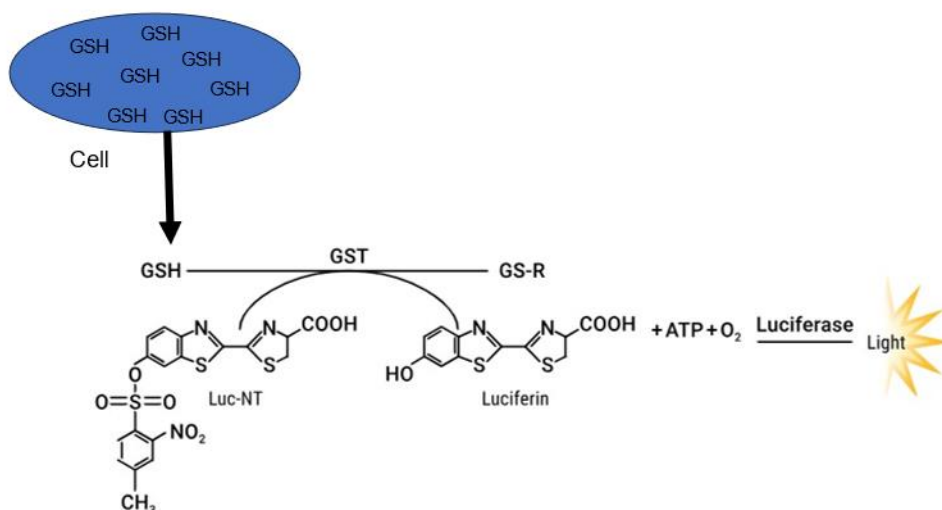


Figure 3.14: Principle of the GSH-Glo™ Glutathione Assay.

Glutathione- S-transferase (GST) catalyses the conversion of a luciferin derivative to luciferin in the presence of GSH. The signal produced is proportional to the amount of glutathione present in the sample. Abbreviations: GSH = glutathione, GS-R = glutathione reductase, and GST = glutathione S-transferase.

In brief, 2.0×10^4 cells were seeded in triplicate into a white luminometric plate. The cells were allowed to adhere to the plate overnight. Rooibos concentrations of 60, 125, and 250 $\mu\text{g}/\text{mL}$ were pipetted directly onto the appropriate cavities (wells) after the culture fluid was aspirated (24 hours Rooibos treatment). Following the Rooibos pre-treatment, H_2O_2 at concentrations of 150 μM was introduced to the cells for 3 hours. The wells were then washed with 100 μL of 0.1 M PBS. The GSH-Glo™ assay reagents were prepared as directed by the manufacturer. Pipetting prepared GSH standard solution (glutathione, 5 mM) of known concentration (0-50 μM) in triplicate (10 μL) generated a standard curve. Each well received 100 μL of the GSH-Glo™ test reagent, followed by a quick agitation (30 seconds). The plate was incubated at room temperature and in the dark for 30 minutes. The Luciferin Detection Reagent (100 μL) was then added, followed by a 15-minute incubation in the dark at room temperature. Luminometric emission was measured with a multiplate reader (SpectraMax i3X, San Jose, CA, USA). The data is given as concentration (μM), which was determined by extrapolating from the standard curve.

3.10. Antioxidant enzyme activity

3.10.1. Superoxide dismutase activity

Total SOD activity (Cu/ZnSOD [SOD1] and MnSOD [SOD2]) was measured in cell lysate using the manufacturer's SOD colorimetric Activity Kit test. In brief, in the presence of O_2 , xanthine oxidase produces superoxide ($O_2^{\cdot-}$), which converts the colourless substrate in the detection reagent into a yellow-coloured result. The absorbance of the coloured product is measured at 450 nm. Increased SOD levels in the samples decrease $O_2^{\cdot-}$ concentration and yellow colour (Figure 3.15) (Wang et al., 2019).

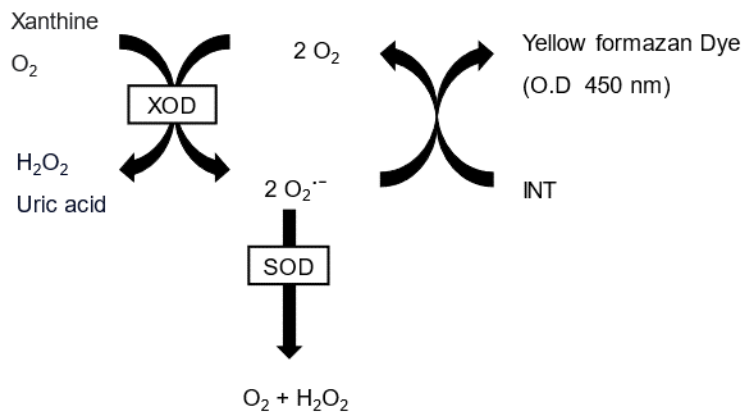


Figure 3.15: Schematic of the superoxide dismutase (SOD) activity assay principle.

Xanthine Oxidase (XOD) can catalyse the reaction of iodinitrotetrazolium (INT) with superoxide ($O_2^{\cdot-}$) in the presence of oxygen (O_2) to yield a water-soluble formazan colour. Because SOD can catalyse the disproportionation of superoxide anions to yield O_2 and hydrogen peroxide (H_2O_2), the reaction can be inhibited, and the activity of SOD has a negative correlation with the amount of formazan dye. As a result, the activity of SOD can be measured by colorimetric measurement of INT products.

The cells were extracted and resuspended in ice-cold 0.1 M PBS (1 mL) before being transferred to an ice-cold microcentrifuge tube following cell culture methods. According to the kit instructions, the cells were centrifuged for 10 minutes at 4 °C at $250 \times g$, the supernatant was removed, and the tubes were placed on ice. The pellet was then sonicated for 15 minutes in 500 μ L of 0.1 M

PBS using a UMC5 sonicator. The supernatant was collected and examined immediately following a 10-minute centrifugation at $1,500 \times g$ at 4°C . The wells were filled with pipetted $10\ \mu\text{L}$ SOD standards/samples. Following that, each well got $50\ \mu\text{L}$ of diluted substrate. The plate was incubated at room temperature for 20 minutes after each well received $25\ \mu\text{L}$ of diluted XOD. Superoxide dismutase absorbance was measured at $450\ \text{nm}$ using a microplate reader (SpectraMax i3X, San Jose, CA, USA). Using the standard curve, the activities of each sample were calculated and expressed as U/mL.

3.10.2. Catalase activity

Catalase activity was measured with a CAT colorimetric activity kit, with only minimal changes to the manufacturer's procedure. This assay kit uses the catalytic activity of CAT and horseradish peroxidase (HRP) to evaluate enzyme activity. Horseradish peroxidase reacts with a substrate in the presence of an appropriate concentration of H_2O_2 to transform a colourless substrate into a pink-coloured product. The wavelength of the coloured product is $560\ \text{nm}$ (Figure 3.16). Increased CAT activity in the samples reduces the concentration of H_2O_2 as well as the pink product.

Horseradish peroxidase, a class III peroxidase isolated and purified from the horseradish root can catalyse the reaction of H_2O_2 with electron-donating substrates (Hynninen et al., 2010; Vazquez-Alvarado et al., 2023), offering numerous advantages (Huang et al., 2021). Indeed, specific substrates can react with HRP to yield highly coloured products, making the combination of HRP with a suitable chromogen a potent analytical tool (Vazquez-Alvarado et al., 2023).

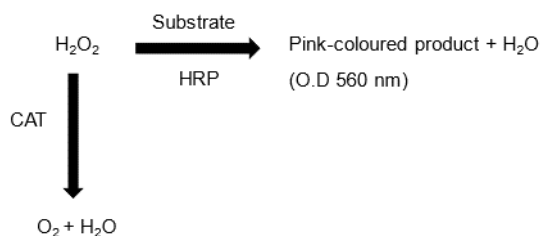


Figure 3.16: Schematic of the catalase colorimetric activity assay principle.

This assay consists of two sequential reactions. Initially, catalase efficiently breaks down hydrogen peroxide (H_2O_2) into water (H_2O) and oxygen (O_2). Any residual H_2O_2 in the mixture then participates in a coupling reaction involving a colorimetric Probe (substrate) and a Horseradish Peroxidase (HRP) catalyst. The resultant coupling product is then measured at 560nm to determine the quantity of H_2O_2 remaining in the reaction mixture.

Human neuroblastoma SH-SY5Y cells were seeded in 25 cm³ flasks with a cell density of 3.5×10^4 cells/cm². When the cells reached the culturing density of to 80 % confluence (approximately 3.5×10^4 cells/cm²) after 24 hours of incubation, cells were treated with Rooibos extracts for 24 hours, followed by 3 hours of treatment with 150 μ M H₂O₂. Following the addition of 400 μ L of 0.1 M PBS, twice, a rubber policeman was used to gently dislodge adhered cells. The pellet was then sonicated for 15 minutes in 1 mL of cold diluted assay buffer using a UMC5 sonicator. The mixture was centrifuged at 10,000 x g for 15 minutes at 4°C, the supernatant was collected, and the assay was carried out immediately. The optimal conditions for the assay include incubating 25 μ L samples or standards with 25 μ L of H₂O₂ reagent at room temperature for 30 minutes. This was followed by the addition of 25 μ L of substrate and 25 μ L of diluted HRP solution. The plate was then incubated for 15 minutes at RT. The Catalase absorbance at 560 nm was measured with a spectrophotometer (SpectraMax i3X, San Jose, CA, USA). The activities of CAT in each sample were calculated using the standard curve and given as U/mL.

3.11. Cellular Death

3.11.1. Analysis of caspase activity

Caspase activity was measured using the Caspase Glo® 3/7, Caspase Glo® 8, and Caspase Glo® 9 Assay kits. The amino-luciferin-derivatized peptide substrates utilised in these homogeneous assays are synthesised in a buffer solution with caspase activity, luciferase activity, and cell lysis controlled. The Caspase-Glo reagent initiates cell lysis, which is followed by caspase substrate cleavage and the production of luciferase stables (Miret et al., 2006; Brunelle & Zhang, 2010; Maysinger & Hutter, 2015; Procházková et al., 2022). The amount of caspase present influences the luminescent signal produced (Figure 3.17) (Miret et al., 2006; Procházková et al., 2022).

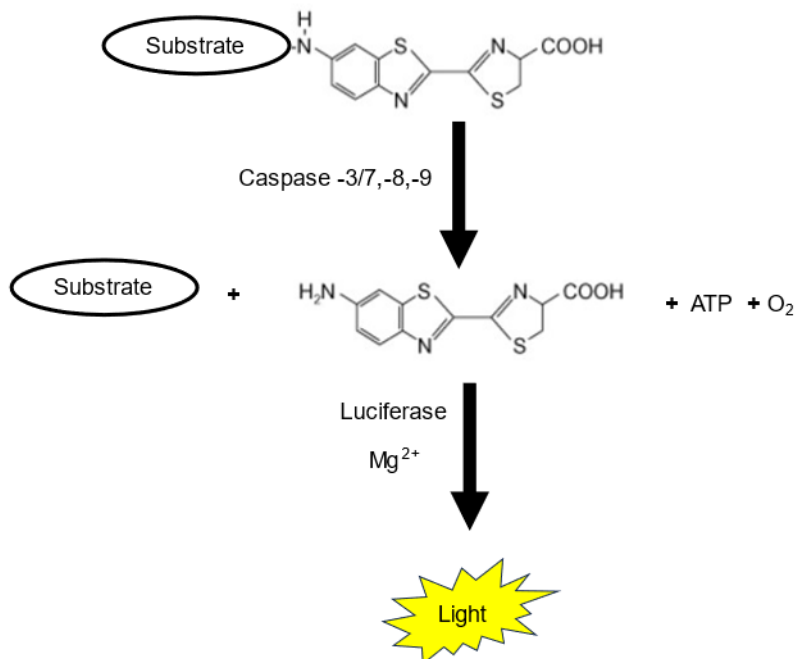


Figure 3.17: Schematic representation of the Caspase-Glo® assay principle.

Following caspase cleavage, a substrate for luciferase (amino luciferin) is released, which results in the luciferase reaction and the production of light in the presence of luciferase and Mg²⁺. Abbreviations: Mg²⁺= magnesium; ATP = adenosine triphosphate, O₂ = Oxygen

In a 96-well white-walled cell culture plate, cells were seeded at a density of 2.0×10^4 cells per well. Cells were pre-treated in triplicate with different Rooibos extracts concentrations after 24 hours (15, 30, 60, 125, 250, and 500 $\mu\text{g}/\text{mL}$). Following incubation, supernatants were aspirated and discarded. For 1, 3, and 24 hours, cells were exposed to optimal H₂O₂ concentrations. After incubation, supernatants were collected and discarded. Caspase activities were determined with slight adjustments using the approach given by Naidoo et al (2017). Wells were rinsed with 100 μL PBS (0.1 M) to eliminate any residual media. Each well in the plate was treated with 25 μL of Caspase Glo® reagents (caspases 3/7,8, and 9) and 25 μL of 0.1 M PBS before being incubated at room temperature for 30 minutes in the dark to allow cell lysis and the enzyme luciferase response. A multiplate reader (SpectraMax i3X, San Jose, CA, USA) was used to correlate the luminescent signal with caspase activity. caspase 3/7, caspase 8, and caspase 9 concentrations are expressed in relative light units (RLU).

3.11.2. The lactate dehydrogenase assay

The LDH assay (Roche CAT: 11644793001) was used to assess cytotoxicity. Lactate dehydrogenase is a cytosolic enzyme found in all cells that is rapidly released into the extracellular space when cellular membrane integrity is disrupted (as in cells undergoing apoptosis, necrosis, or other forms of cellular injury). Therefore, the LDH assay detects LDH enzyme activity in cell culture medium (Kamiloglu et al., 2020; Tabernilla et al., 2021; Azqueta et al., 2022). Lactate dehydrogenase is responsible of converting pyruvate and lactate, as well as NAD^+ and NADH/H^+ . Using NADH/H^+ , a diaphorase catalyses the reduction of a yellow tetrazolium salt to a water-soluble red formazan dye (Kamiloglu et al., 2020; Tabernilla et al., 2021). The LDH activity can be approximated by measuring the consumption of NADH/H^+ using spectrophotometry (Figure 3.18).

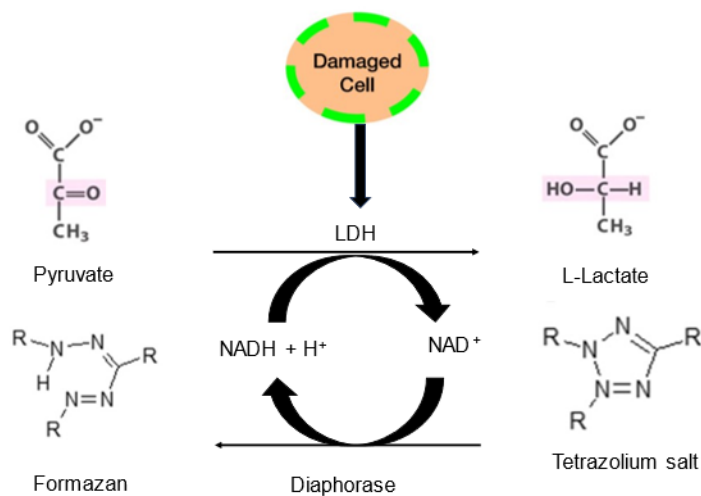


Figure 3.18: The schematic representation of the lactate dehydrogenase (LDH) release assay principle.

The LDH assay measures the integrity of the cell membrane based on the oxidation of yellow tetrazolium salt to a red formazan. Because large amounts of LDH are released from the cytosol during cellular necrosis, it catalyses the conversion of pyruvate to lactate, and the complementary reaction of NADH with tetrazolium salts allows spectroscopic monitoring of LDH enzymatic activity using known initial concentrations of lactate and NAD^+ . Abbreviations: NAD^+ = nicotinamide adenine dinucleotide, NADH = reduced nicotinamide adenine dinucleotide, H^+ = hydrogen ion

Minor changes were made to the protocol described in Docrat et al., (2018). In brief, 100 μ L supernatant was pipetted into 96-well microtiter plates in triplicate. Each well received a 100 μ L reaction mixture containing a diaphorase/NAD⁺ catalyst and a sodium lactate/tetrazolium salt and was incubated for 30 minutes at room temperature in the dark. The optical density (OD) of the formazan product was determined at 500 nm using a multiplate reader (SpectraMax i3X, San Jose, CA, USA). The data is shown as the mean OD.

3.12. Statistical Methods

The results are presented as the mean and standard deviation (SD) of technical triplicate (n=3). To express the precision and repeatability of assays, the coefficients of variation (CV) were calculated using Microsoft® Excel®. All tests were two-tailed with an alpha of 0.05. The one-way analysis of variance (ANOVA) was employed, and multiple comparisons were handled with the Bonferroni correction. The data was analysed with the GraphPad Prism V5.0 software (GraphPad Software Inc., La Jolla, CA, USA).

4. CHAPTER FOUR: RESULTS

To ease data visualization, TPC and AOC of ethanolic and aqueous extracts were compared. In this investigation, the fermented and unfermented samples did not come from the same plant material, which could have contributed to the variance in TPC and AOC as previously noted (Epure et al, 2019; Hussein et al., 2022). Therefore, it was not worthwhile to display comparisons of unfermented aqueous versus fermented ethanolic, etc., because they would just confuse the picture. To compare ethanolic versus aqueous and fermented vs unfermented, each table had to be separated into two different tables. See Appendix 14, Appendix 15 and Appendix 16.

4.1. Determination of total phenolic content of Rooibos extracts

Total phenolic content was determined in fermented and unfermented aqueous and ethanolic extracts at concentrations ranging from 15 to 500 µg/mL and expressed as gallic acid equivalents. The fermented aqueous extract had higher phenolic content than fermented ethanol extract at 15 µg/mL and 500 µg/mL, with a mean difference of 1.5 mg/GAE/L (95 % CI=0.6 mg/GAE/L to 2.4 mg/GAE/L; $P \leq 0.01$) and 12.5 mg/GAE/L (95 % CI=1.1 mg/GAE/L to 23.8 mg/GAE/L; $P \leq 0.05$) respectively. While at the same concentrations unfermented ethanol extract had higher phenolic content than unfermented aqueous extract, with a mean difference of -1.0 mg/GAE/L (95 % CI= -1.9 mg/GAE/L to -0.07 mg/GAE/L; $P \leq 0.05$) and -53.2 mg/GAE/L (95 % CI= -64.6 mg/GAE/L to -41.85 mg/GAE/L; $P \leq 0.001$) respectively. At 30 µg/mL, the phenolic contents of unfermented aqueous and ethanolic extracts were comparable. However, at the same concentration, fermented ethanolic extract had a higher total phenolic content than fermented aqueous extract, with a mean difference of -1.9 mg/GAE/L (95 % CI= -2.5 mg/GAE/L to -1.2 mg/GAE/L; $P \leq 0.001$) (Table 4.1).

Table 4.1 : The total phenolic content of ethanolic, and aqueous extractions compared according to the type of Rooibos.

Extract concentration ($\mu\text{g/mL}$)	Unfermented Rooibos (mg GAE/L)		Fermented Rooibos (mg GAE/L)	
	Aqueous	Ethanolic	Aqueous	Ethanolic
	Mean (SD)	Mean (SD)	Mean (SD)	Mean (SD)
15	0.3 (0.2)	1.3 (0.4) *	1.8 (0.4)	0.7 (0.2) **
30	6.3 (0.4)	6.1 (0.2) ^{ns}	2.4 (0.2)	4.3 (0.1) ***
60	18.1 (1.2)	20.9 (0.5) **	11.7 (0.1)	13.4 (0.5) ^{ns}
125	47.6 (2.3)	64.1 (3.6) ***	37.8 (1.0)	38.2 (1.0) ^{ns}
250	106.2 (4.6)	138.4 (2.9) ***	87.7 (3.1)	90.6 (2.6) ^{ns}
500	189.4 (2.7)	242.3 (6.1) ***	169.2 (4.2)	156.8 (1.4) *

*The total phenolic content of ethanolic, and aqueous extractions compared according to the type of Rooibos tea. Results are expressed as gallic equivalents (GAE), mean, and standard deviations (SD) of triplicate evaluations (n=3). For significant difference aqueous vs ethanolic at $p < 0.05$, * for $P \leq 0.05$ ** for $p \leq 0.01$, *** for $p \leq 0.001$ and ^{ns} for $P > 0.05$*

4.2. Determination of ferric reducing antioxidant power of Rooibos extracts

The ferric- reducing antioxidant power of extracts was measured and expressed as ascorbic acid equivalents in fermented and unfermented aqueous and ethanolic Rooibos extracts. Both extracts demonstrated a dose-dependent increase in antioxidant capacity (Table 4.2). Unfermented and fermented ethanol Rooibos extracts had higher antioxidant capacity than aqueous extracts at concentrations of 30, 60, 125, 250, and 500 $\mu\text{g/mL}$. While at 15 $\mu\text{g/mL}$, fermented aqueous Rooibos extract had better FRAP activity compared to fermented ethanol Rooibos extract with a mean difference of 7.4 $\mu\text{mol AAE/L}$ (95 % CI= 0.8 $\mu\text{mol AAE/L}$ to 14.0 $\mu\text{mol AAE/L}$; $P \leq 0.05$).

Table 4.2: Ferric reducing antioxidant power of ethanolic, and aqueous extractions compared according to the type of Rooibos.

Extract concentration (µg/mL)	Unfermented Rooibos (µmol AAE/L)		Fermented Rooibos (µmol AAE/L)	
	Aqueous	Ethanolic	Aqueous	Ethanolic
	Mean (SD)	Mean (SD)	Mean (SD)	Mean (SD)
15	79.4 (1.2)	176.1 (4.2) ***	85.1 (0.1)	77.5 (1.5) *
30	126.7 (1.7)	208.0 (6.2) ***	91.8 (0.7)	107.7 (1.4) **
60	181.4 (3.1)	309.8 (2.1) ***	147.2 (2.1)	160.8 (0.9) ***
125	353.2 (8.3)	427.4 (12.3) ***	250.5 (2.5)	252.3 (0.0) ns
250	608.3 (16.1)	754.3 (26.8) ***	441.6 (11.3)	451.0 (10.7) ns
500	1106.6 (31.9)	1374.7 (7.5) ***	827.4 (31.9)	831.2 (33.6) ns

*Ferric reducing antioxidant power of ethanolic, and aqueous extractions compared according to the type of Rooibos tea. Results are expressed as ascorbic acid equivalents (µmol AAE/L), mean, and SD of triplicate evaluations (n=3). Ferric-reducing antioxidant power increased in a dose-dependent manner. For significant difference aqueous vs ethanolic at $p < 0.05$, * for $P \leq 0.05$ ** for $p \leq 0.01$, *** for $p \leq 0.001$ and ns for $P > 0.05$*

4.3. Determination of Trolox Equivalent Antioxidant Capacity of Rooibos extracts

The Trolox equivalent antioxidant capacity of extracts was measured and expressed as Trolox equivalents for fermented and unfermented aqueous and ethanolic Rooibos extracts. Both Rooibos extracts demonstrated a dose-dependent increase in antioxidant capacity (Table 4.3). Furthermore, both unfermented ethanol Rooibos extract and fermented ethanol Rooibos extract were comparable to unfermented aqueous Rooibos extract and fermented aqueous Rooibos extract at 15 and 30 µg/mL respectively. Additionally, fermented ethanol Rooibos extract was comparable to fermented aqueous Rooibos extract at 60, 125 and 250 µg/mL. Unfermented ethanol Rooibos extract exhibited a higher antioxidant capacity than unfermented aqueous Rooibos extract at 60, 125, 250, and 500 µg/mL. However, fermented aqueous Rooibos extract had a higher antioxidant activity than fermented ethanol Rooibos extract at 500 µg/mL with a mean difference of 68.7 µmol TE/L (95 % CI= 35.5 µmol TE/L to 101.8 µmol TE/L; $P \leq 0.001$).

Table 4.3: Trolox equivalent antioxidant capacity of ethanolic, and aqueous extractions compared according to the type of Rooibos.

Extract concentration (µg/mL)	Unfermented Rooibos (µmol TE/L)		Fermented Rooibos (µmol TE/L)	
	Aqueous	Ethanolic	Aqueous	Ethanolic
	Mean (SD)	Mean (SD)	Mean (SD)	Mean (SD)
15	105.9 (3.1)	117.1 (3.5) ^{ns}	121.9 (8.4)	107.6 (7.6) ^{ns}
30	162.6 (0.2)	152.3 (2.3) ^{ns}	128.9 (9.5)	136.1 (12.2) ^{ns}
60	249.7 (15.4)	308.6 (26.0) ^{**}	186.1 (2.8)	183.0 (5.8) ^{ns}
125	447.5 (6.3)	562.5 (31.8) ^{***}	333.3 (5.1)	322.0 (16.6) ^{ns}
250	758.6 (19.4)	911.3 (24.3) ^{***}	560.3 (20.8)	547.8 (17.5) ^{ns}
500	1167.5 (5.4)	1263.9 (1.4) ^{***}	904.3 (18.2)	835.6 (13.4) ^{***}

*Trolox equivalent antioxidant capacity (TEAC) of ethanolic, and aqueous extractions compared according to the type of Rooibos tea. Results are expressed as Trolox equivalents (µmol TE/L), mean, and SD of triplicate evaluations (n=3). Trolox equivalent antioxidant capacity increased in a dose-dependent manner. For significant difference aqueous vs ethanolic at $p < 0.05$, ** for $p \leq 0.01$, *** for $p \leq 0.001$ and ns for $P > 0.05$*

4.4. High-performance liquid chromatography analysis of unfermented and fermented Rooibos extracts

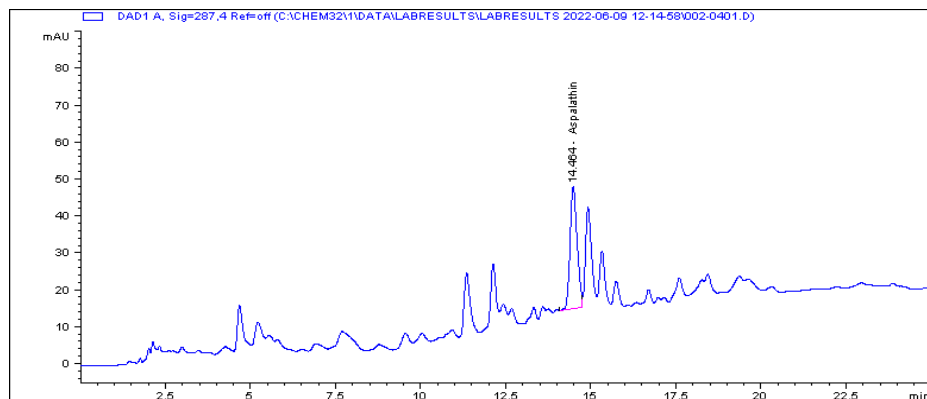
Table 4.4 Figure 4.1, and Figure 4.2 show the quantitative results in mg/L from HPLC-DAD chromatograms of unfermented and fermented Rooibos extracts at 287 and 360 nm. Aspalathin, orientin, iso-orientin, iso-vitexin and vitexin were the major constituents of both unfermented and fermented Rooibos extracts. In general, both fermented and unfermented ethanolic extracts contained higher quantities of these bioactive components, with the unfermented extract containing nearly x3 the quantity of aspalathin, the major bioactive compound, compared to the aqueous extracts.

Table 4.4: Quantitative data of flavonoids detected in ethanolic, and aqueous extracts compared according to the type of Rooibos.

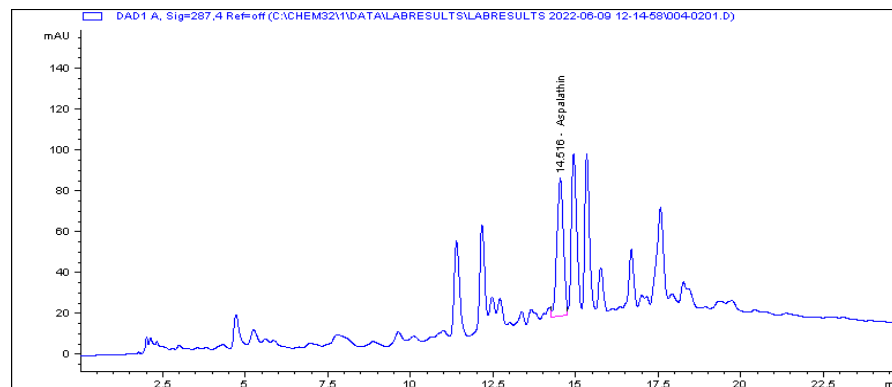
Phytochemical	Unfermented Rooibos (mg/L)		Fermented Rooibos (mg/L)	
	Aqueous	Ethanolic	Aqueous	Ethanolic
Aspalathin	45.2	142.4***	8.1	15.5 ***
Orientin	11.4	16.9 ***	8.2	22.1 ***
Iso-orientin	13.9	24.4 ***	5.8	28.5 ***
Iso-vitexin	3.0	4.5 ***	2.1	6.3 ***
Vitexin	3.5	9.0 ***	0.9	7.6 ***

*Quantitative data of flavonoids detected in ethanolic, and aqueous extracts compared by Rooibos tea type. The results in a single run and injection are given in mg/L. Aspalathin, orientin, iso-orientin, iso-vitexin, and vitexin were the main compounds identified in both unfermented and fermented Rooibos. For significant difference aqueous vs ethanolic at $p < 0.05$, *** for $p \leq 0.001$*

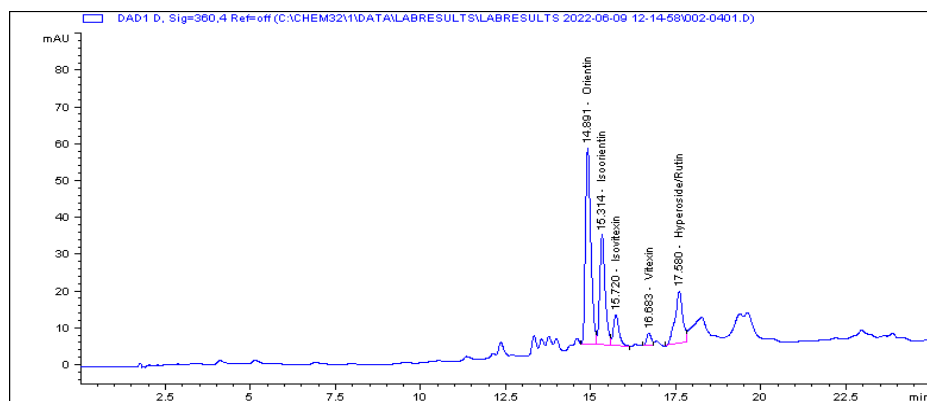
Unfermented aqueous Rooibos extract at 287 nm



Unfermented ethanolic Rooibos extract at 287 nm



Unfermented aqueous Rooibos extract at 360 nm



Unfermented ethanolic Rooibos extract at 360 nm

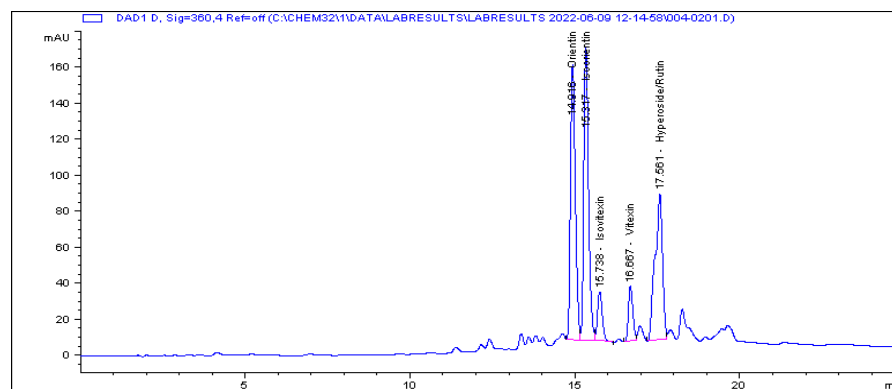
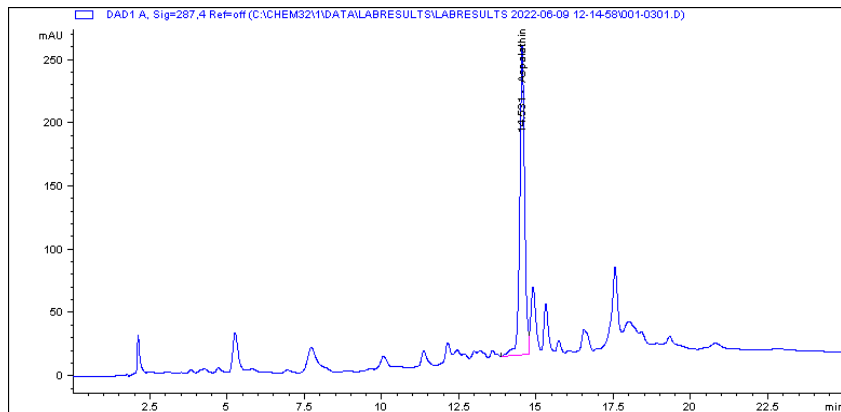


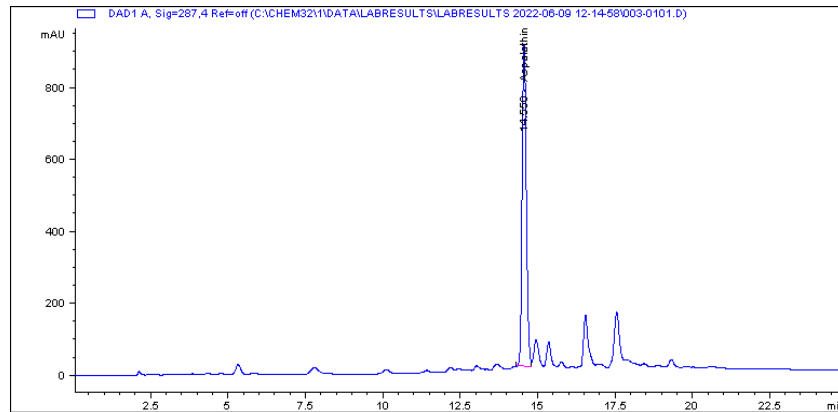
Figure 4.1: High-performance liquid chromatography (HPLC) chromatogram of unfermented Rooibos extracts used in the study.

Peak area obtained for the aspalathin at 287 nm and 360 nm for other flavonoids in unfermented Rooibos extract.

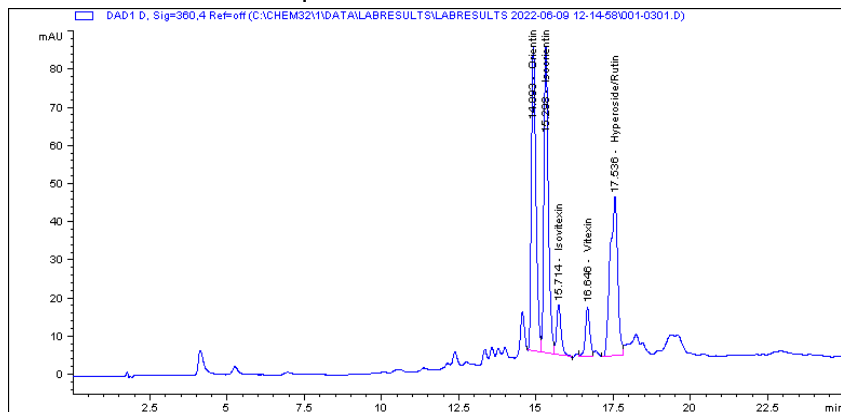
Unfermented aqueous Rooibos extract at 287 nm



Unfermented ethanolic Rooibos extract at 287 nm



Unfermented aqueous Rooibos extract at 360 nm



Unfermented ethanolic Rooibos extract at 360 nm

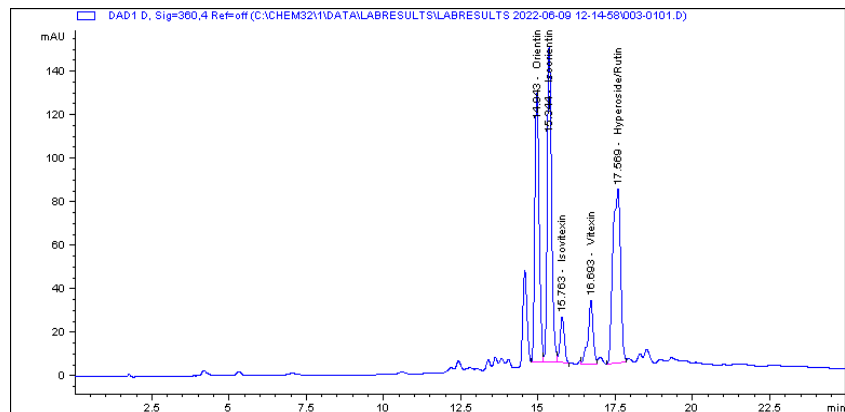


Figure 4.2: High-performance liquid chromatography (HPLC) chromatogram of fermented Rooibos extracts

Peak area obtained for the aspalathin at 287 nm and 360 nm for other flavonoids in fermented Rooibos extract.

4.5. H₂O₂ cytotoxicity on the metabolic activity of SH-SY5Y cells

Human neuroblastoma SH-SY5Y cells were exposed to H₂O₂ (0-1000 µM) for 1, 2, 3, and 24 hours, and cell viability was assessed using the MTT test, with findings expressed as a percentage of control cells. Control cells were incubated in a culture medium and received no treatment for the exposure period. Cell viability decreased gradually as H₂O₂ concentrations increased (**Error! Reference source not found.**). The results demonstrate that at lower concentration (50 µM), H₂O₂ reduced SH-SY5Y cell viability by 87 %, 65 %, 88 %, and 21 % for the 1-hour, 2-hour, 3-hour, and 24-hour exposures (Appendix 6). The results also show that H₂O₂ reduced SH-SY5Y cell viability by at least 50 % at ~75, ~75, and ~150 µM for 1 hour, 2 hours, and 3 hours, respectively. In the presence of 150 µM H₂O₂, there were only 55.75 % (95 % CI= 50.10 % to 61.40 %; P≤0.001) viable cells compared to control cells. In subsequent experiments, 150 µM H₂O₂ was used to induce cytotoxicity in SH-SY5Y cells for 3 hours, since it achieved the desired level of stress without causing excessive cytotoxicity (~50 % cell viability) (Figure 4.3).

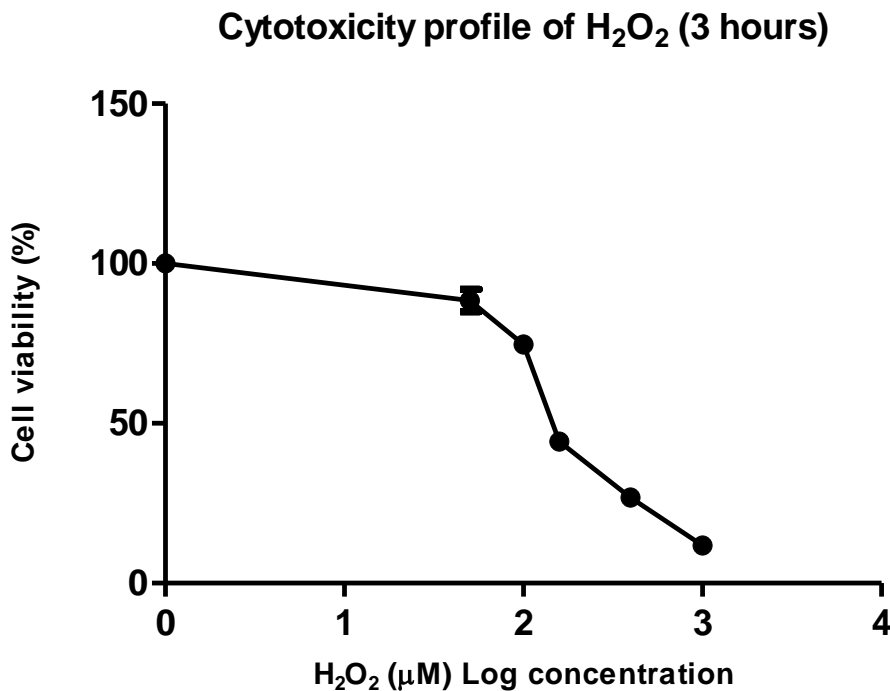


Figure 4.3: Cytotoxicity profile of H₂O₂ (3 hours) in the 3-(4,5-dimethylthiazol-2-yl)-2,5-diphenyl-2H-tetrazolium bromide (MTT) assay expressed as % cell viability.

*The results show a dose-dependent decrease. The optimal concentration was determined to be 150 µM. (***)P≤0.001 compared to control. Since it induced OS while maintaining cell viability (~ 50 % cell viability).*

4.6. The effect of Rooibos extracts on cell viability in SH-SY5Y cells

The MTT assay was used to assess the efficacy of fermented and unfermented Rooibos extracts for any potential cytotoxic effects at concentrations of 15, 30, 60, 125, 250, and 500 $\mu\text{g/mL}$. The data presented are the mean and SD of triplicate experiments. Since none of the extracts were deemed cytotoxic (cell viability $\geq 100\%$), all concentrations were evaluated for their cytoprotective potential against oxidative stress induced by the optimised concentration of H_2O_2 (Figure 4.4).

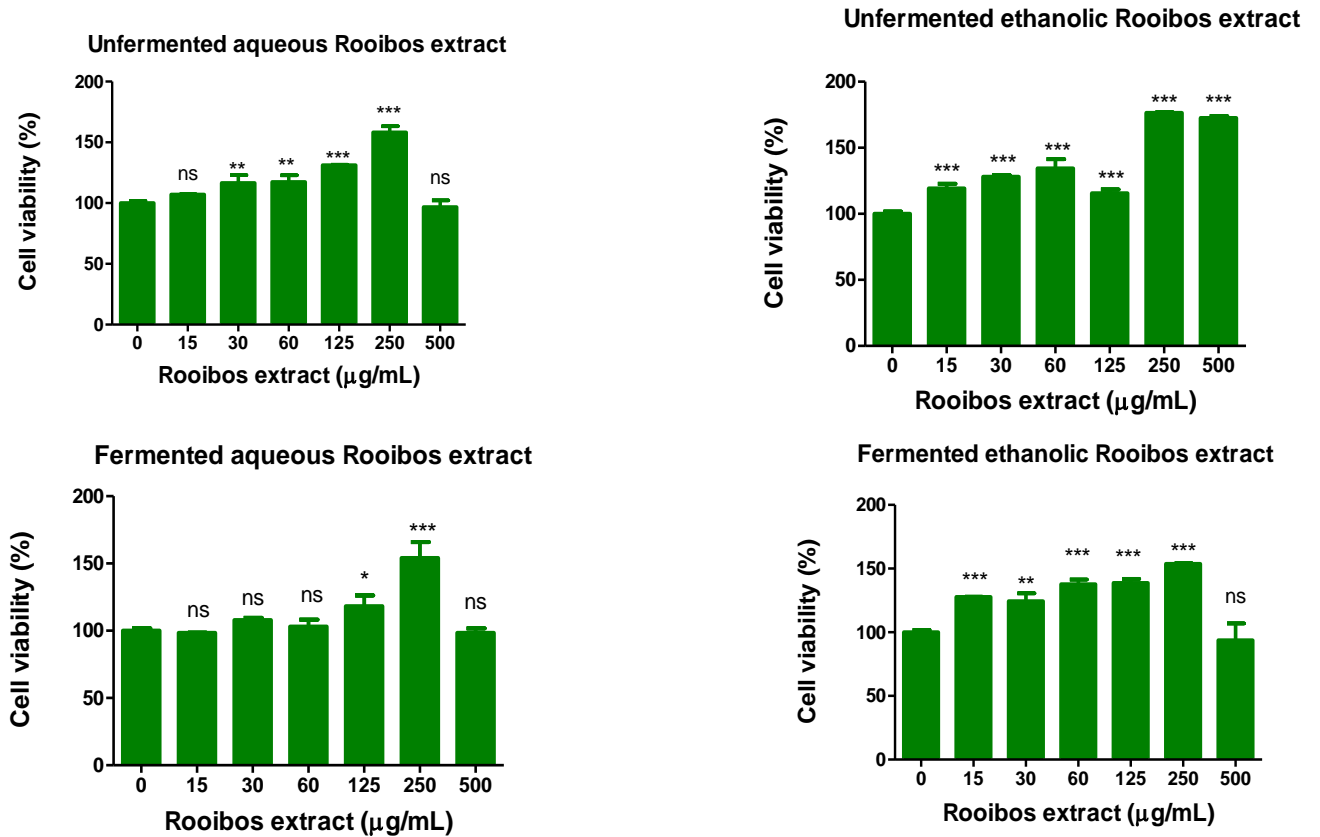


Figure 4.4: The effects of a 24-hour Rooibos treatment.

The control cell received 0 $\mu\text{g/mL}$ Rooibos extracts. For significant difference of the control cells vs Rooibos treatment at $p < 0.05$, * for $P \leq 0.05$, ** for $P \leq 0.01$, and *** for $P \leq 0.001$. The results of the XY analysis are presented in Appendix 12. A bar graph was utilized to enhance the visual appeal of the analysis.

4.7. The effect of Rooibos extracts on SH-SY5Y cell metabolic activity under induced H_2O_2 cytotoxic conditions.

Human neuroblastoma SH-SY5Y cells were pre-treated for 24 hours with unfermented and fermented Rooibos extracts ranging in concentration from 15 to 500 µg/mL. Figure 4.5 shows that when H₂O₂ was used to treat, cell viability decreased with a statistical significance of P≤0.001 compared to the control, whereas unfermented and fermented aqueous Rooibos extracts at concentrations of 60, 125, 250, and 500 µg/mL enhanced cell viability and showed protective effects against H₂O₂ compared to cells treated with only H₂O₂. Furthermore, unfermented, and fermented ethanolic Rooibos extracts treated cells at equivalent concentrations of 15, 30, 60, 125, and 250 µg/mL exhibited considerably higher cell viability than H₂O₂ alone treated cells. Thus, low, medium, and high concentrations of 60, 125, and 250 µg/mL, respectively were selected for further experimental evaluation based on cell viability data. However, when the cells were pretreated with 500 µg/mL fermented ethanolic Rooibos extract, it reduced the cell viability significant with the mean difference of 30 % (95 % CI= 24 % to 36 %; P≤0.001) compared to 250 µg/mL fermented ethanolic Rooibos extract. 2-hour Rooibos extracts pretreatment was not protective against 3-hour H₂O₂ treatment (Appendix 7).

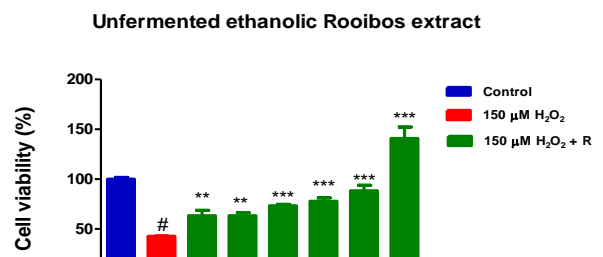
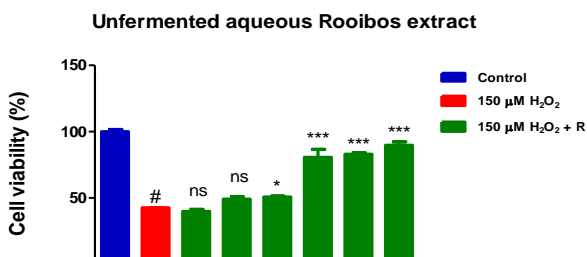


Figure 4.5: Effect of Rooibos extracts on the metabolic output of SH-SY5Y cells challenged with 150 μM H_2O_2 using the 3-(4,5-dimethylthiazol-2-yl)-2,5-diphenyl-2H-tetrazolium bromide (MTT) assay.

The control cells received media only. Hydrogen peroxide significantly decreased the metabolic output of SH-SY5Y cells (# $P \leq 0.001$) compared to control cells and Rooibos significantly increased the metabolic output of SH-SY5Y cells ($P \leq 0.05$), (** $P \leq 0.01$), and (***) $P \leq 0.001$) compared to cells treated with 150 μM H_2O_2 only. 500 $\mu\text{g}/\text{mL}$ fermented ethanolic Rooibos extract, it reduced the cell viability significant (***) $P \leq 0.001$) compared to 250 $\mu\text{g}/\text{mL}$ fermented ethanolic Rooibos extract. Abbreviations: C = Control, R = Rooibos extract. The Appendix 13 contains the results of the XY analysis. However, the bar graph was used to ease data visualisation.*

4.8. The effect of Rooibos extracts on intracellular ATP

The ATP bioluminescent assay is a reliable method for determining cell viability by quantifying ATP (Akinfenwa et al., 2021). Cellular ATP content analysis confirmed that 150 μM H_2O_2 for 3 hours was toxic to the SH-SY5Y cells, with a mean difference of 3.3×10^5 RLU (95% CI= 3.0×10^5 RLU to 3.5×10^5 RLU; $P \leq 0.001$) compared to the control (Figure 4.6). In both unfermented aqueous and ethanol Rooibos extracts, no statistical significance in ATP levels was observed when compared to the H_2O_2 treatment. However, when cells were pre-treated with fermented aqueous Rooibos extract at the lowest concentration (60 $\mu\text{g}/\text{mL}$), the ATP content increased significantly, with a mean difference of -8.1×10^5 RLU (95 % CI= -1.6×10^5 RLU to -5.0×10^5 RLU; $P \leq 0.05$) compared to the H_2O_2 treatment. Fermented ethanol Rooibos extract also increased cellular ATP content at concentrations of 125 and 250 $\mu\text{g}/\text{mL}$, with mean differences of -5.9×10^5

RLU (95 % CI= -8.7×10^5 RLU to -3.1×10^5 RLU; $P \leq 0.001$) and -2.1×10^5 RLU (95 % CI= -2.4×10^5 RLU to -1.9×10^5 RLU; $P \leq 0.001$), respectively compared to the H_2O_2 treatment. Nonetheless, neither fermented aqueous nor ethanol Rooibos extracts were able to maintain ATP levels above control cell levels. Furthermore, all extracts at concentrations $\geq 125 \mu\text{g/mL}$, did not increase ATP levels except for the fermented ethanolic extract. However, fermented aqueous at $60 \mu\text{g/mL}$ increased ATP levels in comparison to the H_2O_2 treatment. A 2-hour Rooibos extracts pretreatment was not protective against 3-hour H_2O_2 treatment (Appendix 8).

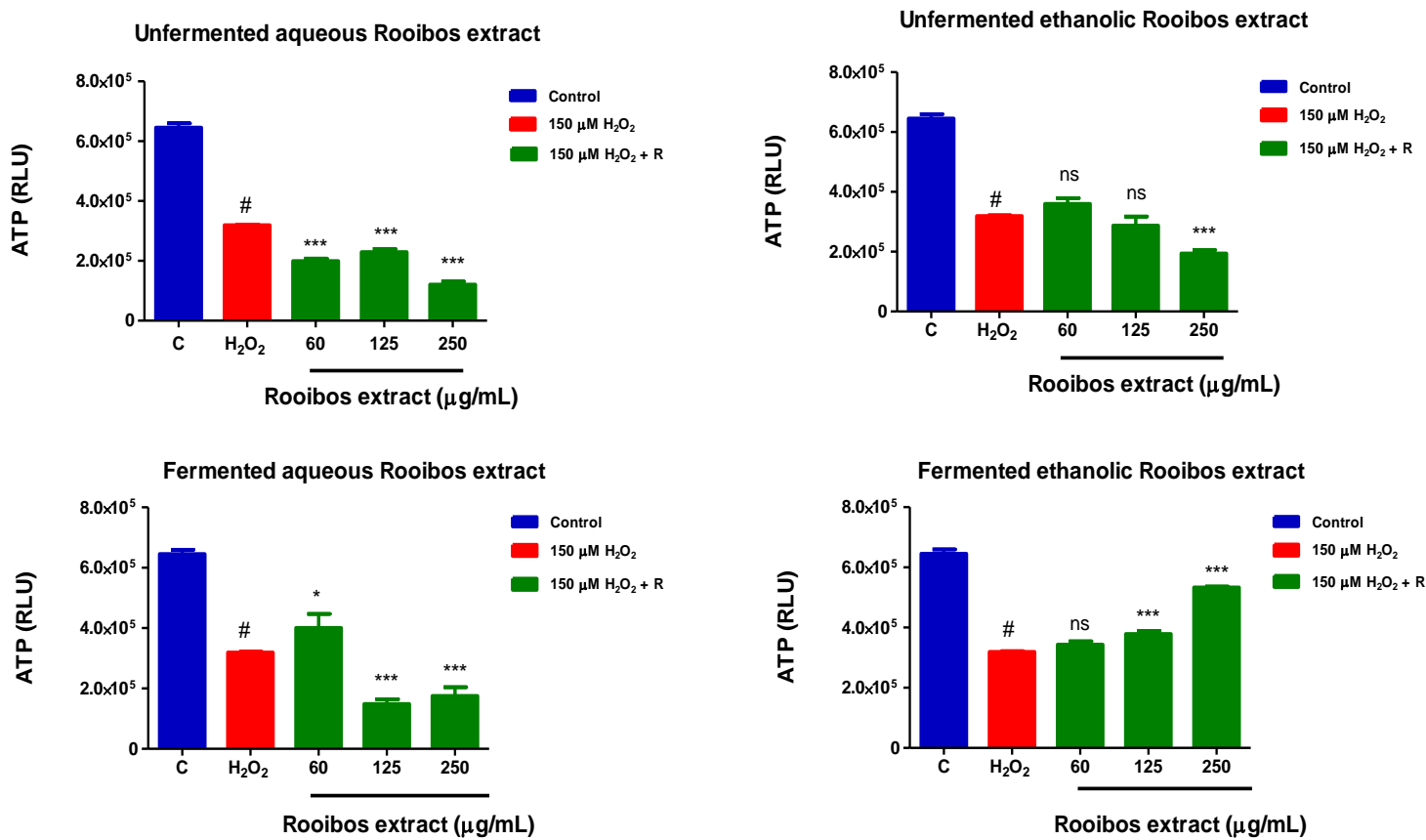


Figure 4.6: Analysis of the effect of 24- Rooibos extracts pretreatment followed by 3-hour H₂O₂ treatment on intracellular adenosine triphosphate (ATP) levels in SH-SY5Y cells.

The statistical significance is observed when cells were pre-treated with 60 μg/mL of fermented aqueous Rooibos extract, 125 and 250 μg/mL of fermented ethanolic Rooibos extract for 24 hrs. Hydrogen peroxide was applied at a concentration of 150 μM (3hrs), (#P≤0.001) when compared to control cells. Unfermented aqueous Rooibos extract (60, 125, 250 μg/mL), unfermented ethanolic Rooibos extract (250 μg/mL) and fermented aqueous Rooibos extract (125 and 250 μg/mL) significantly reduced cell viability compared to cells treated with H₂O₂ only. (*P≤0.05) and (**P≤0.001) when compared to cells treated with H₂O₂ only. Abbreviations: C = Control, R = Rooibos extract, ns = non statistically significant.

4.9. The effect of Rooibos extracts on oxidative damage biomarkers in SH-SY5Y cells

Oxygen radicals, a form of free radical, can cause irreversible severe damage to cellular structures and functions, eventually leading to cell death (Linden et al., 2008). The effects of Rooibos extracts on oxidative damage biomarkers against induced OS in SH-SY5Y cells were determined by measuring LPO and protein carbonylation.

4.9.1. The effect of the Rooibos extracts on lipid peroxidation in H₂O₂-challenged cultured SH-SY5Y cells.

The progression of LPO can be monitored by measuring products of LPO such as CDs and MDA (Devasagayam et al., 2003). The CD assay can be used to determine oxidation degree by measuring all conjugate forms of diene in the early stages of LPO (Li et al., 2023), while MDA, which reacts with TBA to form TBARS is one of the end products of OS, it is also widely known as a biomarker of LPO (Dotan et al., 2004; Li et al., 2023).

4.9.1.1. The effects of the Rooibos extracts on conjugated Dienes

The oxidation of fatty acids leads to CDs (Mehri, 2023), which can indicate the molecular reorganization of PUFAs during the early stages of LPO (Kodali et al., 2020). The change in CD levels observed between the 150 μ M H₂O₂ (3 hours) treatment and the control cells represents a significant increase with a mean difference of -122.9 μ mol/L (95 % CI= -159.7 to -86.1 μ mol/L; P \leq 0.001) (Figure 4.7). When cells were pre-treated with unfermented aqueous Rooibos extract at, 60, 125, and 250 μ g/mL, CD levels decreased significantly, with mean differences of 170.8 μ mol/L (95 % CI= 134.0 to 207.6 μ mol/L; P \leq 0.001), 139.7 μ mol/L (95 % CI= 102.9 to 176.5 μ mol/L; P \leq 0.001) and 163.9 μ mol/L (95 % CI= 127.1 to 200.7 μ mol/L; P \leq 0.001), respectively, compared to the H₂O₂ treatment. Unfermented ethanol Rooibos extract also significantly decreased at concentrations of 60, 125 and 250 μ g/mL, with mean differences of 219.3 μ mol/L (95 % CI= 178.7 to 259.8 μ mol/L; P \leq 0.001), 151.3 μ mol/L (95 % CI= 110.7 to 191.8 μ mol/L; P \leq 0.001) and 58.4 μ mol/L (95 % CI= 17.9 to 99.0 μ mol/L; P \leq 0.01), respectively, compared to the H₂O₂ treatment. Furthermore, when cells were pre-treated with fermented aqueous Rooibos extract, the extract significantly decreased CD levels at concentrations of 125 and 250 μ g/mL, with mean differences of 90.6 μ mol/L (95 % CI= 52.5 to 128.8 μ mol/L; P \leq 0.001), 131.2 μ mol/L (95 % CI= 93.0 to 169.3 μ mol/L; P \leq 0.001) respectively, compared to the H₂O₂ treatment. Fermented ethanol Rooibos extracts significantly also decreased CDs at concentrations of 60, 125 and 250 μ g/mL, with mean differences of 35.0 μ mol/L (95 % CI= 25.1 to 44.9 μ mol/L; P \leq 0.001), 56.7 μ mol/L (95 % CI= 46.9 to 66.5 μ mol/L; P \leq 0.001) and 136.2 μ mol/L (95 % CI= 126.4 to 146.1 μ mol/L; P \leq 0.001), respectively, compared to the H₂O₂ treatment.

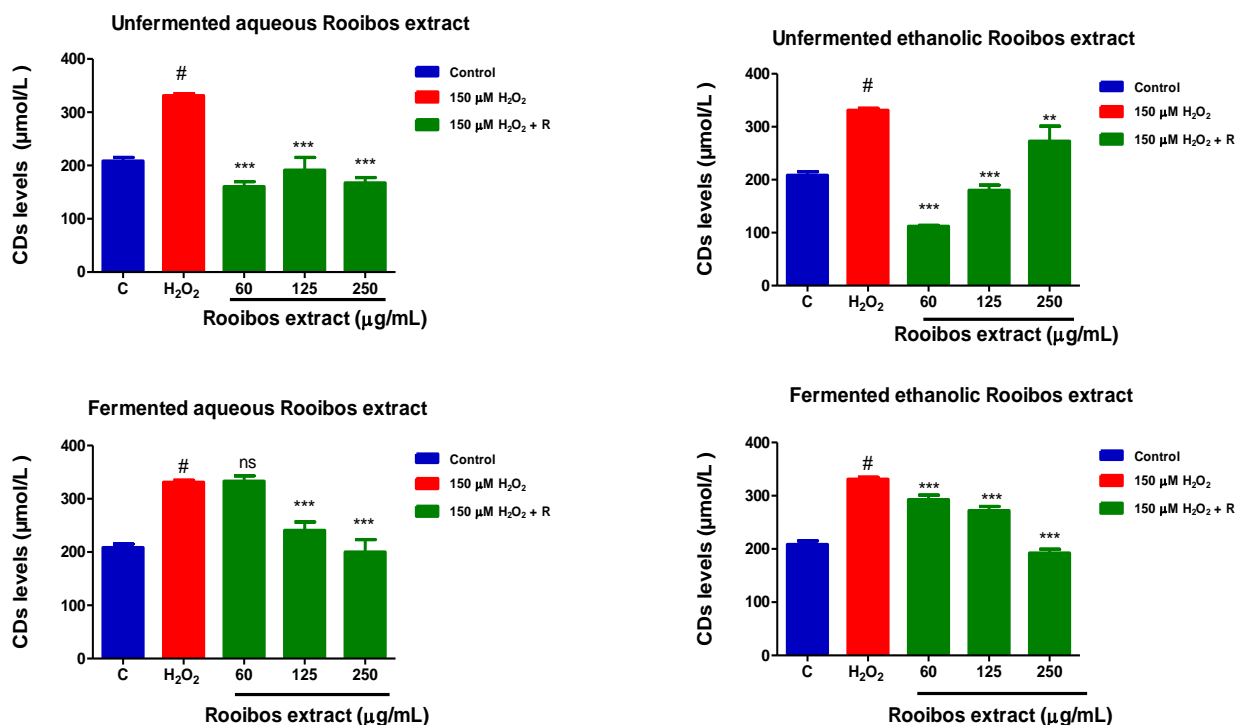


Figure 4.7: Conjugated diene levels in SH-SY5Y cells pre-treated with different concentrations of Rooibos extracts for 24 hours, followed by 150 μM H₂O₂ treatment for 3 hours.

The levels of CDs were significantly increased after the 150 μM H₂O₂ treatment. Conjugated diene levels significantly decreased in cells treated with unfermented aqueous Rooibos extract 60, 125, and 250 μg/mL, and unfermented ethanolic Rooibos extract 60, 125, and 250 μg/mL. A similar trend was observed in unfermented aqueous Rooibos extracts 125, and 250 μg/mL and fermented ethanolic Rooibos extracts 60, 125 and 125 μg/mL. The results show a statistically significant (#P≤0.001) decrease in CDs in H₂O₂-treated cells compared to control cells. (**P≤0.01), and (***)P≤0.001) when compared to cells treated only with H₂O₂. Abbreviations: C = Control, R = Rooibos extract, ns = non statistically significant.

4.9.1.2. The effect of Rooibos extracts on thiobarbituric acid reactive substances (TBARS)

Malondialdehyde (MDA) has been widely used as a marker of LPO in membrane and biological systems since the 1950s due to its facile reactivity with TBA (Hodges et al., 1999; Aguilar Diaz De Leon & Borges, 2020). In the current study, the results show that cells treated with H₂O₂ only had a significant decrease in MDA concentration when compared to the control with the mean difference of 0.1 μM (95 % CI= 0.09 μM to 0.11 μM; P≤0.001) (Figure 4.8). Thus, H₂O₂ at a cytotoxic concentration (150 μM) induced LPO in SH-SY5Y cells after 3 hours of exposure as measured by levels of MDA, a secondary product of PUFA oxidation but not in the expected

trends for toxicity. However, pre-treating cells with 250 µg/mL unfermented ethanolic Rooibos extract, 60 µg/mL fermented aqueous Rooibos extract, and 250 µg/mL fermented ethanolic extract (24 hours) followed by 150 µM H₂O₂ (3 hours) increased MDA concentration compared to H₂O₂ alone treated cells with mean differences of -0.05 µM (95 % CI= -0.06 µM to -0.04 µM; P≤0.001), -0.03 µM (95 % CI= -0.05 µM to -0.007 µM; P≤0.01) and -0.07 µM (95% CI= -0.08 µM to -0.05 µM; P≤0.001), respectively.

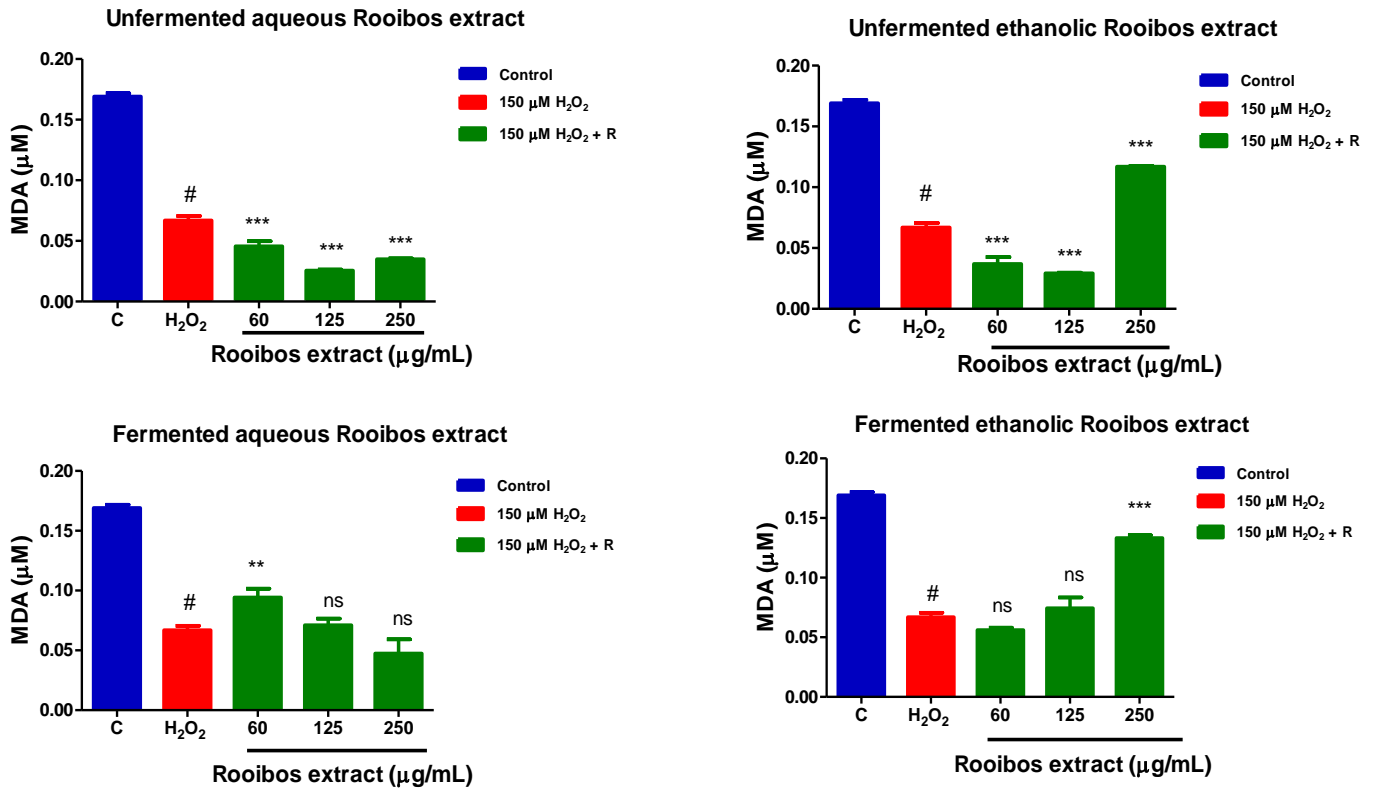


Figure 4.8: Malondialdehyde (MDA) levels in SH-SY5Y cells treated for 24 hours with different concentrations of Rooibos extracts, followed by 3 hours with 150 µM H₂O₂.

The results show a statistically significant (#P≤0.001) decrease in MDA levels in H₂O₂-treated cells (H₂O₂ at cytotoxic concentrations did not induce LPO). The MDA levels increased in cells treated with unfermented ethanolic Rooibos extract 250 µg/mL, with fermented aqueous Rooibos extract 60 µg/mL and fermented ethanolic Rooibos extract 250 µg/mL. While the MDA levels decreased in cells treated with unfermented aqueous Rooibos extract 60, 125, and 250 µg/mL and unfermented ethanolic Rooibos extract 60 and 125 µg/mL. The results show a statistically significant (*P≤0.05), (**P≤0.01), and (***)P≤0.001) when compared to cells treated only with H₂O₂. Abbreviations: C = Control, R = Rooibos extract, ns = non statistically significant.

4.9.2. The effects of Rooibos Extracts on Protein Carbonylation in H₂O₂-challenged cultured SH-SY5Y cells.

To determine the effect of H₂O₂ inducing more oxidative damage to cellular proteins in SH-SY5Y cells, protein carbonyl was assessed. Treatment of SH-SY5Y cells with 150 µM H₂O₂ (3 hours) increased protein carbonyl levels compared to the control by a mean difference of -0.1 nmol/mg protein (95 % CI= -0.2 nmol/mg protein to -0.03 nmol/mg protein; P ≤ 0.001) and pre-treatment with unfermented aqueous extract (250 µg/mL) and ethanol extract (125 µg/mL and 250 µg/mL) significantly reduced this in cell lysates (Figure 4.9). When compared to the H₂O₂ treatment, a 250 µg/mL unfermented aqueous Rooibos extract significantly reduced protein carbonyl levels by 0.1 nmol/mg protein (95 % CI= 0.04 nmol/mg protein to 0.17 nmol/mg protein; P≤0.01). Similarly, at a concentration of 125 µg/mL and 250 µg/mL of unfermented ethanol Rooibos extract, carbonyl protein levels were significantly reduced compared to the H₂O₂ with mean differences of 0.09 nmol/mg protein (95 % CI= 0.04 nmol/mg protein to 0.14 nmol/mg protein; P≤0.001) and 0.06 nmol/mg protein (95 % CI= 0.01 nmol/mg protein to 0.1 nmol/mg protein; P≤0.05) respectively. However, unfermented aqueous with a mean difference of -0.5 nmol/mg protein (95 % CI= -0.6 nmol/mg protein to -0.5 nmol/mg protein; P≤0.001) and ethanolic with mean difference of -0.2 nmol/mg protein (95 % CI= -0.3 nmol/mg protein to -0.2 nmol/mg protein; P≤0.001) significantly increased protein carbonyl levels. Rooibos extracts at 60 µg/mL and 125 µg/mL with mean differences of and -0.2 nmol/mg protein (95 % CI= -0.2 nmol/mg protein to -0.1 nmol/mg protein; P≤0.001) significantly increased protein carbonyl levels. Fermented aqueous Rooibos extract at 125 and 250 µg/mL significantly increased protein carbonyl levels with mean differences of -0.2 nmol/mg protein (95 % CI= -0.2 nmol/mg protein to -0.1 nmol/mg protein; P ≤ 0.001) and -0.2 nmol/mg protein (95 % CI= -0.2 nmol/mg protein to -0.1 nmol/mg protein; P≤0.001) respectively. At 60 µg/mL, fermented ethanolic and aqueous Rooibos extracts with mean differences of -0.18 nmol/mg protein (95 % CI= -0.2 nmol/mg protein to -0.16 nmol/mg protein; P≤0.001), and -0.2 nmol/mg protein (95 % CI= -0.3 nmol/mg protein to -0.2 nmol/mg protein; P≤0.001) respectively, significantly increased protein carbonyl levels.

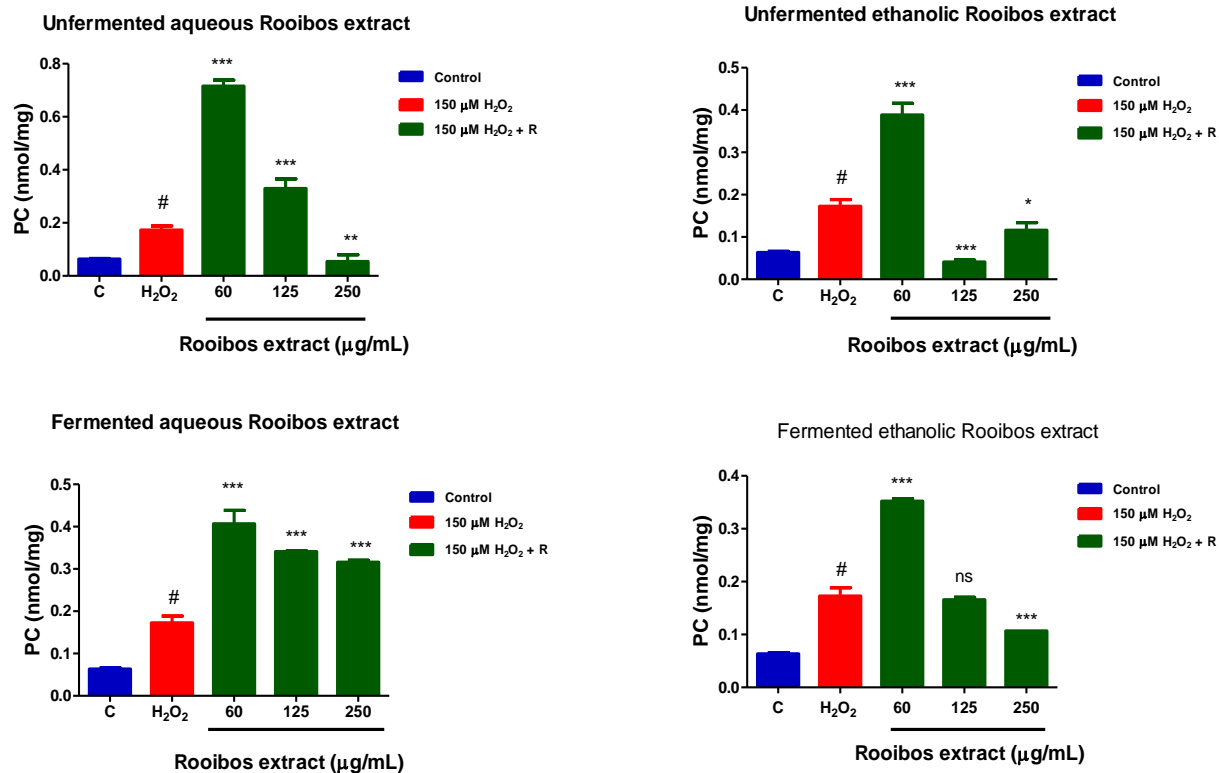


Figure 4.9: The effects of 24-hour treatment of Rooibos extracts, followed by on protein damage in 150 μM H₂O₂ (3 hours) - challenged cultured SH-SY5Y cells.

The results show a significant (# $P \leq 0.001$) increase in protein carbonyls (PCs) which are established biomarkers of protein oxidation, was observed in H₂O₂-treated cells compared to control cells. Significant increases were also observed in cells pre-treated with 60 and 250 μg/mL of unfermented aqueous Rooibos extract, 60 μg/mL unfermented ethanolic Rooibos extract, 60, 125 and 250 μg/mL of fermented aqueous Rooibos extract, and 60 μg/mL of fermented aqueous compared to cells treated only with H₂O₂. However, statistically significant decrease was observed in cells pre-treated with 250 μg/mL of unfermented aqueous Rooibos extract, 125 and 250 μg/mL of unfermented ethanolic Rooibos extract and 250 μg/mL of fermented ethanolic Rooibos extract compared to cells treated only with H₂O₂. The results show a statistically significant (* $P \leq 0.05$), (** $P \leq 0.01$), and (***) $P \leq 0.001$) when compared to cells treated only with H₂O₂. Abbreviations: C = Control, R = Rooibos extract, ns = non statistically significant.

4.10. The effects of Rooibos extracts on reduced glutathione (GSH) in H₂O₂-challenged cultured SH-SY5Y cells.

Luminometric analysis of GSH, a prominent endogenous antioxidant molecule presents in cells, revealed a significant decrease in reduced GSH in SH-SY5Y cells challenged with H₂O₂, with a mean difference of 10.5 μ M (95 % CI= 6.9 μ M to 14.1 μ M; P \leq 0.001) compared to the control (Figure 4.10). when cells pretreated with unfermented aqueous Rooibos extracts at 60, 125 and 250 μ g/mL statistically significant decreased GSH levels with mean differences of 4.5 μ M (95 % CI= 1.5 μ M to 7.6 μ M; P \leq 0.01), 4.8 μ M (95 % CI= 1.8 μ M to 7.8 μ M; P \leq 0.001) and 10.0 μ M (95 % CI= 7.0 μ M to 13.0 μ M; P \leq 0.001) respectively compared to the cells treated with H₂O₂ only. However, when cells were pre-treated with unfermented ethanolic Rooibos extract at the lowest concentration (60 μ g/mL), there was a statistically significant increase in GSH levels with a mean difference of -2.5 μ M (95 % CI= -5.00 μ M to -0.04 μ M; P \leq 0.05) when compared to the H₂O₂ treatment. Furthermore, when cells were pre-treated with unfermented ethanolic Rooibos extract at 125 and 250 μ g/mL, there was a statistically significant decrease in GSH levels with a mean difference of 8.6 μ M (95 % CI= 6.1 μ M to 11.0 μ M; P \leq 0.001) and 8.2 μ M (95 % CI= 5.7 μ M to 10.7 μ M; P \leq 0.001) respectively when compared to the H₂O₂ treatment. Cells pretreated with fermented aqueous Rooibos extracts at 60, 125 and 250 μ g/mL statistically significant decreased GSH levels with mean differences of 5.7 μ M (95 % CI= 2.1 μ M to 9.3 μ M; P \leq 0.01), 8.5 μ M (95 % CI= 4.9 μ M to 12.0 μ M; P \leq 0.001) and 8.6 μ M (95 % CI= 5.1 μ M to 12.2 μ M; P \leq 0.001) respectively compared to the cells treated with H₂O₂ only. The GSH levels for the cells pretreated with fermented ethanolic Rooibos extracts at 60, and 125 μ g/mL were not statistically significant (P \geq 0.05) with those that were treated with H₂O₂ only. However, those that were treated with 250 μ g/mL of fermented ethanolic Rooibos extract had a statistically significant decreased GSH levels with a mean difference of 11.3 μ M (95 % CI= 6.9 μ M to 15.7 μ M; P \leq 0.001) compared to those that were treated with H₂O₂ only.

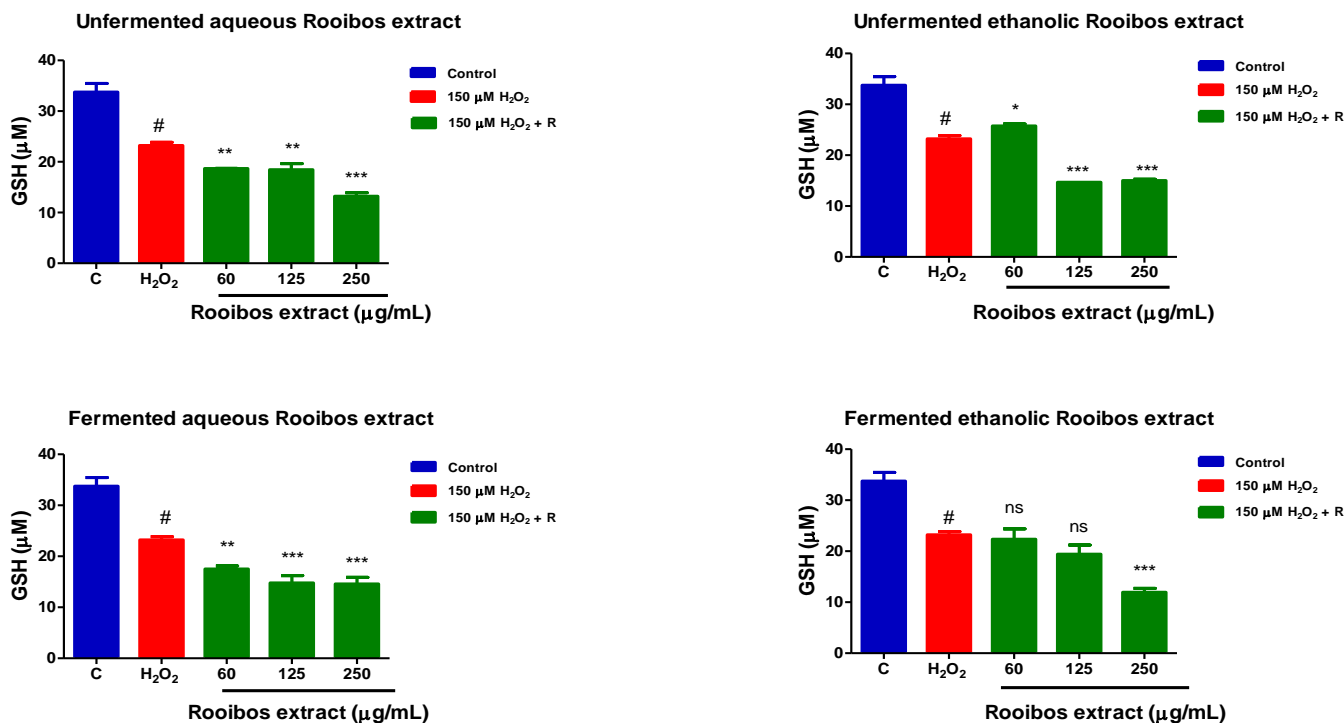


Figure 4.10: Effects of Rooibos extracts on reduced glutathione (GSH) levels in SH-SY5Y cells treated for 24 hours with different concentrations of Rooibos extracts, followed by 3 hours with 150 μM H₂O₂.

The results show a statistically significant ($\#P \leq 0.001$) decrease in GSH in H₂O₂-treated cells. Both unfermented and fermented aqueous Rooibos extracts at 60, 125 and 250 μg/mL statistically significant decreased GSH levels compared with H₂O₂-treated cells. Likewise cells pre-treated with fermented ethanolic Rooibos extracts at 125 and 250 μg/mL statistically significant ($***P \leq 0.001$) decreased GSH levels compared with H₂O₂-treated cells. However cells pretreated with fermented ethanolic Rooibos extracts at 60 μg/mL statistically significant ($*P \leq 0.05$) increased GSH levels compared with H₂O₂-treated cells. Cells pretreated with fermented ethanolic Rooibos extract at 60 and 125 μg/mL were not statistically significant ($^{ns} P \geq 0.05$) compared with H₂O₂-treated cells in GSH levels. However cells pre-treated with fermented ethanolic Rooibos at 250 μg/mL significantly significant ($***P \leq 0.001$) decreased GSH compared to H₂O₂. Abbreviations: C = Control, R = Rooibos extract, ns = non statistically significant.

4.11. The effect of Rooibos extracts pre-treatment on SOD activity in SH-SY5Y cells exposed to 150 μM H₂O₂ for 3 hours.

The consequences of OS are serious, as evidenced by the increased activity of enzymes involved in O₂ detoxification (Alía et al., 2005). Indeed, several lines of evidence support the notion that SODs have a defence function. Thus, they are induced by O₂ exposure (Fridovich, 1986). In the current study, the quantification and detection of SOD activity in cell lysates confirmed that 150 μM H₂O₂ for 3 hours significantly increased the SOD activity in SH-SY5Y cells, with a mean difference of -0.8 units/mL (95 % CI= -1.2 to -0.4 units/mL; $P \leq 0.001$) compared to the control cells (Figure 4.11). When cells were pre-treated with unfermented aqueous Rooibos extract at 125 μg/mL, the SOD activity decreased significantly, with a mean difference of 1.5 units/mL (95

% CI= 1.1 to 1.9 U/mL; $P \leq 0.001$) compared to the H_2O_2 treatment. Unfermented ethanol Rooibos extract also significantly decreased at concentrations of 60 $\mu\text{g/mL}$, with mean differences of 1.3 units/mL (95 % CI= 0.9 to 1.7 U/mL; $P \leq 0.001$) compared to the H_2O_2 treatment. While, when cells were pre-treated with fermented aqueous Rooibos extract significantly decreased SOD activity at concentrations of 60 and 125 $\mu\text{g/mL}$, with mean differences of 1.1 U/mL (95 % CI= 0.7 to 1.5 U/mL; $P \leq 0.001$) and 1.1 U/mL (95 % CI= 0.7 to 1.5 U/mL; $P \leq 0.001$) respectively, compared to the H_2O_2 treatment. Fermented ethanol Rooibos extracts significantly decreased SOD activity at concentrations of 60 and 250 $\mu\text{g/mL}$, with mean differences of 1.1 U/mL (95 % CI= 0.7 to 1.5 U/mL; $P \leq 0.001$) and 1.0 U/mL (95 % CI= 0.6 to 1.4 U/mL; $P \leq 0.001$) respectively, compared to the H_2O_2 treatment.

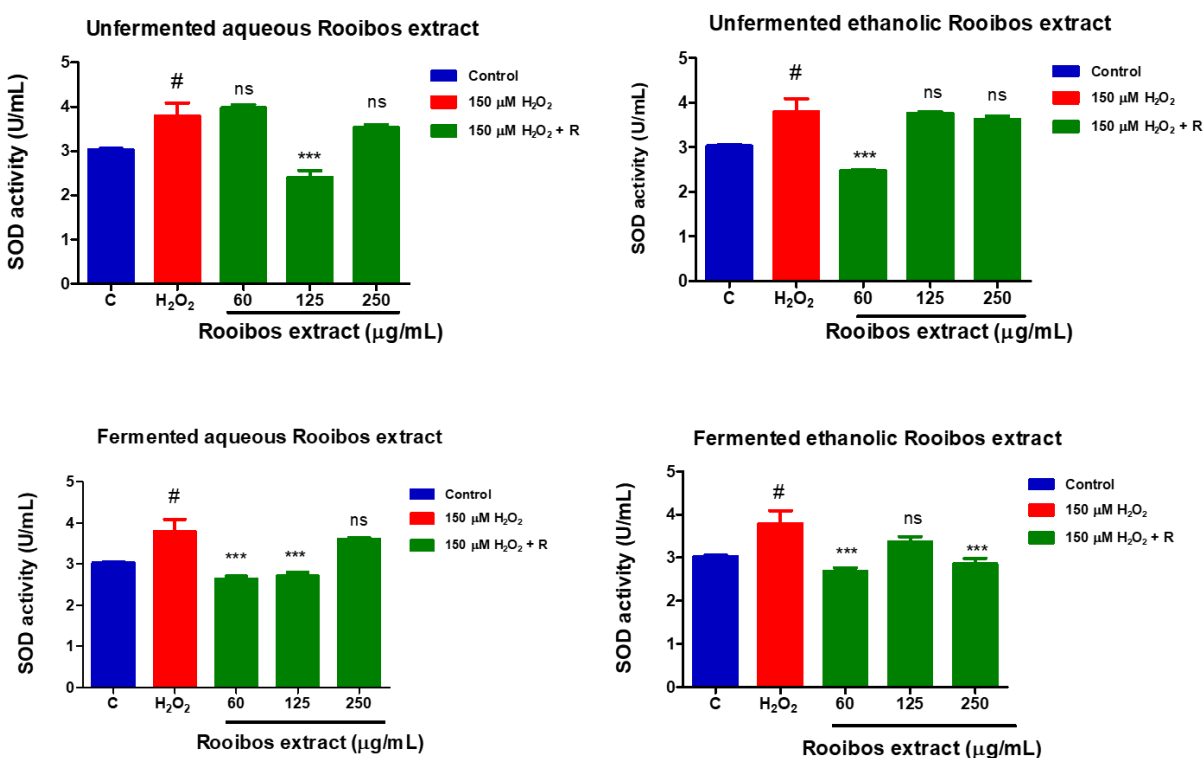


Figure 4.11: The superoxide dismutase (SOD) activity in SH-SY5Y cells pre-treated with different concentrations of Rooibos extracts for 24 hours, followed by 150 μM H_2O_2 treatment for 3 hours.

The SOD activity significantly increased when the cells were treated with 150 μM H_2O_2 . A decrease in SOD activity was observed in cells treated with unfermented aqueous Rooibos extract 125 $\mu\text{g/mL}$, unfermented ethanolic Rooibos extract 60 $\mu\text{g/mL}$, and fermented aqueous Rooibos extract extracts 60 and 125 $\mu\text{g/mL}$, while fermented ethanolic Rooibos extracts 60 and 250 $\mu\text{g/mL}$. The results show a statistically significant ($\#P \leq 0.001$) increase in SOD activity in H_2O_2 -treated cells compared to control cells. ($***P \leq 0.001$) when compared to cells treated only with H_2O_2 . ($\#P \leq 0.001$), ($*P \leq 0.05$) and ($***P \leq 0.001$). Abbreviations: C = Control, R = Rooibos extract, ns = non statistically significant.

4.12. The effects of Rooibos extracts pre-treatment on CAT activity in SH-SY5Y cells exposed to 150 μM H_2O_2 for 3 hours

Catalase (CAT) is a highly active enzyme with four groups of heme-containing iron that facilitates the enzyme's interaction with its substrate, H_2O_2 (Grodner et al., 2022; Shahraki et al., 2023). Catalase inactivation is known to have some deleterious effects and can lead to diseases such as NDDs. When CAT is inactivated, H_2O_2 accumulates in the cell, and increased ROS can lead to cell death (Shahraki et al., 2023). In the current study, the quantification and detection of CAT activity in cell lysates confirmed that 150 μM H_2O_2 for 3 hours resulted in a significant decrease in CAT activity in SH-SY5Y cells, with a mean difference of 143.8 units/mL (95 % CI= 114.4 to 173.1 units/mL; $P \leq 0.001$) compared to the control cells (Figure 4.12). When cells were pre-treated with unfermented aqueous Rooibos extract at the lowest concentration (60 $\mu\text{g}/\text{mL}$), the CAT activity increased significantly, with a mean difference of -46.5 units/mL (95 % CI= -75.90 to -17.14 units/mL; $P \leq 0.01$) compared to the H_2O_2 treatment. However, when cells were pre-treated with unfermented aqueous Rooibos extract at 125 and 250 $\mu\text{g}/\text{mL}$, the CAT activity decreased significantly, with mean differences of 91.3 units/mL (95 % CI= 61.9 to -120.7 units/mL; $P \leq 0.001$) and 202.8 units/mL (95 % CI= 173.5 to 232.2 units/mL; $P \leq 0.001$) respectively compared to the H_2O_2 treatment. Unfermented ethanol Rooibos extract also significantly increased at concentrations of 60 and 125 $\mu\text{g}/\text{mL}$, with mean differences of -138.7 U/mL (95 % CI= -150.7 U/mL to -126.8 U/mL; $P \leq 0.001$) and -18.0 U/mL (95 % CI= -29.96 U/mL to -6.044 U/mL; $P \leq 0.01$), respectively compared to the H_2O_2 treatment. However, when cells were pre-treated with unfermented ethanolic Rooibos extract at 250 $\mu\text{g}/\text{mL}$, the CAT activity decreased significantly, with a mean difference of 50.7 units/mL (95 % CI= 38.8 to 62.7 units/mL; $P \leq 0.001$) compared to the H_2O_2 treatment. Statistical significance decrease in CAT activity was observed when cells were pretreated with fermented aqueous Rooibos extract at 60, 125 and 250 $\mu\text{g}/\text{mL}$ with mean differences of 105.1 U/mL (95 % CI= -69.3 U/mL to 140.9 U/mL; $P \leq 0.001$), 105.1 U/mL (95 % CI= 45.8 U/mL to 117.3 U/mL; $P \leq 0.001$) and 150.6 U/mL (95 % CI= 114.9 U/mL to 186.4 U/mL; $P \leq 0.001$) respectively compared to the H_2O_2 treatment. However, fermented ethanol Rooibos extract significantly increased CAT activity at concentrations of 60 and 125 $\mu\text{g}/\text{mL}$, with mean differences of -133.3 U/mL (95 % CI= -152.5 U/mL to -114.1 U/mL; $P \leq 0.001$) and -65.8 U/mL (95 % CI= -85.0 U/mL to -46.6 U/mL; $P \leq 0.01$), respectively compared to the H_2O_2 treatment. Non statistical significance in CAT activity was observed when cells were pretreated with 250 $\mu\text{g}/\text{mL}$ fermented ethanol Rooibos extract compared with the H_2O_2 treatment.

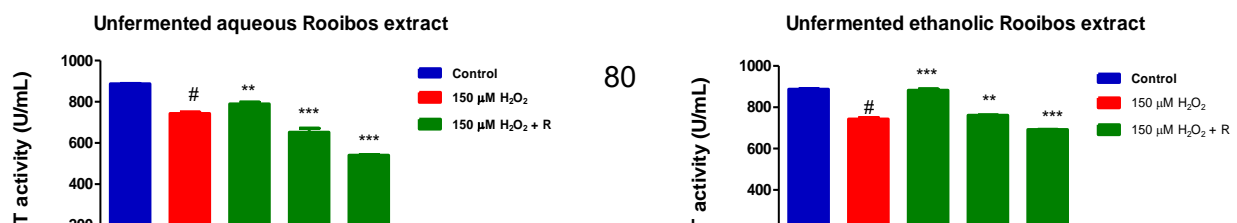


Figure 4.12: Catalase (CAT) activity in SH-SY5Y cells pre-treated with different concentrations of Rooibos extracts for 24 hours, followed by 150 μM H_2O_2 treatment for 3 hours.

*The CAT activity was statistically significantly ($\#P \leq 0.001$) decreased after treatment with 150 μM H_2O_2 compared to control cells. The CAT activity statistically significantly ($**P \leq 0.01$) and ($***P \leq 0.001$) increased in cells treated with unfermented aqueous Rooibos extract 60 $\mu\text{g}/\text{mL}$, unfermented ethanolic Rooibos extract 60 and 125 $\mu\text{g}/\text{mL}$, and fermented ethanolic Rooibos extract 60 and 125 $\mu\text{g}/\text{mL}$. The results also showed statistically significant ($***P \leq 0.001$) decrease in CAT activity in 125 and 250 $\mu\text{g}/\text{mL}$ unfermented aqueous Rooibos extract treated cells compared to cells treated only with H_2O_2 . However, unfermented ethanolic Rooibos extract at 250 $\mu\text{g}/\text{mL}$ statistically significantly ($***P \leq 0.001$) decreased the CAT activity compared to cells treated only with H_2O_2 . Non statistically significantly in CAT activity was observed in cells pretreated with 250 $\mu\text{g}/\text{mL}$ fermented ethanolic Rooibos compared to H_2O_2 treated cells. While cells pretreated with 60, 125 and 250 $\mu\text{g}/\text{mL}$ fermented aqueous Rooibos extract the CAT activity statistically significantly decreased ($***P \leq 0.001$) when compared to cells treated only with H_2O_2 . Abbreviations: C = Control, R = Rooibos extract, ns = non statistically significant.*

4.13. Cellular Death

4.13.1. Effects of Rooibos extract pre-treatment on H_2O_2 -induced caspase-8, -9, and -3/7 activation in SH-SY5Y cells exposed to 150 μM H_2O_2 for 3 hours.

The apoptotic molecular machinery is well understood, and it is critical that caspase, a unique family of cysteine proteases, be activated (Morana et al., 2022). The current study found that treating SH-SY5Y cells with 150 μM H_2O_2 for 3 hours reduced caspase -8, -9, and -3/7 activity significantly when compared to the control with the mean differences of 4.7×10^4 RLU (95 % CI= 1.6×10^3 RLU to 9.3×10^4 RLU; $P \leq 0.05$), 2.6×10^5 RLU (95 % CI= 2.0×10^5 RLU to 3.2×10^5 RLU; $P \leq 0.001$) and 2.9×10^3 RLU (95 % CI= 1.2×10^3 RLU to 4.5×10^3 RLU; $P \leq 0.01$),

respectively. Thus, caspases -8, -9, and -3/7 were not activated in SH-SY5Y cells after 3 hours of treatment with 150 μM H_2O_2 (Figure 4.13, Figure 4.14 and Figure 4.15). However, unfermented, and fermented Rooibos extracts dramatically reduced caspase-8 and caspase-9 activities when compared to treatment of SH-SY5Y cells with 150 μM H_2O_2 (3 hours), respectively. While caspase -3/7 activity was significantly increased when cells were pretreated with unfermented ethanol Rooibos extract (250 $\mu\text{g}/\text{mL}$), fermented aqueous Rooibos (125, 250 $\mu\text{g}/\text{mL}$), and fermented ethanolic Rooibos (60, 125, and 250 $\mu\text{g}/\text{mL}$) compared to treatment of SH-SY5Y cells with 150 μM H_2O_2 (3 hours).

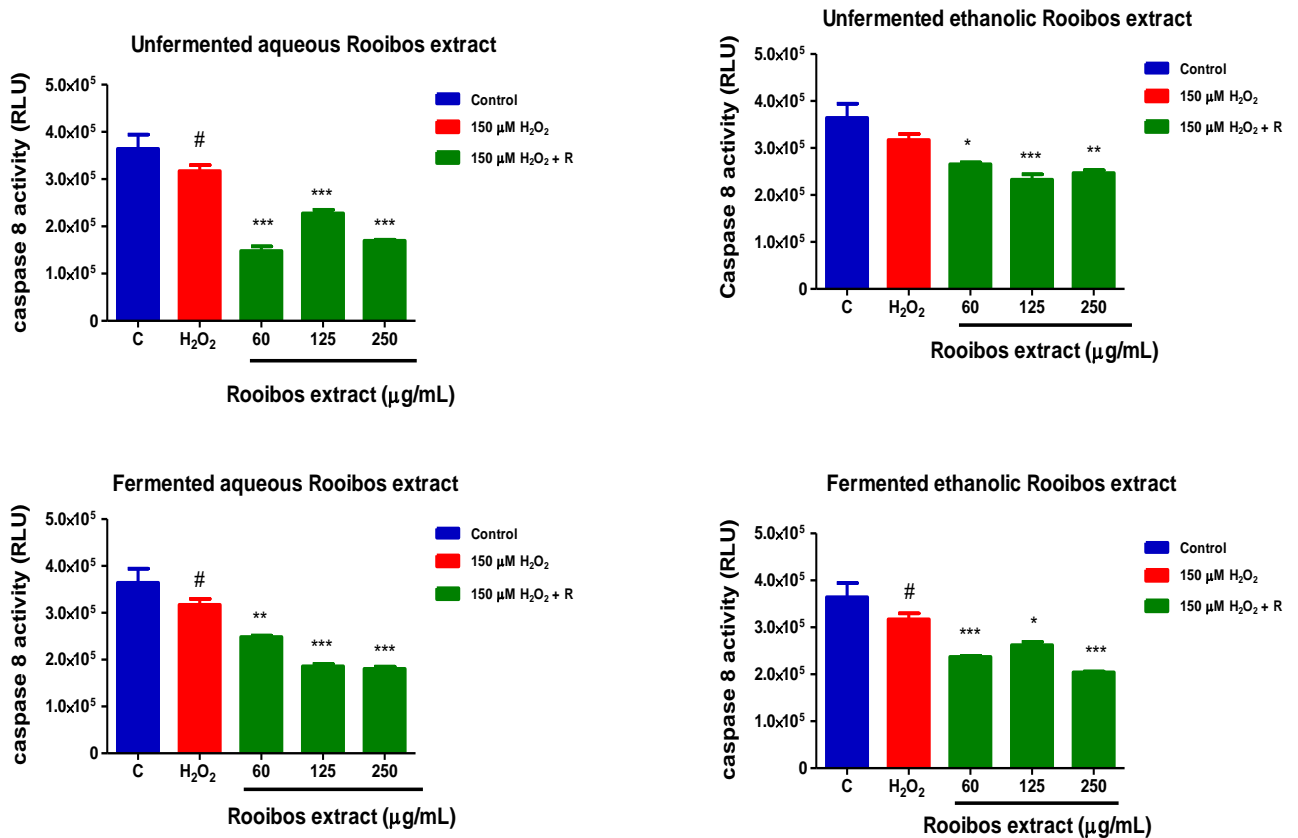


Figure 4.13: Caspase 8 activity in SH-SY5Y cells pre-treated with different concentrations of Rooibos extracts for 24 hours, followed by 150 μM H_2O_2 treatment for 3 hours.

The results show a statistically significant ($\#P \leq 0.001$) decrease in caspase 8 activity in H_2O_2 -treated cells. Caspase 8 activity decreased in cells treated with unfermented aqueous Rooibos extract 60, 125 and 250 $\mu\text{g}/\text{mL}$, unfermented ethanolic Rooibos extract 60, 125, and 250 $\mu\text{g}/\text{mL}$, fermented aqueous Rooibos extract 60, 125 and 250 $\mu\text{g}/\text{mL}$, and fermented ethanolic Rooibos extract 60, 125, and 250 $\mu\text{g}/\text{mL}$. The results show a statistically significant ($*P \leq 0.05$), ($**P \leq 0.01$), and ($***P \leq 0.001$) when compared to cells treated only with H_2O_2 . Abbreviations: C = Control, R = Rooibos extract. ns = non statistically significant.

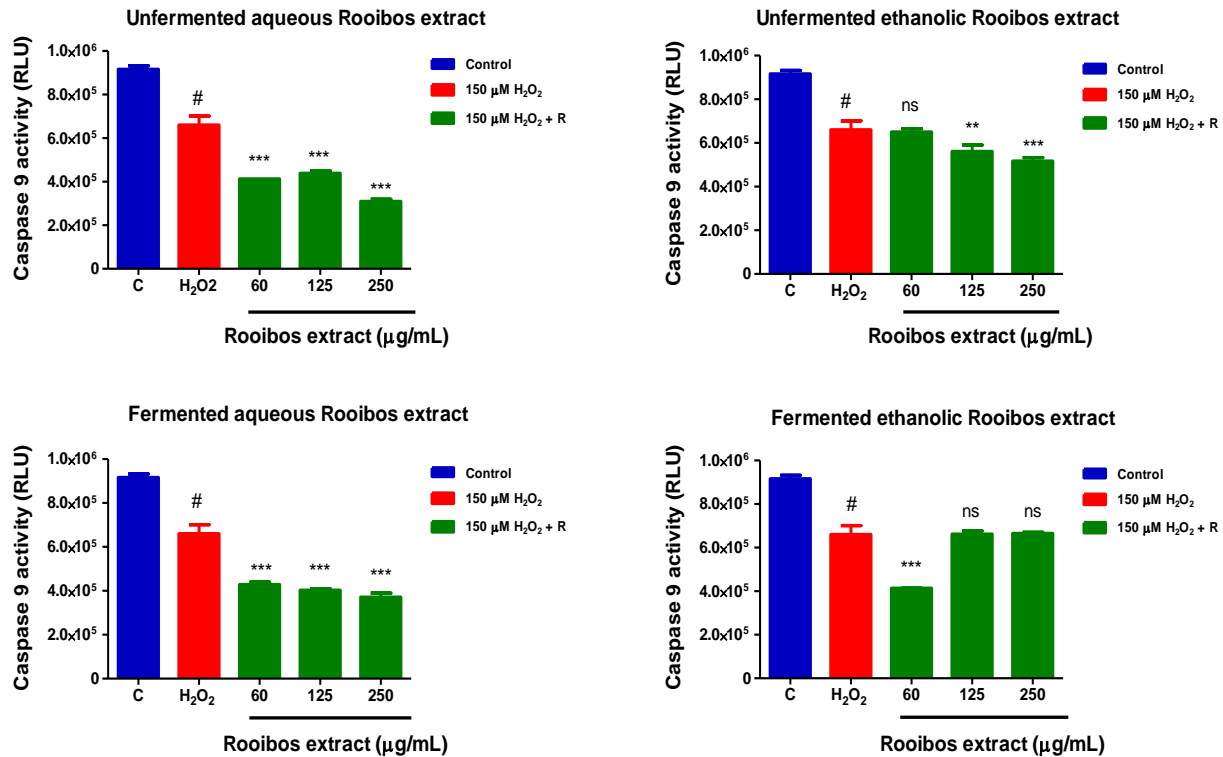


Figure 4.14: Caspase 9 activity in SH-SY5Y cells pre-treated with different concentrations of Rooibos extracts for 24 hours, followed by 150 μM H₂O₂ treatment for 3 hours.

The results show a statistically significant (# $P \leq 0.001$) decrease in caspase 9 activity in H₂O₂-treated cells. Caspase 9 activity decreased in cells treated with unfermented aqueous Rooibos extract 60, 125, and 250 μg/mL, unfermented ethanolic Rooibos extract 125 and 250 μg/mL, fermented aqueous Rooibos extract 60, 125, and 250 μg/mL, and fermented ethanolic Rooibos extract 60 μg/mL. The results show a statistically significant (** $P \leq 0.01$) and (***) $P \leq 0.001$) when compared to cells treated only with H₂O₂. Abbreviations: C = Control, R = Rooibos extract, ns = non statistically significant.

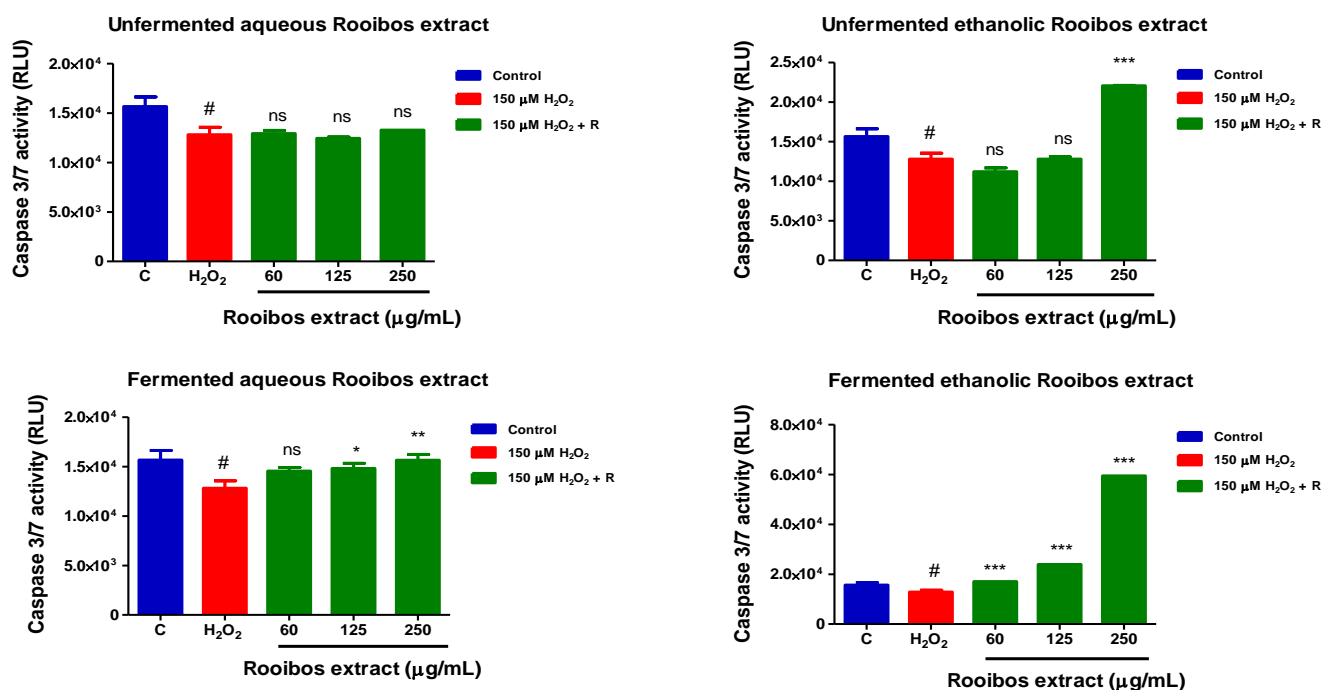


Figure 4.15: Caspase 3/7 activity in SH-SY5Y cells pre-treated with different concentrations of Rooibos extracts for 24 hours, followed by 150 μM H_2O_2 treatment for 3 hours.

The results show a statistically significant ($\#P \leq 0.001$) decrease in caspase 3/7 activity in H_2O_2 -treated cells. Caspase 3/7 activity increased in cells treated with unfermented ethanolic Rooibos extract 250 $\mu\text{g}/\text{mL}$, with fermented aqueous Rooibos extract 125 and 250 $\mu\text{g}/\text{mL}$, and fermented ethanolic Rooibos extract 60, 125, and 250 $\mu\text{g}/\text{mL}$. The results show a statistically significant ($*P \leq 0.05$), ($**P \leq 0.01$), and ($***P \leq 0.001$) when compared to cells treated only with H_2O_2 . Abbreviations: C = Control, R = Rooibos extract, ns = non statistically significant.

4.13.2. Effects of Rooibos extract pre-treatment on H_2O_2 -induced LDH activation in SH-SY5Y cells exposed to 150 μM H_2O_2 for 3 hours.

The LDH assay exhibits linearity, therefore, it can be used to calculate the proportion of necrotic cells in a sample (Chan, Francis Ka-Ming, Kenta Moriwaki, 2013). The current study revealed that cells treated with H_2O_2 only had a 0.1 OD (95 % CI= 0.06 OD to 0.2 OD; $P \leq 0.001$) decrease in LDH activity when compared to the control. (Figure 4.16). Thus, the LDH activity at H_2O_2 at cytotoxic concentration was detected but not in the expected way for toxicity. However, unfermented ethanolic Rooibos extract (125 and 250 $\mu\text{g}/\text{mL}$), fermented aqueous Rooibos extract (60 $\mu\text{g}/\text{mL}$), and fermented ethanolic Rooibos extract (60, 125, and 250 $\mu\text{g}/\text{mL}$) significantly ($*P \leq 0.05$), ($**P \leq 0.01$), and ($***P \leq 0.001$) increased LDH activity compared to H_2O_2 , but not the control.

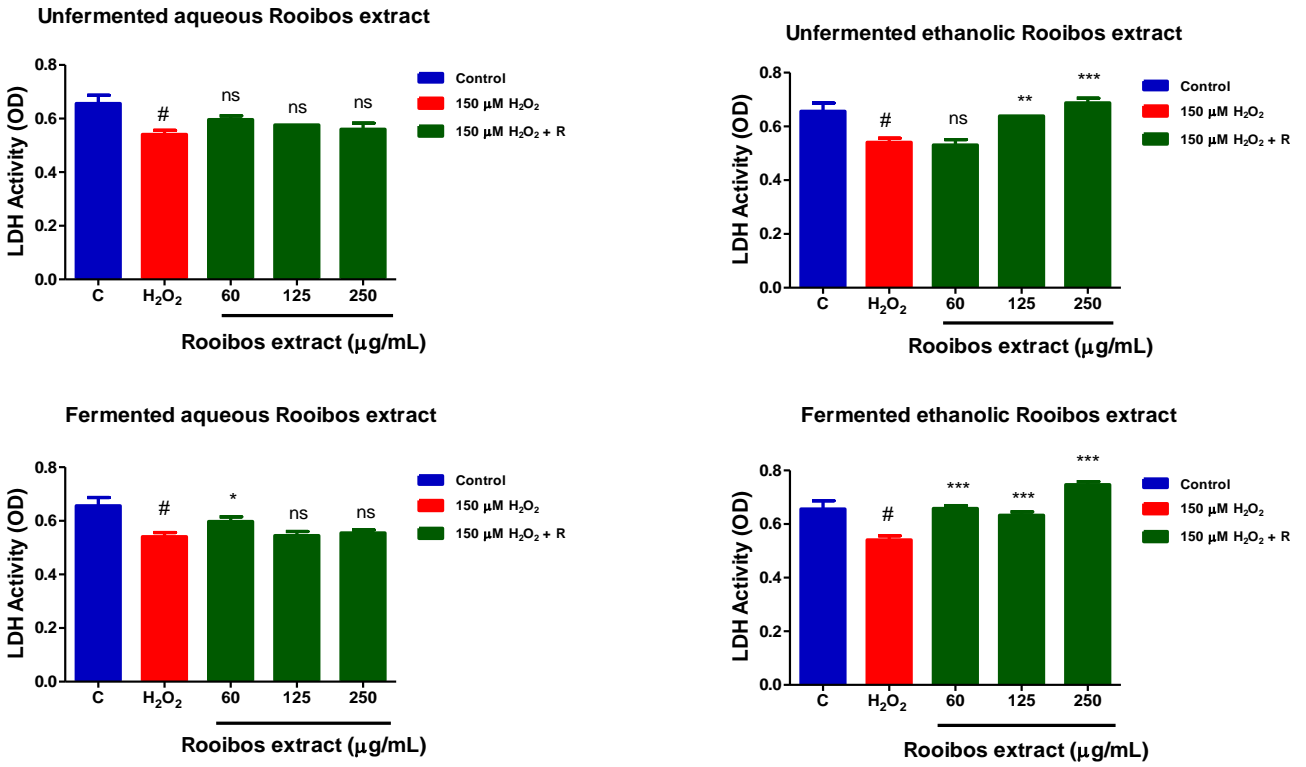


Figure 4.16: The lactate dehydrogenase (LDH) activity in SH-SY5Y cells pre-treated with different concentrations of Rooibos extracts for 24 hours, followed by 150 μM H₂O₂ treatment for 3 hours.

The results show a statistically significant ($\#P \leq 0.001$) decrease in caspase LDH activity in H₂O₂-treated cells (H₂O₂ at cytotoxic concentration did not activate LDH). The LDH activity increased in cells treated with unfermented ethanolic Rooibos extract 125 and 250 μg/mL, with fermented aqueous Rooibos extract 60 μg/mL, and fermented ethanolic Rooibos extract 60, 125 and 250 μg/mL. The results show a statistically significant ($*P \leq 0.05$), ($**P \leq 0.01$), and ($***P \leq 0.001$) when compared to cells treated only with H₂O₂. Abbreviations: C = Control, R = Rooibos extract, ns = non statistically significant.

5. CHAPTER FIVE: DISCUSSION

The growing incidence of NDDs has driven intensive research into possible therapeutic interventions. Among these, natural compounds have gained attention for their antioxidant properties and their potential to mitigate OS, a key contributor to neural cell damage and death. In this context, the present study delves into the neuroprotective effects of Rooibos (*Aspalathus linearis*) extracts, exploring their effect on H₂O₂-induced cytotoxicity in human neuroblastoma SH-SY5Y cells.

Several studies have shown that uncontrolled ROS generation in the brain, exceeding maximum cellular capacity, increases the risk of injury and death of neural cells (Briyal et al., 2023; Fadzil et al., 2023; Olufunmilayo et al., 2023). Therefore, it is reasonable to anticipate that enhancing endogenous antioxidant systems may play an essential role in leveraging novel drug delivery systems to target medications for neurodegeneration prevention (Fadzil et al., 2023; Olufunmilayo et al., 2023).

South African Rooibos (*Aspalathus linearis*), sometimes known as herbal tea, has been related to neuroprotective effects. However, little research has been undertaken directly on nervous system cells or in pre-clinical *in vivo* models of neurodegeneration, indicating the need for additional research (Pyrzanowska, 2022).

Rooibos contains a well-established broad spectrum of phytochemical compounds some of which exhibit AOC (Hussein et al., 2022; Pyrzanowska, 2022). Furthermore, while the chemistry of fermented and unfermented Rooibos differs, both have demonstrated antioxidant activity (Popoola et al., 2019; Hussein et al., 2022). The current study found that Rooibos extracts have a high AOC, which is related to their high total phenolic content (TPC). These results correlate with prior studies that demonstrated the antioxidant properties of both unfermented and fermented Rooibos using cell-free models (López et al., 2022; Abdul & Marnewick, 2022).

The main phytochemical compounds of the extracts were aspalathin, orientin, iso-orientin, iso-vitexin, and vitexin, according to HPLC analysis. The bioactive compounds identified in this study are comparable to those that were previously identified in Rooibos (*Aspalathus linearis*) (Abdul & Marnewick, 2022). The solvent and analytical technique utilised can explain the discrepancies in phytochemical concentrations observed in aqueous and ethanolic extracts. The ability of a solvent to dissolve a given set of antioxidant molecules is determined by its polarity, which influences the

assessment of antioxidant activity (Hussein et al., 2022). Furthermore, polyphenols constitute a significant fraction of antioxidants in plant material (Sadowska-Bartosz & Bartosz, 2022). However, because the Folin-Ciocalteu assay has an indefinitely high redox potential, is not specific to antioxidants. Thus, it is sensitive to interference from a variety of sources including citric acid, reducing sugars and some amino acids (Waterhouse, 2002; Sadowska-Bartosz & Bartosz, 2022). Therefore, in addition to phenolics, water might have extracted other compounds that contribute to the TPC (Hussein et al., 2022). As a result, TPC measurements of fermented Rooibos extracted with water at a higher concentration (500 µg/mL) may be overestimated. The relatively high TPC of fermented Rooibos extracted with water compared to fermented Rooibos extracted with ethanol at 15 µg/mL can be considered as a 'less than' limit of detection. It should be noted that the results below the detection limit are not meaningless; they simply have a higher relative uncertainty than those above this limit (Rousseau, 2001). Furthermore, it is suggested that the TPC (Folin-Ciocalteu method) provided a reliable measurement of Rooibos extracts at concentrations of 30 µg/mL, 60 µg/mL, 125 µg/mL, and 250 µg/mL.

Ethanol was more efficient than H₂O in extracting antioxidant compounds; thus, ethanol may give more convincing evidence of antioxidant effects on the body. In general, adding water increases the polarity of ethanol, which can improve the recovery of phenolic compounds by breaking the hydrogen bonds in polyphenol structure and improving their solubility in organic solvents (Chaabani et al., 2023). Thus, in the extraction of polyphenols, ethanol, and water (80:20 % v/v) may be a more successful solvent mixture for active component extraction than a single solvent (Plaskova & Mlcek, 2023). Furthermore, ethanol-water (80:20 % v/v) mixtures appear to be the most appropriate solvents for extraction because of the different polarity of both solvents and their acceptability for human consumption (Waszkowiak & Gliszczyńska-Świgło, 2016). Such ethanol-water Rooibos extracts could be safely used in neurodegeneration prevention strategies without the possibility of toxic solvent residues. However, TEAC results for 500 µg/mL unfermented ethanolic Rooibos extract correlated well and inversely with 500 µg/mL unfermented aqueous Rooibos extract, indicating that that TPC measurements of unfermented Rooibos extracted with ethanol and water at a higher concentration (≥500 µg/mL) may be overestimated (n=3; Pearson's $r = -0.500$; $P = 1.000$).

Hydrogen peroxide is widely used as an inducer of cellular OS in cellular models because it is highly soluble, easily diffuses through membranes, and has the greatest life span (Zhang et al., 2007; Agapouda et al., 2020). When cultured cells are exposed to H₂O₂, it causes an imbalance in energy metabolism and the negative effects of hydroxyl and peroxy radicals on membrane lipids and proteins (Zhang et al., 2007), making it a suitable candidate for an OS cell model. It is also worth noting that the higher pathological concentration of H₂O₂ in OS conditions can reach up to 150 µM *in vitro* (Sanghai & Tranmer, 2022).

To determine the optimal concentration of H₂O₂ treatment to induce cytotoxicity in SH-SY5Y cells, cells were treated with several dosages of H₂O₂ ranging from 50-1000 µM for 1, 2, 3, and 24 hours, and cell viability was assessed using the MTT assay. The cell viability of SH-SY5Y cells after 3 hours incubation with H₂O₂ exhibited a considerable decrease. Concentrations exceeding 150 µM reduced cell viability to 12-27 %. Therefore, in subsequent experiments, 150 µM H₂O₂ (3 hours), which had approximately 50 % inhibition as indicated by cell viability data, was used to study the cytoprotective effects of unfermented and fermented Rooibos extracts in SH-SY5Y cells. The optimal H₂O₂ concentration selected for this study (150 µM) correlated with the concentration of H₂O₂ used in previous studies despite the differences in exposure periods (Zhang et al., 2007; Law et al., 2014). It is important to note the exposure discrepancies in comparison to previous studies (Premratanachai et al., 2020; Mendes et al., 2022), where cells were treated with 200 µM H₂O₂ for 30 min or 1,2,4 or 24 hours to investigate time-dependent effects of the H₂O₂ treatment on changes in calcineurin levels in SH-SY5Y cells (Premratanachai et al., 2020); and 300 µM H₂O₂ for 24 hours to induce OS in SH-SY5Y (Mendes et al., 2022). Findings of the present study correspond to earlier studies that show that the effect of extracellular H₂O₂ on cell survival begins after a few hours of H₂O₂ exposure (Zhang et al., 2007; Bejarano et al., 2009; Law et al., 2014). The active mitochondrial dehydrogenase enzyme converts dissolved MTT ions to insoluble formazan. As cofactors, reduced equivalents such as NADH and NADPH are involved in the reaction. The reduction in viable cells, likely attributed to OS-induced neurotoxicity, correlates with a decrease in the availability of these reducing equivalents, impacting the MTT assay readout (Reddy et al., 2023).

The current study demonstrated Rooibos' antioxidant properties using a brain cell culture model. Cell viability was not affected by the highest dose of fermented and unfermented Rooibos [500 µg/mL]. Although the highest dose of the unfermented aqueous, fermented aqueous and fermented ethanolic Rooibos extracts used in the MTT assay were comparable with the negative

control. This finding matches the findings of a recent study in which mitochondrial reductive capacity was used as an indication of cell viability in Neuro-2a cells following exposure to increasing concentrations of an unfermented Rooibos extract for 24 hours. Here, a peak was absorbed at 125 µg/mL and 500 µg/mL the unfermented Rooibos extract did not show any inhibitory effect on mitochondrial reductive capacity (López et al., 2022).

The current study showed that the presence of fermented and unfermented Rooibos extracts at 60, 125, and 250 µg/mL (low, medium, and high, respectively) attenuated the oxidative damage induced by 150 µM H₂O₂ (3-hour exposure) and were used in subsequent assays. Given the HPLC data, the Appendix 10 and Appendix 11 provides a rough estimate of how much of the compound is in the extract at these concentrations. In addition, to put these findings in context with Rooibos consumption, consider that a dose of 25 µg/mL extract is roughly comparable to the antioxidants found in one cup of Rooibos tea using the current model and extract. This estimation, however, is based on the standard assumption of 100 % absorption (López et al., 2022). Despite widely investigated for their health properties, many of the flavonoids contained in Rooibos are known to be poorly absorbed in humans with limited number of metabolites identified in urine and blood after ingestion (López et al., 2022; Pyrzanowska, 2022). However, it is reported that the distribution of many of the flavonoids contained in Rooibos, cross the BBB and their direct activity within the brain is possible. Nevertheless, still little is known about the mechanism of permeation or further metabolism in the nervous tissue (Pyrzanowska, 2022). Thus, the low medium and high selected in this study were calculated to be approximately 2, 5, and 25 cups of tea respectively.

These findings support previous research that found Rooibos extracts to be cytoprotective against diesel exhaust particles (DEP)-induced OS in human umbilical vein endothelial cells (HUVECs), resulting in increased cell survival (Lawal, Davids, et al., 2019). Furthermore, the ability of unfermented Rooibos extracts to chelate transition metals has been demonstrated in cell free systems (Vhangani et al., 2022). Indeed, improved cell viability shows that Rooibos extracts could be related to the high antioxidant potential of its unique polyphenols. These polyphenols are known for their redox properties, which enable them to serve as pro-oxidative metal chelators, reducing agents, singlet oxygen quenchers, and hydrogen donors, as well as upregulate the cell's antioxidant defence (Ito, Shinohara, Kator, 1991; Yoo et al., 2008; Lawal, Davids, et al., 2019; López et al., 2022). The safety and toxicity profile of small compounds is an important step in drug research and development. There is currently a wealth of information available about vitexin and its derivatives' toxicity and safety (Abdulai et al., 2021). It is worth noting that 500 µg/mL fermented

ethanolic Rooibos extract reduced cell viability, which could be attributed to iso-vitexin, iso-orientin, and orientin, as the HPLC findings show significant high values of these compounds. These findings are consistent with investigations on neuro-2a cells, A- β 25-35 dramatically reduced cell viability through ROS-mediated toxicity and apoptosis. However, incubation of neuro-2a cells with vitexin (50 μ M) dramatically restored cell viability up to 92.86 ± 5.57 % (Malar et al., 2018). In contrast, isovitexin concentrations of 100 and 500 μ M were shown to be toxic to Caco-2 cells after 4 hours of incubation (Hithamani et al., 2017).

The level of ATP activity in a cell is an important indicator of cellular metabolism and cell function as highlighted in previous studies (Omoruyi et al., 2023). In the current work, intracellular ATP levels in SH-SY5Y cells were evaluated using a luciferase system to confirm that the selected Rooibos extract doses (60, 125, and 250 μ g/mL) maintained metabolic activity. Hydrogen peroxide at 150 μ M for 3 hours oxidatively challenged cells by reducing intracellular ATP production to approximately 50%. This confirms the dual role of H₂O₂, functioning not only as a cytotoxic agent but also as a mitochondrial inhibitor. Hydrogen peroxide depletes ATP primarily by inducing DNA single-strand breaks; as a result, poly ADP ribose polymerase (PARP), a nucleic acid polymerase found in the nucleus, is activated (Lee & Shacter, 2000; Chung et al., 2022). When PARP is activated by DNA damage, it consumes intracellular NAD⁺ to synthesize the polymer of ADP-ribose (PAR) at the damaged site, and immense DNA damage depletes NAD⁺. Intracellular NAD⁺ depletion drastically affects intracellular ATP levels, and so excessive PARP activity reduces cells' ability to generate energy in the form of ATP, ultimately resulting in cell death (Redegeld et al., 1992; Chung et al., 2022). Indeed, a decrease in intracellular ATP levels can result in irreversible degeneration of important cellular activities such as redox balance maintenance, ultimately leading to cell viability loss (Redegeld et al., 1992).

In the current study, pre-treatment of 125 and 250 μ g/mL of fermented ethanolic Rooibos extract for 24 hours reduced H₂O₂ toxicity by increasing intracellular ATP levels in SH-SY5Y cells. These findings support prior research that found *Aspalathus linearis*, aspalathin, and linearthin increased ATP production in SH-SY5Y cells following 1-methyl-4-phenylpyridinium (MPP⁺) toxicity (Omoruyi et al., 2023). Higher ATP levels may promote cell viability by boosting energy-dependent DNA repair processes (Park et al., 2010). Therefore, Rooibos may have improved the recovery of SH-SY5Y cells from oxidative damage by inhibiting PARP (Pantsi et al., 2011).

However, a toxicity was observed when cells were pre-treated with unfermented Rooibos extracts. It is also worth noting that unfermented Rooibos extracts have a higher TPC and antioxidant capacity. These findings contradict a previous study in which exposure to unfermented ethanolic extract in a high glucose induced toxicity model, 4 hours exposure in HepG2 cells-supplemented media significantly elevated ATP at the lower tested concentrations, while a significant decrease in ATP was observed at the highest (1000 µg/mL) tested concentration (Abdul & Marnewick, 2022). There are two possible explanations for the variation. The current study suggests that unfermented Rooibos extracts may have pro-oxidant properties. Indeed, it has been suggested that the ability of Rooibos and its constituents to enhance the Fenton reaction, as well as the metal chelating properties of Rooibos and its polyphenols, may contribute to the pro-oxidant effects at high concentrations (Akinfenwa et al., 2021).

Secondly, agents added to cells in culture can undergo chemical reactions with cell culture media constituents, some resulting in H₂O₂ generation (Halliwell et al., 2000). Several phenolic compounds, such as L-DOPA, dopamine, epigallocatechin, catechin, quercetin, and epigallocatechin gallate, can interact with commonly used cell culture media (e.g., Dulbecco's modified Eagles' medium [DMEM], RPMI, and McCoy's 5A medium) to produce significant amounts of H₂O₂. Some of these compounds can achieve levels of more than 50 µM. Some of the reported effects of these phenolic compounds on cells in culture could be attributed to H₂O₂ production (Halliwell et al., 2000; Long et al., 2000). Thus, it is suggested that unfermented Rooibos extracts were toxic due to H₂O₂ generation in the culture media. However, no data on aspalathin in the literature on this topic could be found.

In this study, the ATP results from unfermented Rooibos extract are more sensitive to cell viability than the MTT assay, confirming previous findings that emphasized the sensitivity of the ATP assay over other cell viability testing methods. These results demonstrate that MTT assay will provide an underestimation of the anti-proliferative effect of Rooibos extracts. It is suggested that careful evaluation of the method for *in vitro* assessment of cell viability and proliferation depending on the chemical nature of botanical supplements (Wang et al., 2010).

Increased ROS production can result in OS, which can damage biomolecules such as proteins, nucleic acids, and lipids. However, as is common among these targets, the oxidation of membrane lipids, known as LPO, is particularly harmful because free radical reactions are easily propagated by LPO products (Zhu et al., 2023). The current study looked at the effects of Rooibos

extracts in SH-SY5Y cells that had been challenged with H₂O₂ as an LPO inducer by measuring CD levels, which are produced in the first step of lipid peroxide formation, and MDA, a byproduct of the oxidation mechanism that breaks down mostly PUFAs into their essential chains. The difference in CD levels observed between the 150 µM H₂O₂ (3 hours exposure) and the control cells indicates a considerable increase in LPO. The increase in CD levels in the H₂O₂-treated group could be attributed to either overproduction of [•]HO and peroxy radicals, which can destroy organelle structure and biomolecules, or to depletion of GSH, which is involved in detoxification of LPO products including MDA (Gerasimenko et al., 2012), an occurrence that we also observed in this study regarding GSH, SOD and protein carbonyls. It is noteworthy to observe that in the present study the activity of the CAT enzyme did not increase after H₂O₂ exposure. Rather a decrease in CAT activity was measured in agreement with what was observed in oxidative status alteration during aerobic-dominant mixed and anaerobic-dominant mixed effort in judokas (Gandouzi et al., 2023).

Pretreatment with Rooibos extracts markedly reduced the observed increase in the SH-SY5Y cells, indicating protection against oxidative lipid damage. These findings are consistent with prior research showing that pre-treatment with fermented or unfermented Rooibos extracts and orientin reduced oxidative stress induced by DEP in HUVECs by decreasing CD levels (Lawal, Davids, et al., 2019). Similarly, fermented aqueous Rooibos dramatically reduced CDs in the livers of Wistar rats exposed to *tert*-butyl-hydroperoxide (*t*-BHP) (Ajuwon et al., 2013). Furthermore, these findings are consistent with a clinical trial study that found that consuming fermented Rooibos significantly decreased oxidative damage biomarkers (MDA and CDs), and a significant increase in GSH:GSSG ratio (a useful biomarker of OS) in individuals who are at a higher risk of developing cardiovascular disease symptoms, most likely due to its notable phenolic compound bioactivities (Marnewick et al., 2011). The ability of Rooibos to preserve cell membranes from H₂O₂-induced LPO as indicated by CD levels can be attributed to one or more of the antioxidant activity of polyphenols, particularly aspalathin, or synergistic interactions of its unique phytochemicals. Rooibos phenolic phytochemicals are known for their antioxidant-mediated pharmacological activities by inhibiting the lipid peroxide cascade, either as a sacrificial antioxidant to scavenge free radicals or as chelators of transition metal ions that participate in a variety of antioxidant defence systems (Zhao, 2019). However, when the concentration of unfermented ethanolic Rooibos increased, so did the formation of CDs. These could be attributed to hormetic effects associated with Rooibos, as previously demonstrated (Akinfenwa et al., 2021).

In contrast to CDs, H₂O₂ induced LPO (measured as MDA) in SH-SY5Y cells, but not as expected for toxicity. Hydrogen peroxide's unexpected impact on inducing LPO, as evidenced by MDA, has also been reported *in vitro* in other cell types (Erba et al., 2003; Linden et al., 2008). Previously, H₂O₂ at 300 µM for 24 hours induced LPO as evaluated by MDA in SH-SY5Y cells (Oliveira et al., 2018). Furthermore, 400 µM H₂O₂ for 24 hours increased LPO estimated by measuring MDA in SH-SY5Y cells by two-fold (Garcimartín et al., 2014). Taken together, these observations indicate that a lack of correlation between different indices related to LPO products may be due to the overall process of LPO, which consists of three steps: an initial "lag" phase, followed by a chain reaction propagation phase, which normally ends when the oxidisable lipids are consumed and termination phase (Dotan et al., 2004; Ayala et al., 2014). The length of the propagation chain depends on many factors, including the lipid to protein ratio in a membrane, the fatty acid composition, the O₂ concentrations, heavy metals (copper, iron, and manganese), and the presence of chain breaking antioxidants, which interrupt the chain reaction by providing an easily donatable hydrogen for abstraction by peroxy radicals (Paciorek et al., 2020; Halliwell, 1997)

However, it is noteworthy to observe that in the present study reduced GSH levels were depleted, and the activity of the CAT enzymes did not increase after H₂O₂ exposure. Rather a decrease in CAT activity was measured, in agreement with what was observed in oxidative status alteration during aerobic-dominant mixed and anaerobic-dominant mixed effort in judokas (Gandouzi et al., 2023). It is important to note that a complex mixture of products that are formed in lipid peroxidation reactions are difficult to analyse (Paciorek et al., 2020). However, it has been reported that CDs are intermediates in the formation of MDA (Facundo et al., 2004) and as mentioned before, the availability of O₂ becomes a limiting factor in LPO under rare conditions (Raveh et al., 2002). Thus, the current work reveals that after 3 hours of exposing cells to 150 µM H₂O₂, the formation of LPO products (MDA) via a well-established sequence of processes comes to a halt when the O₂ concentration in the cells decreases to near zero. Furthermore, LPO alone cannot be utilised as a general indicator of OS (Dotan et al., 2004).

It is noteworthy to observe that in this present study the higher concentrations of unfermented and fermented ethanolic Rooibos extracts (250 µg/mL) increased MDA levels, reaching levels higher than H₂O₂. However, none of these extracts exceeded baseline levels of MDA, with reduced LPO in comparison to control cells. It is noteworthy to observe that unfermented and fermented ethanolic Rooibos extracts are potentially toxic at high concentrations, thus potentiating the effects of H₂O₂, an occurrence that was also observed in this study regarding caspase 3/7

and LDH. As previously highlighted, a dose of 25 µg/mL extract roughly equates to the polyphenolic flavonoids present in one cup of Rooibos herbal tea, according to the current model. Therefore, the cytotoxic effects of a 250 µg/mL extract of Rooibos are not surprising given Rooibos is associated with hormetic effects (Akinfenwa et al., 2021)

Protein carbonyl group formation has been used as a marker of protein oxidation *in vivo* and *in vitro* (Davies et al., 1999). The abrupt depletion of GSH has been demonstrated to result in extensive carbonylation of rat brain proteins (Bizzozero et al., 2006). In the current study, H₂O₂ treatment increased protein carbonylation in SH-SY5Y cells, which was reduced by pre-treatment with the unfermented Rooibos ethanolic extract. These results are consistent with a previous study showing reduced protein carbonylation in a model of glucotoxicity using HepG2 liver cells treated with Rooibos extracts (Abdul & Marnewick, 2022). Similarly, Rooibos extracts were reported to ameliorate OS induced by DEP in HUVECs by reducing protein carbonylation (Lawal, Davids, et al., 2019). The unfermented Rooibos ethanolic extract (125 µg/mL and 250 µg/mL) reduced H₂O₂-induced stress by increasing the direct scavenging of ROS via protein carbonylation. However, in this study, the Rooibos extracts at lower concentrations increased protein carbonyls in conjunction with H₂O₂. *In vitro*, polyphenols have been shown to have oxidative effects on proteins in a dose- and pH-dependent manner (Masuda et al., 2013).

Status modification of the most abundant intracellular antioxidant and free radical scavenger, GSH has long been discussed as a potential therapeutic strategy in OS-related diseases such as AD and PD (Han et al., 1997; Johnson et al., 2012). Glutathione levels can be dramatically reduced due to a variety of factors, including the export of oxidised glutathione, GSSG from cells during enzymatic hydroperoxide removal or non-enzymatic reactions, increased ROS, and decreased GSH synthesis (Han et al., 1997). Increased GSH export appears to be required for apoptosis to occur in many cell types (Ghibelli et al., 1998). It is also important to note that extremely high levels of ROS can deplete GSH and convert apoptotic cell death to necrotic cell death (Hall, 1999). Glutathione-dependent redox regulation is accomplished through bimolecular reactions of GSH with target proteins (Flohé, 2013). Glutathione's cellular antioxidant effects are attributed to enzymes such as GPx, a cytosolic enzyme that employs GSH as a cofactor to reduce H₂O₂, culminating in the formation of GSSG (Ho et al., 2022). Furthermore, literature corroborates GSH depletion, with the inhibition of GPx (Hirano et al., 1997). Thus, maintaining cellular GSH, dependent on *de novo* synthesis, is critical for the adaptive response to OS (Han et al., 1997).

The H₂O₂ depletion of GSH was partially prevented (not significantly) by pre-treatment with 60 µg/mL of unfermented ethanolic Rooibos extract. It is noteworthy to observe that in the present study, unfermented extract contained nearly three times the quantity of aspalathin, the major bioactive compound, compared to the aqueous extract as indicated by the HPLC quantification results. These findings support earlier research that has shown the ability of unfermented Rooibos ethanolic extracts to increase cellular GSH, which may be expected to support GSH-dependent pathways (Sheik Abdul & Marnewick, 2022). The observed protection could be attributed to *de novo* GSH synthesis, regulated by the level of γ-glutamylcysteine synthetase in the cell (Ferguson & Bridge, 2016; Lawal, Oluyede, et al., 2019).

It is important to note that chronic consumption of Rooibos polyphenols, especially in high dosages, has been linked to pro-oxidative effects (Joubert et al., 2005). Their prooxidant activity is catalysed mainly by transition metals (copper and iron) and results from the generation of a redox complex with a transition metal ion or a phenoxy radical (Duda-Chodak & Tarko, 2023). It is known that flavonoids with a catechol group on the B-ring may lead to GSH conjugation (Van Der Merwe et al., 2015). Studies in hepatocytes indicated that flavonoids with the catechol group possessing low redox potentials such as luteolin and quercetin, depleted hepatocyte GSH (Galati et al., 2002). It is noteworthy that unfermented Rooibos extract flavonoids containing a B- ring catechol arrangement include aspalathin, isoorientin and orientin (Van Der Merwe et al., 2015). It is plausible that prolonged exposure to high levels of aspalathin enriched unfermented ethanolic extract result in a large reduction in cellular GSH since GSH conjugation is the main pathway in the metabolism of major Rooibos flavonoids. Rooibos extracts also interact with GSH by regulating its levels and activity within cells, an occurrence that was also observed in a previous study regarding polyphenol/GSH interactions in which it disrupted the GSH redox cycle in rats fed a dietary aspalathin-enriched green Rooibos extract for 28 or 90 days (Van Der Merwe et al., 2015). In this regard, it is suggested that Rooibos dosage and exposure as well as Rooibos interaction with the redox state of the environment appear to be of primary importance; especially when precise redox modulation is needed to allow a physiological function or to promote a deleterious effect. Thus, polyphenol dosage and exposure should be closely monitored.

Oxidative stress induced by toxic damage has been associated to changes in the status of antioxidant enzymes (Ajuwon et al., 2013). Understanding the intrinsic cell functions, metabolic specialization, and external conditions to which the cells are exposed (such as oxygenation levels and the presence of metabolites) aids in determining the antioxidant enzyme activity of cells

(Wijeratne et al., 2005). The current study found that 150 μM H_2O_2 (3 hours)-induced cell viability decreases were associated with decreased CAT activity and increased SOD activity in human neuroblastoma SH-SY5Y cells. A substantial increase in O_2 concentration is expected at the site of CAT action, hence inside the cell, due to a process known as disproportionation (Heck et al., 2010; Ransy et al., 2020). This increase in intracellular O_2 increases the likelihood that it will be reduced by the leakage of a single electron from cellular metabolism. Hence, this directly explains the observed increase in cellular $\text{O}_2^{\cdot-}$ production and SOD activity (Ransy et al., 2020). Additionally, the increase in the SOD enzyme is induced by the increased in the formation of CDs that causes hyperoxia. Thus, the increase in SOD can be attributed to the formation of ROS such as H_2O_2 and $\text{O}_2^{\cdot-}$ (Halliwell & Gutteridge, 1981). The ROS scavenging activity of SOD is effective only when it is followed by the activity of CAT and GPx, because the dismutase activity of SOD generates H_2O_2 from the superoxide ion which is more toxic than oxygen derived from free radicals and requires to be scavenged further by CAT and GPx (Wang et al., 2005). A decrease in SOD activity in the 250 $\mu\text{g}/\text{mL}$ fermented ethanolic Rooibos extract treated group in this study may be due to a previously reported pro-oxidant effect of Rooibos extracts (Joubert et al., 2005). It is known that the biological effects of polyphenols as well as their *in vitro* and *in vivo* outcomes, to be strongly associated with a hormetic effects where polyphenols low doses usually are usually associated with beneficial effects while high doses usually have a toxic effect (Shaito et al., 2020). In this regard, evidence suggests that Rooibos' hormetic property may be due to its dose associated biphasic effects on the cellular redox state which was reported to be antioxidant at low doses and a pro-oxidant at high doses.

The current study demonstrated that pretreatment with Rooibos extracts restored the changes in SOD activity induced by H_2O_2 in the cells. These findings correlate with previous research that found that consuming fermented Rooibos reduced SOD activity *t*-BHP- induced OS in Wistar rats' liver (Canda et al., 2014). Similarly, Rooibos extracts have been shown in previous studies to be potent antioxidants via increasing CAT activity (Awoniyi et al., 2012; Hong et al., 2014). These findings reveal that the effect of an antioxidant enzyme in a biological system can have synergistic or antagonistic interactions with other compounds and enzymes in the cellular environment (Wijeratne et al., 2005). Thus, the synergistic interactions of CAT and SOD may have protected

each other from the harmful effects of free radicals (Kono & Fridovich, 1982; Blum & Fridovich, 1985; Wijeratne et al., 2005). This can be supported by the correlation between increased CAT activity and decreased SOD activity in Rooibos-treated cells. Additionally, GSH acts as a scavenger of ROS and as a substrate for GPx to reduce H₂O₂ (AlBasher et al., 2020; Uçkan et al., 2022). Therefore, it has a major role in antagonising oxidative action which may explain the reduced levels of GSH after H₂O₂ treatment which agrees with what was observed in patients with polycystic ovary syndrome (Uçkan et al., 2022). Interestingly pretreatment of Rooibos extracts, markedly alleviated the toxic effect and oxidative damage induced by H₂O₂. Thus, formation of CDs, GSH concentration, SOD and CAT activities were normalised. The attenuating effects of Rooibos extracts on oxidative destruction induced by H₂O₂ may result from its antioxidant potential. Rooibos extracts may synergistically act with antioxidant enzymes via the following mechanisms: chelating pro-oxidative transition metal cations, scavenging free radicals, and quenching O₂ radicals. However, it is important to consider that other factors could also influence enzymatic activity related to OS.

Hydrogen peroxide induces apoptosis at moderate concentrations and necrotic cell death at elevated concentrations in an OS model (Watanabe et al., 2015). However, necrosis can also prevent or result from aborted apoptosis (Borutaite & Brown, 2001). In this study, after 3 hours of treatment with 150 µM H₂O₂, caspase 3/7, 8, or 9 activities were detected at reduced levels from the baseline in SH-SY5Y cells. Similarly, LDH activity was detected in the medium but at reduced levels from the baseline. These findings correlate with previous studies that found that treating cells with H₂O₂ inhibits caspase-9 proteolytic cleavage (Lee & Shacter, 2000; Nishida et al., 2022). Taken together, these findings suggest that under 150 µM H₂O₂ for 3 hours, ATP-dependent caspases-9 activation via apoptosome formation may have been impaired. Indeed, in the current study, there was a decrease in ATP levels, which may have affected the upstream step in caspase-9 cleavage, leading it to be suppressed by 3 hours of exposure to 150 µM H₂O₂. Caspase-9 activation is an energy-dependent process, which activate the effector caspases 3 and causes apoptosis (Lee & Shacter, 2000). In addition, caspase-8 may have been inhibited in response to TNFα activation, resulting in necrosis induction (Nishida et al., 2022). Reduced ATP levels with increased caspase 3/7 activity is suggestive of mitochondrial-dependent apoptosis (Cordier et al., 2021). It is noteworthy to observe that in the present study, a large decrease in ATP was measured after H₂O₂ treatment, however, caspase 3/7 activity also decreased. Thus, it is suggesting a non-caspase-dependent route of cytotoxicity. Excessive ATP depletion can transition cell death from apoptosis to necrosis (Cordier et al., 2021; Eguchi et al., 1997; Leist et

al., 1997; Tsujimoto, 1997), which may explain the lack of caspase 3/7 activity. Corroborating the cell death observed, GSH levels were also reduced at low concentrations after H₂O₂ treatment. It has been proposed that GSH depletion via efflux regulates intracellular apoptotic signalling (Franco & Cidlowski, 2009). However, excess GSH depletion predisposes cells to necrosis (Mcconkey, 1998). Indeed, reports indicate that when cells are subjected to chemicals such as H₂O₂, cellular GSH depletion shifts the cell death pathways from apoptosis to necrosis (Baigi et al., 2008). Buthionine sulphoximine, a γ -GCS inhibitor, shifted the mode of cell death in human leukemic cells from apoptosis to necrosis (Fernandes, 1994).

In this study, treatment of human neuroblastoma SH-SY5Y cells with 150 μ M H₂O₂ (3 hours) depleted GSH levels by approximately 30% compared to controls, while H₂O₂ only depleted intracellular ATP levels to approximately 50% of the initial levels. These data support the concept that GSH depletion occurs at an earlier stage of cell death and only when it is preceded or followed by delayed ATP depletion (Redegeld et al., 1992). Furthermore, the Gibbs free energy equation links mitochondrial dysfunction with GSH depletion, resulting in reduced ATP generation (Schütt et al., 2012). Thus, reduced intracellular ATP levels in age-related diseases, especially NDDs, can lead to decreased GSH levels, accelerating neurodegeneration. Lactate dehydrogenase is released into the extracellular space when the plasma membrane ruptures or is disrupted (Kendig & Tarloff, 2007; Parhamifar et al., 2019). Furthermore, LDH is released early in necrosis but late in apoptosis, therefore a lack of increase does not necessarily imply no toxicity (Parhamifar et al., 2019). Indeed, when combined with other methods, the release of LDH from cells has been widely used as a biomarker for necrotic cell death (Kendig & Tarloff, 2007). However, two factors will influence the accuracy of LDH measurement: (1) the extracellular half-life of the enzyme, which is 9 hours for LDH; and (2) the difficulty in determining the time of LDH release into the extracellular space because the actual time from the onset of apoptosis to the time the cell ruptures is usually undeterminable, unless the therapy causes immediate necrotic cell death (Chizenga, 2022).

The current study attempted to evaluate LDH release in human neuroblastoma SH-SY5Y cells. The MTT assay demonstrated reduced viability, with fewer SH-SY5Y cells in H₂O₂-treated wells and depleted ATP levels, indicative of compromised viability. Despite these observations, LDH activity in the medium was detected but at reduced levels from the baseline, suggesting that H₂O₂ may have induced necrosis in the cells. These results are consistent with prior studies that established the potential of H₂O₂ to reduce LDH activity in epithelial-like pig kidney cell lines (LLC-

PK1) by oxidizing NADH rather than inactivating LDH (Kendig & Tarloff, 2007). Additionally, the pH indicator phenol red is commonly used in tissue culture medium (Parhamifar et al., 2019). However, phenol red can be sufficient to significantly reduce assay sensitivity and/or completely obscure detection of cellular LDH (Parhamifar et al., 2019).

5.1. Conclusion

The findings of this study have provided a foundation for targeting neuroprotection with pre-exposure to Rooibos extracts at certain levels. However, the biological effects of some of the extracts, as well as their *in vitro* results (including GSH, ATP, CDs, and caspases), except for protein carbonyls (where 60 µg/mL increased protein carbonyl levels), appear to be strongly associated with a hormetic effect, with low doses of Rooibos extracts usually resulting in beneficial effects and high doses producing toxic ones on the SH-SY5Y cell line after exposure to H₂O₂. Evidence suggests that Rooibos extracts have a biphasic effect on cellular redox status, acting as an antioxidant at low doses and a pro-oxidant at high doses. Both unfermented and fermented aqueous and ethanolic extracts at 60 µg/mL showed the highest neuroprotective effects and should be explored further.

5.2. Study limitations and future recommendations

A notable limitation of the study is the reliance on a single cell line for investigating the molecular mechanism. While this approach provides valuable insights, primary cells could be explored, thus offering a more comprehensive understanding of its broader implications. Moreover, incorporating an *in vitro* BBB modelling with co-cultured neural progenitor cell-derived astrocytes and neurons is recommended. This would advance knowledge of the potential of Rooibos tea components to cross the BBB.

Notwithstanding the substantial number of *in vitro* and *in vivo* studies that support the beneficial and neuroprotective effects of Rooibos (Hong et al., 2014; Akinrinmade et al., 2017; Pyrzanowska et al., 2019; Pyrzanowska et al., 2021; López et al., 2022; Omoruyi et al., 2023), future studies should include *in vivo* models as a better holistic approach. Moreover, the molecular mechanism of Rooibos action needs to be better identified. The current *in vitro* study contributes valuable insights, but it is crucial to acknowledge the differences between an *in vitro* and *in vivo* investigation. Cells *in vitro* may not fully capture the systemic effects of Rooibos and its active constituents.

6. REFERENCES

- Abdulai, I.L., Kwofie, S.K., Gbewonyo, W.S., Boison, D., Puplampu, J.B. and Adinortey, M.B., 2021. Multitargeted effects of vitexin and isovitexin on diabetes mellitus and its complications. *The Scientific World Journal*. 6641128–20.
- Abeyrathne, E.D.N.S., Nam, K. & Ahn, D.U. 2021. Analytical methods for lipid oxidation and antioxidant capacity in food systems. *Antioxidants*, 10(10).
- Agapouda, A., Butterweck, V., Hamburger, M., De Beer, D., Joubert, E., Eckert, A. & Mendonça Junior, F.J.B. 2020. Honeybush Extracts (*Cyclopia* spp.) Rescue Mitochondrial Functions and Bioenergetics against Oxidative Injury. *Oxidative Medicine and Cellular Longevity*, 2020.

- Aguilar Diaz De Leon, J. & Borges, C.R. 2020. Evaluation of oxidative stress in biological samples using the thiobarbituric acid reactive substances assay. *Journal of Visualized Experiments*, 2020(159).
- Ahotupa, M. 1996. Simple methods of quantifying oxidation products and antioxidant potential of low-density lipoproteins. *Clinical Biochemistry*, 29(2): 139.
- Ajuwon, O.R., Katengua-Thamahane, E., Van Rooyen, J., Oguntibeju, O.O. & Marnewick, J.L. 2013. Protective Effects of Rooibos (*Aspalathus linearis*) and/or Red Palm Oil (*Elaeis guineensis*) Supplementation on tert-Butyl Hydroperoxide-Induced Oxidative Hepatotoxicity in Wistar Rats. *Evidence-Based Complementary and Alternative Medicine*, 2013: 984273–19.
- Akagawa, M. 2021. Protein carbonylation: molecular mechanisms, biological implications, and analytical approaches. *Free Radical Research*, 55(4): 307–320.
- Akinfenwa, A.O., Abdul, N.S., Marnewick, J.L. & Hussein, A.A. 2021. Protective effects of linearthin and other chalcone derivatives from *Aspalathus linearis* (Rooibos) against uvb induced oxidative stress and toxicity in human skin cells. *Plants*, 10(9).
- Akinrinmade, O., Omoruyi, S., Dietrich, D. & Ekpo, O. 2017. Long-term consumption of fermented rooibos herbal tea offers neuroprotection against ischemic brain injury in rats. *Acta Neurobiologiae Experimentalis*, 77(1): 94–105.
- Alavi Naini, S.M. & Soussi-Yanicostas, N. 2015. Tau Hyperphosphorylation and Oxidative Stress, a Critical Vicious Circle in Neurodegenerative Tauopathies? *Oxidative Medicine and Cellular Longevity*, 2015: 151979–17.
- Albarracin, S.L., Stab, B., Casas, Z., Sutachan, J.J., Samudio, I., Gonzalez, J., Gonzalo, L., Capani, F., Morales, L. & Barreto, G.E. 2012. Effects of natural antioxidants in neurodegenerative disease. *Nutritional Neuroscience*, 15(1): 1–9.
- AlBasher, G., Abdel-Daim, M.M., Almeer, R., Ibrahim, K.A., Hamza, R.Z., Bungau, S. & Aleya, L. 2020. Synergistic antioxidant effects of resveratrol and curcumin against fipronil-triggered oxidative damage in male albino rats. *Environmental Science and Pollution Research International*, 27(6): 6505–6514.
- Ali, F., Manzoor, U., Khan, F.I., Lai, D., Khan, M.K.A., Chandrashekharaiyah, K.S., Singh, L.R. & Dar, T.A. 2022. Effect of polyol osmolytes on the structure-function integrity and aggregation propensity of catalase: A comprehensive study based on spectroscopic and molecular dynamic simulation measurements. *International Journal of Biological Macromolecules*, 209(PA): 198–210. <https://doi.org/10.1016/j.ijbiomac.2022.04.013>.

- Alía, M., Ramos, S., Mateos, R., Bravo, L. & Goya, L. 2005. Response of the antioxidant defence system to tert-butyl hydroperoxide and hydrogen peroxide in a human hepatoma cell line (HepG2). *Journal of Biochemical and Molecular Toxicology*, 19(2): 119–128.
- Alvi, A.M., Siuly, S. and Wang, H., 2022. Neurological abnormality detection from electroencephalography data: a review. *Artificial Intelligence Review*, 55(3), pp.2275-2312. <https://doi.org/10.1007/s10462-021-10062-8>.
- Angelova, P.R., Esteras, N. & Abramov, A.Y. 2021. Mitochondria and lipid peroxidation in the mechanism of neurodegeneration: Finding ways for prevention. *Medicinal Research Reviews*, 41(2): 770–784.
- Araya, L.E., Soni, I. V., Hardy, J.A. & Julien, O. 2021. Deorphanizing Caspase-3 and Caspase-9 Substrates in and out of Apoptosis with Deep Substrate Profiling. *ACS Chemical Biology*, 16(11): 2280–2296.
- Artal-Sanz, M. & Tavernarakis, N. 2005. Proteolytic mechanisms in necrotic cell death and neurodegeneration. *FEBS letters*, 579(15): 3287–3296.
- Asghari, M. and Aghdam, M.S., 2010. Impact of salicylic acid on post-harvest physiology of horticultural crops. *Trends in Food Science & Technology*, 21(10), pp.502-509.
- Ataie, A., Shadifar, M. & Ataee, R. 2016. Review paper: Polyphenolic antioxidants and neuronal regeneration. *Basic and Clinical Neuroscience*, 7(2): 81–90.
- Augustyniak, E., Adam, A., Wojdyla, K., Rogowska-Wrzesinska, A., Willetts, R., Korkmaz, A., Atalay, M., Weber, D., Grune, T., Borsa, C., Gradinaru, D., Chand Bollineni, R., Fedorova, M. & Griffiths, H.R. 2015. Validation of protein carbonyl measurement: A multi-centre study. *Redox Biology*, 4: 149–157.
- Awoniyi, D.O., Aboua, Y.G., Marnewick, J. & Brooks, N. 2012. The Effects of Rooibos (*Aspalathus linearis*), Green Tea (*Camellia sinensis*) and Commercial Rooibos and Green Tea Supplements on Epididymal Sperm in Oxidative Stress-induced Rats. *Phytotherapy research*, 26(8): 1231–1239.
- Ayala, A., Muñoz, M.F. & Argüelles, S. 2014. Lipid Peroxidation: Production, Metabolism, and Signaling Mechanisms of Malondialdehyde and 4-Hydroxy-2-Nonenal. *Oxidative Medicine and Cellular Longevity*, 2014: 360438–31.
- Azqueta, A., Stopper, H., Zegura, B., Dusinska, M. & Møller, P. 2022. Do cytotoxicity and cell death cause false positive results in the *in vitro* comet assay? *Mutation Research - Genetic Toxicology and Environmental Mutagenesis*, 881: p503520.

- Babaei, F., Moafizad, A., Darvishvand, Z., Mirzababaei, M., Hosseinzadeh, H. & Nassiri-Asl, M. 2020. Review of the effects of vitexin in oxidative stress-related diseases. *Food Science and Nutrition*, 8(6): 2569–2580.
- Bai, R., Guo, J., Ye, X.-Y., Xie, Y. & Xie, T. 2022. Oxidative stress: The core pathogenesis and mechanism of Alzheimer's disease. *Ageing Research Reviews*, 77: 101619. <https://doi.org/10.1016/j.arr.2022.101619>.
- Baigi, M.G., Brault, L., Néguesque, A., Beley, M., Hilali, R. El, Gaüzère, F. & Bagrel, D. 2008. Apoptosis/necrosis switch in two different cancer cell lines: Influence of benzoquinone- and hydrogen peroxide-induced oxidative stress intensity, and glutathione. *Toxicology in Vitro*, 22(6): 1547–1554.
- Balboa, M.A. & Balsinde, J. 2021. Phospholipases: From structure to biological function. *Biomolecules*, 11(3): 1–4.
- Bartosz, G. 2003. Generation of reactive oxygen species in biological systems. *Comments On Toxicology*, 9(1): 5.
- Beelders, T., Kalili, K.M., Joubert, E., De Beer, D. & De Villiers, A. 2012. Comprehensive two-dimensional liquid chromatographic analysis of Rooibos (*Aspalathus linearis*) phenolics. *Journal of Separation Science*, 35(14): 1808–1820.
- De Beer, D., Malherbe, C.J., Beelders, T., Willenburg, E.L., Brand, D.J. & Joubert, E. 2015. Isolation of aspalathin and nothofagin from rooibos (*Aspalathus linearis*) using high-performance countercurrent chromatography: Sample loading and compound stability considerations. *Journal of Chromatography A*, 1381: 29–36. <http://dx.doi.org/10.1016/j.chroma.2014.12.078>.
- Behl, T., Makkar, R., Sehgal, A., Singh, S., Sharma, N., Zengin, G., Bungau, S., Andronie-Cioara, F.L., Munteanu, M.A., Brisc, M.C., Uivarosan, D. & Brisc, C. 2021. Current trends in neurodegeneration: Cross talks between oxidative stress, cell death, and inflammation. *International Journal of Molecular Sciences*, 22(14).
- Bejarano, I., Espino, J., González-Flores, D., Casado, J.G., Redondo, P.C., Rosado, J.A., Barriga, C., Pariente, J.A. and Rodríguez, A.B., 2009. Role of calcium signals on hydrogen peroxide-induced apoptosis in human myeloid HL-60 cells. *International Journal of Biomedical Science: IJBS*, 5(3), p.246.
- Bell, M. & Zempel, H. 2022. SH-SY5Y-derived neurons: A human neuronal model system for investigating TAU sorting and neuronal subtype-specific TAU vulnerability. *Reviews in the Neurosciences*, 33(1): 1–15.

- Bizzozero, O.A., Ziegler, J.L., De Jesus, G. & Bolognani, F. 2006. Acute depletion of reduced glutathione causes extensive carbonylation of rat brain proteins. *Journal Of Neuroscience Research*, 83(4): 656–667.
- Blanckenberg, J., Bardien, S., Glanzmann, B., Okubadejo, N.U. and Carr, J.A., 2013. The prevalence and genetics of Parkinson's disease in sub-Saharan Africans. *Journal of the neurological sciences*, 335(1-2), pp.22-25.
- Blum, J. and Fridovich, I., 1985. Inactivation of glutathione peroxidase by superoxide radical. *Archives of Biochemistry and Biophysics*, 240(2), pp.500-508.
- Borutaite, V. & Brown, G.C. 2001. Caspases are reversibly inactivated by hydrogen peroxide. *FEBS letters*, 500(3): 114–118.
- Bramati, L., Minoggio, M., Gardana, C., Simonetti, P., Mauri, P. and Pietta, P., 2002. Quantitative characterization of flavonoid compounds in Rooibos tea (*Aspalathus linearis*) by LC– UV/DAD. *Journal of agricultural and food chemistry*, 50(20), pp.5513-5519.
- Briyal, S., Ranjan, A.K. & Gulati, A. 2023. Oxidative stress: A target to treat Alzheimer's disease and stroke. *Neurochemistry International*, 165: 105509–105509.
- Brunelle, J.K. & Zhang, B. 2010. Apoptosis assays for quantifying the bioactivity of anticancer drug products. *Drug Resistance Updates*, 13(6): 172–179. <http://dx.doi.org/10.1016/j.drug.2010.09.001>.
- Butterfield, D.A., Swomley, A.M. & Sultana, R. 2013. Amyloid β -Peptide (1-42)-induced oxidative stress in alzheimer disease: Importance in disease pathogenesis and progression. *Antioxidants and Redox Signaling*, 19(8): 823–835.
- Canda, B.D., Oguntibeju, O.O. & Marnewick, J.L. 2014. Effects of Consumption of Rooibos (*Aspalathus linearis*) and a Rooibos-Derived Commercial Supplement on Hepatic Tissue Injury by tert-Butyl Hydroperoxide in Wistar Rats. *Oxidative Medicine and Cellular Longevity*, 2014: 716832–9.
- Carrasco, R.A., Stamm, N.B. & Patel, B.K.R. 2003. One-step cellular Caspase-3/7 assay. *BioTechniques*, 34(5): 1064–1067.
- Carrier, P., Debette-Gratien, M., Jacques, J., Grau, M. & Loustaud-Ratti, V. 2021. Rooibos, a fake friend. *Clinics and Research in Hepatology and Gastroenterology*, 45(2): 20–22.
- Cavallaro, R.A., Nicolia, V., Fiorenza, M.T., Scarpa, S. & Fuso, A. 2017. S-Adenosylmethionine and Superoxide Dismutase 1 Synergistically Counteract Alzheimer's Disease Features Progression in TgCRND8 Mice. *Antioxidants*, 6(4): 76.
- Cazzola, M., Rogliani, P., Salvi, S.S., Ora, J. & Matera, M.G. 2021. Use of Thiols in the Treatment of COVID-19: Current Evidence. *Lung*, 199(4): 335–343.

- Cetin, S., Knez, D., Gobec, S., Kos, J. and Pišlar, A., 2022. Cell models for Alzheimer's and Parkinson's disease: At the interface of biology and drug discovery. *Biomedicine & Pharmacotherapy*, 149, p.112924.
- Chaabani, E., Abert Vian, M., Bettaieb Rebey, I., Bourgou, S., Zar Kalai, F., Chemat, F. & Ksouri, R. 2023. Ethanol–water binary solvent affects phenolic composition and antioxidant ability of *Pistacia lentiscus* L. fruit extracts: a theoretical versus experimental solubility study. *Journal of Food Measurement & Characterization*, 17(5): 4705–4714.
- Cháfer-Pericás, C. 2021. Lipid peroxidation in neurodegeneration. *Antioxidants*, 10(3): 1–2.
- Chan, F.K.M., Moriwaki, K. and De Rosa, M.J., 2013. Detection of necrosis by release of lactate dehydrogenase activity. *Immune Homeostasis: Methods and Protocols*, pp.65-70.
- Chavan, S., Sava, L., Saxena, V., Pillai, S., Sontakke, A. & Ingole, D. 2005. Reduced glutathione: Importance of specimen collection. *Indian Journal of Clinical Biochemistry*, 20(1): 150–152.
- Chen, J. 2022. A Case of Early-Onset Alzheimer's Disease with MAPT P301L Mutation and Literature Review: 4–11. DOI: <https://doi.org/10.21203/rs.3.rs-1231300/v1>
- Chen, J.J., Thiyagarajah, M., Song, J., Chen, C., Herrmann, N., Gallagher, D., Rapoport, M.J., Black, S.E., Ramirez, J., Andrezza, A.C., Oh, P., Marzolini, S., Graham, S.J. & Lanctôt, K.L. 2022. Altered central and blood glutathione in Alzheimer's disease and mild cognitive impairment: a meta-analysis. *Alzheimer's Research and Therapy*, 14(1): 1–17.
- Chen, W., Sulcove, J., Frank, I., Jaffer, S., Ozdener, H. & Kolson, D.L. 2002. Development of a Human Neuronal Cell Model for Human Immunodeficiency Virus (HIV)-Infected Macrophage-Induced Neurotoxicity: Apoptosis Induced by HIV Type 1 Primary Isolates and Evidence for Involvement of the Bcl-2/Bcl-xL-Sensitive Intrinsic Apoptosis Pa. *Journal of Virology*, 76(18): 9407–9419.
- Cheng, X., Xu, H.D., Ran, H.H., Liang, G. & Wu, F.G. 2021. Glutathione-Depleting Nanomedicines for Synergistic Cancer Therapy. *ACS Nano*, 15(5): 8039–8068.
- Chizenga, E.P. 2022. Biosynthesis and analysis of a nano-immunophthalocyanine compound for use in photodynamic therapy of human papillomavirus-transformed cervical cancer cells (Doctoral dissertation, University of Johannesburg).
- Christiansen, L., Petersen, H.C., Bathum, L., Frederiksen, H., McGue, M. & Christensen, K. 2004. The catalase -262C/T promoter polymorphism and aging phenotypes. *Journals of Gerontology - Series A Biological Sciences and Medical Sciences*, 59(9): 886–889.
- Chung, K.A., Back, J.S. & Jang, J.H. 2022. The Preventive Effect of 5-Iodo-6-Amino-1,2-Benzopyrone on Apoptosis of Rat Heart-derived Cells induced by Oxidative Stress. *Biomedical Science Letters*, 28(4): 237–246.

- Cilia, R., Akpalu, A., Cham, M., Bonetti, A., Amboni, M., Faceli, E. & Pezzoli, G. 2011. Parkinson's disease in sub-Saharan Africa: step-by-step into the challenge. *Neurodegenerative Disease Management*, 1(3): 193–202.
- Clausen, A., Doctrow, S. & Baudry, M. 2010. Prevention of cognitive deficits and brain oxidative stress with superoxide dismutase/catalase mimetics in aged mice. *Neurobiology of Aging*, 31(3): 425–433.
- Clausen, A., Xu, X., Bi, X. & Baudry, M. 2012. Effects of the Superoxide Dismutase/Catalase Mimetic EUK-207 in a Mouse Model of Alzheimer's Disease: Protection Against and Interruption of Progression of Amyloid and Tau Pathology and Cognitive Decline. *Journal of Alzheimer's Disease*, 30: 183–208.
- Cordier, W., Yousaf, M., Nell, M.J. & Steenkamp, V. 2021. Underlying mechanisms of cytotoxicity in HepG2 hepatocarcinoma cells exposed to arsenic, cadmium, and mercury individually and in combination. *Toxicology In Vitro*, 72: 105101.
- Costa, M., Losada-Barreiro, S., Paiva-Martins, F. & Bravo-Díaz, C. 2021. Polyphenolic antioxidants in lipid emulsions: Partitioning effects and interfacial phenomena. *Foods*, 10(3).
- Crispi, S. & Filosa, S. 2021. Novel perspectives for neurodegeneration prevention: effects of bioactive polyphenols. *Neural Regeneration Research*, 16(7): 1411–1412.
- da Cruz, N.O., Galuppo, A.G., Silva, A.G., Lima, L. da S., Streit, D.P., Fischer, V. & Godoy, L. 2022. Assessment of viability in coral oocytes: a biochemical approach to achieve reliable assays. *Marine Biology*, 169(7): 1–8. <https://doi.org/10.1007/s00227-022-04086-z>.
- D'Aloia, A., Pastori, V., Blasa, S., Campioni, G., Peri, F., Sacco, E., Ceriani, M., Lecchi, M. & Costa, B. 2024. A new advanced cellular model of functional cholinergic-like neurons developed by reprogramming the human SH-SY5Y neuroblastoma cell line. *Cell Death Discovery*, 10(1): 24–24.
- Datta, A., Sarmah, D., Mounica, L., Kaur, H., Kesharwani, R., Verma, G., Veeresh, P., Kotian, V., Kalia, K., Borah, A., Wang, X., Dave, K.R., Yavagal, D.R. & Bhattacharya, P. 2020. Cell Death Pathways in Ischemic Stroke and Targeted Pharmacotherapy. *Translational Stroke Research*, 11(6): 1185–1202.
- Davies, M.J., Fu, S., Wang, H. & Dean, R.T. 1999. Stable markers of oxidant damage to proteins and their application in the study of human disease. *Free Radical Biology and Medicine*, 27(11–12): 1151–1163.
- Davis, A.A., Leyns, C.E.G. & Holtzman, D.M. 2018. Intercellular Sp read of Protein Aggregates in Neurodegenerative Disease. *Annual Review of Cell and Developmental Biology*, 34: 545–568.

- Day, B.J. 2009. Catalase and glutathione peroxidase mimics. *Biochemical Pharmacology*, 77(3): 285–296.
- Dekker, M.C.J., Coulibaly, T., Bardien, S., Ross, O.A., Carr, J. & Komolafe, M. 2020. Parkinson's Disease Research on the African Continent: Obstacles and Opportunities. *Frontiers in Neurology*, 11.
- Demirci-Çekiç, S., Özkan, G., Avan, A.N., Uzunboy, S., Çapanoğlu, E. & Apak, R. 2022. Biomarkers of Oxidative Stress and Antioxidant Defense. *Journal of Pharmaceutical and Biomedical Analysis*, 209: 114477. <https://doi.org/10.1016/j.jpba.2021.114477>.
- Devasagayam, T.P.A., Bloor, K.K. & Ramasarma, T. 2003. Methods for estimating lipid peroxidation: an analysis of merits and demerits. *Indian Journal of Biochemistry & Biophysics*, 40(5): 300–308.
- Docrat, T.F., Nagiah, S., Krishnan, A., Naidoo, D.B. & Chuturgoon, A.A. 2018. Atorvastatin induces MicroRNA-145 expression in HEPG2 cells via regulation of the PI3K/AKT signalling pathway. *Chemico-Biological Interactions*, 287: 32–40. <https://doi.org/10.1016/j.cbi.2018.04.005>.
- Docrat, T.F., Nagiah, S., Naicker, N., Baijnath, S., Singh, S. & Chuturgoon, A.A. 2020. The protective effect of metformin on mitochondrial dysfunction and endoplasmic reticulum stress in diabetic mice brain. *European Journal of Pharmacology*, 875: 173059.
- Dong, Y. & Yong, V.W. 2022. Oxidized phospholipids as novel mediators of neurodegeneration. *Trends in Neurosciences*, 45(6): 419–429. <https://doi.org/10.1016/j.tins.2022.03.002>.
- Dotan, Y., Lichtenberg, D. & Pinchuk, I. 2004. Lipid peroxidation cannot be used as a universal criterion of oxidative stress. *Progress in Lipid Research*, 43(3): 200–227.
- Dringen, R., Pawlowski, P.G. & Hirrlinger, J. 2005. Peroxide detoxification by brain cells. *Journal of Neuroscience Research*, 79(1–2): 157–165.
- Duda-Chodak, A. & Tarko, T. 2023. Possible Side Effects of Polyphenols and Their Interactions with Medicines. *Molecules (Basel, Switzerland)*, 28(6): 2536.
- Eguchi, Y., Shimizu, S. and Tsujimoto, Y., 1997. Intracellular ATP levels determine cell death fate by apoptosis or necrosis. *Cancer research*, 57(10), pp.1835-1840.
- Engels, M., Wang, C., Matoso, A., Maidan, E. & Wands, J. 2013. Tea not Tincture: Hepatotoxicity Associated with Rooibos Herbal Tea. *ACG Case Reports Journal*, 1(1): 58–60.
- Epure, A., Oniga, I., Benedec, D., Hanganu, D., Gheldiu, A.M., Toiu, A. and Vlase, L., 2019. Chemical analysis and antioxidant activity of some rooibos tea products. *Farmacia*, 67(6).
- Erba, D., Riso, P., Criscuoli, F. and Testolin, G., 2003. Malondialdehyde production in Jurkat T cells subjected to oxidative stress. *Nutrition*, 19(6), pp.545-548.
- Erdelmeier, I., Gérard-Monnier, D., Régnard, K., Moze-Henry, N., Yadan, J.C. & Chaudière, J. 1998. Reactions of 1-methyl-2-phenylindole with malondialdehyde and 4- hydroxyalkenals. Analytical

- applications to a colorimetric assay of lipid peroxidation. *Chemical Research in Toxicology*, 11(10): 1176–1183.
- Erekat. 2022. Apoptosis and its therapeutic implications in neurodegenerative diseases. *Clinical Anatomy*, 35(1): 65–78.
- Erekat, N.S., 2018. Apoptosis and its Role in Parkinson's Disease. *Exon Publications*, pp.65-82.
- Erekat, N.S. 2017. Cerebellar Purkinje cells die by apoptosis in the shaker mutant rat. *Brain Research*, 1657: 323–332. <http://dx.doi.org/10.1016/j.brainres.2016.12.025>.
- Erekat, N.S. 2022. Programmed cell death in cerebellar Purkinje neurons. *Journal of Integrative Neuroscience*, 21(1): 30–30.
- Erlwanger, K.H. & Ibrahim, K.G. 2017. Aspalathin a unique phytochemical from the South African rooibos plant (*Aspalathus linearis*): A Mini-Review. *Journal of African Association of Physiological Sciences*, 5(1): 1–6.
- Erukainure, O.L., Salau, V.F., Chukwuma, C.I. & Islam, Md.S. 2020a. Kolaviron: A Biflavonoid with Numerous Health Benefits. *Current Pharmaceutical Design*, 27(4): 490–504.
- Erukainure, O.L., Matsabisa, M.G., Salau, V.F. & Islam, M.S. 2020b. Tetrahydrocannabinol-Rich Extracts from Cannabis Sativa L. Improve Glucose Consumption and Modulate Metabolic Complications Linked to Neurodegenerative Diseases in Isolated Rat Brains. *Frontiers in Pharmacology*, 11.
- Facundo, H.T.F., Brandt, C.T., Owen, J.S. & Lima, V.L.M. 2004. Elevated levels of erythrocyte-conjugated dienes indicate increased lipid peroxidation in schistosomiasis mansoni patients. *Brazilian Journal of Medical and Biological Research*, 37(7): 957–962.
- Fadzil, M.A.M., Mustar, S. & Rashed, A.A. 2023. The Potential Use of Honey as a Neuroprotective Agent for the Management of Neurodegenerative Diseases. *Nutrients*, 15(7): 1558.
- Fakih, W., Zeitoun, R., AlZaim, I., Eid, A.H., Kobeissy, F., Abd-Elrahman, K.S. & El-Yazbi, A.F. 2022. Early metabolic impairment as a contributor to neurodegenerative disease: Mechanisms and potential pharmacological intervention. *Obesity*, 30(5): 982–993.
- Farhoosh, R. 2022. New insights into the kinetic and thermodynamic evaluations of lipid peroxidation. *Food Chemistry*, 375: 131659.
- Feles, S., Overath, C., Reichardt, S., Diegeler, S., Schmitz, C., Kronenberg, J., Baumstark-Khan, C., Hemmersbach, R., Hellweg, C.E. and Liemersdorf, C., 2022. Streamlining culture conditions for the neuroblastoma cell line SH-SY5Y: a prerequisite for functional studies. *Methods and Protocols*, 5(4), p.58.
- Feng, Y. and Wang, X., 2012. Antioxidant therapies for Alzheimer's disease. *Oxidative Medicine and Cellular Longevity*, 472932.

- Ferguson, G. & Bridge, W. 2016. Glutamate cysteine ligase and the age-related decline in cellular glutathione: The therapeutic potential of γ -glutamylcysteine. *Archives of Biochemistry and Biophysics*, 593: 12–23.
- Fernandes, R. 1994. Apoptosis or necrosis: intracellular levels of glutathione influence mode of cell death. *Biochemical Pharmacology*, 48(4): 675.
- Flohé, L. 2013. The fairytale of the GSSG/GSH redox potential. *Biochimica et Biophysica Acta - General Subjects*, 1830(5): 3139–3142. <http://dx.doi.org/10.1016/j.bbagen.2012.10.020>.
- Folch, J., Lees, M. and Sloane Stanley, G.H., 1957. A simple method for the isolation and purification of total lipids from animal tissues. *Journal of Biological Chemistry*, 226(1), pp.497-509.
- Fragoso-Morales, L.G., Correa-Basurto, J. & Rosales-Hernández, M.C. 2021. Implication of nicotinamide adenine dinucleotide phosphate (NADPH) oxidase and its inhibitors in Alzheimer's disease murine models. *Antioxidants*, 10(2): 1–22.
- Franco, R. & Cidlowski, J.A. 2009. Apoptosis and glutathione: Beyond an antioxidant. *Cell Death and Differentiation*, 16(10): 1303–1314.
- Fridovich, I. 1986. Biological effects of the superoxide radical. *Archives of Biochemistry and Biophysics*, 247(1): 1–11.
- Fujita, K., Yamafuji, M., Nakabeppu, Y. and Noda, M., 2012. Therapeutic approach to neurodegenerative diseases by medical gases: focusing on redox signaling and related antioxidant enzymes. *Oxidative Medicine and Cellular Longevity*, 324256.
- Von Gadow, A., Joubert, E. & Hansmann, C.F. 1997. Comparison of the antioxidant activity of rooibos tea (*Aspalathus linearis*) with green, oolong and black tea. *Food Chemistry*, 60(1): 73–77.
- Galati, G., Sabzevari, O., Wilson, J.X. & O'Brien, P.J. 2002. Prooxidant activity and cellular effects of the phenoxyl radicals of dietary flavonoids and other polyphenolics. *Toxicology (Amsterdam)*, 177(1): 91–104.
- Galaup, C., Picard, C., Couderc, F., Gilard, V. & Collin, F. 2022. Luminescent lanthanide complexes for reactive oxygen species biosensing and possible application in Alzheimer's diseases. *FEBS Journal*, 289(9): 2516–2539.
- Gandouzi, I., Fekih, S., Selmi, O., Chalghaf, N., Turki, M., Ayedi, F., Guelmami, N., Azaiez, F., Souissi, N., Marsigliante, S. & Muscella, A. 2023. Oxidative status alteration during aerobic-dominant mixed and anaerobic-dominant mixed effort in judokas. *Heliyon*, 9(10): e20442–e20442.
- Garcimartín, A., Merino, J.J., González, M.P., Sánchez-Reus, M.I., Sánchez-Muniz, F.J., Bastida, S. & Benedí, J. 2014. Organic silicon protects human neuroblastoma SH-SY5Y cells against hydrogen peroxide effects. *BMC Complementary and Alternative Medicine*, 14(1): 1–9.

- Gerasimenko, M.N., Titova, N.M., Zukov, R.A., Dykhno, Y.A. and Peretoka, E.S., 2013. Lipid peroxidation and antioxidant system in erythrocytes of patients with renal cell carcinoma. *Bulletin of Experimental Biology and Medicine*, 154, pp.728-730.
- Ghani, M.A., Barril, C., Bedgood, D.R. & Prenzler, P.D. 2017. Measurement of antioxidant activity with the thiobarbituric acid reactive substances assay. *Food Chemistry*, 230: 195–207.
- Ghibelli, L., Fanelli, C., Rotilio, G., Lafavia, E., Coppola, S., Colussi, C., Civitareale, P. & Ciriolo, M.R. 1998. Rescue of cells from apoptosis by inhibition of active GSH extrusion. *The FASEB Journal*, 12(6): 479–486.
- Głuchowska, K., Pliszka, M. & Szablewski, L. 2021. Expression of glucose transporters in human neurodegenerative diseases. *Biochemical and Biophysical Research Communications*, 540: 8–15.
- Gonzalez-Pinto, A., Martinez-Cengotitabengoa, M., Arango, C., Baeza, I., Otero-Cuesta, S., Graell-Berna, M., Soutullo, C., Leza, J.C. & Micó, J.A. 2012. Antioxidant defense system and family environment in adolescents with family history of psychosis. *BMC Psychiatry*, 12.
- Grochowska, M., Laskus, T. & Radkowski, M. 2019. Gut Microbiota in Neurological Disorders. *Archivum Immunologiae et Therapiae Experimentalis*, 67(6): 375–383. <https://doi.org/10.1007/s00005-019-00561-6>.
- Grodner, B., Napiórkowska, M. & Pisklak, D.M. 2022. Catalase Inhibition by Aminoalkanol Derivatives with Potential Anti-Cancer Activity—*In Vitro* and In Silico Studies Using Capillary Electrophoresis Method. *International Journal of Molecular Sciences*, 23(13).
- Gudoityte, E., Arandarcikaite, O., Mazeikiene, I., Bendokas, V. & Liobikas, J. 2021. Ursolic and Oleanolic Acids: Plant Metabolites with Neuro-modulatory Potential. www.preprints.org.
- Gülcan, H.O. & Orhan, I.E. 2020. The Main Targets Involved in Neuroprotection for the Treatment of Alzheimer's Disease and Parkinson Disease. *Current Pharmaceutical Design*, 26(4): 509–516.
- Hakeem, I.J. & Hodges, N.J. Michelangeli, F. 2020. Cytotoxicity of SH-SY5Y Neuroblastoma Cells to the Antipsychotic Drugs, Chlorpromazine and Trifluoperazine, is via a Ca²⁺ -Mediated Apoptosis Process and Differentiation of These Cells with Retinoic Acid Makes Them More Resistant to Cell Death. *Clinical Oncology and Research*: 1–7.
- Hall, A.G. 1999. The role of glutathione in the regulation of apoptosis. *European Journal of Clinical Investigation*, 29(3): 238–245.
- Halliwell, B. 2003. Oxidative stress in cell culture: an under-appreciated problem? *FEBS Letters*, 540(1): 3–6.
- Halliwell, B., Clement, M.V., Ramalingam, J. and Long, L.H., 2000. Hydrogen peroxide. Ubiquitous in cell culture and *in vivo*? *IUBMB life*, 50(4-5), pp.251-257.

- Halliwell, B. and Gutteridge, J.M., 1981. Formation of a thiobarbituric-acid-reactive substance from deoxyribose in the presence of iron salts: the role of superoxide and hydroxyl radicals. *FEBS Letters*, 128(2), pp.347-352.
- Halliwell, B. (King's C. 1997. Antioxidants and human disease: a general introduction. *Nutrition Reviews*, 55(1): S44–S49.
- Han, D., Handelman, G., Marcocci, L., Sen, C.K., Roy, S., Kobuchi, H., Tritschler, H.J., Flohé, L. & Packer, L. 1997. Lipoic acid increases de novo synthesis of cellular glutathione by improving cystine utilization. *BioFactors*, 6(3): 321–338.
- Haque, M.E., Akther, M., Azam, S., Kim, I.S., Lin, Y., Lee, Y.H. & Choi, D.K. 2022. Targeting α -synuclein aggregation and its role in mitochondrial dysfunction in Parkinson's disease. *British Journal of Pharmacology*, 179(1): 23–45.
- Heck, D.E., Shakarjian, M., Kim, H.D., Laskin, J.D. & Vetrano, A.M. 2010. Mechanisms of oxidant generation by catalase. *Annals of the New York Academy of Sciences*, 1203(1): 120–125.
- Heydarnezhad Asl, M., Pasban Khelejani, F., Bahojb Mahdavi, S.Z., Emrahi, L., Jebelli, A. & Mokhtarzadeh, A. 2022. The various regulatory functions of long noncoding RNAs in apoptosis, cell cycle, and cellular senescence. *Journal of Cellular Biochemistry*, 123(6): 995–1024.
- Hirano, T., Yamaguchi, Y. & Kasai, H. 1997. Inhibition of 8-Hydroxyguanine Repair in Testes after Administration of Cadmium Chloride to GSH-Depleted Rats. *Toxicology and Applied Pharmacology*, 147(1): 9–14.
- Hithamani, G., Kizhakayil, D. & Srinivasan, K. 2017. Uptake of phenolic compounds from plant foods in human intestinal Caco-2 cells. *Journal of Biosciences*, 42(4): 603–611.
- Ho, T., Ahmadi, S. & Kerman, K. 2022. Do glutathione and copper interact to modify Alzheimer's disease pathogenesis? *Free Radical Biology and Medicine*, 181: 180–196. <https://doi.org/10.1016/j.freeradbiomed.2022.01.025>.
- Hodges, D.M., DeLong, J.M., Forney, C.F. & Prange, R.K. 1999. Improving the thiobarbituric acid-reactive-substances assay for estimating lipid peroxidation in plant tissues containing anthocyanin and other interfering compounds. *Planta*, 207(4): 604–611.
- Hoffmann, L., Martins, A., Majolo, F., Contini, V., Laufer, S. & Goettert, M. 2023. Neural regeneration research model to be explored: SH-SY5Y human neuroblastoma cells. *Neural Regeneration Research*, 18(6): 1265–1266.
- Holbrook, J.A., Jarosz-Griffiths, H.H., Caseley, E., Lara-Reyna, S., Poulter, J.A., Williams-Gray, C.H., Peckham, D. & McDermott, M.F. 2021. Neurodegenerative Disease and the NLRP3 Inflammasome. *Frontiers in Pharmacology*, 12: 1–15.

- Hong, I.S., Lee, H.Y. & Kim, H.P. 2014. Anti-oxidative effects of Rooibos tea (*Aspalathus linearis*) on immobilization-induced oxidative stress in rat brain. *PLoS ONE*, 9(1): 1–9.
- Hoosen, M. 2019. The Effects of *Aspalathus linearis* (Rooibos Tea) on Nitric Oxide (NO) and Cytokine Activity. *International Journal of Human and Health Sciences*, 3(3): 150.
- Huang, B., Liu, J., Fu, S., Zhang, Y., Li, Y., He, D., Ran, X., Yan, X., Du, J., Meng, T., Gao, X. & Liu, D. 2020. α -Cyperone Attenuates H₂O₂-Induced Oxidative Stress and Apoptosis in SH-SY5Y Cells via Activation of Nrf2. *Frontiers in Pharmacology*, 11: 1–10.
- Huang, S.L., He, H.B., Zou, K., Bai, C.H., Xue, Y.H., Wang, J.Z. & Chen, J.F. 2014. Protective effect of tomatine against hydrogen peroxide-induced neurotoxicity in neuroblastoma (SH-SY5Y) cells. *Journal of Pharmacy and Pharmacology*, 66(6): 844–854.
- Huang, Y., Lin, J., Zou, J., Xu, J., Wang, M., Cai, H., Yuan, B. & Ma, J. 2021. ABTS as an electron shuttle to accelerate the degradation of diclofenac with horseradish peroxidase-catalysed hydrogen peroxide oxidation. *The Science of the total environment*, 798: 149276–149276.
- Hussein, E.A., Thron, C., Ghaziasgar, M., Vaccari, M., Marnewick, J.L. and Hussein, A.A., 2021. Comparison of phenolic content and antioxidant activity for fermented and unfermented Rooibos samples extracted with water and methanol. *Plants*, 11(1), p.16.
- Hynninen, P.H., Kaartinen, V. & Kolehmainen, E. 2010. Horseradish peroxidase-catalyzed oxidation of chlorophyll a with hydrogen peroxide Characterization of the products and mechanism of the reaction. *Biochimica et Biophysica Acta - Bioenergetics*, 1797(5): 531–542.
- Icer, M.A., Arslan, N. & Gezmen-Karadag, M. 2021. Effects of vitamin e on neurodegenerative diseases: An update. *Acta Neurobiologiae Experimentalis*, 81(1): 21–33.
- Imbriani, P., Martella, G., Bonsi, P. & Pisani, A. 2022. Oxidative stress and synaptic dysfunction in rodent models of Parkinson's disease. *Neurobiology of Disease*, 173: 105851–105851.
- Ioghen, O.C., Ceafalan, L.C. & Popescu, B.O. 2023. SH-SY5Y Cell Line *In Vitro* Models for Parkinson Disease Research-Old Practice for New Trends. *Journal of Integrative Neuroscience*, 22(1): 20–20.
- Iranshahy, M., Javadi, B. & Sahebkar, A. 2022. Protective effects of functional foods against Parkinson's disease: A narrative review on pharmacology, phytochemistry, and molecular mechanisms. *Phytotherapy Research*, 36(5): 1952–1989.
- Iskusnykh, I.Y., Zakharova, A.A. & Pathak, D. 2022. Glutathione in Brain Disorders and Aging. *Molecules*, 27(1): 1–13.
- Ito A, Shinohara K, Kator K. 1991. *Protective action of rooibos tea (Aspalathus linearis) extract against inactivation of L5178Y cells by H₂O₂. In: Proceedings of the international symposium on tea science, The Organizing Committee of ISTS, Shizuoka, pp 381–384.*

- Juchi, K., Takai, T. & Hisatomi, H. 2021. Cell Death via Lipid Peroxidation and Protein Aggregation Diseases. *Biology (Basel, Switzerland)*, 10(5): 399.
- Jaganjac, M., Cindrić, M., Jakovčević, A., Žarković, K. and Žarković, N., 2021. Lipid peroxidation in brain tumors. *Neurochemistry International*, 149, p.105118.
- Jain, A. & Zoncu, R. 2022. Organelle transporters and inter-organelle communication as drivers of metabolic regulation and cellular homeostasis. *Molecular Metabolism*, 60: 101481. <https://doi.org/10.1016/j.molmet.2022.101481>.
- Jin, Y. & Wang, H. 2019. Naringenin Inhibit the Hydrogen Peroxide-Induced SH-SY5Y Cells Injury Through Nrf2/HO-1 Pathway. *Neurotoxicity Research*, 36(4): 796–805.
- Johar, K., Priya, A. & Wong-Riley, M.T.T. 2014. Regulation of Na⁺/K⁺-ATPase by neuron-specific transcription factor Sp4: Implication in the tight coupling of energy production, neuronal activity, and energy consumption in neurons. *European Journal of Neuroscience*, 39(4): 566–578.
- Johnson, W.M., Wilson-Delfosse, A.L. & Mieyal, J.J. 2012. Dysregulation of glutathione homeostasis in neurodegenerative diseases. *Nutrients*, 4(10): 1399–1440.
- Joubert, E. & de Beer, D. 2012. Phenolic content and antioxidant activity of Rooibos food ingredient extracts. *Journal of Food Composition and Analysis*, 27(1): 45–51.
- Joubert, E., Gelderblom, W.C.A., Louw, A. & de Beer, D. 2008. South African herbal teas: *Aspalathus linearis*, *Cyclopia* spp. and *Athrixia phylicoides*-A review. *Journal of Ethnopharmacology*, 119(3): 376–412.
- Joubert, E., Winterton, P., Britz, T.J. & Gelderblom, W.C.A. 2005. Antioxidant and pro-oxidant activities of aqueous extracts and crude polyphenolic fractions of Rooibos (*Aspalathus linearis*). *Journal of Agricultural and Food Chemistry*, 53(26): 10260–10267.
- Juan, C.A., de la Lastra, J.M.P., Plou, F.J. & Pérez-Lebeña, E. 2021. The chemistry of reactive oxygen species (ROS) revisited: Outlining their role in biological macromolecules (DNA, lipids, and proteins) and induced pathologies. *International Journal of Molecular Sciences*, 22(9).
- Kalani, A., Chaturvedi, P., Brunetti, D. & Kalani, K. 2023. Editorial: Mitochondrial therapy in neurodegeneration. *Frontiers in Pharmacology*, 14: 1144093–1144093.
- Kamiloglu, S., Sari, G., Ozdal, T. and Capanoglu, E., 2020. Guidelines for cell viability assays. *Food Frontiers*, 1(3), pp.332-349.
- Kee, K.T., Koh, M., Oong, L.X. & Ng, K. 2013. Screening culinary herbs for antioxidant and α-glucosidase inhibitory activities. *International Journal of Food Science and Technology*, 48(9): 1884–1891.
- Kehm, R., Baldensperger, T., Raupbach, J. & Höhn, A. 2021. Protein oxidation - Formation mechanisms, detection, and relevance as biomarkers in human diseases. *Redox Biology*, 42.

- Kendig, D.M. & Tarloff, J.B. 2007. Inactivation of lactate dehydrogenase by several chemicals: Implications for *in vitro* toxicology studies. *Toxicology in Vitro*, 21(1): 125–132.
- Kermer, P., Liman, J., Weishaupt, J.H. & Bähr, M. 2004. Neuronal apoptosis in neurodegenerative diseases: From basic research to clinical application. *Neurodegenerative Diseases*, 1(1): 9–19.
- Khovarnagh, N. & Seyedalipour, B. 2021. Antioxidant, histopathological and biochemical outcomes of short-term exposure to acetamiprid in liver and brain of rat: The protective role of N-acetylcysteine and S-methylcysteine. *Saudi Pharmaceutical Journal*, 29(3): 280–289.
- Kim, N. & Lee, H.J. 2021. Redox-active metal ions and amyloid-degrading enzymes in Alzheimer's disease. *International Journal of Molecular Sciences*, 22(14).
- Kinoshita, C., Kubota, N. & Aoyama, K. 2022. Glutathione Depletion and MicroRNA Dysregulation in Multiple System Atrophy: A Review. *International Journal of Molecular Sciences*, 23(23).
- Kodali, S.T., Kauffman, P., Kotha, S.R., Yenigalla, A., Veeraraghavan, R., Pannu, S.R., Hund, T.J., Satoskar, A.R., McDaniel, J.C., Maddipati, R.K. and Parinandi, N.L., 2020. Oxidative lipidomics: analysis of oxidized lipids and lipid peroxidation in biological systems with relevance to health and disease. *Measuring Oxidants and Oxidative Stress in Biological Systems*, pp.61-92.
- Kono, Y. & Fridovich, I. 1982. Superoxide radical inhibits catalase. *Journal of Biological Chemistry*, 257(10): 5751–5754.
- Krueger, A., Baumann, S., Krammer, P.H. & Kirchhoff, S. 2001. FLICE-Inhibitory Proteins: Regulators of Death Receptor-Mediated Apoptosis. *Molecular and Cellular Biology*, 21(24): 8247–8254.
- Kulkarni, P. 2021. Bacopa monnieri (Brahmi): A potential treatment course for neurological disorders: Review. ~ 10 ~ *International Journal of Herbal Medicine*, 9(4): 10–18. www.florajournal.com.
- Kumari, R., Dkhar, D.S., Mahapatra, S., Divya, Kumar, R. & Chandra, P. 2022. Nano-bioengineered sensing technologies for real-time monitoring of reactive oxygen species in *in vitro* and *in vivo* models. *Microchemical Journal*, 180: 107615. <https://doi.org/10.1016/j.microc.2022.107615>.
- Kurutas, E.B. 2016. The importance of antioxidants which play the role in cellular response against oxidative/nitrosative stress: Current state. *Nutrition Journal*, 15(1): 1–22. <http://dx.doi.org/10.1186/s12937-016-0186-5>.
- Kwakowsky, A., Prasad, A.A., Peña-Ortega, F. & Lim, S.A.O. 2023. Editorial: Neuronal network dysfunction in neurodegenerative disorders. *Frontiers in Neuroscience*, 17: 1151156–1151156.
- Lampinen, R., Belaya, I., Saveleva, L., Liddell, J.R., Rait, D., Huuskonen, M.T., Giniatullina, R., Sorvari, A., Soppela, L., Mikhailov, N., Boccuni, I., Giniatullin, R., Cruz-Haces, M., Konovalova, J., Koskivi, M., Domanskyi, A., Hämäläinen, R.H., Goldsteins, G., Koistinaho, J., Malm, T., Chew, S., Rilla, K., White, A.R., Marsh-Armstrong, N. & Kanninen, K.M. 2022. Neuron-astrocyte transmitophagy is altered in Alzheimer's disease. *Neurobiology of Disease*, 170: 105753.

- Lampthey, R.N.L., Chaulagain, B., Trivedi, R., Gothwal, A., Layek, B. & Singh, J. 2022. A Review of the Common Neurodegenerative Disorders: Current Therapeutic Approaches and the Potential Role of Nanotherapeutics. *International Journal of Molecular Sciences*, 23(3): 1851.
- Law, B.N.T., Ling, A.P.K., Koh, R.Y., Chye, S.M. & Wong, Y.P. 2014. Neuroprotective effects of orientin on hydrogen peroxide-induced apoptosis in SH-SY5Y cells. *Molecular Medicine Reports*, 9(3): 947–954.
- Lawal, A.O., Davids, L.M. & Marnewick, J.L. 2019. Rooibos (*Aspalathus linearis*) and honeybush (*Cyclopia* species) modulate the oxidative stress associated injury of diesel exhaust particles in human umbilical vein endothelial cells. *Phytomedicine (Stuttgart)*, 59: 152898–152898.
- Lawal, A.O., Oluyede, D.M., Adebimpe, M.O., Olumegbon, L.T., Awolaja, O.O., Elekofehinti, O.O. & Crown, O.O. 2019. The cardiovascular protective effects of rooibos (*Aspalathus linearis*) extract on diesel exhaust particles induced inflammation and oxidative stress involve NF- κ B- and Nrf2-dependent pathways modulation. *Heliyon*, 5(3): e01426. <https://doi.org/10.1016/j.heliyon.2019.e01426>.
- Lee, Y.-J. & Shacter, E. 2000. Hydrogen peroxide inhibits activation, not activity, of cellular caspase-3 *in vivo*. *Free Radical Biology & Medicine*, 29(7): 684–692.
- Lee, Y.M., He, W. & Liou, Y.C. 2021. The redox language in neurodegenerative diseases: oxidative post-translational modifications by hydrogen peroxide. *Cell Death and Disease*, 12(1).
- Leist, M., Single, B., Castoldi, A.F., Kühnle, S. and Nicotera, P., 1997. Intracellular adenosine triphosphate (ATP) concentration: a switch in the decision between apoptosis and necrosis. *The Journal of Experimental Medicine*, 185(8), pp.1481-1486. <http://rupress.org/jem/article-pdf/185/8/1481/1682403/5497.pdf>.
- Levin, J., Högen, T., Hillmer, A.S., Bader, B., Schmidt, F., Kamp, F., Kretschmar, H.A., Bötzel, K. & Giese, A. 2011. Generation of ferric iron links oxidative stress to α -synuclein oligomer formation. *Journal of Parkinson's Disease*, 1(2): 205–216.
- Li, Y., Si, D., Sabier, M., Liu, J., Si, J. and Zhang, X., 2023. Guideline for screening antioxidant against lipid-peroxidation by spectrophotometer. *eFood*, 4(2), p.e80.
- Li, Z., Wang-Heaton, H., Cartwright, B.M., Makinwa, Y., Hilton, B.A., Musich, P.R., Shkriabai, N., Kvaratskhelia, M., Guan, S., Chen, Q., Yu, X. & Zou, Y. 2021. ATR prevents Ca^{2+} overload-induced necrotic cell death through phosphorylation-mediated inactivation of PARP1 without DNA damage signaling. *FASEB Journal*, 35(5): 1–18.
- Linden, A., Gülden, M., Martin, H.J., Maser, E. & Seibert, H. 2008. Peroxide-induced cell death and lipid peroxidation in C6 glioma cells. *Toxicology in Vitro*, 22(5): 1371–1376.

- Liu, T., Sun, L., Zhang, Y., Wang, Y. & Zheng, J. 2022. Imbalanced GSH/ROS and sequential cell death. *Journal of Biochemical and Molecular Toxicology*, 36(1): 1–9.
- Liu, W., Wang, Y. and Youdim, M.B., 2022. A novel neuroprotective cholinesterase-monoamine oxidase inhibitor for treatment of dementia and depression in Parkinson's disease. *Ageing and Neurodegenerative Diseases*, 2(1).
- Long, L.H., Clement, M.V. & Halliwell, B. 2000. Artifacts in cell culture: Rapid generation of hydrogen peroxide on addition of (-)-epigallocatechin, (-)-epigallocatechin gallate, (+)-catechin, and quercetin to commonly used cell culture media. *Biochemical and Biophysical Research Communications*, 273(1): 50–53.
- Lopes, R., Costa, M., Ferreira, M., Gameiro, P., Fernandes, S., Catarino, C., Santos-Silva, A. & Paiva-Martins, F. 2021. Caffeic acid phenolipids in the protection of cell membranes from oxidative injuries. Interaction with the membrane phospholipid bilayer. *Biochimica et Biophysica Acta - Biomembranes*, 1863(12).
- López, V., Cásedas, G., Petersen-Ross, K., Powrie, Y. & Smith, C. 2022. Neuroprotective and anxiolytic potential of green rooibos (*Aspalathus linearis*) polyphenolic extract. *Food and Function*, 13(1): 91–101.
- López-Ortiz, S., Pinto-Fraga, J., Valenzuela, P.L., Martín-Hernández, J., Seisdedos, M.M., García-López, O., Toschi, N., Di Giuliano, F., Garaci, F., Mercuri, N.B., Nisticò, R., Emanuele, E., Lista, S., Lucia, A. & Santos-Lozano, A. 2021. Physical exercise and Alzheimer's disease: Effects on pathophysiological molecular pathways of the disease. *International Journal of Molecular Sciences*, 22(6): 1–29.
- Lopez-Suarez, L., Awabdh, S. Al, Coumoul, X. & Chauvet, C. 2022. The SH-SY5Y human neuroblastoma cell line, a relevant *in vitro* cell model for investigating neurotoxicology in human: Focus on organic pollutants. *Neurotoxicology (Park Forest South)*, 92: 131–155.
- Lu, Y., Chen, Y., Jiang, Z., Ge, Y., Yao, R., Geng, S., Zhang, J., Chen, F., Wang, Y., Chen, G. & Yang, D. 2023. Research progress of ferroptosis in Parkinson's disease: a bibliometric and visual analysis. *Frontiers in Aging Neuroscience*, 15: 1278323–1278323.
- Lv, H., Zhen, C., Liu, J., Yang, P., Hu, L. & Shang, P. 2019. Unraveling the Potential Role of Glutathione in Multiple Forms of Cell Death in Cancer Therapy. *Oxidative Medicine and Cellular Longevity*, 2019: 3150145–16.
- Lwi, S.J., Ford, B.Q., Casey, J.J., Miller, B.L., Levenson, R.W. & Fiske, S.T. 2017. Poor caregiver mental health predicts mortality of patients with neurodegenerative disease. *Proceedings of the National Academy of Sciences of the United States of America*, 114(28): 7319–7324.

- Maccioni, R.B., Calfío, C., González, A. & Lüttges, V. 2022. Novel Nutraceutical Compounds in Alzheimer Prevention. *Biomolecules*, 12(2): 249. <https://www.mdpi.com/2218-273X/12/2/249>.
- Maciotta, S., Meregalli, M. and Torrente, Y., 2013. The involvement of microRNAs in neurodegenerative diseases. *Frontiers in cellular neuroscience*, 7, p.265.
- Mahrus, S., Trinidad, J.C., Barkan, D.T., Sali, A., Burlingame, A.L. & Wells, J.A. 2008. Global sequencing of proteolytic cleavage sites in apoptosis by specific labelling of protein N termini. *Cell*, 134(5): 866–876.
- Makoni, N.J. & Nichols, M.R. 2021. The intricate biophysical puzzle of caspase-1 activation. *Archives of Biochemistry and Biophysics*, 699: 108753. <https://doi.org/10.1016/j.abb.2021.108753>.
- Malar, D.S., Suryanarayanan, V., Prasanth, M.I., Singh, S.K., Balamurugan, K. & Devi, K.P. 2018. Vitexin inhibits A β 25-35 induced toxicity in Neuro-2a cells by augmenting Nrf-2/HO-1 dependent antioxidant pathway and regulating lipid homeostasis by the activation of LXR- α . *Toxicology In Vitro*, 50: 160–171.
- Mancilla, H., Maldonado, R., Cereceda, K., Villarroel-Espíndola, F., Montes de Oca, M., Angulo, C., Castro, M.A., Slebe, J.C., Vera, J.C., Lavandero, S. & Concha, I.I. 2015. Glutathione Depletion Induces Spermatogonial Cell Autophagy. *Journal of Cellular Biochemistry*, 116(10): 2283–2292.
- Mann, H., McCoy, M.T., Subramaniam, J., Van Remmen, H. & Cadet, J.L. 1997. Overexpression of superoxide dismutase and catalase in immortalized neural cells: Toxic effects of hydrogen peroxide. *Brain Research*, 770(1–2): 163–168.
- Marnewick, J.L. 2009. Rooibos and Honeybush: Recent Advances in Chemistry, Biological Activity and Pharmacognosy. 1021: 277–294.
- Marnewick, J.L., Gelderblom, W.C.A. & Joubert, E. 2000. An investigation on the antimutagenic properties of South African herbal teas. *Mutation Research - Genetic Toxicology and Environmental Mutagenesis*, 471(1–2): 157–166.
- Marnewick, J.L., Rautenbach, F., Venter, I., Neethling, H., Blackhurst, D.M., Wolmarans, P. & MacHaria, M. 2011. Effects of rooibos (*Aspalathus linearis*) on oxidative stress and biochemical parameters in adults at risk for cardiovascular disease. *Journal of Ethnopharmacology*, 133(1): 46–52.
- Martemucci, G., Costagliola, C., Mariano, M., D'andrea, L., Napolitano, P. & D'Alessandro, A.G. 2022. Free Radical Properties, Source and Targets, Antioxidant Consumption and Health. *Oxygen*, 2(2): 48–78.
- Massaad, C.A., Washington, T.M., Pautler, R.G. & Klann, E. 2009. Overexpression of SOD-2 reduces hippocampal superoxide and prevents memory deficits in a mouse model of Alzheimer's disease. *Proceedings of the National Academy of Sciences - PNAS*, 106(32): 13576–13581.

- Masuda, T., Inai, M., Miura, Y., Masuda, A. & Yamauchi, S. 2013. Effect of polyphenols on oxymyoglobin oxidation: Prooxidant activity of polyphenols *in vitro* and inhibition by amino acids. *Journal of Agricultural and Food Chemistry*, 61(5): 1097–1104.
- Mathur, S., Gawas, C., Ahmad, I.Z., Wani, M. & Tabassum, H. 2023. Neurodegenerative disorders: Assessing the impact of natural vs drug-induced treatment options. *Aging Medicine*, 6(1): 82–97.
- Maysinger, D. & Hutter, E. 2015. Nanoparticle-based caspase sensors. *Nanomedicine*, 10(3): 483–501.
- McConkey, D.J., 1998. Biochemical determinants of apoptosis and necrosis. *Toxicology letters*, 99(3), pp.157-168.
- Mehri, S. 2023. Relevance of oxidative stress biomarkers, haemoglobin A1c, troponin-I, and angiotensin-converting enzyme metabolism to blood pressure in acute myocardial infarction: a case-control study. *Redox report: Communications in Free Radical Research.*, 28(1): 2209360.
- Mendes, S., Jolner, F., Almeida, S. De & Dargesso, M. 2022. Sesamol prevents mitochondrial impairment and pro - inflammatory alterations in the human neuroblastoma SH - SY5Y cells: role for Nrf2. *Metabolic Brain Disease*: 607–617. <https://doi.org/10.1007/s11011-021-00875-5>.
- Van Der Merwe, J.D., De Beer, D., Joubert, E. & Gelderblom, W.C.A. 2015. Short-term and sub-chronic dietary exposure to aspalathin-enriched green rooibos (*Aspalathus linearis*) extract affects rat liver function and antioxidant status. *Molecules*, 20(12): 22674–22690.
- Mgwatyu, Y., Stander, A.A., Ferreira, S., Williams, W. & Hesse, U. 2020. Rooibos (*Aspalathus linearis*) genome size estimation using flow cytometry and k-mer analyses. *Plants*, 9(2).
- Millar, D.A., Bowles, S., Windvogel, S.L., Louw, J. & Muller, C.J.F. 2020. Effect of Rooibos (*Aspalathus linearis*) extract on atorvastatin-induced toxicity in C3A liver cells. *Journal of Cellular Physiology*, 235(12): 9487–9496.
- Miret, S., De Groene, E.M. & Klaffke, W. 2006. Comparison of *in vitro* assays of cellular toxicity in the human hepatic cell line HepG2. *Journal of Biomolecular Screening*, 11(2): 184–193. <https://doi.org/10.1177/1087057105283787>.
- Mohideen, K., Krithika, C., Jeddy, N., Shamsuddin, S., Basheer, S.A., Sainudeen, S., Alomar, A.A., Sahly, S.A., Mushtaq, S., Raj, A.T., Zanza, A., Testarelli, L. & Patil, S. 2022. Depleting levels of endogenous antioxidant superoxide dismutase in oral sub-mucous fibrosis: A systematic review and meta-analysis: Superoxide dismutase and oral sub-mucous fibrosis. *Journal of Oral Biology and Craniofacial Research*, 12(3): 343–351.
- Mongirdienė, A., Skrodenis, L., Varoneckaitė, L., Mierkytė, G. & Gerulis, J. 2022. Reactive Oxygen Species Induced Pathways in Heart Failure Pathogenesis and Potential Therapeutic Strategies. *Biomedicines*, 10(3).

- Morana, O., Wood, W. & Gregory, C.D. 2022. The Apoptosis Paradox in Cancer. *International Journal of Molecular Sciences*, 23(3): 1328.
- Moreno-García, A., Kun, A., Calero, M. & Calero, O. 2021. The neuromelanin paradox and its dual role in oxidative stress and neurodegeneration. *Antioxidants*, 10(1): 1–19.
- Moujalled, D., Strasser, A. & Liddell, J.R. 2021. Molecular mechanisms of cell death in neurological diseases. *Cell Death & Differentiation*: 2029–2044. <http://dx.doi.org/10.1038/s41418-021-00814-y>.
- Mulaudzi, N., Combrinck, S., Vermaak, I., Joubert, E. & Viljoen, A. 2022. High performance thin layer chromatography fingerprinting of rooibos (*Aspalathus linearis*) and honeybush (*Cyclopia genistoides*, *Cyclopia intermedia* and *Cyclopia subternata*) teas. *Journal of Applied Research on Medicinal and Aromatic Plants*, 30: 100378.
- Munteanu, I.G. & Apetrei, C. 2021. Analytical methods used in determining antioxidant activity: A review. *International Journal of Molecular Sciences*, 22(7).
- Naidoo, D.B., Chuturgoon, A.A., Phulukdaree, A., Guruprasad, K.P., Satyamoorthy, K. & Sewram, V. 2017. Centella asiatica modulates cancer cachexia associated inflammatory cytokines and cell death in leukaemic THP-1 cells and peripheral blood mononuclear cells (PBMC's). *BMC Complementary and Alternative Medicine*, 17(1): 377–377.
- Nandi, A., Yan, L.J., Jana, C.K. & Das, N. 2019. Role of catalase in oxidative stress-and age-associated degenerative diseases. *Oxidative medicine and cellular longevity*, 2019. *Oxidative Medicine and Cellular Longevity*, 2019: 1–19.
- Nasri, Z., Ahmadi, M., Striesow, J., Ravandeh, M., von Woedtke, T. and Wende, K., 2022. Insight into the Impact of Oxidative Stress on the Barrier Properties of Lipid Bilayer Models. *International Journal of Molecular Sciences*, 23(11), p.5932.
- Nelson, G., Nelson, G., Ndlovu, N., Christofides, N., Hlungwani, T.M., Faust, I., Racette, B.A. & Racette, B.A. 2020. Validation of Parkinson's Disease-Related Questionnaires in South Africa. *Parkinson's Disease*, 2020.
- Nilles, J., Weiss, J. & Theile, D. 2022. Crystal violet staining is a reliable alternative to bicinchoninic acid assay-based normalization. *BioTechniques*, 73(3): 131–135.
- Nishida, T., Naguro, I. & Ichijo, H. 2022. NAMPT-dependent NAD + salvage is crucial for the decision between apoptotic and necrotic cell death under oxidative stress. *Cell Death Discovery*, 8(1): 195–195.
- Nowak, E., Kammerer, S. & Küpper, J.H. 2018. ATP-based cell viability assay is superior to trypan blue exclusion and XTT assay in measuring cytotoxicity of anticancer drugs Taxol and Imatinib,

- and proteasome inhibitor MG-132 on human hepatoma cell line HepG2. *Clinical Hemorheology and Microcirculation*, 69(1–2): 327–336.
- Oancea, M., Mazumder, S., Crosby, M.E. & Almasan, A. 2006. Apoptosis assays. *Methods Molecular Medicine*, 129: 279–290.
- Oboh, G., Atoki, A.V., Ademiluyi, A.O. & Ogunsuyi, O.B. 2023. African Jointfir (*Gnetum africanum*) and Editan (*Lasianthera africana*) leaf alkaloid extracts exert antioxidant and anticholinesterase activities in fruit fly (*Drosophila melanogaster*). *Food Science & Nutrition*: 1–11.
- Oliveira, M.C., Yusupov, M., Bogaerts, A. and Cordeiro, R.M., 2021. Lipid oxidation: role of membrane phase-separated domains. *Journal of Chemical Information and Modeling*, 61(6), pp.2857-2868.
- de Oliveira, M.R., de Bittencourt Brasil, F. and Fürstenau, C.R., 2018. Sulforaphane promotes mitochondrial protection in SH-SY5Y cells exposed to hydrogen peroxide by an Nrf2-dependent mechanism. *Molecular Neurobiology*, 55, pp.4777-4787.
- Olufunmilayo, E.O., Gerke-Duncan, M.B. and Holsinger, R.D., 2023. Oxidative stress and antioxidants in neurodegenerative disorders. *Antioxidants*, 12(2), p.517.
- Omoruyi, S.I., Akinfenwa, A.O., Ekpo, O.E. & Hussein, A.A. 2023. Aspalathin and linearthin from *Aspalathus linearis* (Rooibos) protect SH-SY5Y cells from MPP⁺-induced neuronal toxicity. *South African Journal of Botany*, 157: 53–63.
- Orlando, P., Chellan, N., Louw, J., Tiano, L., Cirilli, I., Dłudla, P., Joubert, E. & Muller, C.J.F. 2019. Aspalathin-rich green Rooibos extract lowers LDL-cholesterol and oxidative status in high-fat diet-induced diabetic vervet monkeys. *Molecules (Basel, Switzerland)*, 24(9): 1713.
- Oshino, N., Oshino, R. & Chance, B. 1973. The characteristics of the ‘peroxidatic’ reaction of catalase in ethanol oxidation. *The Biochemical Journal*, 131(3): 555–563.
- Paciorek, P., Żuberek, M. and Grzelak, A., 2020. Products of lipid peroxidation as a factor in the toxic effect of silver nanoparticles. *Materials*, 13(11), p.2460.
- Padanilam, B.J., 2003. Cell death induced by acute renal injury: a perspective on the contributions of apoptosis and necrosis. *American Journal of Physiology-Renal Physiology*, 284(4), pp. F608-F627. <http://www.ajprenal.org>.
- Pantsi, W.G., Marnewick, J.L., Esterhuysen, A.J., Rautenbach, F. & van Rooyen, J. 2011. Rooibos (*Aspalathus linearis*) offers cardiac protection against ischaemia/reperfusion in the isolated perfused rat heart. *Phytomedicine (Stuttgart)*, 18(14): 1220–1228.
- Parhamifar, L., Andersen, H. & Moghimi, S.M. 2019. Lactate dehydrogenase assay for assessment of polycation cytotoxicity. *Methods in Molecular Biology*, 1943: 291–299.

- Park, H.R., Lee, H., Park, H., Jeon, J.W., Cho, W.K. & Ma, J.Y. 2015. Neuroprotective effects of Liriope platyphylla extract against hydrogen peroxide-induced cytotoxicity in human neuroblastoma SH-SY5Y cells. *BMC Complementary and Alternative Medicine*, 15(1): 1–11.
- Park, J., Halliday, G.M., Surjana, D. & Damian, D.L. 2010. Nicotinamide prevents ultraviolet radiation-induced cellular energy loss. *Photochemistry and Photobiology*, 86(4): 942–948.
- Piek, H., Venter, I., Rautenbach, F. & Marnewick, J.L. 2019. Rooibos herbal tea: An optimal cup and its consumers. *Health SA Gesondheid*, 24: 1–9.
- Plaskova, A. & Mlcek, J. 2023. New insights of the application of water or ethanol-water plant extract rich in active compounds in food. *Frontiers in Nutrition (Lausanne)*, 10: 1118761–1118761.
- Popoola, O.K., Adedara, T.O., Ajao, A.T., Akinrinlola, M. and Olasanmi, A.O., 2019. Effect of Fermentation on the Factor of Skin Pigmentation Inhibitory Activity and Total Antioxidant Capacities Demonstrated by the South African Rooibos (*Aspalathus linearis*). *Biomed J Sci & Tech Res*, 20(4), pp.15195-15202.
- Premratanachai, A., Suwanjang, W., Govitrapong, P. & Chetsawang, J. 2020. Melatonin prevents calcineurin-activated the nuclear translocation of nuclear factor of activated T-cells in human neuroblastoma SH-SY5Y cells undergoing hydrogen peroxide-induced cell death. *Journal of Chemical Neuroanatomy*, 106: 101793. <https://doi.org/10.1016/j.jchemneu.2020.101793>.
- Procházková, M., Killinger, M., Prokeš, L. & Klepárník, K. 2022. Miniaturized bioluminescence technology for single-cell quantification of caspase-3/7. *Journal of Pharmaceutical and Biomedical Analysis*, 209: 114512. <https://doi.org/10.1016/j.jpba.2021.114512>.
- Putcha, G. V., Harris, C.A., Moulder, K.L., Easton, R.M., Thompson, C.B. & Johnson, E.M. 2002. Intrinsic and extrinsic pathway signaling during neuronal apoptosis: Lessons from the analysis of mutant mice. *Journal of Cell Biology*, 157(3): 441–453.
- Pyrzanowska, J., 2023. Pharmacological activity of *Aspalathus linearis* extracts: pre-clinical research in view of prospective neuroprotection. *Nutritional Neuroscience*, 26(5), pp.384-402.
- Pyrzanowska, J., Fecka, I., Mirowska-guzel, D. & Joniec-maciejak, I. 2019. Long-term administration of *Aspalathus linearis* infusion affects spatial memory of adult Sprague-Dawley male rats as well as increases their striatal dopamine content. *Journal of Ethnopharmacology*, 238: 111881. <https://doi.org/10.1016/j.jep.2019.111881>.
- Pyrzanowska, J., Joniec-Maciejak, I., Blecharz-Klin, K., Piechal, A., Mirowska-Guzel, D., Fecka, I. & Widy-Tyszkiewicz, E. 2021. *Aspalathus linearis* infusion affects hole-board test behaviour and amino acid concentration in the brain. *Neuroscience Letters*, 747: 135680. <https://doi.org/10.1016/j.neulet.2021.135680>.

- Quarshie, J.T., Mensah, E.N., Quaye, O. & Aikins, A.R. 2021. The Current State of Parkinsonism in West Africa: A Systematic Review. *Parkinson's Disease*, 2021.
- Rahman, A. 2020. Studies in natural products chemistry. *Elsevier*. 1st Edition, Volume 67
- Ransy, C., Vaz, C., Lombès, A. & Bouillaud, F. 2020. Use of H₂O₂ to cause oxidative stress, the catalase issue. *International Journal of Molecular Sciences*, 21(23): 1–14.
- Raveh, O., Pinchuk, I., Fainaru, M. and Lichtenberg, D., 2002. Oxygen availability as a possible limiting factor in LDL oxidation. *Free radical research*, 36(10), pp.1109-1114.
- Re, R., Pellegrini, N., Proteggente, A., Pannala, A., Yang, M. & Rice-Evans, C. 1999. Antioxidant activity applying an improved ABTS radical cation decolorization assay. *Free Radical Biology & Medicine*, 26(9): 1231–1237.
- Recknagel, R. & Glende, E. 1984. [40] Spectrophotometric detection of lipid conjugated dienes. *Methods in Enzymology*, 105: 331–337.
- Reddy, P., Pradeep, S., S. M., G., Dharmashekar, C., G., D., M. R., S.C., Srinivasa, C., Shati, A.A., Alfaifi, M.Y., Elbehairi, S.E.I., Achar, R.R., Silina, E., Stupin, V., Manturova, N., Shivamallu, C. & Kollur, S.P. 2023. Cell cycle arrest and apoptotic studies of *Terminalia chebula* against MCF-7 breast cancer cell line: an *in vitro* and *in silico* approach. *Frontiers in Oncology*, 13: 1221275–1221275.
- Redegeld, F.A.M., Moison, R.M.W., Koster, A.S. & Noordhoek, J. 1992. Depletion of ATP but not of GSH affects viability of rat hepatocytes. *European Journal of Pharmacology: Environmental Toxicology and Pharmacology*, 228(4): 229–236.
- Richard, R. & Mousa, S. 2022. Necroptosis in Alzheimer's disease: Potential therapeutic target. *Biomedicine & Pharmacotherapy*, 152: 113203–113203.
- Rosa, A.C., Corsi, D., Cavi, N., Bruni, N. & Dosio, F. 2021. Superoxide dismutase administration: A review of proposed human uses. *Molecules*, 26(7): 1–40.
- Rosini, E. & Pollegioni, L. 2022. Reactive oxygen species as a double-edged sword: The role of oxidative enzymes in antitumor therapy. *BioFactors*, 48(2): 384–399.
- Rousseau, R.M., 2001. Detection limit and estimate of uncertainty of analytical XRF results. *Rigaku J*, 18(2), pp.33-47.
- Sadowska-Bartosz, I. and Bartosz, G., 2022. Evaluation of the antioxidant capacity of food products: Methods, applications, and limitations. *Processes*, 10(10), p.2031.
- Sahin, M., Oncu, G., Yilmaz, M.A., Ozkan, D. & Saybasili, H. 2021. Transformation of SH-SY5Y cell line into neuron-like cells: Investigation of electrophysiological and biomechanical changes. *Neuroscience Letters*, 745: 135628.

- Saleem, S., 2021. Apoptosis, autophagy, necrosis and their multi galore crosstalk in neurodegeneration. *Neuroscience*, 469, pp.162-174.
- Sánchez, M.C., Llama-Palacios, A., Marín, M.J., Figuero, E., León, R., Blanc, V., Herrera, D. & Sanz, M. 2013. Validation of ATP bioluminescence as a tool to assess antimicrobial effects of mouthrinses in an *in vitro* subgingival-biofilm model. *Medicina Oral, Patología Oral y Cirugía Bucal*, 18(1).
- Sanghai, N. & Tranmer, G.K. 2022. Hydrogen peroxide and amyotrophic lateral sclerosis: From biochemistry to pathophysiology. *Antioxidants*, 11(1).
- Saxena, P., Selvaraj, K., Khare, S.K. & Chaudhary, N. 2022. Superoxide dismutase as multipotent therapeutic antioxidant enzyme: Role in human diseases. *Biotechnology Letters*, 44(1): 1–22.
- Schmidt, M.F., Gan, Z.Y. & Komander, D. 2021. Ubiquitin signalling in neurodegeneration: mechanisms and therapeutic opportunities. *Cell Death & Differentiation*: 570–590. <http://dx.doi.org/10.1038/s41418-020-00706-7>.
- Schütt, F., Aretz, S., Auffarth, G.U. & Kopitz, J. 2012. Moderately reduced ATP levels promote oxidative stress and debilitate autophagic and phagocytic capacities in human RPE cells. *Investigative Ophthalmology & Visual Science*, 53(9): 5354–5361.
- Shahraki, S., Shiri, F. & Razmara, Z. 2023. Improving enzymatic performance of antioxidant enzyme catalase in combination with [Mn (phen)2Cl.H₂O] Cl.tu complex. *Applied Organometallic Chemistry*, 37(4).
- Shaito, A., Posadino, A.M., Younes, N., Hasan, H., Halabi, S., Alhababi, D., Al-Mohannadi, A., Abdel-Rahman, W.M., Eid, A.H., Nasrallah, G.K. & Pintus, G. 2020. Potential Adverse Effects of Resveratrol: A Literature Review. *International Journal of Molecular Sciences*, 21(6): 2084.
- Sheik Abdul, N. & Marnewick, J.L. 2022. Green Rooibos extract attenuates high glucose induced oxidative stress in a human derived (HepG2) liver cell line. *South African Journal of Botany*, 151: 852–865. <https://doi.org/10.1016/j.sajb.2022.11.002>.
- Sheik Abdul, N. & Marnewick, J.L. 2021. Rooibos, a supportive role to play during the COVID-19 pandemic? *Journal of Functional Foods*, 86.
- Sheng, Y., Abreu, I.A., Cabelli, D.E., Maroney, M.J., Miller, A.F., Teixeira, M. & Valentine, J.S. 2014. Superoxide dismutases and superoxide reductases. *Chemical Reviews*, 114(7): 3854–3918.
- Shiple, M.M., Mangold, C.A. and Szpara, M.L., 2016. Differentiation of the SH-SY5Y human neuroblastoma cell line. *JoVE (Journal of Visualized Experiments)*, (108), p.e53193.
- Shrivastava, A.N., Triller, A. & Melki, R. 2020. Cell biology and dynamics of Neuronal Na⁺/K⁺-ATPase in health and diseases. *Neuropharmacology*, 169: 107461.
- Sies, H. 2020. Oxidative stress: Concept and some practical aspects. *Antioxidants*, 9(9): 1–6.

- Sies, H. & Jones, D.P. 2020. Reactive oxygen species (ROS) as pleiotropic physiological signalling agents. *Nature Reviews Molecular Cell Biology*, 21(7): 363–383.
- Singh, A., Kukreti, R., Saso, L. & Kukreti, S. 2019. Oxidative stress: A key modulator in neurodegenerative diseases. *Molecules*, 24(8).
- Singh, R. & Singh, S. 2019. Redox-dependent catalase mimetic cerium oxide-based nanozyme protect human hepatic cells from 3-AT induced acatalasemia. *Colloids and Surfaces B: Biointerfaces*, 175(September 2018): 625–635. <https://doi.org/10.1016/j.colsurfb.2018.12.042>.
- Singleton et al. 1999. Analysis of total phenols and other oxidation substrates and antioxidants by means of folin-ciocalteu reagent. *Methods in Enzymology*, 299: 152–178.
- Sinisalo, M., Enkovaara, A.-L. & Kivistö, K.T. 2010. Possible hepatotoxic effect of Rooibos tea: a case report. *European Journal of Clinical Pharmacology*, 66(4): 427–428.
- Sirotkin, A. V. 2021. Rooibos (*Aspalathus linearis*) influence on health and ovarian functions. *Journal of Animal Physiology and Animal Nutrition*: 1–5.
- Situnayake, R.D., Crump, B.J., Zezulka, A.V., Davis, M., McConkey, B. and Thurnham, D.I., 1990. Measurement of conjugated diene lipids by derivative spectroscopy in heptane extracts of plasma. *Annals of Clinical Biochemistry*, 27(3), pp.258-266.
- Smadi, M.A., Hammadeh, M.E., Batiha, O., Al Sharu, E., Altalib, M.M., Jahmani, M.Y., Mahdy, A. & Amor, H. 2021. Elevated seminal protein carbonyl concentration is correlated with asthenozoospermia and affects adversely the laboratory intracytoplasmic sperm injection (ICSI) outcomes. *Andrologia*, 53(11): 1–8.
- Strother, L., Miles, G.B., Holiday, A.R., Cheng, Y. & Doherty, G.H. 2021. Long-term culture of SH-SY5Y neuroblastoma cells in the absence of neurotrophins: A novel model of neuronal ageing. *Journal of Neuroscience Methods*, 362: 109301. <https://doi.org/10.1016/j.jneumeth.2021.109301>.
- Su, B., Wang, X., Lee, H., Tabaton, M., Perry, G., Smith, M.A. & Zhu, X. 2010. Chronic oxidative stress causes increased tau phosphorylation in M17 neuroblastoma cells. *Neuroscience Letters*, 468(3): 267–271.
- Suhail, M., 2010. Na⁺, K⁺-ATPase: ubiquitous multifunctional transmembrane protein and its relevance to various pathophysiological conditions. *Journal of clinical medicine research*, 2(1), p.1.
- Swaminathan, A., Basu, M., Bekri, A., Drapeau, P. & Kundu, T.K. 2019. The dietary flavonoid, luteolin, negatively affects neuronal differentiation. *Frontiers in Molecular Neuroscience*, 12.
- Tabernilla, A., Rodrigues, B.D.S., Pieters, A., Caufriez, A., Leroy, K., Campenhout, R. Van, Cooreman, A., Gomes, A.R., Arnesdotter, E., Gijbels, E. & Vinken, M. 2021. *In vitro* liver toxicity testing of chemicals: A pragmatic approach. *International Journal of Molecular Sciences*, 22(9).

- Takalani, N.B., Adefolaju, G.A., Henkel, R.R. & Opuwari, C.S. 2022. *In vitro* effects of aqueous extract of unfermented Rooibos on human spermatozoa. *Andrologia*: 1–10.
- Taurone, S., Ralli, M., Artico, M., Madia, V.N., Scarpa, S., Nottola, S.A., Maconi, A., Betti, M., Familiari, P., Nebbioso, M., Costi, R. & Micera, A. 2022. Oxidative Stress and Visual System: a Review. *EXCLI Journal*, 21: 544–553.
- Tefera, T.W., Steyn, F.J., Ngo, S.T. & Borges, K. 2021. CNS glucose metabolism in Amyotrophic Lateral Sclerosis: a therapeutic target? *Cell and Bioscience*, 11(1): 1–17. <https://doi.org/10.1186/s13578-020-00511-2>.
- Tobin, J., 2018. Rooibos fermentation-Characterising phenolic changes using chemometric analysis and kinetic modelling (Doctoral dissertation, Stellenbosch: Stellenbosch University).
- Toledo, A.R.L., Monroy, G.R., Salazar, F.E., Lee, J.Y., Jain, S., Yadav, H. and Borlongan, C.V., 2022. Gut–brain axis as a pathological and therapeutic target for neurodegenerative disorders. *International Journal of Molecular Sciences*, 23(3), p.1184.
- Tönnies, E. and Trushina, E., 2017. Oxidative stress, synaptic dysfunction, and Alzheimer’s disease. *Journal of Alzheimer's Disease*, 57(4), pp.1105-1121.
- Tretter, V., Hochreiter, B., Zach, M.L., Krenn, K. & Klein, K.U. 2022. Understanding cellular redox homeostasis: A challenge for precision medicine. *International Journal of Molecular Sciences*, 23(1).
- Tsikakos, D. 2017. Assessment of lipid peroxidation by measuring malondialdehyde (MDA) and relatives in biological samples: Analytical and biological challenges. *Analytical Biochemistry*, 524: 13–30.
- Tsujimoto, Y. 1997. Apoptosis and necrosis: intracellular ATP level as a determinant for cell death modes. *Cell death and Differentiation*, 4(6): 429.
- Uçkan, K., Demir, H., Turan, K., Sarıkaya, E. & Demir, C. 2022. Role of Oxidative Stress in Obese and Nonobese PCOS Patients. *International Journal of Clinical Practice (Esher)*, 2022: 4579831–9.
- Ul-Islam, S., Shehzad, A., Bilal Ahmed, M. & Lee, Y.S. 2020. Intranasal delivery of nanoformulations: A potential way of treatment for neurological disorders. *Molecules*, 25(8): 1–27.
- Uversky, V.N., Li, J. & Fink, A.L. 2001. Metal-triggered structural transformations, aggregation, and fibrillation of human α -synuclein: A possible molecular link between Parkinson’s disease and heavy metal exposure. *Journal of Biological Chemistry*, 276(47): 44284–44296.
- Vazquez-Alvarado, M., Vanasupa, S.L., Valdez, E.H., Pama, A.M., Crowder, M.J., Vanasupa, L., Martinez, N.W. & Martinez, A.W. 2023. Evaluation of chromogenic substrates for horseradish peroxidase on paper-based microfluidic devices. *Sensors and Actuators B: Chemical*, 377.

- Vhangani, L.N., Favre, L.C., Rolandelli, G., Van Wyk, J. & Del Pilar Buera, M. 2022. Optimising the Polyphenolic Content and Antioxidant Activity of Green Rooibos (*Aspalathus linearis*) Using Beta-Cyclodextrin Assisted Extraction. *Molecules (Basel, Switzerland)*, 27(11): 3556.
- Villalpando-Rodriguez, G.E. and Gibson, S.B., 2021. Reactive oxygen species (ROS) regulates different types of cell death by acting as a rheostat. *Oxidative Medicine and Cellular Longevity*, 2021.
- Waki, T., Nakanishi, I., Matsumoto, K.I., Kitajima, J., Chikuma, T. & Kobayashi, S. 2012. Key role of chemical hardness to compare 2,2-diphenyl-1-picrylhydrazyl radical scavenging power of flavone and flavonol O-glycoside and C-glycoside derivatives. *Chemical and Pharmaceutical Bulletin*, 60(1): 37–44.
- Wang, P., Henning, S.M. & Heber, D. 2010. Limitations of MTT and MTS-based assays for measurement of antiproliferative activity of green tea polyphenols. *PLoS ONE*, 5(4).
- Wang, Q.-S., Xie, K.-Q., Zhang, C., Zhu, Y.-J., Zhang, L.-P., Guo, X. & Yu, S. 2005. Allyl chloride-induced time dependent changes of lipid peroxidation in rat nerve tissue. *Neurochemical Research*, 30(11): 1387–1395.
- Wang, W., Wu, S., Wang, J., Li, Z., Cui, H., Lin, S., Zhu, J. & Chen, Q. 2019. Superoxide dismutase transcellular shuttle constructed from dendritic MOF and charge reversible protein derivatives. *Chemical Science (Cambridge)*, 10(16): 4476–4485.
- Waszkowiak, K. & Gliszczyńska-Świątło, A. 2016. Binary ethanol–water solvents affect phenolic profile and antioxidant capacity of flaxseed extracts. *European food Research & Technology*, 242(5): 777–786.
- Watanabe, T., Sekine, S., Naguro, I., Sekine, Y. & Ichijo, H. 2015. Apoptosis signal-regulating kinase 1 (ASK1)-p38 pathway-dependent cytoplasmic translocation of the orphan nuclear receptor NR4A2 is required for oxidative stress-induced necrosis. *Journal of Biological Chemistry*, 290(17): 10791–10803.
- Waterhouse, A.L., 2002. Determination of total phenolics. *Current Protocols in Food Analytical Chemistry*, 6(1), pp. I1-1.
- Widhiantara, G., Permatasari, A.A.A.P. and Wiradana, P.A., 2021. The effect of sembung leaf extract (*Blumea balsamifera*) on the number and diameter of rats Leydig cells induced by high-fat diet. *Plant Archives*, 21(no 1).
- Wijeratne, S.S.K., Cuppett, S.L. & Schlegel, V. 2005. Hydrogen peroxide induced oxidative stress damage and antioxidant enzyme response in Caco-2 human colon cells. *Journal of Agricultural and Food Chemistry*, 53(22): 8768–8774.
- Winterbourn, C.C. 2020. Biological chemistry of superoxide radicals. *ChemTexts*, 6(1): 1–13.

- Xie, L., Zhu, Q. & Lu, J. 2022. Can We Use Ginkgo Biloba Extract to Treat Alzheimer's Disease? Lessons from Preclinical and Clinical Studies. *Cells*, 11(3): 479. <https://www.mdpi.com/2073-4409/11/3/479>.
- Yang, J., Yang, J., Liang, S.H., Xu, Y., Moore, A. and Ran, C., 2016. Imaging hydrogen peroxide in Alzheimer's disease via cascade signal amplification. *Scientific Reports*, 6(1), p.35613.
- Yanowsky-Escatell, F.G., Andrade-Sierra, J., Pazarín-Villaseñor, L., Santana-Arciniega, C., Torres-Vázquez, E. de J., Chávez-Iñiguez, J.S., Zambrano-Velarde, M.Á. & Preciado-Figueroa, F.M. 2020. The role of dietary antioxidants on oxidative stress in diabetic nephropathy. *Iranian Journal of Kidney Diseases*, 14(2): 81–94.
- Yoo, K.M., Lee, C.H., Lee, H., Moon, B.K. & Lee, C.Y. 2008. Relative antioxidant and cytoprotective activities of common herbs. *Food Chemistry*, 106(3): 929–936.
- Yu, Y., Tang, D., Liu, C., Zhang, Q., Tang, L., Lu, Y. and Xiao, H., 2022. Biodegradable polymer with effective near-Infrared-II absorption as a photothermal agent for deep tumour therapy. *Advanced Materials*, 34(4), p.2105976.
- Yun, B., King, M., Draz, M.S., Kline, T. and Rodriguez-Palacios, A., 2022. Oxidative reactivity across kingdoms in the gut: Host immunity, stressed microbiota, and oxidised foods. *Free Radical Biology and Medicine*, 178, pp.97-110. <https://doi.org/10.1016/j.freeradbiomed.2021.11.009>.
- Zhang, B., Pan, C., Feng, C., Yan, C., Yu, Y., Chen, Z., Guo, C. & Wang, X. 2022. Role of mitochondrial reactive oxygen species in homeostasis regulation. *Redox Report*, 27(1): 45–52.
- Zhang, L., Yu, H., Sun, Y., Lin, X., Chen, B., Tan, C., Cao, G. & Wang, Z. 2007. Protective effects of salidroside on hydrogen peroxide-induced apoptosis in SH-SY5Y human neuroblastoma cells. *European Journal of Pharmacology*, 564(1–3): 18–25. <http://dx.doi.org/10.1016/j.ejphar.2007.01.089>.
- Zhang, P., Li, T., Wu, X., Nice, E.C., Huang, C. & Zhang, Y. 2020. Oxidative stress and diabetes: antioxidative strategies. *Frontiers of Medicine*, 14(5): 583–600.
- Zhang, Y., Yang, H., Wei, D., Zhang, X., Wang, J., Wu, X. & Chang, J. 2021. Mitochondria-targeted nanoparticles in treatment of neurodegenerative diseases. *Exploration*, 1(3): 20210115.
- Zhao, Z. 2019. Iron and oxidizing species in oxidative stress and Alzheimer's disease. *Aging Medicine*, 2(2): 82–87.
- Zhu, X., Lee, H.G., Casadesus, G., Avila, J., Drew, K., Perry, G. and Smith, M.A., 2005. Oxidative imbalance in Alzheimer's disease. *Molecular neurobiology*, 31, pp.205-217.
- Zhu, Y., Gong, P., Wang, J., Cheng, J., Wang, W., Cai, H., Ao, R., Huang, H., Yu, M., Lin, L. and Chen, X., 2023. Amplification of lipid peroxidation by regulating cell membrane unsaturation to enhance chemodynamic therapy. *Angewandte Chemie*, 135(12), p.e202218407.

7. APPENDIX

Appendix 1: Recipe for preparation of TPC reagents

Ethanol	10%: In a 1L media bottle, add 100 mL of ethanol (Saarchem Cat Nr: 2233540LP) to 900 mL H ₂ O.
Folin Reagent	In a 15 mL screw cap tube, add 1 mL Folin-Ciocalteus phenol reagent (Merck Cat Nr: 109001) (Reagent rack) to 9 mL H ₂ O and mix well. Prepare fresh on day of analysis. This mix should have a bright yellow colour, if otherwise discard.
Sodium Carbonate:	7.5 %: In a 100 mL media bottle, weigh 7.50 g Na ₂ CO ₃ (Aldrich Cat Nr: 223530) (Reagent rack) and add 100 mL H ₂ O. Mix until dissolved. Store at room temperature for up to a month.
Gallic acid standard	In a 50 mL screw cap tube, dissolve 40 mg (0.040 g) gallic acid (Sigma Cat Nr: G7384) (Reagent rack) in 50 mL 10% ethanol to give a stock standard concentration of 800 mg/L. Prepare fresh. Use this solution as the stock standard. Check: When diluted 50 x with 10 % ethanol this solution should give an absorbance of 0.509 ± 0.010 at 280 nm.
Control:	<p>In a 50 mL screw cap tube, dissolve 10 mg (0.010 g) gallic acid (Sigma Cat Nr: G7384) (Reagent rack) in 50 mL 10 % ethanol (200 mg/L). Prepare fresh. Use this solution as the control.</p> <p>Check: When diluted 12.5 x with 10 % ethanol this solution should give an absorbance of 0.509 ± 0.010 at 280 nm.</p>

Appendix 2: Recipe for preparation of FRAP reagents

Acetate Buffer:	300 mM, pH 3.6
	In a 1 L media bottle add the following:
	1.627 g Sodium acetate (Reagent rack)
	16 mL Glacial acetic acid (SAARCHEM Cat Nr.: 1021000) (Reagent rack)
	Make up with dH ₂ O to 1 L
	Check pH, Store at room temperature for up to a month.
Dilute HCl:	40mM (SAARCHEM Cat Nr.: 100319 LP)
	In a 1 L media bottle add the following:
	1.46 mL concentrated HCl (32 % HCl) (Reagent rack)
	Make up with dH ₂ O to 1 L
	Store at room temperature for up to 6 months
TPTZ (2,4,6-tri[2-pyridyl]-s-triazine)	10 mM (Sigma Cat Nr.: T1253)
	In a 15 mL conical tube, add the following:
	0.0093g TPTZ (Fridge)
	3 mL of 40 mM HCl
	Make fresh on day of assay
Iron (III) chloride hexahydrate:	20 mM (F2877)
	In a 15 mL conical tube, add the following:
	0.054 g FeCl ₃ .6H ₂ O (Reagent rack)

10 mL dH₂O

Make fresh on day of assay.

L-Ascorbic acid Standard

L-Ascorbic acid (Sigma Cat Nr.: A5960)

Prepare 1.0 mM solution: Weigh 0.0088 g Ascorbic acid (Reagent rack) in a 50 mL centrifuge tube and add 50 mL dH₂O. Mix until dissolved. Prepare fresh. Use this solution as the stock solution.

Check: In an eppendorf tube, dilute 125 μ l of this stock solution with 1375 μ l H₂O to obtain a concentration of 83 μ M. This solution should give an absorbance of 0.830 ± 0.010 at 265nm.

Control

L-Ascorbic acid 400 μ M (Sigma Cat Nr.: A5960)

Weigh 0.00352 g ascorbic acid (Reagent rack) in a 50 mL centrifuge tube and add 50 mL dH₂O. Mix until dissolved. Use this solution as the control.

Check: In an eppendorf tube, dilute 311 μ l of this solution with 1189 μ l H₂O to obtain a concentration of 83 μ M. This solution should give an absorbance of 0.830 ± 0.010 at 265nm.

Appendix 3: Recipe for preparation of TEAC reagents

ABTS (2,2'-Azino-bis(3-ethylbenzothiazoline-6-sulfonic acid) Diammonium salt:	7mM (Sigma Cat nr.: A1888) Weigh 0.0192 g of ABTS (Fridge) in a 15 mL screw cap tube and add 5 mL distilled water. Mix until dissolve. Prepare fresh.
Potassium-peroxodisulphate:	140mM (Merck Cat Nr.: 105091) Weigh 0.1892 g K ₂ S ₂ O ₈ (Reagent rack) in a 15 mL screw cap tube and add 5 mL distilled water. Mix until dissolve. Prepare fresh.
ABTS mix (This must be done 24 hours before starting the assay):	Add 88µl of the potassium-peroxodisulphate solution to 5 mL of the ABTS solution in a 15 mL screw cap tube. Mix well. Leave in the dark at room temperature for 24 hours before use.
Standard (Trolox also known as 6-Hydrox-2,5,7,8-tetramethylchroman-2-carboxylic acid):	1.0mM (Aldrich Cat nr.: 238831) Weigh 0.0125 g Trolox in a 50 mL screw cap tube and add 50 mL of Ethanol (Saarchem Cat Nr: 2233540LP) (Reagent rack). Mix until dissolved. Prepare fresh. Use this solution as the stock standard. Check: When diluted 5x with ethanol this solution should give an absorbance of 0.650 ±0.015 at 289 nm.
Control (Trolox):	200µM (Aldrich Cat nr.: 238831): Dissolve 0.0025 g Trolox (Reagent rack) in 50 mL of Ethanol (Saarchem Cat Nr: 2233540LP). Prepare fresh. Use this solution as the stock control. Check: When used as is this solution should give an absorbance of 0.650 ±0.015 at 289 nm.

Appendix 4: Recipe for preparation of TBARS reagents

Phosphoric acid (H_3PO_4) stocks (can be stored at room temperature)	Prepare 2 % H_3PO_4 by pipetting 1177 μL H_3PO_4 in 48.823 mL dH_2O in pre-labelled glass test tubes Prepare 7% H_3PO_4 by mixing (4.1 ml H_3PO_4 in 45.9 mL dH_2O).
Acid and Base stocks to adjust pH	Prepare 1 M HCl 4.92mL from 32 % HCl topped to 50 mL 3 mM HCl (30 μL from 1M stock in 9.97 mL dH_2O) 20 mM Butylated hydroxytoluene (BHT) stock by [440.8 mg BHT in 100 mL ethanol] TBA/Butylated hydroxytoluene (BHT) solution 0.1 g sodium hydroxide [NaOH]; 0.5 g TBA; 250 μL BHT from 20 mM stock all dissolved and made up to 50 mL using dH_2O),

Appendix 5: Recipe for preparation of protein carbonyl reagents

DNPH	9.8 mg DNPH [2.46 mL; 37% HCl in 7.53 mL dH ₂ O]
2,5M HCl	16.36 mL HCL in 1000 mL of DH ₂ O
20 % w/v trichloroacetic acid (TCA)	(20g TCA in 100 mL of dH ₂ O),
ethanol-ethyl acetate	(1:1 v/v)
6 M guanidine hydrochloride	(20 mL in 6.6 mL of dH ₂ O)

Appendix 6: Optimal H₂O₂ concentrations

Concentration of H ₂ O ₂ (μM)	% cell viability			
	1-hour exposure mean (SD)	2-hour exposure mean (SD)	3-hour exposure mean (SD)	24-hour exposure mean (SD)
0	100.0 (11.4)	100.0 (0.6)	100.0 (1.5)	100.0 (1.3)
50	87.1 (2.4)	65.6 (4.3)	88.4 (3.5)	21.3 (1.5)
100	39.2 (1.3)	31.9 (3.2)	74.7 (2.0)	10.9 (0.5)
150	38.8 (6.0)	29.5 (2.2)	44.3 (1.6)	10.5 (0.6)
400	28.0 (0.5)	28.5 (1.4)	26.5 (2.1)	11.0 (0.1)
1000	18.6 (0.6)	19.8 (0.5)	11.8 (1.1)	9.8 (0.3)

SH-SY5Y cells may have developed a level of resistance or adaptation to moderate levels of H₂O₂. The cells might have upregulated antioxidant defences or repair mechanisms, making them less vulnerable to OS after being exposed to H₂O₂ for 3 hours. cultured cells, particularly malignant cells, tend to adapt, with numerous changes in gene expression and protein levels, which are triggered in part by the oxidative stress component of "culture shock." Cellular adaptation to the OS of 'culture shock' in the minority of cells that survive could, in theory, involve increasing antioxidant defences, downregulating levels of ROS-generating enzymes, adapting electron transport chains to become less leaky and thus produce less superoxide, or altering cellular targets of oxidative damage to become more resistant to damage by ROS (Halliwell, 2003).

Appendix 7: The effect of 2-hour Rooibos extracts pretreatment followed by 3-hour H₂O₂ treatment on SH-SY5Y cell metabolic activity

Concentrations of Rooibos extract (µg/mL) plus optimal H ₂ O ₂ concentration	% cell viability			
	Aqueous unfermented Rooibos	Ethanol unfermented Rooibos	Aqueous fermented Rooibos	Ethanol Fermented Rooibos
0	100.0 (1.95)	100.0 (1.95)	100.0 (4.75)	100.0 (4.75)
150 µM H ₂ O ₂	37.2 (1.05)	37.2 (1.05)	40.2 (0.02)	40.2 (0.02)
15 µg/mL + 150 µM H ₂ O ₂	31.6 (0.03)	43.9 (1.15)	22.2 (0.09)	24.5 (1.13)
30 µg/mL + 150 µM H ₂ O ₂	40.3 (1.03)	57.7 (0.09)	29.4 (4.12)	37.1 (0,20)
60 µg/mL + 150 µM H ₂ O ₂	44.4 (0.01)	61.2 (0.01)	40.1 (2.64)	39.5 (0,11)
125 µg/mL + 150 µM H ₂ O ₂	44.0 (1.31)	63.1 (0.01)	46.9 (3.64)	42.0 (0,41)
250 µg/mL + 150 µM H ₂ O ₂	46.9 (3.20)	76.2 (0.31)	38.3 (0.39)	46.2 (6,17)
500 µg/mL + 150 µM H ₂ O ₂	71.3 (0.01)	80.4 (0.01)	43.4 (0.73)	57.4 (0,51)

Appendix 8: Intracellular ATP levels after SH-SY5Y cells pretreated with Rooibos extracts for 2 hours followed by 3-hour treatment with H₂O₂

Rooibos extracts and H ₂ O ₂ treatment groups	ATP Levels (RLU)			
	Aqueous unfermented Rooibos Mean (SD)	Ethanol unfermented Rooibos Mean (SD)	Aqueous fermented Rooibos Mean (SD)	Ethanol fermented Rooibos Mean (SD)
Cells only	4.6 10 ⁵ (7795)	4.6 10 ⁵ (7795)	4.6 10 ⁵ (7795)	4.6 10 ⁵ (7795)
150 µM H ₂ O ₂	4.9 10 ⁴ (2121)	4.9 10 ⁴ (2121)	4.9 10 ⁴ (2121)	4.9 10 ⁴ (2121)
125 µg/mL + 150 µM H ₂ O ₂	2.4 10 ⁴ (1306)	2.9 10 ⁴ (304)	2.8 10 ⁴ (1744)	3.5 10 ⁴ (3179)
250 µg/mL + 150 µM H ₂ O ₂	3.1 10 ⁴ (1262)	4.0 10 ⁴ (1036)	3.0 10 ⁴ (802)	3.5 10 ⁴ (1878)
500 µg/mL + 150 µM H ₂ O ₂	1.7 10 ⁴ (393)	2.9 10 ⁴ (1392)	2.1 10 ⁴ (431)	2.3 10 ⁴ (2529)

Appendix 9: Protein quantitation and standardisation after SH-SY5Y cells pretreated with Rooibos extracts from 24 hours followed by H₂O₂ treatment for 3 hours

Treatment Groups	Concentration of crude protein (µg/mL)			
	Aqueous unfermented Rooibos	Ethanol unfermented Rooibos	Aqueous fermented Rooibos	Ethanol fermented Rooibos
Cells only	1792.5	1792.5	1792.5	1792.5
150 µM H ₂ O ₂	2218.7	2218.7	2218.7	2218.7
60 µg/mL + 150 µM H ₂ O ₂	2405.3	1756.5	1757.5	1643.9
125 µg/mL + 150 µM H ₂ O ₂	2179.1	1672.4	1585.2	2230.5
250 µg/mL + 150 µM H ₂ O ₂	1398.8	2036.4	1885.3	1928.6

Bicinchoninic acid (BCA) was used to quantify the protein and is only used for standardization. Since no conclusions can be derived from this data, no statistics are required.

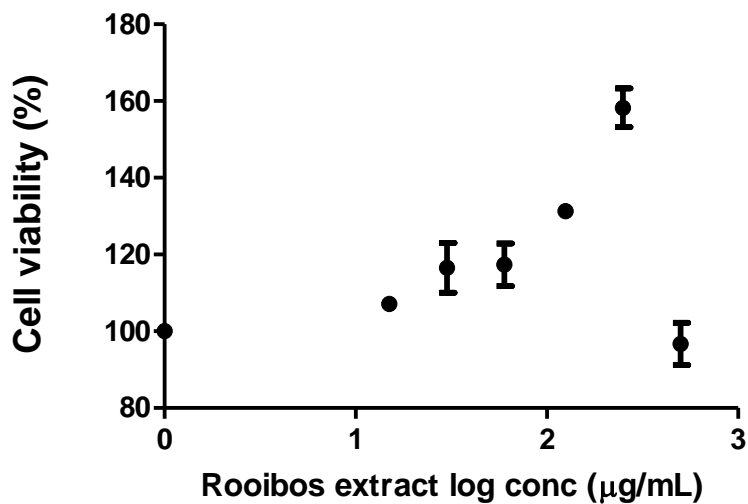
Appendix 10: Estimate the quantity of flavonoids identified in unfermented ethanolic and aqueous Rooibos extracts.

	Unfermented Rooibos (mg/L)					
	Aqueous			Ethanolic		
	60 µg/mL	125 µg/mL	250 µg/mL	60 µg/mL	125 µg/mL	250 µg/mL
Aspalathin	1.35	2.82	5.64	4.27	8.90	17.80
Orientin	0.34	0.71	1.43	0.51	1.06	2.12
Iso-orientin	0.42	0.87	1.74	0.73	1.52	3.05
Iso-vitexin	0.09	0.19	0.37	0.14	0.28	0.57
Vitexin	0.10	0.22	0.44	0.27	0.56	1.13

Appendix 11: Estimate the quantity of flavonoids identified in fermented ethanolic and aqueous Rooibos extracts.

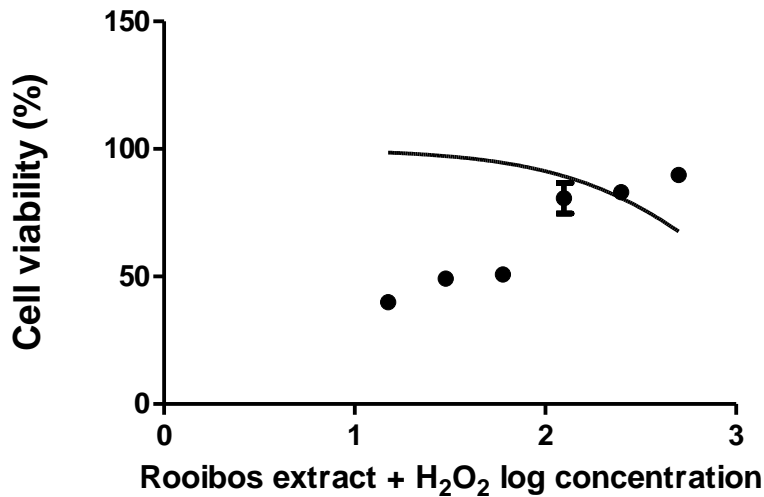
	Fermented Rooibos (mg/L)					
	Aqueous			Ethanolic		
	60 µg/mL	125 µg/mL	250 µg/mL	60 µg/mL	125 µg/mL	250 µg/mL
Aspalathin	0.24	0.51	1.01	0.46	0.97	1.93
Orientin	0.25	0.51	1.03	0.66	1.38	2.76
Iso-orientin	0.17	0.36	0.73	0.86	1.78	3.56
Iso-vitexin	0.06	0.13	0.27	0.19	0.39	0.79
Vitexin	0.03	0.06	0.11	0.23	0.47	0.95

Unfermented aqueous Rooibos extracts



Appendix 12: The effects of a 24-hour unfermented aqueous Rooibos extract treatment

unfermented aqueous Rooibos extracts



Appendix 13: Effect of unfermented aqueous Rooibos extracts on the metabolic output of SH-SY5Y cells challenged with 150 μM H₂O₂ using the 3-(4,5-dimethylthiazol-2-yl)-2,5-diphenyl-2H-tetrazolium bromide (MTT) assay.

Appendix 14: The total phenolic content of unfermented, and unfermented Rooibos compared according to the extraction methods.

Extract concentration ($\mu\text{g/mL}$)	Aqueous (mg GAE/L)		Ethanollic (mg GAE/L)	
	Unfermented	Fermented	Unfermented	Fermented
	Mean (SD)	Mean (SD)	Mean (SD)	Mean (SD)
15	0.3 (0.2)	1.8 (0.4)	1.3 (0.4)	0.7 (0.2)
30	6.3 (0.4)	2.4 (0.2)	6.1 (0.2)	4.3 (0.1)
60	18.1 (1.2)	11.7 (0.1)	20.9 (0.5)	13.4 (0.5)
125	47.6 (2.3)	37.8 (1.0)	64.1 (3.6)	38.2 (1.0)
250	106.2 (4.6)	87.7 (3.1)	138.4 (2.9)	90.6 (2.6)
500	189.4 (2.7)	169.2 (4.2) No	242.3 (6.1)	156.8 (1.4) No

Appendix 15: Ferric reducing antioxidant power of unfermented, and fermented Rooibos compared according to the extraction methods.

Extract concentration (µg/mL)	Aqueous (µmol AAE/L)		Ethanollic (µmol AAE/L)	
	Unfermented	Fermented	Unfermented	Fermented
	Mean (SD)	Mean (SD)	Mean (SD)	Mean (SD)
15	79.4 (1.2)	85.1 (0.1)	176.1 (4.2)	77.5 (1.5)
30	126.7 (1.7)	91.8 (0.7)	208.0 (6.2)	107.7 (1.4)
60	181.4 (3.1)	147.2 (2.1)	309.8 (2.1)	160.8 (0.9)
125	353.2 (8.3)	250.5 (2.5)	427.4 (12.3)	252.3 (0.0)
250	608.3 (16.1)	441.6 (11.3)	754.3 (26.8)	451.0 (10.7)
500	1106.6 (31.9)	827.4(31.9) r=1.000; P=0.333	1374.7 (7.5)	831.2(33.6) r=1.000; P=0.33

Appendix 16: Trolox equivalent antioxidant capacity of unfermented, and fermented Rooibos compared according to the extraction methods.

Extract concentration (µg/mL)	Aqueous (µmol TE/L)		Ethanollic (µmol TE/L)	
	Unfermented	Fermented	Unfermented	Fermented
	Mean (SD)	Mean (SD)	Mean (SD)	Mean (SD)
15	105.9 (3.1)	121.9 (8.4)	117.1 (3.5)	107.6 (7.6)
30	162.6 (0.2)	128.9 (9.5)	152.3 (2.3)	136.1 (12.2)
60	249.7 (15.4)	186.1 (2.8)	308.6 (26.0)	183.0 (5.8)
125	447.5 (6.3)	333.3 (5.1)	562.5 (31.8)	322.0 (16.6)
250	758.6 (19.4)	560.3 (20.8)	911.3 (24.3)	547.8 (17.5)
500	1167.5 (5.4)	904.3 (18.2) r=1.000; P=0.333	1263.9 (1.4)	835.6 (13.4) r=-0.500; P=1.000

Appendix 17: Ethics certificate



HEALTH AND WELLNESS SCIENCES RESEARCH ETHICS COMMITTEE (HWS-REC)
Registration Number NHREC: REC- 230408-014

P.O. Box 1906 • Bellville 7535 South Africa
Symphony Road Bellville 7535
Tel: +27 21 959 6917
Email: sethn@cput.ac.za

25 May 2023

REC Approval Reference No:
CPUT/HWS-REC 2022/H11 (renewal)

Faculty of Health and Wellness Sciences

Dear Mr. Elias Chipofya

Re: APPLICATION TO THE CPUT HWS-REC FOR ETHICS CLEARANCE

Approval was granted by the Health and Wellness Sciences-REC to **Mr. E Chipofya** for ethical clearance. This approval is for research activities related to research for **Mr. E Chipofya** at Cape Peninsula University of Technology.

TITLE: The neuroprotective effects of Rooibos extracts against oxidative stress-induced cytotoxicity in human neuroblastoma SH-SY5Y cells

Supervisor: Prof .Marnewick and Dr. Docrat

Comment:

Approval will not extend beyond 26 May 2024. An extension should be applied for 6 weeks before this expiry date should data collection and use/analysis of data, information and/or samples for this study continue beyond this date.

The investigator(s) should understand the ethical conditions under which they are authorized to carry out this study and they should be compliant to these conditions. It is required that the investigator(s) complete an **annual progress report** that should be submitted to the CPUT HWS-REC in December of that particular year, for the CPUT HWS-REC to be kept informed of the progress and of any problems you may have encountered.

Kind Regards



Ms. Carolynn Lackay
Chairperson – Research Ethics Committee
Faculty of Health and Wellness Sciences